EJA

European Journal of Anatomy

Volume 27 - Number 5 September 2023

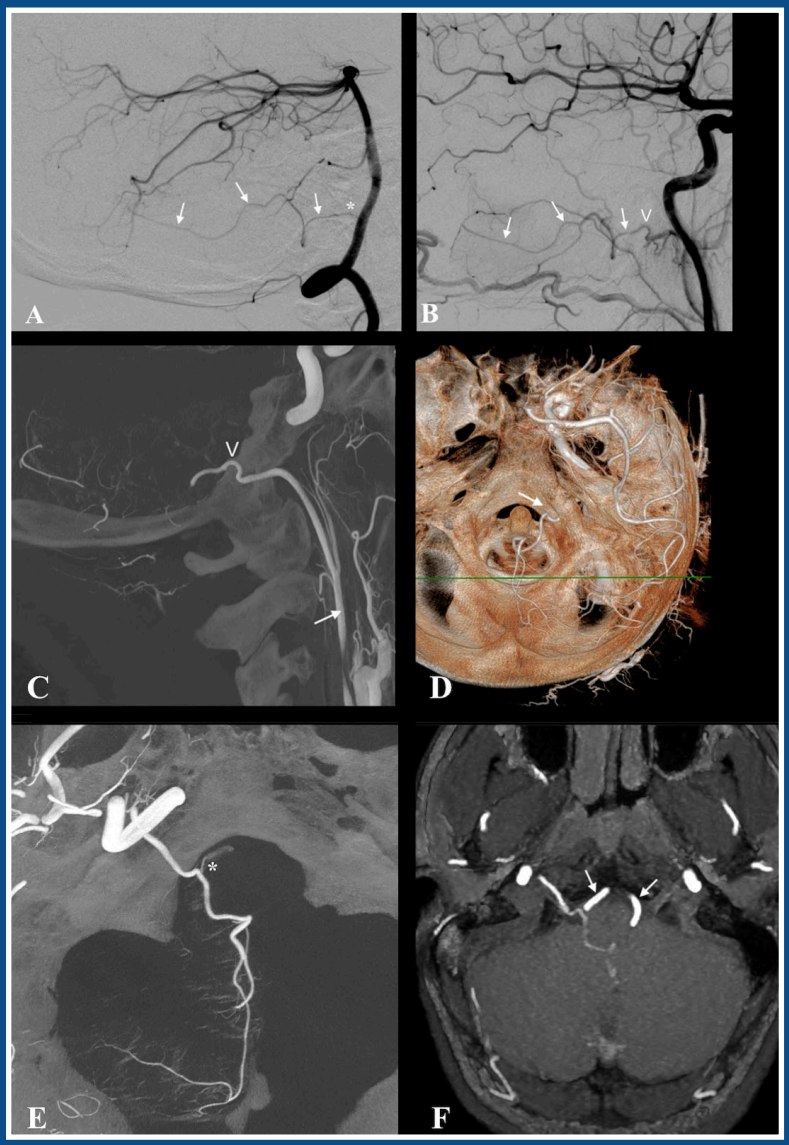

Indexed in:

CLARIVATE
- JCR:2020
- Q4 (21/23)
- I.F. J.C.I.: 0.19

DIALNET

EMBASE / Excerpta Medica

SCOPUS
- SJCR: 2020
- Q4 (31/39)
- I.F.: 0.162

Emerging Sources Citation Index

LATINDEX. Catálogo v1.0 (2002-2017)

Official Journal of the Spanish Society of Anatomy

Published by: **LOKI & DIMAS**

www.eurjanat.com

EJA
European Journal of Anatomy

Volume 27 - Number 5 September 2023

Lycopene attenuates oxidative stress, apoptosis, and biochemical fluctuations induced by bisphenol A in the kidney of rats

Mohammed Alorini

Department of Basic Medical Sciences, Unaizah College of Medicine and Medical Sciences, Qassim University, Unaizah, Kingdom of Saudi Arabia

SUMMARY

Bisphenol A (BPA) is an environmental pollutant that harms different body systems. Previous investigations indicated that BPA exposure is linked to renal dysfunction. Among carotenoids, lycopene (Lyc) is one of the strongest antioxidants. This work was conducted to assess the potential protective benefits of Lyc on oxidative stress and biochemical and histological abnormalities induced by BPA in the kidney. Adult male rats were divided into: control group, Lyc group (4 mg/kg /day), BPA group (50 mg/kg/day), and Lyc-BPA group. The agents were given orally for eight weeks.

BPA induced a marked increment in malondialdehyde (MDA) and a marked decrement in the superoxide dismutase (SOD) level. A marked rise in creatinine and urea levels was also reported. Marked histopathological alterations were demonstrated in the renal cortex. Atrophy of the renal corpuscles, dilated tubules with degenerated epithelium, dilated congested cortical renal blood vessels, and cellular infiltration were demonstrated. Up-regulation of the immune expression of desmin and down-regulation of Bcl2 were also detected. Interestingly, co-administration of Lyc and BPA ameliorated to a great extent most of the biochemical and histopathological alterations induced by BPA. In conclusion, BPA had a harmful impact on the kidney of rats and Lyc protected against renal damage through its antioxidant, anti-inflammatory, and anti-apoptotic effects.

Key words: Bcl2 – Desmin – Creatinine – Urea – Oxidative stress

INTRODUCTION

Bisphenol A (BPA), an environmental hazard, is an extensively manufactured chemical (Eweda et al., 2020). BPA is primarily utilized as an epoxy resin precursor and a monomer in creating polycarbonate plastics. Polycarbonate plastics are used in beverage and food containers, and the resins are used to cover metal items such as water supply pipes, bottle caps, and cans. Additionally, BPA is utilized to create thermal paper, flame retardants, various resins, and polyvinyl chloride plastic manufacturing (Haroun et al., 2019). BPA-containing items are widely used, leading to extensive global human exposure (Vandenberg et al., 2010). Although inhalation and transder-

Corresponding author:
Mohammed Alorini, MD. Department of Basic Medical Sciences, Unaizah College of Medicine and Medical Sciences, Qassim University, 44159 Unaizah, Kingdom of Saudi Arabia. Phone: 00966503975705, Fax: 0020504985900. E-mail: m.alorini@qu.edu.sa

Submitted: February 15, 2023. **Accepted:** March 17, 2023

https://doi.org/10.52083/FGZO9858

mal absorption are potential additional exposure pathways, especially for individuals who work in organizations that make BPA-based goods, ingestion is the most common route of BPA exposure. (Kang et al., 2006, Zalko et al., 2011).

BPA is an endocrine disruptor that mimics estrogen and thyroid hormones (Eweda et al., 2020). Experiments employing laboratory animals and cultured cells revealed that BPA could accumulate and interfere with various essential organ activities, such as the pancreas, brain, liver, heart, and testis (Kobroob et al., 2018). Human epidemiological research implies a link between high BPA levels in urine and the possibility of hypertension or albuminuria (Moreno-Gómez-Toledano et al., 2022). Additionally, (Olea-Herrero et al., 2014) reported high urinary excretion of albumin and podocytopathy after five weeks of exposure to BPA. Saura et al. (2014) also reported that exposure to BPA was linked to hypertension in mice. Such results raised concerns about the likelihood that routine BPA exposure might harm the kidney and contribute to cumulative renal impairment, which worsens over time.

The principal carotenoid, lycopene (Lyc), is a fat-soluble red pigment in tomatoes, pink grapefruit, papaya, and watermelon (Stojiljković et al., 2020). Lyc has recently attracted special attention as the most potent antioxidant among carotenoids (Rao and Agarwal, 2000). It was stated that utilization of Lyc reduced oxidative injury to biological molecules like proteins, DNA, and lipids (Palabiyik et al., 2013). Additionally, previous research revealed that Lyc had anti-inflammatory properties. Lyc slowed the aging process and offered protection from various diseases, including heart diseases, Alzheimer's disease, and other malignancies (Kaya et al., 2015).

A beneficial relationship has been established between dietary antioxidant supplementation and the decrement of harmful impacts of numerous environmental and toxicant factors (Pandir et al., 2016). In view of the aforementioned medicinal qualities of Lyc, this experimental work was conducted to assess the potential protective benefits of Lyc on oxidative stress and toxicity caused by BPA-induced biochemical and histological alterations in the kidney.

MATERIALS AND METHODS

Animals

This investigation employed 40 mature male albino rats (190 ± 20 g). The animals were kept in three-animal polypropylene rat cages. The rats were acclimatized to regular laboratory settings for at least seven days before treatment, with temperatures ranging from 25 ± 2°C and 30-70% relative humidity and a 12/12-hour light-dark cycle. Animals ate experimental rat pellets and drank purified water. The research was done following the Laboratory Animal Care and Use Guide, and during the light phase (National Institute of Health Publication No. 80– 23, revised 1996).

Chemicals

Sigma Chemical Company supplied BPA powder (CAS register no. 239658) (St. Louis, MO), and Puritan's Pride, INC, USA supplied Lyc with 20 mg capsules.

Study protocol

Four groups of 10 rats each were assigned:

Group I (Control group) was then divided into subgroup (I), which was kept untreated, and subgroup (II), which was given 0.5 mL of corn oil, the diluting vehicle for Lyc and BPA; group II (Lyc group) was dosed with Lyc of 4 mg/kg /day (Pandir et al., 2016); group III (BPA group) received BPA at a dose of 50 mg/kg/day (Amin et al., 2023), and group IV (Lyc-BPA group) was given both Lyc and BPA as in previous groups. All preceding treatments were supplied orally by gavage as a single, newly generated daily dose for eight weeks.

After the investigation, the animals were sacrificed under ethyl ether anesthesia (Shalaby et al., 2019). Blood samples were taken through a heart puncture and coagulated at room temperature. After centrifuging the samples at 3000 rpm for 15 minutes, the separated sera were frozen at -20 C for future urea and creatinine biochemical analysis. After opening the abdominal wall, both kidneys were taken out, cleaned with cold saline, dried with filter paper and weighed. The right kidneys were kept at -80 degrees Celsius in liquid nitrogen until tissue homogenates were made. The

left kidneys were immersed in 10% buffered formalin for histological evaluation.

Biochemical analysis

Creatinine and urea levels in blood were determined using commercial kits from the French company Biolabo.

Assessment of oxidative stress

Superoxide dismutase (SOD) and malondialdehyde (MDA) levels were measured in kidney homogenates according to Marklund and Marklund (1974) and Uchiyama and Mihara (1978), respectively.

Light microscopic studies

The left kidney of each animal was divided lengthwise into two halves, fixed in a 10% buffered formalin solution for 24 hours, dried in increasing strength ethanol, and then embedded in paraffin. The following procedures were applied to serial sections of 5 µm thickness:

- Hematoxylin and Eosin (H&E) stain: to highlight the major histological characteristics.
- Periodic acid-Schiff (PAS) stain: to show the brush border and basement membrane of the proximal and distal convoluted tubules and the parietal layer of the Bowman's capsule (Layton and Bancroft, 2013).
- Immunohistochemical staining with the streptavidin-biotin-peroxidase method as described by Shalaby et al., (2020b), Shalaby et al., (2020a).

The slides were dewaxed and then treated in PBS with 3% H2O2 to quell any remaining endogenous peroxidase activity. After each procedure, PBS was used to clean up any residue (Alabiad et al., 2021a, Khayal et al., 2022). Antigenic retrieval of proteins required 15 minutes at 95 degrees Celsius in sodium citrate solution (10 mM, pH 6.0) (Alabiad et al., 2021b, Ahmed et al., 2021). Non-specific staining was prevented by incubating the slides in 10% normal goat serum in PBS for one hour at room temperature. Next, the slides were incubated with diluted primary antibodies, a mouse monoclonal antibody against desmin (cat # M 0760, Dako, Carpentaria California, USA) at a dilution of 1:100, and a mouse monoclonal antibody against Bcl2 (SC-7480, Dako, Carpentaria California, USA) at a dilution of 1:100, at 4 C overnight. The slides were treated with the appropriate biotinylated secondary antibody (Alabiad et al., 2021b, Elsalam et al., 2021). Then the slides were treated with the avidin-biotin combination. These immunopositive responses were induced by the addition of diaminobenzidine (DAB). Finally, Mayer's hematoxylin was applied to the sections as a counterstain.

Morphometric study

For image analysis, the "Image J version 1.47 software", National Institute of Health Bethesda, Maryland, USA (Tawfeek et al., 2021, Khayal et al., 2021), was utilized to measure the area percentages of desmin and Bcl2 expressions in the stained kidney sections immunohistochemically, as well as the area percentages of PAS-positive reaction.

Statistical Analysis

For each group, the morphometric data were displayed as mean ± SD. One-way analysis of variance (ANOVA) was used for statistical analysis, and $P < 0.05$ was used as the significance threshold for the post hoc Tukey test. The software Statistical Package for Social Sciences version 17 (SPSS Inc., Chicago, Illinois, USA) was used to analyze the data.

RESULTS

No deaths were observed among experimental rats.

Kidney weight results

The rats' kidney weight increased significantly ($p < 0.001$) after receiving BPA treatment compared to controls. Compared to rats given BPA alone, treatment with Lyc substantially decreased the higher kidney weight ($p < 0.001$) (Table 1).

Biochemical results

Comparing the BPA group to the control group, a substantial rise ($p < 0.001$) in the blood levels of urea and creatinine was observed, while Lyc treatment in the Lyc-BPA group significantly lowered their levels ($p < 0.001$) and succeeded in normalizing them (Table 1).

Oxidative stress results

The BPA group depicted a marked reduction in the SOD level and a marked rise in the MDA level versus the control group ($p < 0.001$). On the contrary, treatment with both Lyc and BPA significantly lowered MDA and elevated SOD compared with animals administrated BPA alone ($p < 0.001$) (Table 1).

Table 1. The effect of BPA, Lyc, Lyc-BPA combination on kidney weight, urea, creatinine, MDA, SOD, Area % of PAS, Area % of desmin, and optical density of Bcl2 levels in the kidney's rat.

	Control group (Group I)	Lyc group (Group II)	BPA group (Group III)	Lyc-BPA Group (Group IV)	ANOVA	
	Mean ± SD	Mean ± SD	Mean ± SD	Mean ± SD	F	P-value
Kidney weight (g)	1.52 ± 0.05	1.53 ± 0.09	2.53 ± 0.27	1.66 ± 0.05	55.037	<0.001*
Urea (mg dL– 1)	21.86 ± 1.21	22.48 ± 1.16	47.50 ± 1.77	23.56 ± 1.11	431.500	<0.001*
Creatinine (mg dL– 1)	0.74 ± 0.01	0.73 ± 0.03	2.15 ± 0.40	0.80 ± 0.01	60.076	<0.001*
MDA (mmol/mg tissue)	3.82 ± 0.34	3.62 ± 0.47	9.42 ± 1.18	4.09 ± 0.35	84.138	<0.001*
SOD (U/mg protein)	9.78 ± 0.35	10.01 ± 0.76	5.05 ± 0.45	9.06 ± 0.56	88.297	<0.001*
Area % of PAS	31.40 ± 2.30	30.40 ± 1.94	16.40 ± 1.14	29.39 ± 2.07	67.574	<0.001*
Area % of desmin	0.36 ± 0.03	0.35 ± 0.02	3.07 ± 0.50	0.44 ± 0.04	140.010	<0.001*
Optical density of Bcl2	0.86 ± 0.03	0.84 ± 0.02	0.57 ± 0.04	0.82 ± 0.02	130.683	<0.001*

TUKEY'S Test						
	I&II	I&III	I&IV	II&III	II&IV	III&IV
Kidney weight (g)	0.999	<0.001*	0.449	<0.001*	0.523	<0.001*
Urea (mg dL– 1)	0.883	<0.001*	0.227	<0.001*	0.592	<0.001*
Creatinine (mg dL– 1)	1.000	<0.001*	0.968	<0.001*	0.968	<0.001*
MDA (mmol/mg tissue)	0.967	<0.001*	0.916	<0.001*	0.692	<0.001*
SOD (U/mg protein)	0.911	<0.001*	0.202	<0.001*	0.063	<0.001*
Area % of PAS	0.842	<0.001*	0.381	<0.001*	0.842	<0.001*
Area % of desmin	1.000	<0.001*	0.966	<0.001*	0.961	<0.001*
Optical density of Bcl2	0.642	<0.001*	0.122	<0.001*	0.643	<0.001*

One-way ANOVA and Tukey's post-hoc test, n=5
* Indicates Significance.

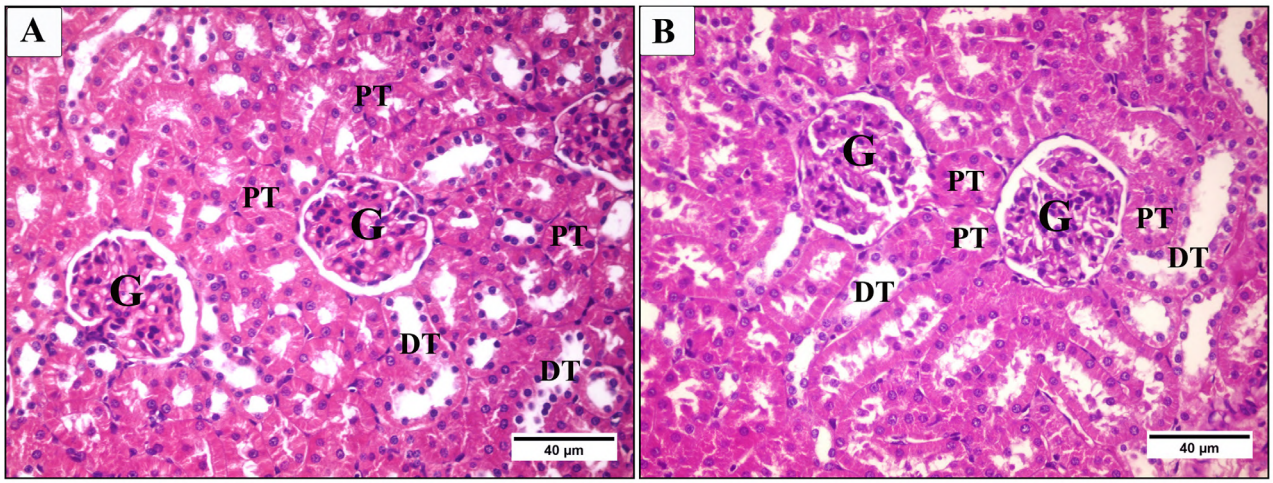

Fig. 1.- A: Control group and **B:** Lyc group showing normal glomeruli (G), distal convoluted tubules (DT), and proximal convoluted tubules (PT). (H&E ×400, scale bars = 40 µm).

Histopathological results

H&E-stained results

The control group and the Lyc group showed the normal structure of the renal cortex, which consisted of glomeruli, proximal convoluted tubules with deeply acidophilic cytoplasm and narrow lumen, and distal convoluted tubules with less acidophilic cytoplasm and a wider lumen (Fig. 1A, B). Administration of BPA for eight weeks induced changes in the renal cortex which included shrunken glomeruli and dilated tubules with atrophied epithelium and pyknotic nuclei (Fig. 2A). Dilated congested blood vessels, cellular infiltration, and edema between tubules were also detected (Fig. 2B, C), in addition to the presence of casts inside tubule (Fig. 2D). On the contrary, co-administration of both Lyc and BPA attenuated the histological alterations induced by BPA regarding glomeruli and tubules, as they appeared normal (Fig. 3A). Nevertheless, small foci of cellular infiltration were present (Fig. 3B).

PAS-stained results

A strong PAS-positive reaction was observed in the brush border of the tubules and in the basement membrane of the Bowman's capsule of the glomerulus and renal tubules in the control group and in the Lyc group (Fig. 4A, B), although the BPA group demonstrated loss of PAS-positive reaction in the brush border in most tubules with an ill-defined basement membrane (Fig. 4C). Regarding the Lyc-BPA group, it showed a strong PAS-positive reaction (Fig. 4D). The mean area fraction of PAS was found to be significantly decreased in the BPA group ($p < 0.001$) when compared to the control group. Contrarily, when Lyc and BPA were administered together, the mean area percentage of PAS was considerably higher ($p < 0.001$) than in the BPA group (Table 1).

Desmin immunohistochemistry results

Weak desmin expression within podocytes of the glomerulus was demonstrated in both the control and Lyc groups (Fig. 5A, B), whereas the

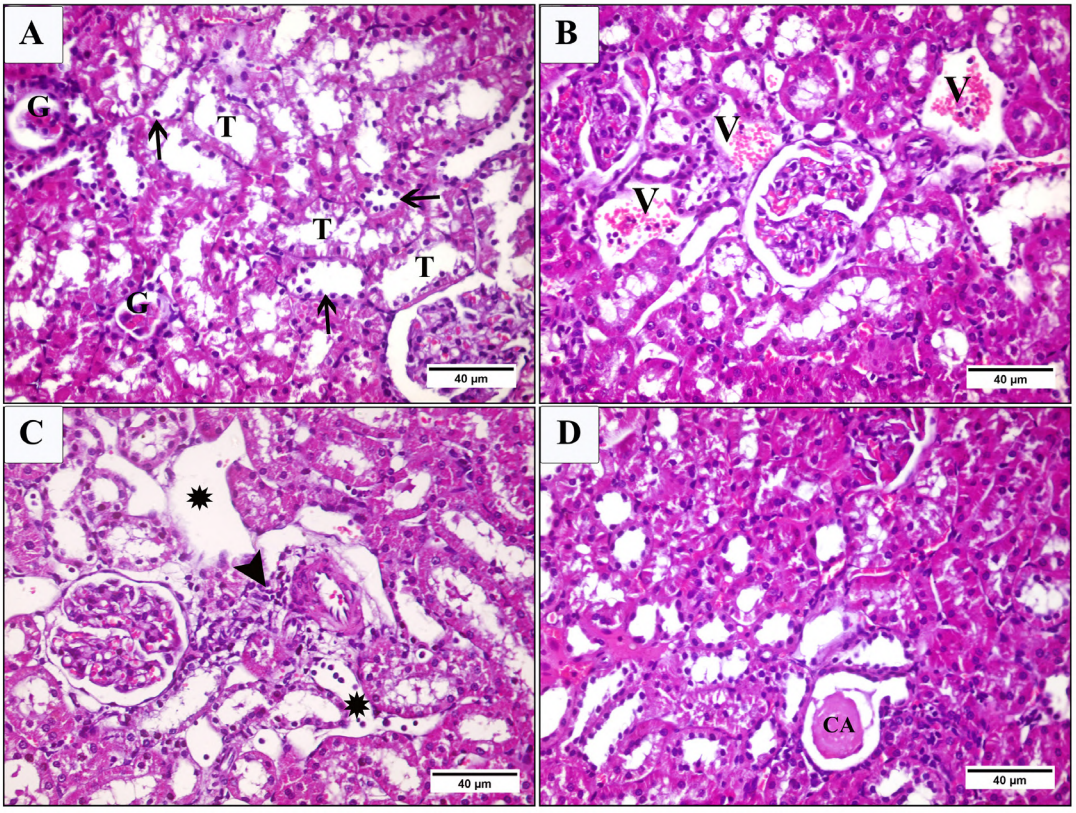

Fig. 2.- BPA group demonstrating: **A:** Shrunken glomeruli (G), dilated tubules (T) with atrophied epithelium and pyknotic nuclei (arrows); **B:** dilated congested blood vessels (V) in-between tubules; **C:** cellular infiltration (arrowhead) and edema (asterisks) in-between tubules; **D:** cast (C) inside tubule. (H&E ×400, scale bars = 40 µm).

BPA group demonstrated up-regulation of desmin expression (Fig. 5C). Regarding the Lyc-BPA group, IT displayed down-regulation of desmin expression (Fig. 5D). A significant increment ($p < 0.001$) in the mean area fraction of desmin expression in the BPA group in opposition to control group was reported. While administration of both Lyc and BPA significantly reduced ($p < 0.001$) the area fraction of desmin expression in opposition to the BPA group (Table 1).

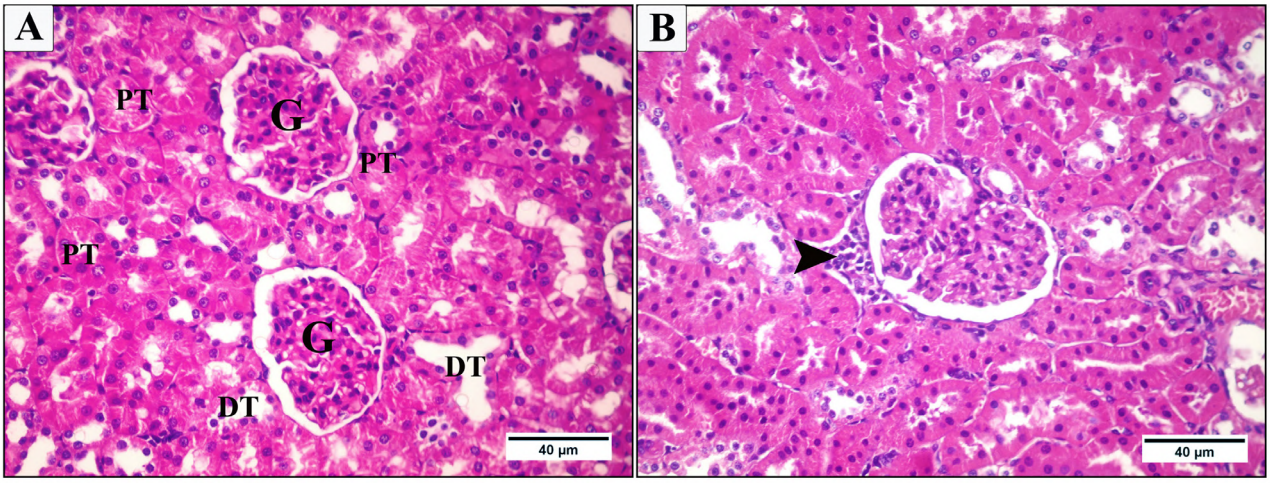

Fig. 3.- Lyc-BPA group demonstrating: **A:** normal glomeruli (G), distal convoluted tubules (DT), and proximal convoluted tubules (PT); **B:** a small focus of cellular infiltration (arrowhead). (H&E ×400, scale bars = 40 µm).

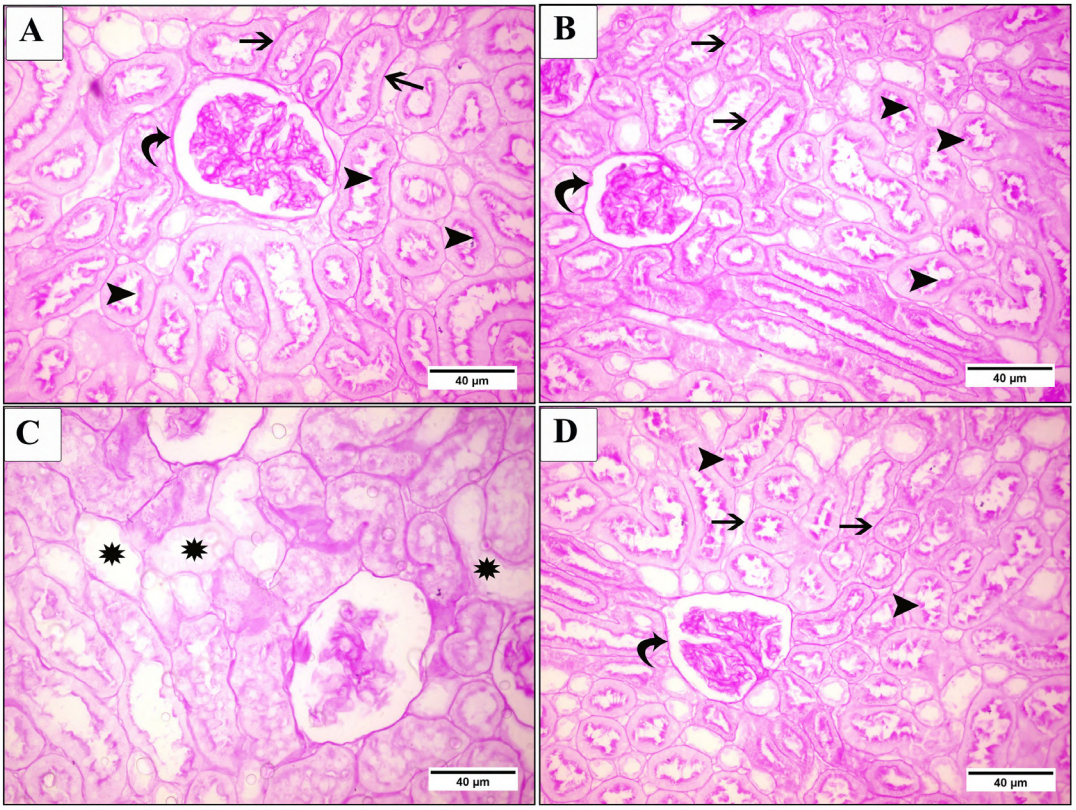

Fig. 4.- A: Control group and **B:** Lyc group demonstrating strong PAS positive reaction in brush border of tubules (arrowheads) and the basement membrane of Bowman capsule of glomerulus (curved arrow) and renal tubules (arrows). **C:** BPA group demonstrating; loss of PAS positive reaction in the brush border of tubules (asterisks) with ill-defined basement membrane. **D:** Lyc-BPA group revealing strong PAS positive reaction in brush border of tubules (arrowheads) and the basement membrane of Bowman capsule of glomerulus (curved arrow) and renal tubules (arrows). (PAS ×400, scale bars = 40 µm).

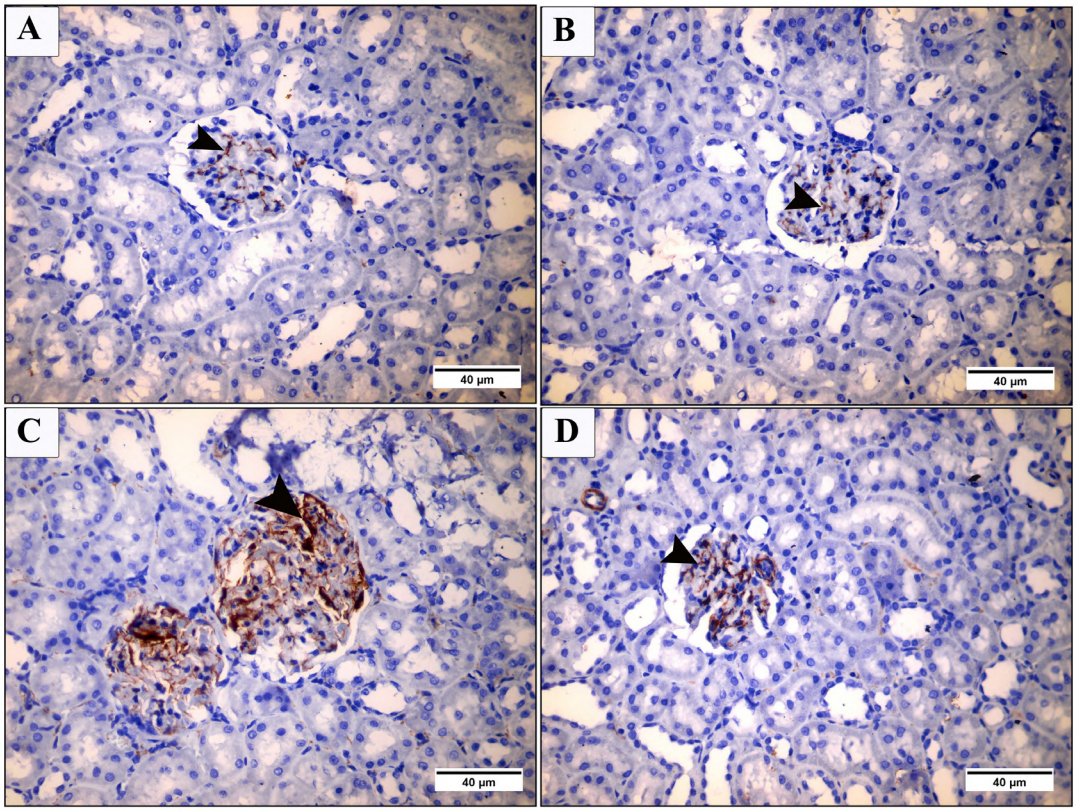

Fig. 5.- A: Control group and **B:** Lyc group revealing weak demin expression within podocytes of glomerulus (arrowhead). **C:** BPA group demonstrating; up-regulation of desmin expression (arrowhead). **D:** Lyc-BPA group displaying down-regulation of desmin expression (arrowhead). (Desmin immunostaining ×400, scale bars = 40 µm).

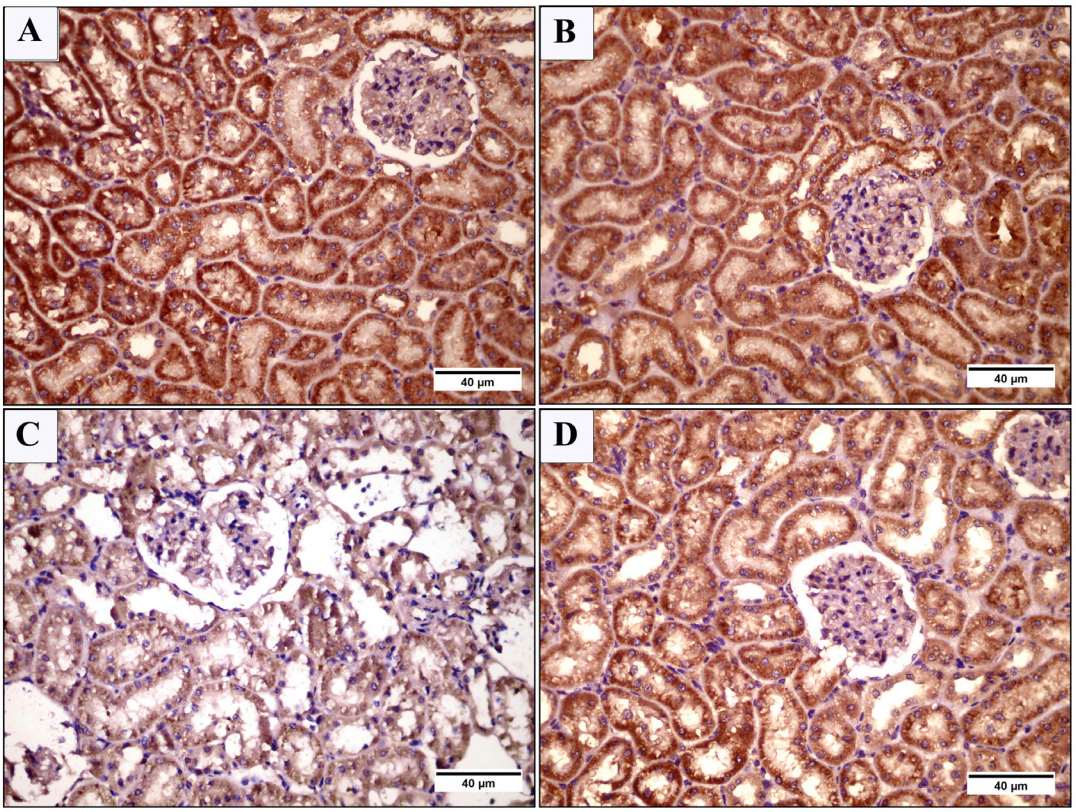

Fig. 6.- A: Control group and **B:** Lyc group demonstrating strong Bcl2 expression within glomerulus and tubules. **C:** BPA group demonstrating; down-regulation of Bcl2 expression. **D:** Lyc-BPA group displaying up-regulation of Bcl2 expression. (Bcl2 immunostaining ×400, scale bars = 40 µm).

Bcl2 immunohistochemistry results

Strong Bcl2 expression within the glomerulus and tubules was detected in both the control and Lyc groups (Fig. 6A, B). Down-regulation of Bcl2 expression was demonstrated in the BPA group (Fig. 6C). Up-regulation of Bcl2 expression was demonstrated in the Lyc-BPA group (Fig. 6D). The mean optical density of Bcl2 expression was significantly lower ($p < 0.001$) in the BPA group when compared to the control group. But when Lyc and BPA were administered together, the mean optical density of Bcl2 expression was considerably higher ($p < 0.001$) than in the BPA group (Table 1).

DISCUSSION

Concerns regarding the impact of BPA exposure on human health have lately been raised, since extensive exposure has been found among populations in numerous nations. (Björnsdotter et al., 2017). Because BPA is used in so many daily plastic items, it has the potential to drastically damage the environment, either by leaking from plastic water and food containers or as a consequence of manufacturing. As a result, the principal sources of exposure are food and drink. (Helal et al., 2013). The main goal of this investigation is to evaluate the efficacy of Lyc as a protecting agent against the renal impacts of BPA. The study's findings validate the effect of BPA on the kidney and provide new insight into the possible effective role of Lyc in mitigating the detrimental cellular consequences associated with BPA exposure.

The current research reported a marked increment in the weight of the kidney of rats that were administered BPA. This result coincided with Poormoosavi et al., (2018), who detected the same finding in their work on rats. They indicated that BPA is a xenoestrogen and could activate the estrogen receptors in the kidney, subsequently promoting the growth of epithelial cells. On the other side, BPA may result in hydronephrosis by increasing the volume of the renal tubules. The present work revealed that BPA deteriorated kidney functions, as confirmed by the significant rise in the serum levels of creatinine and urea. This was in harmony with Edres et al., (2018), who indicated comparable results in their investigation on rats that were administered BPA. The accumulation of BPA-toxic compounds in the kidney with the inability to remove them led to nephrotoxicity, with a subsequent rise in creatinine and urea levels (Wahby et al., 2017). Kobroob et al., (2018) also added that BPA damaged the kidney glomeruli with decreased glomerular filtration, which could explain impaired kidney function.

Regarding the influence of BPA on oxidative/antioxidative markers in rat kidney tissues, the current work depicted that BPA caused oxidative stress in the kidney of rats, as evidenced by the marked increase in MDA coupled with a marked reduction in the level of SOD. This finding was in agreement with Poormoosavi et al. (2018), who had comparable results in rats that were administered BPA. BPA was reported to increase reactive oxygen species (ROS) production (Asahi et al., 2010). In the same line, Morgan et al. (2014) discovered that BPA treatment caused lipid peroxidation in testicular, brain, and kidney tissue, as evidenced by considerably lower GSH concentrations and higher MDA levels. Furthermore, Eid et al. (2015) reported a reduction in antioxidant capacity and an increase in MDA levels after exposure to BPA. Additionally, patients using BPA-containing polysulfone dialysers had also been found to have high serum levels of BPA and elevated indicators of oxidative stress (Bosch-Panadero et al., 2016).

The analysis of the renal cortex histology of the current study in BPA-treated rats showed atrophied renal corpuscles, dilated tubules with degenerated epithelium, dilated congested cortical renal blood vessels, and infiltration of mononuclear cells. These findings were in harmony with the earlier work of Korkmaz et al. (2011) and Ahmed et al. (2015), who observed similar findings in the kidney of BPA-exposed rats. These changes could be attributed to oxidative damage caused by BPA (Kobayashi et al., 2020). It was stated that increased ROS levels by BPA caused mutations, accelerated cell proliferation, lipid peroxidation, DNA damage, mitochondrial malfunction, and protein alteration, all contributing to renal damage and inflammation (Priego et al., 2021).

According to in vitro research, BPA enhanced the generation of pro-inflammatory cytokines,

such as TNF-α and IL-6 (Lee and Lim, 2010). In a recent study conducted in rats, ingestion of BPA for four weeks increased pro-inflammatory cytokine generation and secretion, with a subsequent decrease in renal function (Alekhya Sita et al., 2019). Furthermore, mice exposed to BPA for a long time showed a rise in the amount of $CD3^+$ T lymphocytes in the interstitium of the kidney, which was more noticeable in damaged kidneys, leading to the generation and secretion of more inflammatory mediators (Priego et al., 2021).

Up-regulation of desmin expression was demonstrated in rats administered BPA in our research. Consistent with our results, Fadda et al. (2019) indicated that podocyte injury was enhanced in rats with a subsequent increase in desmin expression. Previously, increased desmin expression in podocytes was shown in various rat renal diseases, including diabetic nephropathy (Kakimoto et al., 2014). Desmin and vimentin, two intermediate filament proteins, are expressed in podocytes. Desmin is mostly detected in vascular smooth muscle and mesangial cells, with podocytes showing extremely faint expression (Zou et al., 2006). Thus, desmin expression is a reliable indicator of early podocyte damage (Gross et al., 2003).

The present work indicated that BPA induced apoptosis in the renal cortex, as confirmed by the marked decrease in Bcl2 expression. This finding was in agreement with Fadda et al. (2019), who demonstrated apoptosis in renal cells after exposure to BPA. In the same line, Peerapanyasut et al. (2019) indicated a significant increase in pro-apoptotic genes in the kidney after exposure to BPA. According to Bosch-Panadero et al. (2018), BPA promotes mitochondrial damage, oxidative stress, and apoptosis in renal tubules in a concentration-dependent manner. Moreover, Olea-Herrero et al. (2014) discovered that different concentrations of BPA could elicit podocyte death after nine days in culture using the tunnel assay.

The present investigation revealed that Lyc administration improved renal function and reduced the biochemical and histopathological changes caused by BPA in rats. The current study reported normalization of serum creatinine and urea levels in rats that were co-administered Lyc and BPA. This finding coincided with a prior work of Karahan et al. (2005), who indicated that Lyc treatment normalized serum creatinine and urea levels in nephrotoxicity caused by gentamicin. Also, Gori et al. (2021) indicated that Lyc treatment improved renal functions and lowered the high serum levels of urea and creatinine in adenine-induced renal damage in rats, and attributed this to improved glomerular filtration rate with subsequent enhancement of toxin metabolism.

A marked decline in the MDA level coupled with a rise in the SOD level in rats administrated both Lyc and BPA, suggesting the antioxidant effect of Lyc. In the same line, Hussein et al. (2018) indicated that Lyc treatment significantly increased kidney antioxidant enzymes in diabetic nephropathy in rats. Furthermore, Lyc treatment protected renal cells from lipid peroxidation caused by furan, the level of deceased MDA, and the increase in SOD (Pandir et al., 2016). Moreover, Lyc is an effective scavenger of free radicals and has a constant physical rate of quenching with ROS (Koul et al., 2010, Palabiyik et al., 2013).

The current investigation demonstrated that Lyc supplementation attenuated the histopathological changes caused by BPA. According to Pandir et al.(2016), Lyc could prevent furan-induced oxidative damage to the rat kidney by enhancing renal function, minimizing histopathologic alterations, lowering MDA generation, and restoring antioxidant enzyme activities. Additionally, a prior study by Yilmaz et al.(2006) found that Lyc prevented the kidney alterations brought on by adriamycin, and they attributed this result to the antioxidant capabilities of Lyc. Numerous investigations also discovered that it protects against chemically induced kidney injury (Aydin et al., 2013, Palabiyik et al., 2013). Moreover, Lyc drastically reduced the generation of inflammatory cytokines in rats with diabetic nephropathy (Tabrez et al., 2015). The suppression of pro-inflammatory cytokine synthesis and secretion and modification of signal transduction pathways could explain the anti-inflammatory effect of Lyc (Palozza et al., 2010).

Down-regulation of desmin expression was demonstrated in rats that were co-administered Lyc and BPA. El-Gerbed (2014) indicated that Lyc treatment improved alterations in the podocyte

foot process and protected podocytes. These data corroborate our findings. In our investigation, co-administration of both Lyc and BPA caused up-regulation of Bcl2 immune expression. This was consistent with the earlier study that concluded that Lyc reduces apoptosis (Buyuklu et al., 2015). Lyc administration significantly enhanced the anti-apoptotic gene Bcl-2 and reduced pro-apoptotic gene levels in rats treated with cisplatin, suggesting that Lyc had anti-apoptotic effects (Dogukan et al., 2011).

CONCLUSION

Lycopene (Lyc), which had been shown to have antioxidant, anti-apoptotic, and anti-inflammatory properties, lessened BPA-induced kidney damage. The use of Lyc supplements as a natural nephroprotective component is recommended, as humans consume Lyc in large amounts through goods such as tomatoes, tomato sauce, watermelons, melons, and grapefruits.

ACKNOWLEDGMENTS

I would like to thank my colleagues and laboratory technicians at the Unaizah College of Medicine for the technical assistance and use of their equipment and facilities. Also, I would like to thank Prof. Dr. Mohamed Ali Alabiad and Prof. Dr. Amany Mohamed Shalaby for their role in reviewing the study design of the manuscript and their assistance in interpreting the microscopic images. In addition, I would like to express my gratitude to Mr. Mohamed Fathy for helping with the statistical tests.

REFERENCES

AHMED MM, GEBRIEL MG, MORAD EA, SABER IM, ELWAN A, SALAH M, FAKHR AE, SHALABY AM, ALABIAD MA (2021) Expression of immune checkpoint regulators, cytotoxic T-lymphocyte antigen-4, and programmed death-ligand 1 in Epstein-Barr virus-associated nasopharyngeal carcinoma. *Appl Immunohistochem Mol Morphol*, 29(6): 401-408.

AHMED WM, MOSELHY WA, NABIL T (2015) Bisphenol A toxicity in adult male rats: hematological, biochemical and histopathological approach. *Global Veterinaria,* 14: 228-238.

ALABIAD M, HARB O, MANDOUR D, HEMEDA R, AHMED RZ, EL-TAHER A, OSMAN G, SHALABY A, ALNEMR AA, ABDELFATTAH MT (2021a) Prognostic and clinicopathological implications of expression of Beclin-1 and hypoxia-inducible factor 1α in serous ovarian carcinoma: an immunohistochemical study. *Pol J Pathol*, 72(1): 23-38.

ALABIAD MA, HARB OA, HEFZI N, AHMED RZ, OSMAN G, SHALABY AM, ALNEMR AA, SARAYA YS (2021b) Prognostic and clinicopathological significance of TMEFF2, SMOC-2, and SOX17 expression in endometrial carcinoma. *Exp Mol Pathol*, 122: 104670.

ALEKHYA SITA GJ, GOWTHAMI M, SRIKANTH G, KRISHNA MM, RAMA SIREESHA K, SAJJARAO M, NAGARJUNA K, NAGARJUNA M, CHINNABOINA GK, MISHRA A (2019) Protective role of luteolin against bisphenol A-induced renal toxicity through suppressing oxidative stress, inflammation, and upregulating Nrf2/ARE/HO-1 pathway. *IUBMB Life,* 71: 1041-1047.

AMIN MAS, SONPOL HMA, GOUDA RHE, ABOREGELA MA (2023) Bisphenol A enhances apoptosis, fibrosis, and biochemical fluctuations in the liver of adult male rats with possible regression after recovery. *Anat Rec (Hoboken)*, 306(1): 213-225.

ASAHI J, KAMO H, BABA R, DOI Y, YAMASHITA A, MURAKAMI D, HANADA A, HIRANO T (2010) Bisphenol A induces endoplasmic reticulum stress-associated apoptosis in mouse non-parenchymal hepatocytes. *Life Sci,* 87: 431-438.

AYDIN S, PALABIYIK ŞS, ERKEKOGLU P, SAHIN G, BAŞARAN N, GIRAY BK (2013) The carotenoid lycopene protects rats against DNA damage induced by Ochratoxin A. *Toxicon,* 73: 96-103.

BJÖRNSDOTTER MK, DE BOER J, BALLESTEROS-GÓMEZ A (2017) Bisphenol A and replacements in thermal paper: A review. *Chemosphere,* 182: 691-706.

BOSCH-PANADERO E, MAS S, SANCHEZ-OSPINA D, CAMARERO V, PÉREZ-GÓMEZ MV, SAEZ-CALERO I, ABAIGAR P, ORTIZ A, EGIDO J, GONZÁLEZ-PARRA E (2016) The choice of hemodialysis membrane affects bisphenol A levels in blood. *J Am Soc Nephrol,* 27: 1566-1574.

BOSCH-PANADERO E, MAS S, CIVANTOS E, ABAIGAR P, CAMARERO V, RUIZ-PRIEGO A, ORTIZ A, EGIDO J, GONZÁLEZ-PARRA E (2018) Bisphenol A is an exogenous toxin that promotes mitochondrial injury and death in tubular cells. *Environ Toxicol,* 33: 325-332.

BUYUKLU M, KANDEMIR F, OZKARACA M, SET T, BAKIRCI E, TOPAL E, ILERITURK M, TURKMEN K (2015) Benefical effects of lycopene against contrast medium-induced oxidative stress, inflammation, autophagy, and apoptosis in rat kidney. *Human Exp Toxicol,* 34: 487-496.

DOGUKAN A, TUZCU M, AGCA CA, GENCOGLU H, SAHIN N, ONDERCI M, OZERCAN, İH, İLHAN N, KUCUK O, SAHIN K (2011) A tomato lycopene complex protects the kidney from cisplatin-induced injury via affecting oxidative stress as well as Bax, Bcl-2, and HSPs expression. *Nutrition Cancer,* 63: 427-434.

EDRES, HA, TAHA NM, MANDOUR AE-WA, LEBDA MA (2018) Impact of l-carnitine on bisphenol A-induced kidney damage in rats. *Alexandria J Vet Sci,* 56.

EID JI, EISSA SM, EL-GHOR AA (2015) Bisphenol A induces oxidative stress and DNA damage in hepatic tissue of female rat offspring. *J Basic Appl Zool,* 71: 10-19.

EL-GERBED MS (2014) Protective effect of lycopene on deltamethrin-induced histological and ultrastructural changes in kidney tissue of rats. *Toxicol Indust Health,* 30: 160-173.

ELSALAM SA, MANSOR AE, SARHAN MH, SHALABY AM, GOBRAN MA, ALABIAD MA (2021) Evaluation of apoptosis, proliferation, and adhesion molecule expression in trophoblastic tissue of women with recurrent spontaneous abortion and infected with Toxoplasma gondii. *Int J Gynecol Pathol*, 40(2): 124-133.

EWEDA SM, NEWAIRY ASA, ABDOU HM, GABER AS (2020) Bisphenol A-induced oxidative damage in the hepatic and cardiac tissues of rats: The modulatory role of sesame lignans. *Exp Therap Med,* 19: 33-44.

FADDA WA, ESSAWY AS, FARIED MA (2019) Green tea extract protects the renal cortex against bisphenol A-induced nephrotoxicity in the adult male albino rat: a histological and immunohistochemical study. *Eur J Anat,* 23: 415-424.

GORI P, PATEL A, SOLANKI N, SHAH U, PATEL V, PATEL S (2021) Protective effects of lycopene against adenine-induced chronic renal failure in rats. *Indian J Physiol Pharmacol,* 65: 74-85.

GROSS M-L, EL-SHAKMAK A, SZABÓ A, KOCH A, KUHLMANN A, MÜNTER K, RITZ E, AMANN K (2003) ACE-inhibitors but not endothelin receptor blockers prevent podocyte loss in early diabetic nephropathy. *Diabetologia,* 46: 856-868.

HAROUN MR, ZAMZAM IS, METWALLY ES, EL-SHAFEY RS (2019) Effect of vitamin C on bisphenol A induced hepato-nephrotoxicity in albino rats. *Egypt J Forensic Sci Appl Toxicol,* 16: 57-85.

HELAL EG, SOLIMAN MG, BADAWI MM, ABDEL-KAWI NA, FADEL HA, ABOZAID NM (2013) Physiological and histopathological studies on Bisphenol-A compound as xenoestrogen in male albino rats. *Egypt J Hosp Med,* 50: 127-136.

HUSSEIN SA, HASSANEIN MR, AWADALLA MA (2018) Lycopene and its potential role in diabetic nephropathy induced in rats. *Benha Vet Med J,* 34: 26-41.

KAKIMOTO T, OKADA K, HIROHASHI Y, RELATOR R, KAWAI M, IGUCHI T, FUJITAKA K, NISHIO M, KATO T, FUKUNARI A (2014) Automated image analysis of a glomerular injury marker desmin in spontaneously diabetic Torii rats treated with losartan. *J Endocr,* 222: 43-51.

KANG J-H, KONDO F, KATAYAMA Y (2006) Human exposure to bisphenol A. *Toxicology,* 226: 79-89.

KARAHAN İ, ATEŞŞAHIN A, YıLMAZ S, ÇERIBAŞ A, SAKIN F (2005) Protective effect of lycopene on gentamicin-induced oxidative stress and nephrotoxicity in rats. *Toxicology,* 215: 198-204.

KAYA C, KARABULUT R, TURKYILMAZ Z, SONMEZ K, KULDUK G, GÜLBAHAR Ö, KÖSE F, BASAKLAR AC (2015) Lycopene has reduced renal damage histopathologically and biochemically in experimental renal ischemia-reperfusion injury. *Renal Failure,* 37: 1390-1395.

KHAYAL EE-S, ALABIAD MA, ELKHOLY MR, SHALABY AM, NOSERY Y, EL-SHEIKH AA (2022) The immune modulatory role of marjoram extract on imidacloprid induced toxic effects in thymus and spleen of adult rats. *Toxicology*, 471: 153174.

KHAYAL EES, IBRAHIM HM, SHALABY AM, ALABIAD MA, EL-SHEIKH AA (2021) Combined lead and zinc oxide-nanoparticles induced thyroid toxicity through 8-OHdG oxidative stress-mediated inflammation, apoptosis, and Nrf2 activation in rats. *Environ Toxicol*, 36(12): 2589-2604.

KOBAYASHI K, LIU Y, ICHIKAWA H, TAKEMURA S, MINAMIYAMA Y (2020) Effects of bisphenol A on oxidative stress in the rat brain. *Antioxidants,* 9: 240.

KOBROOB A, PEERAPANYASUT W, CHATTIPAKORN N, WONGMEKIAT O (2018) Damaging effects of bisphenol A on the kidney and the protection by melatonin: Emerging evidences from in vivo and in vitro studies. *Oxidat Med Cell Longevity,* 2018: 3082438.

KORKMAZ A, AYDOĞAN M, KOLANKAYA D, BARLAS N (2011) Vitamin C coadministration augments bisphenol A, nonylphenol, and octylphenol induced oxidative damage on kidney of rats. *Environ Toxicol,* 26: 325-337.

KOUL A, ARORA N, TANWAR L (2010) Lycopene mediated modulation of 7, 12 dimethlybenz (A) anthracene induced hepatic clastogenicity in male Balb/c mice. *Nutricion Hospitalaria,* 25: 304-310.

LAYTON C, BANCROFT J (2013) Carbohydrates. In: Suvarna SK, Layton CH, Bancroft JD, (eds.) *Bancroft's Theory & Practice of histological techniques.* 7th ed. Churchill Livingstone/Elsevier, London.

LEE J, LIM K-T (2010) Expression of TNF-α and IL-6 in HMC-1 cells treated with bisphenol A is attenuated by plant-originating glycoprotein (75 kDa) by blocking p38 MAPK. *Naunyn-Schmiedeberg's Arch Pharmacol,* 382: 51-61.

MARKLUND S, MARKLUND G (1974) Involvement of the superoxide anion radical in the autoxidation of pyrogallol and a convenient assay for superoxide dismutase. *Eur J Biochem,* 47: 469-474.

MORENO-GÓMEZ-TOLEDANO R, ARENAS MI, MUÑOZ-MORENO C, OLEA-HERRERO N, REVENTUN P, IZQUIERDO-LAHUERTA A, ANTÓN-CORNEJO A, GONZÁLEZ-SANTANDER M, ZARAGOZA C, SAURA M (2022) Comparison of the renal effects of bisphenol A in mice with and without experimental diabetes. Role of sexual dimorphism. *Biochim Biophys Acta (BBA)-Mol Basis Dis,* 1868: 166296.

MORGAN AM, EL-BALLAL SS, EL-BIALY BE, EL-BORAI NB (2014) Studies on the potential protective effect of cinnamon against bisphenol A-and octylphenol-induced oxidative stress in male albino rats. *Toxicol Rep,* 1: 92-101.

OLEA-HERRERO N, ARENAS MI, MUÑÓZ-MORENO C, MORENO-GÓMEZ-TOLEDANO R, GONZÁLEZ-SANTANDER M, ARRIBAS I, BOSCH RJ (2014) Bisphenol-A induces podocytopathy with proteinuria in mice. *J Cell Physiol,* 229: 2057-2066.

PALABIYIK SS, ERKEKOGLU P, ZEYBEK ND, KIZILGUN M, BAYDAR DE, SAHIN G, GIRAY BK (2013) Protective effect of lycopene against ochratoxin A induced renal oxidative stress and apoptosis in rats. *Exp Toxicol Pathol,* 65: 853-861.

PALOZZA P, PARRONE N, CATALANO A, SIMONE R (2010) Tomato lycopene and inflammatory cascade: basic interactions and clinical implications. *Curr Med Chemist,* 17: 2547-2563.

PANDIR D, UNAL B, BAS H (2016) Lycopene protects the diabetic rat kidney against oxidative stress-mediated oxidative damage induced by furan. *Brazilian Arch Biol Technol,* 59.

PEERAPANYASUT W, KOBROOB A, PALEE S, CHATTIPAKORN N, WONGMEKIAT O (2019) Activation of sirtuin 3 and maintenance of mitochondrial integrity by N-acetylcysteine protects against bisphenol A-induced kidney and liver toxicity in rats. *Int J Mol Sci,* 20: 267.

POORMOOSAVI SM, NAJAFZADEHVARZI H, BEHMANESH MA, AMIRGHOLAMI R (2018) Protective effects of Asparagus officinalis extract against Bisphenol A-induced toxicity in Wistar rats. *Toxicol Rep,* 5: 427-433.

PRIEGO AR, PARRA EG, MAS S, MORGADO-PASCUAL JL, RUIZ-ORTEGA M, RAYEGO-MATEOS S (2021) Bisphenol A modulates autophagy and exacerbates chronic kidney damage in mice. *Int J Mol Sci,* 22: 7189.

RAO AV, AGARWAL S (2000) Role of antioxidant lycopene in cancer and heart disease. *J Am Coll Nutrit,* 19: 563-569.

SAURA M, MARQUEZ S, REVENTUN P, OLEA-HERRERO N, ARENAS MI, MORENO-GÓMEZ-TOLEDANO R, GÓMEZ-PARRIZAS M, MUÑÓZ-MORENO C, GONZÁLEZ-SANTANDER, ZARAGOZA C (2014) Oral administration of bisphenol A induces high blood pressure through angiotensin II/CaMKII-dependent uncoupling of eNOS. *FASEB J,* 28: 4719-4728.

SHALABY AM, HAMID IBRAHIM MAA, ABOREGELA AM (2019) Effect of aspartame on the placenta of adult albino rat. A histological and immunohistochemical study. *Ann Anat-Anat Anz,* 224: 133-141.

SHALABY AM, ABOREGELA AM, ALABIAD MA, EL SHAER DF (2020a) Tramadol promotes oxidative stress, fibrosis, apoptosis, ultrastructural and biochemical alterations in the adrenal cortex of adult male rat with possible reversibility after withdrawal. *Microscopy Microanalysis*, 26: 509-523.

SHALABY AM, ALABIAD MA, EL SHAER DF (2020b) Resveratrol ameliorates the seminiferous tubules damages induced by finasteride in adult male rats. *Microscopy Microanalysis,* 26: 1176-1186.

STOJILJKOVIĆ N, ILIĆ S, STOJANOVIĆ N, STOJANOVIĆ S, STOILJKOVIĆ M (2020) Lycopene improves methotrexate-induced functional alterations of the Madin–Darby kidney cells in a concentration-dependent manner. *Canad J Physiol Pharmacol,* 98: 111-116.

TABREZ S, AL-SHALI KZ, AHMAD S (2015) Lycopene powers the inhibition of glycation-induced diabetic nephropathy: A novel approach to halt the AGE-RAGE axis menace. *Biofactors,* 41: 372-381.

TAWFEEK SE, SHALABY AM, ALABIAD MA, ALBACKOOSH A-AA, ALBAKOUSH KMM, OMIRA MMA (2021) Metanil yellow promotes oxidative stress, astrogliosis, and apoptosis in the cerebellar cortex of adult male rat with possible protective effect of scutellarin: a histological and immunohistochemical study. *Tissue Cell*, 73: 101624.

UCHIYAMA M, MIHARA M (1978) Determination of malonaldehyde precursor in tissues by thiobarbituric acid test. *Analytical Biochem,* 86: 271-278.

VANDENBERG LN, CHAHOUD I, HEINDEL JJ, PADMANABHAN V, PAUMGARTTEN FJ, SCHOENFELDER G (2010) Urinary, circulating,

and tissue biomonitoring studies indicate widespread exposure to bisphenol A. *Environ Health Perspect,* 118: 1055-1070.

WAHBY MM, ABDALLAH ZM, ABDOU HM, YOUSEF MI, NEWAIRY A-SA (2017) Mitigating potential of Ginkgo biloba extract and melatonin against hepatic and nephrotoxicity induced by Bisphenol A in male rats. *Egypt J Basic Appl Sci,* 4: 350-357.

YILMAZ S, ATESSAHIN A, SAHNA E, KARAHAN I, OZER S (2006) Protective effect of lycopene on adriamycin-induced cardiotoxicity and nephrotoxicity. *Toxicology,* 218: 164-171.

ZALKO D, JACQUES C, DUPLAN H, BRUEL S, PERDU E (2011) Viable skin efficiently absorbs and metabolizes bisphenol A. *Chemosphere,* 82: 424-430.

ZOU J, YAOITA E, WATANABE Y, YOSHIDA Y, NAMETA M, LI H, QU Z, YAMAMOTO T (2006) Upregulation of nestin, vimentin, and desmin in rat podocytes in response to injury. *Virchows Archiv,* 448: 485-492.

Pancreatic beta cell regenerative effect of Costus pictus D Don leaf extracts on streptozotocin induced diabetes on Wistar rats

Anitha Nancy[1], Jeneth Berlin Raj[2], Manimekalai K.[3]

[1] Department of Anatomy, [2] Department of Physiology, [3] Department of Pharmacology, Mahatma Gandhi Medical College & Research Institute, Sri Balaji Vidyapeeth (Deemed to be University), Puducherry-607402, India

SUMMARY

With the increasing prevalence of diabetes and the economic burden caused by its treatment, people seek alternative medicine. Costus pictus D Don, belonging to the family Costaceae, commonly called Insulin plant/spiral ginger, is preferred by many in recent days. The current study was carried out to determine the effect of methanolic leaf extract of Costus pictus D Don on the pancreas of diabetic-induced albino Wistar rats.

Methanolic extract from C.pictus was prepared by soxhalation. The effect of this extract at the dose of 100 mg and 200 mg/kg bw was studied biochemically on blood glucose and blood insulin levels. Histological and histo-morphological observations were studied on the pancreas after 21 days of treatment. The parameters were compared with diabetic and normal rats. Glucose-lowering effect of the plant extract was observed biochemically in diabetic animals treated with both doses of the extracts. It was observed that the effect was more pronounced with 200 mg/kg BW of the extract. The presence of hyperchromic islet cells, granulated beta cells, increase in diameter of islets and number of beta cells as observed by histological examination and histo-morphometric analysis revealed the pancreatic beta cell regenerative property of Costus pictus D Don.

Key words: Diabetes – Costus pictus D Don methanolic leaf extract – Glucose-lowering effect – Pancreatic regeneration

INTRODUCTION

The prevalence of diabetes is increasing year after year sparing no country. Diabetes has been the cause of 1.5 million deaths in the year 2019. Raised blood glucose levels have been associated with 20% of cardiovascular death and nearly 4.6 million deaths from renal diseases (WHO, 2023). There has been a huge economic burden on countries in controlling this non-communicable disease. Uncontrolled diabetes leads to many microvascular and macrovascular complications. The cost of medicines used to control the glycemic status in diabetic patients has been estimated as one of the major contributors to this economic burden (Ramachandran et al., 2022). Adjunct therapy with plants and plant-derived products will reduce the economic burden in treating and controlling diabetes. Around 21,000 potential medical plant spe-

Corresponding author:
Dr. Jeneth Berlin Raj T. Department of Physiology, Mahatma Gandhi Medical College & Research Institute Sri Balaji Vidyapeeth (Deemed to be University), Puducherry-607402, India. Phone: 9994737997. E-mail: jenethberlinraj@gmail.com

Submitted: February 11, 2023. **Accepted:** March 21, 2023

https://doi.org/10.52083/KKOB4199

cies are identified worldwide and have been used by 80% of the world population (Chowdhury et al., 2009). Around 2500 medicinal plants are found in India, which is considered the botanical garden of medical plants. Most of these plants have diverse medical properties, and many of them are used to lower blood glucose levels. This forces many researchers to do extensive research to improve the therapy and minimize the chance of developing chronic complications in diabetes (Seth and Sharma, 2004).

One such medical plant which has been recently studied by researchers for extensive medical properties such as antimicrobial (Raj and Kalaivani, 2018), anthelminthic (Raj and Kalaivani, 2016), hepatoprotective (Nancy et al., 2019), anticancerous (Nandumane et al., 2011), etc., is *Costus pictus D Don*. In this study, we have made an attempt to check for the beta-cell protective effect of *Costus pictus D Don* on albino Wistar rats.

MATERIALS AND METHODS

Plant materials

Leaves from one-year-old *Costus pictus D Don* plants were collected from the local garden of Pondicherry during summer. The plant specimen was identified and authenticated by the Department of Botany, Annamalai University, Chidambaram (No.326). The Voucher specimen of the same is preserved at the department of Pharmacology, Mahatma Gandhi Medical College and Research Institute (MGMCRI), Sri Balaji Vidyapeeth, Pondicherry.

Preparation of plant extract

The leaves of *Costus pictus D Don* were washed and shade-dried for 5-7 days, and then powered. Since methanolic extract was proved to preserve more phytochemicals (Jothivel et al., 2007), methanolic extract was prepared using soxahalator. The final extract was dried with a rotary evaporator and refrigerated in a brown airtight container.

Experimental animals

After obtaining ethical clearance (C3/IAEC/MG/2016), 16 weeks old healthy male adult Wistar rats weighing > 250 g procured from Kings Institute, Chennai, were used in this study. The animals were maintained in a standard cage under controlled temperature (25±2 °C) and light (12:12 light-dark cycle) in MGMCRI central animal house. The animals will be fed with standard rat pellets and hygienic water *ad libitum.*

Drugs and Chemicals

Methanol was procured from Changshu Yangyuan Chemicals; Streptozotocin and Sodium pentobarbital were purchased from Sigma-Aldrich.

Experimental design

After an accommodation period of one week, 24 adult Wistar rats of either sex were randomized into 4 groups with 6 animals each as described in Table 1.

Table 1. Grouping of animals into study and control group.

Group 1	Normal control
Group 2	Diabetic control
Group 3	Diabetic rats treated with 100 mg/kg BW of *Costus pictus D Don* methanolic leaf extract orally
Group 4	Diabetic rats treated with 200 mg/kg BW of *Costus pictus D Don* methanolic leaf extract orally

Induction and confirmation of diabetes

Diabetes was induced by administering a single intra-peritoneal (i.p) injection of 65 mg/kg BW of Streptozotocin (STZ) after an overnight fast. No mortality was observed after inducing diabetes with STZ. The hyperglycemic status was confirmed after 2 weeks by estimating blood glucose level and fasting insulin level by drawing blood from the tail vein. Blood glucose levels were estimated by one touch select simple glucometer by Johnson and Johnson and fasting insulin level by ELISA kit method (Crystal Chem Inc. - Downer Grove, USA) (Raj et al., 2022). Following confirmation of diabetic status, methanolic leaf extract of *Costus pictus D Don* was ingested using a lavage tube for 21 days, and the biochemical tests were repeated.

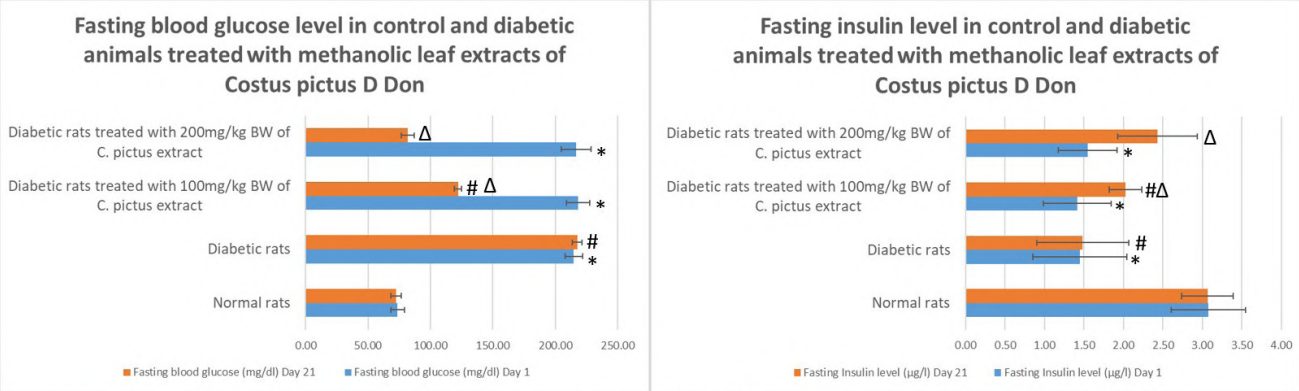

Data expressed in Mean ± SD and analyzed for statistical significance ($P < 0.001$) by Tukey multiple comparison test.
* - day 0 data compared with control. # - Day 21 data compared with control, Δ – data compared with diabetic rats.

Fig. 1.- Fasting blood glucose and insulin level in control and treatment groups.

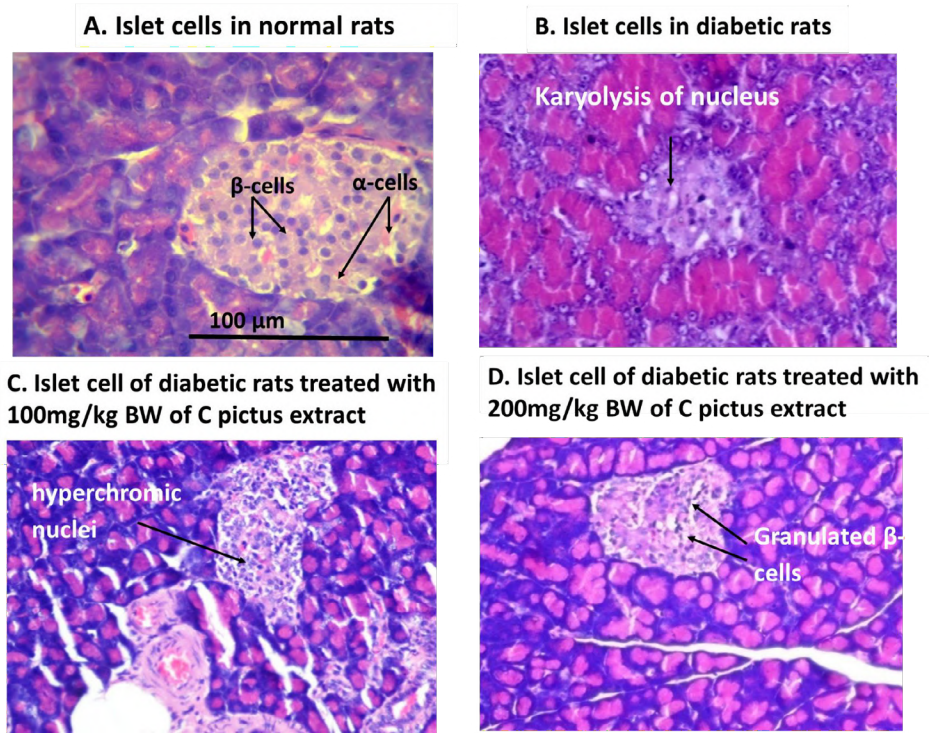

Fig. 2.- Histological changes in the pancreas of animals in control and treatment groups studied. x40.

Histology and histo-morphometric analysis

After 21 days of treatment with methanolic leaf extract, all the animals were sacrificed using sodium pentobarbital (120 mg/kg BW, i.p). The pancreas was excised carefully, washed with saline, and used for studying histological changes using hematoxylin and eosin stain (H&E). Histo-morphometric analysis was performed by measuring the diameter of pancreatic islets of Langerhans and counting the number of beta cells per section. The diameter of pancreatic islets was assessed using a liner scale & an ocular micrometer (Olympus research microscope) and the number of islets per square centimeter using an ocular grid.

RESULTS

The fasting blood glucose and insulin levels were significantly higher in the animals induced with diabetes with 35 mg/kg of Streptozotocin. The raised levels of insulin and fasting glucose were reduced to near normal in animals treated with the plant extract for 21 days (Fig. 1).

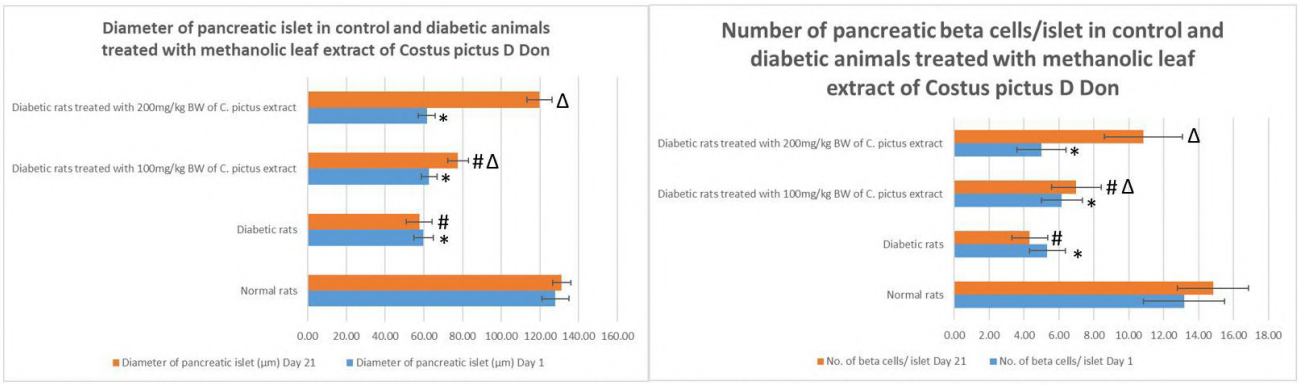

Data expressed in Mean ± SD and analyzed for statistical significance (P < 0.001) by Tukey multiple comparison test.
* - day 0 data compared with control. # - Day 21 data compared with control, Δ – data compared with diabetic rats.

Fig. 3.- Histomorphometric changes in islet cells of animals in control and treatment groups.

The histological study in pancreatic sections stained with H&E showed that in normal control (Group 1) the normal architecture of islets with the normal number of β-cells was seen. In Diabetic control (Group 2), streptozotocin caused severe necrotic changes in pancreatic islets, especially in the center of islets with a higher concentration of β-cells. Nuclear changes, karyolysis, and distortion of normal architecture were visible. Relative reduction of the size of the islets and severe reduction of ß-cells was clearly seen. A study of the pancreas treated with 100 mg/kg of Costus pictus D Don methanolic leaf extract the section showed an increased size of islets and hyperchromic nuclei in the section stained with H&E, and also in Group 4, which was treated with 200 mg/kg of Costus pictus D Don methanolic leaf extract, there was a relative increase of granulated and normal

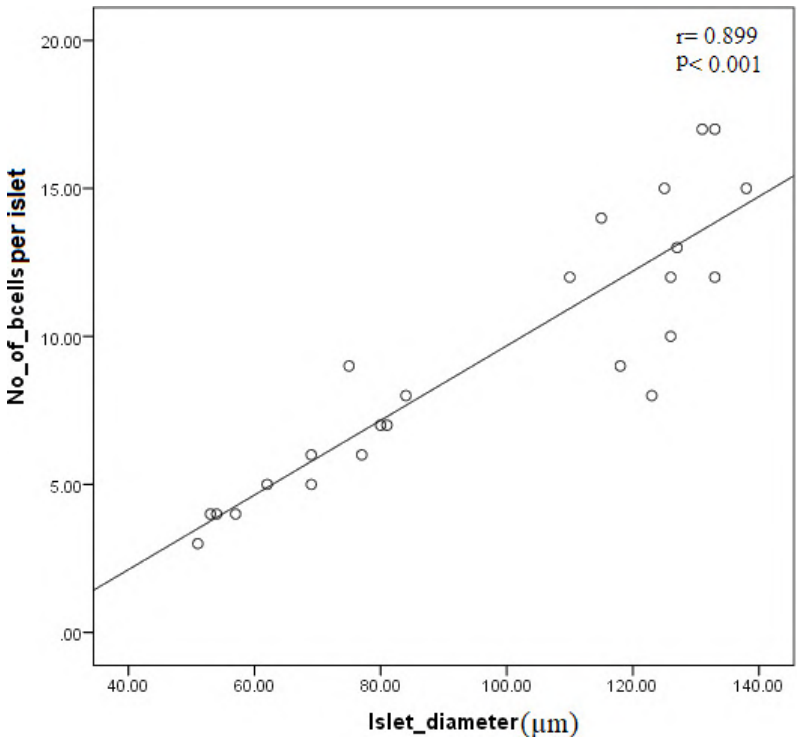

Fig. 4.- Linear relationship between the increase in islet diameter and number of beta cells per islet in the control and treatment group as analyzed by Pearson correlation coefficient.

ß-cells, (Fig. 2). The islets size and the number of beta cells increased significantly in the islets of Group 4 in comparison with a diabetic group, which signifies the regeneration of islets or beta cells in the group that received plant extract (Fig. 3). Pearson correlation coefficient was used to analyze the linear relationship between the increase in the diameter of islet to the number of beta cells (Fig. 4), which was statistically evident with p value < 0.001.

The data about fasting glucose levels, fasting insulin levels, the diameter of pancreatic islets cells, and the number of beta cells per islets were expressed in Mean ± SD and comparison between groups was analyzed for statistical significance (P < 0.001) by Tukey multiple comparison test.

DISCUSSION

Streptozotocin (STZ) damages pancreatic β-cells by the alkylating property induced by the cytotoxic nitrosourea compound, and result in decreased insulin production and poor glycemic control (Graham et al., 2011). The same was evident in our study with the increased blood glucose level and decreased insulin levels in animals induced with diabetes. Histological observation on pancreatic beta cells of these animals also revealed necrotic changes in islets of Langerhans and decreased number of beta cells. Similar changes were also observed in the study by Arora et al. (2021) in STZ-induced diabetic Sprague-Dawley rats and also by Jin et al. (2008) in STZ-induced diabetic rats treated with aucubin. In diabetic control, the pancreas section showed moderate hyperplasia of islet cells, severe congestion in pancreatic parenchyma, and mild infiltration of inflammatory cells. In diabetic animals treated with MECP, the pancreas section showed mild hyperplasia of islet cells and congestion of pancreatic parenchyma (Nandumane et al., 2011).

In our study, the histo-morphometric analysis revealed that the necrotic changes induced by STZ in diabetic animals were restored back to near normal when the diabetic animals were treated with both 100 mg/kg and 200 mg/kg of the plant extract for 21 days. This was evident with increased granulation of the cells in the islets, increased islet cell diameter, and increased cell count per section. Increased granulation of cells signifies the restoration of cell architecture after tissue damage.

The diameter of the islets in the diabetic animals treated with 100 mg/kg and 200 mg/kg were almost three-fold larger when compared to diabetic animals. Similarly, there was an two-fold increase of cells in the animals treated with both doses of the plant extract. These changes point to the fact that the methanolic leaf extract of Costus pictus D Don exerts a regenerative effect on the pancreatic beta cells in the animal model. The blood glucose level which was elevated in diabetic animals was also kept well under control in diabetic animals treated with both doses of the plant extract. Similarly, the decreased insulin level was normal in diabetic animals treated with the plant extracts, and rationalized the increased islet cell and diameter, proving the efficacy of the plant extract in maintaining glucose homeostasis. Our result was in accordance with the study by Gireesh et al. (2009), where the authors found that the antihyperglycemic effect of Costus pictus extracts correlates with the circulating insulin level by the stimulation of the surviving pancreatic beta cells (Jin et al., 2008).

CONCLUSION

The prevalence of diabetes increases year after year in India, making it the capital of diabetes in the world. The economic burden of the disease treatment on individuals, as well as on the country, is excruciating. This forces people and researchers to look for a safe alternative. Natural products derived from plants can be a better alternative. Costus pictus D Don, with its diverse medicinal properties, has proven to be protective to beta cells and also induces regenerative changes in animal models, especially in the dose of 200 mg/kg. However, its efficacy in humans may differ and needs to be evaluated. Basic staining using H&E has been a limitation of this study. Special staining techniques like aldehyde fuchsin method and immunostaining for insulin releasing content and lineage factors of the cells would have added more details of the extract on pancreatic beta cells.

REFERENCES

ARORA SK, VERMA PR, ITANKAR PR, PRASAD SK, NAKHATE KT (2021) Evaluation of pancreatic regeneration activity of Tephrosia purpurea leaves in rats with streptozotocin-induced diabetes. *J Tradit Complement Med*, 11(5): 435-445.

CHOWDHURY MSH, KOIKE M, MUHAMMED N, MD. HALIM A, SAHA N, KOBAYASHI H (2009) Use of plants in healthcare: a traditional ethno-medicinal practice in rural areas of southeastern Bangladesh. *Int J Biodiver Sci Manag*, 5(1): 41-51.

GIREESH G, THOMAS SK, JOSEPH B, PAULOSE CS (2009) Antihyperglycemic and insulin secretory activity of Costus pictus leaf extract in streptozotocin induced diabetic rats and in in vitro pancreatic islet culture. *J Ethnopharmacol*, 123: 470-474.

GRAHAM ML, JANECEK JL, KITTREDGE JA, HERING BJ, SCHUURMAN H-J (2011) The streptozotocin-induced diabetic nude mouse model: differences between animals from different sources. *Comp Med*, 61(4): 356-360.

JIN L, XUE HY, JIN LJ, LI SY, XU YP (2008) Antioxidant and pancreas-protective effect of aucubin on rats with streptozotocin-induced diabetes. *Eur J Pharmacol*, 582(1-3): 162-167.

JOTHIVEL N, PONNUSAMY SP, APPACHI M, SINGARAVEL S, et al. (2007) Anti-diabetic activity of methanol leaf extract of Costus pictus D. Don in alloxan-induced diabetic rats. *J Health Sci*, 53(6): 655-663.

NANCY A, RAJ JB, MANIMEKALAI K (2019) Comparative evaluation of the hepatoprotective effect of Costus pictus D Don methanolic leaf extract and silymarin on paracetamol induced liver damage in albino Wistar rats. *Int J Anat Res*, 7(3.1): 6722-6726.

NANDUMANE VK, RAJASHEKAR S, NARAYANA P, ADINARAYANA S, VIJAYAN S, PRAKASH S, SHARMA A (2011) Evaluation of the anti-cancer potential of costus pictus on fibrosarcoma (HT-1080) cell line. *J Natural Pharmaceutical*, 2(2): 72-76.

RAJ JB, KALAIVANI R (2016) Comparative in-vitro evaluation of anthelmintic property of leaves and rhizome of Costus pictus D. Don against albendazole. *Natl J Physiol Pharm Pharmacol*, 6(5): 438-441.

RAJ JB, KALAIVANI R (2018) In-vitro evaluation of antimicrobial activity of Costus pictus D. Don aqueous leaf extract. *Natl J Physiol Pharm Pharmacol*, 8(8): 1107-1109.

RAJ JB, PARTHASARATHY S, KUMARAPPAN M, SRINIVASAN AR (2022) Effect of costus pictus D don methanolic leaf extract on induced prediabetic behavioral change in albino Wistar rats. *Asian J Pharm Res Health Care*, 14: 224-230.

RAMACHANDRAN A, SNEHALATHA C, VISWANATHAN V (2002) Burden of type 2 diabetes and its complications - the Indian scenario. *Curr Sci*, 83: 1471-1476.

SETH SD, SHARMA B (2004) Medicinal plants in India. *Indian J Med Res*, 120(1): 9-11.

WHO.int. (2023) Diabetes. Last assessed on 31Jan 2023. Available from: https://www.who.int/news-room/fact-sheets/detail/diabetes

Role of mesenchymal stem cells and taurine in chronic pancreatitis in adult albino rats

Nahla S. Saad, Ghada S. El-dien Abdelkader, Noha A.H. Salem, Mona H. Mohammed Ali, Magdy M.O. El-Fark

Human Anatomy and Embryology Department, Faculty of Medicine, Suez Canal University, Ismailia, Egypt

SUMMARY

Chronic pancreatitis (CP) is an inflammatory disease of the pancreas that leads to pancreatic fibrosis. The current treatment of the disease is not efficient or adequate. Therefore, more efficient interventions are required to diminish the substantial burden of the disease.

The present study aimed to assess the potential therapeutic value of bone marrow-derived mesenchymal stem cells (BMSCs) and/or taurine supplementation in CP-induced, using intraperitoneal injection of L-arginine. Forty-five rats were randomly divided into five groups (9 rats each): 1) control group, 2) CP group, 3) CP+BMSCs, 4) CP+Taurine, and 5) CP+BMSCs+Taurine. At the end of the experimental period, the pancreatic tissues were collected, weighed, and prepared for light, electron, and immunohistochemical (α-SMA) microscopic examination. The CP group showed destruction of the pancreatic tissues including fatty degeneration, minimal zymogen granules, and focal degranulation of the rER. Some of the islets degenerated with intense immunoreactivity of α-SMA in the stroma. The groups treated with BMSCs or taurine alone showed improvement of the pancreatic architecture with the presence of some cytoplasmic vacuolation, fewer zymogen granules than the control group, and minimal inflammatory cell infiltrate. The CP+BMSCs+Taurine group showed apparently normal architecture. The combined therapy of both BMSCs and taurine could ameliorate CP progression by suppressing inflammation and fibrosis.

Key words: Chronic pancreatitis – Mesenchymal stem cells – Taurine – L-arginine

INTRODUCTION

Chronic pancreatitis (CP) is a pathological fibro-inflammatory syndrome of the pancreas in individuals with genetic, environmental, and/or other contributing risk factors that develop persistent pathological responses to parenchymal injury or stress. CP results in the development of diabetes mellitus and/or maldigestion due to endocrine and exocrine insufficiency. Moreover, CP patients have an increased risk of developing pancreatic adenocarcinoma with increased overall mortality (Whitcomb et al., 2016).

The pathophysiology of CP is complex and not completely understood (JC and Parks, 2021). Additionally, the current treatments for CP mainly target the symptoms rather than the pathological process (Singh et al., 2019).

Corresponding author:
Magdy M. Omar El-Fark. Human Anatomy and Embryology Department, Faculty of Medicine, Suez Canal University, 4.5 Km the Ring Road, Ismailia, Egypt. Phone: +201228282092. E-mail: magdy_omar@med.suez.edu.eg / anatomist1996@yahoo.com

Submitted: January 30, 2023. **Accepted:** March 28, 2023

https://doi.org/10.52083/JKLG9096

Mesenchymal stem cells (MSCs) are a subset of the mesodermal adult stem cells population that is present in numerous living tissues including bone marrow, adipose tissue, and amniotic fluid. As a result of MSCs' immunomodulatory capabilities, and differentiation potential to any type of cells, they have a driving force of regenerative medicine (Andrzejewska et al., 2019). However, only a few studies have explored the therapeutic potential of MSCs on CP (Scuteri and Monfrini, 2018).

Taurine, 2-aminoethanesulfonic acid, is a semi-essential amino acid, which acts as an anti-inflammatory and antioxidant, and is protective against lipid peroxidation, reperfusion injury, and excessive extracellular matrix deposition. It has been demonstrated that the administration of taurine could improve pancreatic fibrosis in an experimental model of CP (Shirahige et al., 2008).

This study was conducted to evaluate the possible therapeutic role of BMSCs and taurine supplementation, alone or in combination, for the treatment of CP in L-arginine-injection-induced chronic pancreatitis.

MATERIALS AND METHODS

Animals

Fifty-one (forty-five females and six males) adult albino rats were used, with an average weight of ≥250 g. Animals were kept in the animal house of the Faculty of Medicine, Suez Canal University. All animals were housed in special wire mesh cages at room temperature with regular day and night cycles with water and food ad libitum. Rats were kept for 2 weeks before the start of the experiment for acclimatization. Male rats were used only as a source for MSCs (Marrache et al., 2008). The Research Ethics Committee of the Faculty of Medicine, Suez Canal University, Egypt, examined and approved this study protocol (SCU3253). The study followed the National Institutes of Health's guidelines for the handling and use of laboratory animals (NIH Publications No. 85-23, revised 1996).

Chemicals

L-arginine monohydrochloride: Powder (L-arginine – reagent grade, ≥ 98%), obtained from Sigma Chemical St. Louis, MO, USA.

Taurine extra pure: Molecular weight 125.15, obtained from Alpha Chemika (400 053, Maharashtra, India).

BMSCs isolation and culture

This was carried out at the Center of Excellence in Molecular and Cellular Medicine, Suez Canal University. BMSCs were obtained from the femora and tibiae of the male rats after scarification and extraction in complete aseptic conditions. Cells were cultured in complete media (DMEM + 10% FPS+ 1% Penicillin/streptomycin) and incubated at 37°C humidified atmosphere containing a 5% CO_2 (Lotfy et al., 2014). Media were changed every 3 days until the cells reached 90-100% of confluence on the twelfth day, and then the cells were harvested through trypsinization to be subcultured for 3 days. BMSCs were harvested and cell mixtures of 2 x 10^6 /ml of PBL were prepared (Huang et al., 2015).

Flow cytometry analysis

This was carried out at NSA Lab Cairo, Egypt. Approximately 1x10^6 BMSCs at the second passage were harvested. Cell preparations were treated with the monoclonal antibody against CD34 labeled with fluorescein isothiocyanate (FITC), and against CD44 labeled with phycoerythrin (PE). The protocols used were those described by the manufacturer. The cell preparations were analyzed by the flow cytometer (Calibur, BD, USA) for the expression of the mentioned markers (Li et al., 2014).

PCR detection of male-derived BMSCs

This was carried out at the Applied Biotechnology Lab, Ismailia, Egypt. Primer sequences for *SRY* gene (forward 5'-AGATCTTGATTTTTAGTGTTC-3'), (reverse 5'-TGCAGCTCTACTCCAGTCTTG-3') were obtained and mixed with 1 µg pancreatic DNA and Taq polymerase. The PCR products were separated by electrophoresis in 0.8% agarose gel and stained with ethidium bromide. Agarose gel of PCR products of *SRY* gene was detected as a Trans-illuminated line (An et al., 1997).

Experimental Design

Forty-five female rats were randomly divided into five groups (9 rats each) as the following:

- Group A: control (sham) group: rats received two IP injections of normal saline 1 hour apart on day 1, followed by additional injections on days four, seven, and ten in the same way as day 1 (González et al., 2011).
- Group B: chronic pancreatitis-induced group (CP): rats were kept fasted for 12 hours, then received two injections of 20% L-arginine hydrochloride in normal saline solution at a dose of 200 mg/100 g body 1 hour apart on day 1 (Soliman et al., 2014), followed by injections on days four, seven and ten in the same manner as day 1 (González et al., 2011).
- Group C: chronic pancreatitis treated with bone marrow mesenchymal stem cells group (CP+BMSCs): chronic pancreatitis was induced as in group B. On the 5th day after the last L-arginine injection, rats were injected once with 2 X 10^{6} BMSCs, intravenous (IV) through the tail vein in 100 µL of phosphate buffered solution (PBS) per animal (Zhou et al., 2013).
- Group D: chronic pancreatitis treated with taurine group (CP+Taurine). Chronic pancreatitis was induced as in group B. On the 5th day after the last L-arginine injection, rats were treated with IP taurine injection once daily at a dose of 1000 mg/kg for four weeks (Mas et al., 2006).
- Group E: chronic pancreatitis treated with BMSCs and taurine group (CP+BMSCs+Taurine). Chronic pancreatitis was induced as in group B. On the 5th day after the last L-arginine injection, rats were treated with both BMSCs and taurine in the same dose and course as previously mentioned (Yusop et al., 2018).

All rats were sacrificed at the end of the experiment by cervical decapitation. The pancreas was extracted, weighed, and divided into two parts; one was prepared for light microscopy and the second for electron microscopy.

Light microscopic examination of the pancreas

The prepared pancreatic tissues were stained with haematoxylin and eosin (H&E) stain. Slides were examined by Olympus DP70 light microscope (Tokyo, Japan).

Immunohistochemical staining

Endogenous peroxidase of deparaffinized sections was blocked with 3% hydrogen peroxide. Sections were incubated overnight at 4°C with a monoclonal antibody mouse α- SMA (1:800 dilutions, Santa Cruz, California, USA). Envision™ Detection Kit was used for antibody detection (Yang et al., 2012).

Transmission electron microscopic (TEM) examination

Pancreatic specimens were fixed in 2% buffered glutaraldehyde, washed then dehydrated in alcohol, and embedded in epoxy resins. Semithin sections were cut at 1 µm thickness followed by Ultrathin sections (80-90 nm) obtained and stained with uranyl acetate and lead citrate (Bozzola and Russell, 1999). The sections were examined with a JEOL-1010 (Japan) transmission electron microscope (TEM), at the regional center for Mycology and Biotechnology transmitting electron unit (Al-Azhar University, Cairo, Egypt), and photographed under different magnifications.

Morphometric study

In α-SMA immunostained sections, the surface area percentage of immunostained sections were measured in five non-overlapping fields from five different sections at a magnification of 100/slide using ImageJ 2 software.

Statistical analysis

Data processing and analysis were done through SPSS V.24. ANOVA test with Bonferroni post-hock test. Data were expressed as mean and standard deviation. Significance was considered when P-value was less than 0.05 ($P < 0.05$).

RESULTS

Cultivation and characterization of rat BMSCs

Bone marrow cells were incubated at 37°C with 5% CO_2. On day 1, the cells were floating, rounded, and small with a central nucleus (Fig. 1A). On the

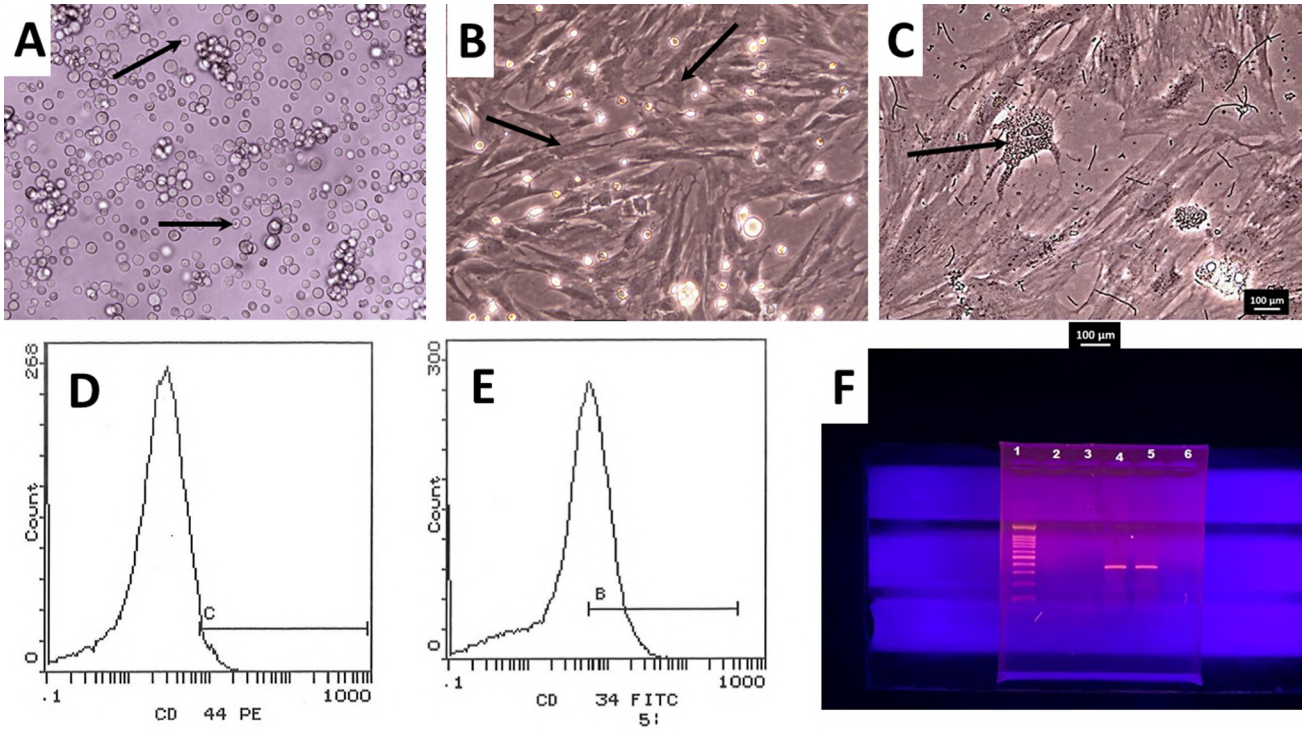

Fig. 1.- Photomicrographs of the cultured BMSCs. **(A)** On the 1st day of incubation; they appeared rounded, floating with a central nucleus (arrows). **(B)** On the 8th day of incubation; spindle-shaped BMSCs were formed (arrows) that reached about 80% confluence. **(C)** On the 3rd day of subculture; the cells had a polygonal appearance, prominent nucleolus, and cell processes (arrow). Scale bar = 100 µm. **(D)** Flow cytometry analysis of BMSCs showing positive expression of CD 44 and **(E)** negative expression of BMSCs of CD 34. **(F)** PCR product was obtained from the reaction of the primer with pancreatic genomic DNA. The first lane was the standards /100 base pair ladder; the second, third, and sixth lanes were empty which were of groups A, B, and D. Fourth and fifth lanes are positive for *SRY* gene which were of groups C and E. BMSCs, bone marrow mesenchymal stem cells; PCR, polymerase chain reaction.

8th day of incubation, adherent spindle-shaped BMSCs were formed with about 80% confluence (Fig. 1B). On the 12th day, a cell sheet of BMSCs was formed that reached about 100% confluence. Cells were harvested and subcultured at 37°C with 5% CO_2. On the 3rd day of the subculture, well-defined BMSCs were seen having a polygonal appearance with a prominent nucleolus and a well-defined cell process (Fig. 1C).

Flow cytometric analysis of BMSCs surface markers of the subcultured cells revealed moderate positive expression of CD 44 marker in most of the adherent cells (43%) (Fig. 1D).

On the other hand, the majority of adherent cells were negative for CD 34 surface marker expression, with only 4% of the cells being positive (Fig. 1E).

The male SRY gene was successfully traced in the rat pancreas of groups C and E, which were treated by BMSCs. In contrast, the test failed to trace the male SRY sequences in the pancreatic tissue of the other groups (Fig. 1F).

Body weight assessment (Table 1)

The initial body weights were approximated among the study groups. Rats in two groups showed weight gain (Control and CP+BMSCs+Tau-

Table1. Weight parameters (g) in different study groups.

	Control	CP	CP+BMSCs	CP+Taurine	CP+BMSCs + Taurine
Initial body weight	263.6±2.8	264.3±9.2	262.7±9.2	260.1±6.5	262.0±6.9
Final body weight	278.0± 5.0	244.6± 11.1	258.0± 8.5	253.2± 10.0	271.0± 10.1
Body weight (gain/loss)	18.4±3.8	-19.8±3.5 [b,c,d,f]	-3.7±8.8 [b,e]	-6.9±4.9 [b,f]	7.0±4.3 [a]
Weight of the pancreas	3.06± 0.18	2.08± 0.28 [b,f]	2.49± 0.26 [a]	2.21± 0.36 [b,e]	2.77± 0.37

Results are expressed as Mean ± SD, n= (9). Significance of differences among groups was evaluated by one-way ANOVA followed by Bonferroni Post Hoc Test.
a- P<0.01 vs. control group. **b-** P<0.001 vs. control group. **c-** P <0.001 vs. CP+BMSCs group. **d-** P<0.001 vs. CP+Taurine group. **e-** P<0.01 vs. CP+BMSCs+Taurine group. f- P <0.001 vs. CP+BMSCs+Taurine group.

rine). This increase in the body weight at the end of the study was in the control group 18.4±3.8, representing an increase of 6.98% from the initial body weight; and, in the CP+BMSCs+Taurine group, 7.0±4.3, representing an increase by 2.67% from the initial body weight. Rats in the other three treated groups showed weight loss (CP, CP+BMSCs, and CP+Taurine). This decrease in the body weight at the end of the study recorded in the CP group was of-19.8±3.5, representing a decrease of 7.49% from the initial body weight; in the CP+BMSCs group, -3.7±8.8, representing a decrease by 1.41% from the initial body weight; and in the CP+Taurine group, -6.9±4.9, representing a decrease by 2.65% from the initial body weight. When compared to the control group, there was a significant decrease in body weight in different study groups; CP ($P<0.001$), CP+BMSCs ($P<0.001$), CP+Taurine ($P<0.001$), and CP+BMSCs+Taurine ($P<0.01$). There was a significant decrease ($P<0.001$) in body weight at the end of the study in rats in the CP group when compared to the CP+BMSCs, CP+Taurine, and CP+BMSCs+Taurine groups. In the three groups treated with BMSCs and taurine, the CP+BMSCs+Taurine group showed a considerable increase in weight gain; there was a significant decrease in body weight at the end of the study in both the CP+BMSCs ($P<0.01$) and CP+Taurine ($P<0.001$) groups, when compared to the CP+BMSCs+Taurine group.

Weight of the pancreas (Table 1)

Rats in the control group showed a pancreatic weight of 3.06± 0.18 g. There was a decrease in the weight of the pancreas with different degrees in the four treated groups, with the lowest values in the CP (2.08± 0.28), CP+Taurine (2.21± 0.36), and CP+BMSCs (2.49± 0.26) groups, and the highest value among these four treated groups was in the CP+BMSCs+Taurine group (2.77± 0.37). The decrease in the weight of the pancreas was significant in both the CP and CP+Taurine groups ($P<0.001$), and CP+BMSCs ($P<0.01$) when compared to the control group. Rats in the CP+BMSCs+Taurine group showed a non- significant decrease in the weight of the pancreas when compared to the control group. On the other hand, there was a significant decrease in the weight of the pancreas in both the CP ($P<0.001$) and CP+Taurine groups ($P <0.00$) when compared to the CP+BMSCs+Taurine group.

Light microscopic examination of the pancreas

H&E-stained sections of the pancreas of the control group showed pancreatic lobules of closely packed acini forming the main bulk of the gland and islets of Langerhans. The pancreatic acini were seen formed of wedge-shaped cells arranged around a central narrow lumen. The cells were with basophilic cytoplasm, basal rounded vesicular nuclei with prominent nucleoli, and apical acidophilic secretory zymogen granules. The centro-acinar cells appeared at the central lumen of the acini representing the beginning of the duct system of the exocrine pancreas, the lobules were separated by interlobular septae containing blood vessels and interlobular ducts with cuboidal epithelium, filled with homogeneous colloid material, and surrounded by connective tissue (Fig. 2A).

The islets of Langerhans varied in size and were composed of masses and cords of secretory cells with numerous fenestrated capillaries in-between. Some endocrine cells exhibited pale acidophilic cytoplasm and pale prominent nuclei mostly situated at the center. Other cells with strong acidophilic cytoplasm and dark nuclei were found mainly at the periphery of the islets. The blood capillaries within the islets were recognized by the flat nuclei of the capillary endothelium. (Fig. 2B). Sections of the CP group showed severe destruction of the acinar cells' architecture, with areas of fatty degeneration. There were multiple dilated congested blood vessels and inflammatory cells infiltrate (Fig. 2C). The interlobular duct showed glandular hyperplasia in the form of an increased number and size of the pancreatic ductal glands. Some of the islets of Langerhans degenerated with dark pyknotic nuclei. (Fig. 2D). Sections of the CP+BMSCs group showed less pancreatic destruction. Some acini showed cytoplasmic vacuolation with a reduction of their zymogen granules accompanied by minimal inflammatory cell infiltrate (Fig. 3A). Moreover, congestion of blood vessels was still evident and a few areas of the islet of Langerhans' cellular degeneration were still present (Fig. 3B). In CP+Taurine, taurine administra-

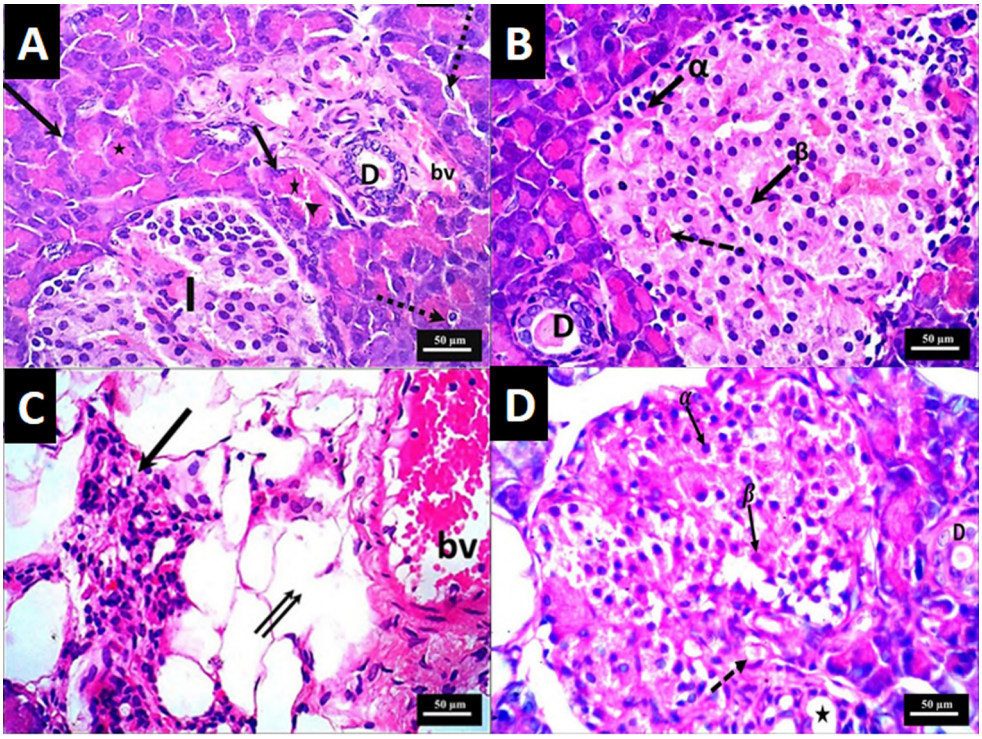

Fig. 2.- H&E-stained sections of the pancreas. **(A)** The control group had the pancreatic acini formed of wedge-shaped cells arranged around a central narrow lumen (arrowhead). The cells had basal rounded vesicular nuclei (arrow), apical acidophilic granules (*), centroacinar cells (dashed arrow), an islet of Langerhans (I), blood vessel (bv), and intralobular duct (D). **(B)** A pale stained islet of Langerhans of the control group that was rich in capillaries (dashed arrow). Some endocrine cells have pale acidophilic cytoplasm and pale prominent nuclei (β), while other cells have strongly acidophilic cytoplasm and dark nuclei (α) and intralobular duct filled with the colloid material (D). **(C)** The CP group showed massive acinar destruction (double arrow), and inflammatory cell infiltrates (arrow), with congested and dilated blood vessels (bv). **(D)** The islets of Langerhans of the CP group showed dilated blood capillaries (dashed arrow), areas of degeneration (*), cells with a pale nucleus and pale cytoplasm (β), cells with a dark nucleus and acidophilic cytoplasm (α). H&E, x400; scale bars = 50 µm. H&E, hematoxylin and eosin; CP, chronic pancreatitis.

tion reduced the pancreatic tissue destruction induced by L-arginine, despite the presence of areas of tissue degeneration in the form of vacuolation of the cytoplasm and fatty infiltration. However, these changes were less than that noticed in the CP group (Fig. 3C). The islets of Langerhans showed small areas of cellular degeneration with some apoptotic bodies and vascular congestion (Fig. 3D). The pancreas of the CP+BMSCs+Taurine group showed nearly normal architecture similar to that of the control group with the restoration of the secretory acini with their basal basophilia and apical acidophilia of the zymogen granules. Few vacuolations were seen within some acini.

Normal interlobular ducts and blood vessels were noticed in the interlobular spaces (Fig. 3E). The islets of Langerhans showed apparent normal structure, like that of the control group, with cells of pale nuclei and cytoplasm at the center and cells with strong acidophilic cytoplasm and dark nuclei found mainly at the periphery of the islets (Fig. 3F).

Alpha smooth muscle actin (*α*-SMA) immunohistochemistry

The pancreas of the control group showed minimal expression of α-SMA in the smooth muscle cells in the wall of the blood vessels, with negative expression in the wall of the ducts, stroma, and islet of Langerhans. (Fig. 4A). The CP group showed intense immunoreactivity of α-SMA in the stroma, also around the ducts and blood vessels, with minimal expression in the islets of Langerhans (Fig. 4B). The CP+BMSCs group showed moderate expression of α-SMA immunoreactivity in the stroma around the blood vessels and ducts, with negative expression in the islet of Langerhans (Fig. 4C). The CP+Taurine treated group showed moderate immunoreactivity of α-SMA in the stroma around the blood vessels and ducts, with minimal expression in the islets of Langerhans (Fig. 4D).

The CP+BMSCs+Taurine group showed minimal immunoreactivity of α-SMA around the stromal

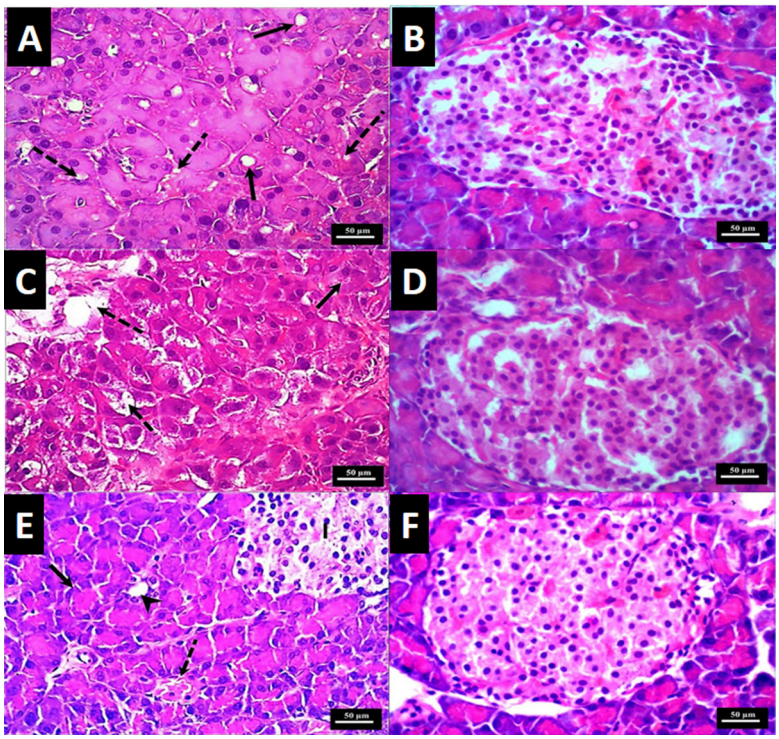

Fig. 3.- H&E-stained sections of the pancreas. **(A)** CP+BMSCs group showing preservation of most of the acinar architecture. Some acini show vacuolation of their cytoplasm (dashed arrows) with decreased zymogen granules and fatty infiltration (arrows). **(B)** CP+BMSCs group showing islets of Langerhans, with small areas of tissue degeneration in between their cords of cells. **(C)** CP+Taurine group showing areas of tissue degeneration (dashed arrows) intermingled with normal acinar architecture (arrow). **(D)** CP+Taurine group showing an islet of Langerhans with nearly normal architecture with few areas of cellular degeneration. **(E)** the CP+BMSCs+Taurine group showed pancreatic acini with nearly normal architecture (arrow), intralobular duct (arrowhead), normal blood vessel (dashed arrow), and the islet of Langerhans (I). **(F)** CP+BMSCs+Taurine group shows islet of Langerhans with a structure resembling that of the control group. H&E, x400; scale bars = 50 µm. H&E, hematoxylin and eosin; CP, chronic pancreatitis; BMSCs, bone marrow mesenchymal stem cells.

blood vessels and ducts, with negative expression in the islet of Langerhans (Fig. 4E).

Area percentage of α-SMA immunostaining

The pancreas of the control group showed a minimal value of area percentage of α-SMA immunostaining (1.89±0.62); rats in the CP group showed a high area percentage of α-SMA immunostaining (30.22±4.78), while the other three treated groups showed lower percentages of α- SMA immunostaining as follows: CP+BMSCs, 8.8±4.06; CP+Taurine, 8.16±4.17, and, finally, CP+BMSCs+Taurine, 4.37±0.86). There was a significant increase in the area percentage of α-SMA immunostaining in the CP group when compared to the control ($P<0.01$), CP+Taurine ($P<0.05$), CP+BMSCs ($P<0.05$), and CP+BMSCs+Taurine ($P<0.05$) groups. On the other hand, the CP groups treated with BMSCs alone, taurine alone, or with a combination of both showed a non-significant increase in the area percentage of α-SMA immunostaining when compared to the control group. (Fig. 5).

Transmission electron microscopy (TEM)

Ultrathin examination of the pancreatic acini of the control group showed pyramidal acinar cells and intercellular space containing interdigitations of adjacent cells, representing canaliculi that are connected to the acinar lumen. The acinar cells appeared to have basally located, spherical, euchromatic nuclei with prominent nucleoli. Variable-sized electrodense secretory zymogen granules occupied most of the apical portion of the cytoplasmic compartment. The rough endoplasmic reticulum lay adjacent to the nucleus and was heavily studded with ribosomes. The mitochondriae were scattered in-between the rough endoplasmic reticulum and contained fairly arranged parallel shelf-like cisternae (Fig. 6A). The ultrastructure of ß cell of islets of Langerhans showed euchromatic nuclei with prominent nucleoli and evenly distributed chromatin with some concentration at the nuclear membrane, abundant secretory granules of varying sizes with electron-lucent halo structure between the limiting

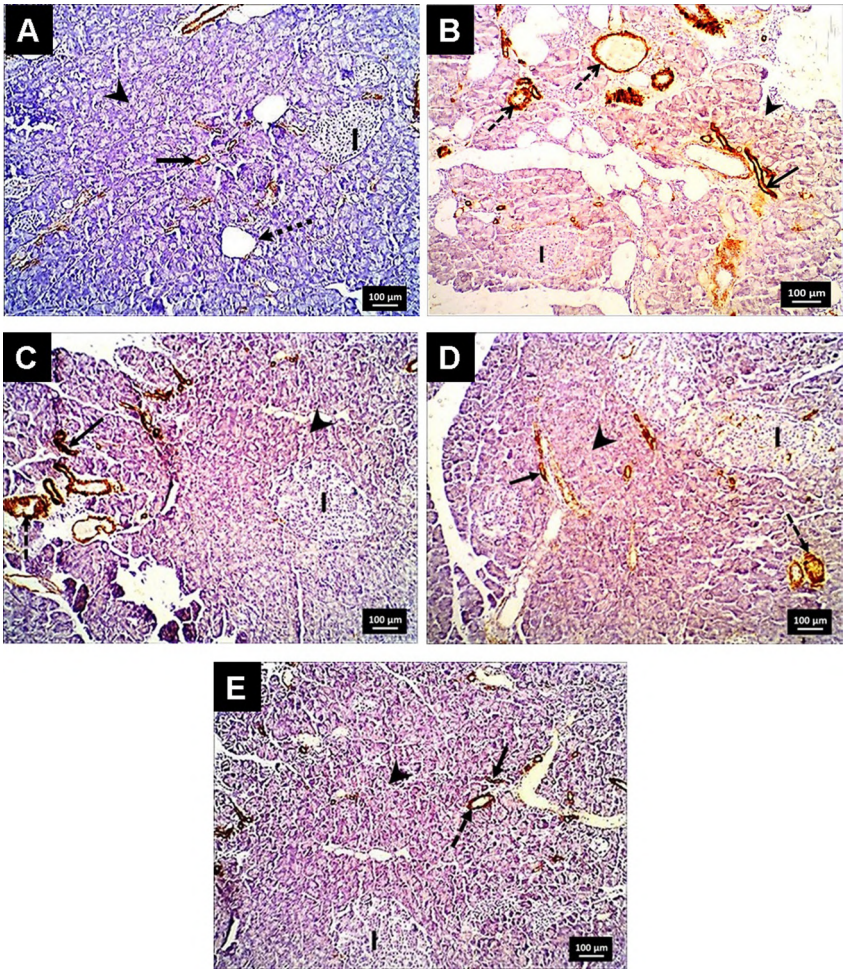

Fig. 4.- α-SMA-immunostained sections of the pancreas. **(A)** Control group; showing minimal brownish immunoreactivity around the blood vessels and negative expression in the wall of the and islet of Langerhans. **(B)** CP group showing intense brownish immunoreactivity in the stroma, around the blood vessels and ducts with minimal expression in the islet of Langerhans. **(C)** CP+BMSCs group showed moderate brownish immunoreactivity in the stroma, around the blood vessels, ducts, and negative expression in the islet of Langerhans. **(D)** CP+Taurine group showed moderate brownish immunoreactivity in the stroma, around the blood vessels and ducts, and minimal expression in the islet of Langerhans. **(E)** CP+BMSCs+Taurine group showed minimal brownish immunoreactivity in the stroma, around the blood vessels and ducts, and negative expression in the islet of Langerhans. α-SMA immunostaining, x100; scale bars = 100 µm. A-SMA, α smooth muscle actin; CP, chronic pancreatitis; BMSCs, bone marrow mesenchymal stem cells.

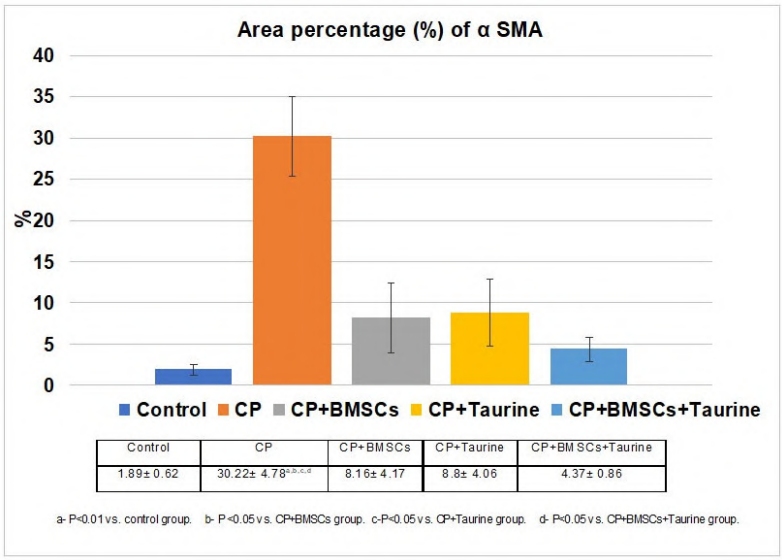

Fig. 5.- Area percentage of α-SMA among different study groups (Mean±SD).

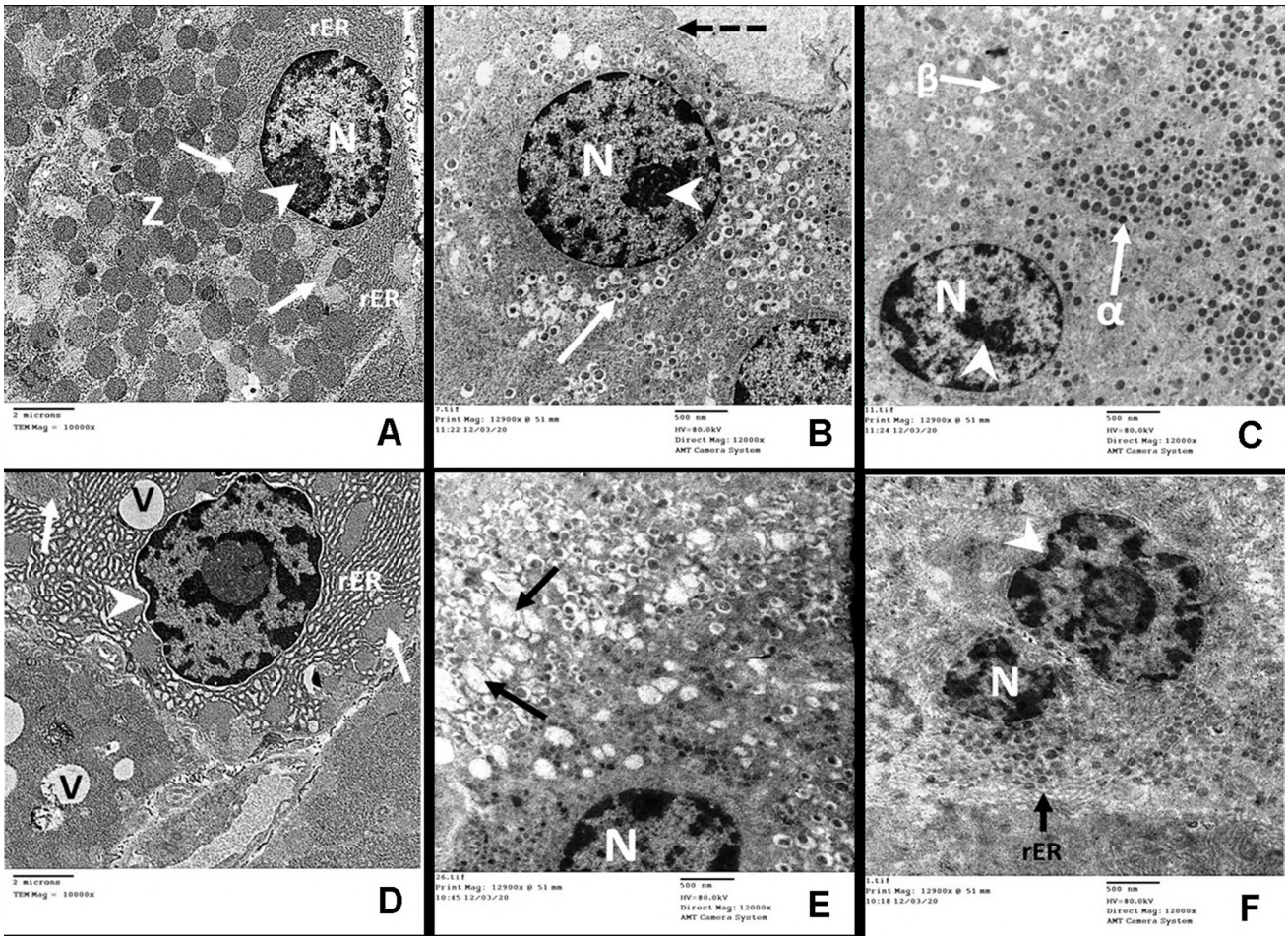

Fig. 6.- Electron micrograph sections of the pancreas. **(A)** A pancreatic acinar cell of the control group showing euchromatic nucleus (N) and nucleolus (arrowhead), apical electron-dense zymogen granules (Z), rough endoplasmic reticulum (rER), and mitochondria (arrows) (TEM, x10,000). **(B)** ß cell of the islets of Langerhans of the control group showing a euchromatic nucleus (N) with prominent nucleolus (arrowhead) and secretory granules with variable electron-dense cores and wide halos (arrow), the endothelium of the blood capillary (dashed arrow) (TEM, x12,000). **(C)** α cell of islets of Langerhans of the control group showing euchromatic nuclei (N) with prominent double nucleoli (arrowhead) and variable size electron-dense secretory granules (α arrow), β cell appear adjacent to α cell with β cell granules (β arrow) (TEM, x12,000). **(D)** A pancreatic acinar cell of the CP group showing dilation and focal degranulation of the rough endoplasmic reticulum (rER), mitochondrial swelling (arrows), irregular nuclear membrane (arrowhead), and vacuolation of the cytoplasm (V) (TEM, x10,000). **(E)** β cell of islets of Langerhans of the CP group showing euchromatic nuclei (N) and some empty secretory granules (arrows) (TEM, x12,000). **(F)** α cell of islets of Langerhans of the CP group showing shrinkage of the nucleus with increased heterochromatin (N), irregular nuclear membrane (arrowhead), dilated cisternae of the rough endoplasmic reticulum (rER arrow), and minimal secretory granules. (TEM, x12,000). Scale bars: A, D = 2 µm; B, C. E, F = 500 nm. TEM, transmission electron microscope; CP, chronic pancreatitis.

membrane and the granule proper. The endoplasmic reticulum of the rough type was seen filling the cytoplasm (Fig. 6B). The α cell of the islets of Langerhans had euchromatic nuclei with prominent nucleolus and variable size electron-dense secretory granules (Fig. 6C). The CP group showed massive acinar cell necrosis with minimal zymogen granules, dilation and focal degranulation of the rough endoplasmic reticulum, mitochondrial swelling with vacuolation of the cytoplasm, and some contained electron-dense bodies. The blood capillaries were congested with increased collagen deposition around their walls (Fig. 6D). The atrophied islet of Langerhans was noticed as a small hypodense area with irregular nuclei. β cell of islets of Langerhans showed some empty secretory granules (Fig. 6E). While the α cells showed wide, rough endoplasmic reticulum and irregular shrunken nucleus (Fig. 6F), the ultrastructure of the CP+BMSCs group showed marked improvement. However, some zymogen granules were still less electron-dense than that of the control group, and some mitochondrial edema was still present (Fig. 7A). The β and α cells of the islets of Langerhans showed a structure resembling that of the control group (Fig. 7B and C) respectively. The

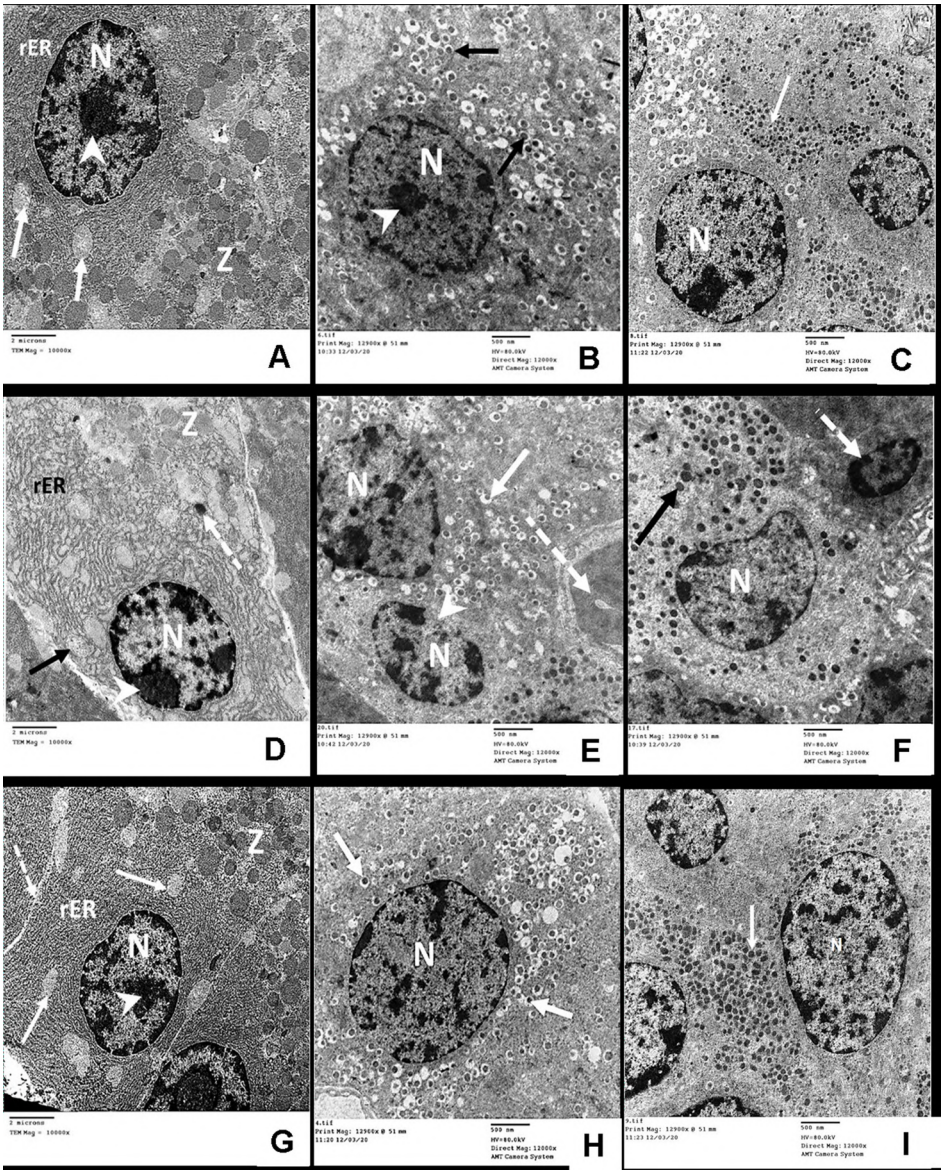

Fig. 7.- Electron micrograph sections of the pancreas. **(A)** The acinar cell of the CP+BMSCs group showing euchromatic vesicular nucleus (N), nucleolus (arrowhead), rough endoplasmic reticulum (rER), hypodense zymogen granules (Z) and some mitochondrial edema (arrows) (TEM, x10,000). **(B)** ß cell of islets of Langerhans of the CP + BMSCs group showing euchromatic nucleus (N) with prominent nucleolus (arrowhead) and variable secretory granules (arrows) (TEM, x12,000). **(C)** α cell of islets of Langerhans of the CP+BMSCs group showing with euchromatic nuclei (N) minimal variable size electron-dense secretory granules (arrow) (TEM, x12,000). **(D)** The acinar cell of the CP+Taurine group showed euchromatic nucleus (N), nucleolus (arrowhead), dilated rough endoplasmic reticulum (rER) with few zymogen granules (Z), swollen mitochondria (arrow), and single electrodense free ribosome (dashed arrow) (TEM, x10,000). **(E)** ß cell of islets of Langerhans of the CP+Taurine group showing euchromatic nucleus (N), and another one with damaged nuclear membrane (arrowhead) secretory granules (arrow) and blood capillary (dashed arrow) (TEM, x12,000). **(F)** α cell of islets of Langerhans of the CP+Taurine group showing euchromatic nucleus (N), another nucleus with chromatin condensation (dashed arrow), and electron-dense secretory granules (arrow) (TEM, x12,000). **(G)** The acinar cell of the CP+BMSCs+Taurine group showed a euchromatic nucleus (N) with prominent nucleolus (arrowhead), mitochondria (arrows), rough endoplasmic reticulum (rER), multiple electrodense zymogen granules (Z), and intercellular space (dashed arrow) (TEM, x10,000). **(H)** ß cell of islets of Langerhans of the CP+BMSCs+Taurine group showing euchromatic nuclei (N), secretory granules (arrows) (TEM, x12,000). **(I)** α cell of islets of Langerhans of the CP+BMSCs+Taurine group showing euchromatic nuclei (N), electron-dense secretory granules (arrow) (TEM, x12,000). Scale bars: A, D, G = 2 µm; B, C. E, F, H, I = 500 nm. TEM, transmission electron microscope; CP, chronic pancreatitis; BMSCs, bone marrow mesenchymal stem cells.

blood capillaries were seen scattered among the islet's cells with flat endothelium and blood cells in their lumen. The CP group treated with taurine showed moderate restoration of most of the normal cellular architecture with narrow intercellular spaces. Dilatation of the rough endoplasmic reticulum was still present. The mitochondriae were swollen with the loss of their cisternae. Single free ribosomes appeared as electron-dense dots in the cytoplasm were seen (Fig. 7D). The β cells showed a damaged nuclear membrane (Fig. 7E), while the α cells of the islets of Langerhans

showed a structure resembling that of the control group, but the nucleus had appeared with condensed chromatin (Fig. 7F). The CP+BMSCs+Taurine treated group showed restoration of the architecture of the acinar cell to normal, appearing with a basal euchromatic nucleus and prominent nucleolus, while their apical part showed multiple zymogen granules. Abundant parallel stacks of rough endoplasmic reticulum speckled with ribosomes were noticed, with scattered mitochondriae containing parallel shelf-like cisternae (Fig. 7G). The ß cells of the islets of Langerhans showed euchromatic nuclei with prominent nucleoli, abundant secretory granules of varying sizes with an electron-lucent halo structure between the limiting membrane and surrounding the granule proper (Fig. 7H). The α cells of the islets of Langerhans had euchromatic nuclei with prominent nucleolus and variable size electron-dense secretory granules (Fig. 7I).

DISCUSSION

MSCs are considered an excellent candidate for cell therapy due to their low immunogenicity, accessibility, broad differentiation potential, and immunomodulatory effects (Lennon and Caplan, 2006). Additionally, it was demonstrated that antioxidant supplementation led to a significant reduction in the oxidative stress related to pancreatic fibrosis in CP (Swentek et al., 2021).

In the current study, the subcultured BMSCs had a well-defined polygonal appearance with many cytoplasmic processes. This is consistent with Yusop et al. (2018), who noticed that MSCs have a heterogeneous morphology. Moreover, BMSCs showed moderate positive expression of the CD 44 marker and negative expression for CD 34, which agrees with He et al. (2018). Therefore, the BMSCs used in this study met the standard criteria of the ISCT, which include adherence to the culture flask and positive expression of stromal CD markers (Dominici et al., 2006).

SRY gene could be traced in the pancreas of groups treated with the BMSCs. These findings agree with Zhao et al. (2016), Sun et al. (2017). However, Eggenhofer et al. (2012) reported that MSCs were found only in the lung for 1 hour after intravenous infusion and in the liver for 24 hours after infusion, and could not be tracked in any other organ 72 hours after infusion.

In the current study, there was a significant reduction in the body weight of rats of groups CP, CP+ MSCs, and CP+Taurine when compared to the control group. This is in accordance with Robles et al. (2014) and Sharma et al. (2017), who reported a significant decrease in the body weight of rats with L-arginine-induced CP. In controversy, Obafemi et al. (2018) demonstrated that rats were losing weight at the beginning of the experiment but started to regain weight two weeks after induction of the tissue injury.

Reduced body weight of L-arginine-treated rats could be due to increased peroxidation of lipids as a consequence of L-arginine-induced oxidative stress, as explained by Sharma et al. (2017). Additionally, it was reported that the degree of weight loss corresponded directly to the degree of malnutrition. This malnutrition was the result of malabsorption and maldigestion of fats with increased metabolic activity due to the inflammatory components of CP (Rasmussen et al., 2013).

On the other hand, rats in the CP+BMSCs+Taurine treated group showed a significant increase in body weight when compared to the CP group. This is in agreement with Mas et al. (2006), who reported that taurine-treated group could gain weight after 28 days of taurine treatment.

Regarding the weight of the pancreas, the present study showed a significant decrease in the CP group. This is in agreement with Sharma et al. (2017) and Obafemi et al. (2018). There was a significant increase in the pancreatic weight of CP groups treated with MSCs alone or in combination with taurine respectively. This is in the match with Sun et al. (2017) who noticed an increase in pancreatic weight after MSCs treatment.

In the present study, the CP group had severely destructed pancreatic architecture histologically and ultra-structurally. This is consistent with Zhang et al. (2016), Kanika et al. (2015) and Sharma et al. (2017), who used L-arginine for the induction of chronic pancreatitis. On the other hand, the current findings are contradictory to Obafemi et al. (2018) who noticed self-recovery of

pancreatic injury after four weeks of induction of CP.

It was reported that L-arginine increases oxidative and nitrosative stress, as it is metabolized to NO; a highly reactive free radical; by NO synthase leading to inflammatory response and finally acinar cell damage (Buchwalow et al., 2013). This is associated with the infiltration of monocytes and macrophages into the injured pancreas which releases TNF-α, which is one of the main factors for CP-induced inflammatory response, as TNF-α can increase the release of other pro-inflammatory factors (such as IL-6). It also increases the expression of chemokines and adhesion molecules, which induces the recruitment of inflammatory cells (Chen et al., 2019). Furthermore, massive enlargement and damage of the pancreatic mitochondria were attributed to the appearance of intracytoplasmic vacuolation, as mentioned by Kui et al. (2014).

The hydropic degeneration of the islets of Langerhans of the CP group was in agreement with Roy et al. (2020), who noticed the depletion of β cells with the development of diabetes mellitus in CP rats. On the other hand, Robles et al. (2014) and Sharma et al. (2017) reported that no morphological changes were affecting the islets of Langerhans. The survival of the islet cells is due to the protective effects of regenerating proteins produced by acinar cells of the pancreas, which are upregulated at the early stage of CP and then reduced as a result of the exocrine pancreatic insufficiency late in CP (Huan et al., 2019).

In the present work, the interlobular duct showed glandular hyperplasia. In accordance, human exocrine tissues from patients with pancreatitis showed ductal metaplasia and cell proliferation (Zhou and Melton, 2018).

BMSCs made some improvements to pancreatic tissue architecture, which are compatible with Zhou et al. (2013) and Sun et al. (2017). On the other hand, Kawakubo et al. (2016) reported that MSCs transplantation could not suppress tissue fibrosis and inflammatory cell infiltration. It was reported that the paracrine secretion of growth factors by MSCs has antiapoptotic, immunoregulatory, and angiogenic functions, which reduce the number of neutrophils and mast cells binding to vascular endothelial cells and limit the mobilization of these cells to the area of damage (Andrzejewska et al., 2019).

Treatment with taurine showed restoration of most of the normal pancreatic architecture. This is consistent with Mas et al. (2006), Shirahige et al. (2008) and Matsushita et al. (2012). Taurine improves the tissue oxidative stress and inhibits TNF, which enhances the survival of acinar cells and prevents complications of pancreatitis (Mas et al., 2006). Also, taurine increases the cellular content of the BCL-2 protein which has antiapoptotic properties (Matsushita et al., 2012).

Combined treatment with BMSCs and taurine showed restoration of the normal pancreatic architecture. Antioxidant treatment behaves like a preconditioning agent that increases the secretion of favorable MSCs paracrine activity and decreases the risk of the early death of the engrafted MSCs in the damaged tissue (Lou et al., 2019). Moreover, Mashyakhy et al. (2021) demonstrated that taurine increased the TERT gene expression ,which encodes the TERT protein, which is responsible for the restoration of telomeric length in MSCs.

In the present study, results revealed that the CP group had an intense expression of α-SMA. This is in accordance with Qin et al. (2014), Zhou et al. (2013) and Sun et al. (2017). Normally, PSCs are inactive and characterized by α-SMA-negative staining. In CP, inflammatory cells release many inflammatory mediators, which activate the PSCs that start to change their morphological features and increase the expression of α-SMA, and then start to secrete extracellular matrix components, such as collagen and fibronectin leading to pancreatic fibrosis (Qin et al., 2014). In the current study, rats of the CP+Taurine group presented with less pancreatic fibrosis. This is compatible with Shirahige et al. (2008).

In the present work, rats of the CP+ BMSCs and CP+ BMSCs+Taurine groups showed a decrease in the expression of α-SMA when compared to the CP group. This agrees with Qin et al. (2014) and Zhou et al. (2013), who reported that MSCs could suppress PSCs activity by inhibiting the infiltration of

inflammatory cells, and the expression of fibrosis-related inflammatory cytokines and chemokines. On the other hand, Kawakubo et al. (2016) showed that the MSCs did not affect pancreatic fibrosis.

Also in the present work, it was found that the group treated with both BMSCs and taurine showed minimal expression of α-SMA around the stromal blood vessels. This agrees with Liao et al. (2020), who reported that the antioxidant could promote MSCs viability through reducing the oxidative stress and inhibit cell apoptosis.

CONCLUSION

In the current study, L-arginine injection resulted in severe pancreatic tissue destruction and fibrosis observed in CP. On the other hand, treatment with BMSCs or taurine alone could improve the pancreatic histopathological changes to some extent, but the combination of both BMSCs or taurine in the CP+ BMSCs+Taurine treated group resulted in good results regarding the pancreatic histopathological changes, pointing to an antioxidant's synergistic effect on both.

REFERENCES

AN J, BEAUCHEMIN N, ALBANESE J, ABNEY T, SULLIVAN A (1997) Use of a rat cDNA probe specific for the Y chromosome to detect male derived cells. *J Androl,* 18: 289-293.

ANDRZEJEWSKA A, LUKOMSKA B, JANOWSKI M (2019) Concise review: mesenchymal stem cells: from roots to boost. *Stem Cells,* 37(7): 855-864.

BOZZOLA JJ, RUSSELL LD (1999) Specimen preparation for scanning electron microscopy. In: Bozzola JJ, Russell LD (eds). *Electron microscopy: principles and techniques for biologists*. 2nd edition (Ch. 3). Jones and Bartlett.

BUCHWALOW I, SCHNEKENBURGER J, TIEMANN K, SAMOILOVA V, BANKFALVI A, POREMBA C, SCHLEICHER C, NEUMANN J, BOECKER W (2013) L-arginine-NO-cGMP signaling pathway in pancreatitis. *Sci Rep,* 3: 1899.

CHEN L, CHEN Y, YUN H, JIANLI Z (2019) Tetramethylpyrazine (TMP) protects rats against acute pancreatitis through NF-κB pathway. *Bioengineered*, 10(1): 172-181.

DOMINICI M, LE BLANC K, MUELLER I, SLAPER-CORTENBACH I, MARINI F, KRAUSE D, DEANS R, KEATING A, PROCKOP D, HORWITZ E (2006) Minimal criteria for defining multipotent mesenchymal stromal cells. The International Society for Cellular Therapy position statement. *Cytotherapy,* 8(4): 315-317.

EGGENHOFER E, BENSELER V, KROEMER A, POPP F, GEISSLER E, SCHLITT H, BAAN C, DAHLKE M, HOOGDUIJN M (2012). Mesenchymal stem cells are short-lived and do not migrate beyond the lungs after intravenous infusion. *Front Immunol,* 3: 297.

GONZÁLEZ AM, GARCIA T, SAMPER E, RICKMANN M, VAQUERO EC, MOLERO X (2011) Assessment of the protective effects of oral tocotrienols in arginine chronic-like pancreatitis. *Am J Physiol Gastrointest Liver Physiol,* 301(5): G846-855.

HE Q, YE Z, ZHOU Y, TAN WS (2018) Comparative study of mesenchymal stem cells from rat bone marrow and adipose tissue. *Turk J Bio,* 42: 477-489.

HUAN C, STANEK A, MUELLER C, OU P, DONG S, ZHANG J, ABDELNABY R, GRUESSNER R (2019) Loss of Reg proteins' protection of islet β cells in chronic pancreatitis: A potential mechanism for the pathogenesis of type 3c diabetes. *Curr Opin Endocr Metab Res,* 5: 21-28.

HUANG S, XU L, SUN Y, WU T, WANG K, LI G (2015) An improved protocol for isolation and culture of mesenchymal stem cells from mouse bone marrow. *J Orthop Translat,* 3(1): 26-33.

JC C, PARKS RW (2021) Chronic pancreatitis-update on pathophysiology and therapeutic approaches. *Indian J Surg,* 83(Suppl 3): 701-708.

KANIKA G, KHAN S, JENA G (2015) Sodium butyrate ameliorates L-arginine-induced pancreatitis and associated fibrosis in wistar rat: role of inflammation and nitrosative stress. *J Biochem Mol Toxicol,* 29(8): 349-359.

KAWAKUBO K, OHNISHI S, FUJITA H, KUWATANI M, ONISHI R, MASAMUNE A, TAKEDA H, SAKAMOTO N (2016) Effect of fetal membrane-derived mesenchymal stem cell transplantation in rats with acute and chronic pancreatitis. *Pancreas,* 45(5): 707-713.

KUI B, BALLA Z, VEGH E, PALLAGI P, VENGLOVECZ V, IVÁNYI B, TAKÁCS T, HEGYI P, RAKONCZAY Z (2014) Recent advances in the investigation of pancreatic inflammation induced by large doses of basic amino acids in rodents. *Lab Invest,* 94(2): 138-149.

LENNON DP, CAPLAN AI (2006) Isolation of rat marrow-derived mesenchymal stem cells. *Exp Hematol,* 34(11): 1606-1607.

LI X, BAI J, JI X, LI R, XUAN Y, WANG Y (2014) Comprehensive characterization of four different populations of human mesenchymal stem cells as regards their immune properties, proliferation and differentiation. *Int J Mol Med,* 34(3): 695-704.

LIAO N, SHI Y, WANG Y, LIAO F, ZHAO B, ZHENG Y, ZENG Y, LIU X, LIU J (2020) Antioxidant preconditioning improves therapeutic outcomes of adipose tissue-derived mesenchymal stem cells through enhancing intrahepatic engraftment efficiency in a mouse liver fibrosis model. *Stem Cell Res Ther,* 11(1): 237.

LOTFY A, SALAMA M, ZAHRAN F, ELENA J, AHMED B, SOBH M (2014) Characterization of mesenchymal stem cells derived from rat bone marrow and adipose tissue: a comparative study. *Int J Stem Cells,* 7(2): 135-142.

LOU D, YE J, YANG L, WU Z, ZHENG W, ZHANG H (2019) Icariin stimulates differentiation of bone marrow-derived mesenchymal stem cells (BM-MSCs) through activation of cAMP/PKA/CREB. *Braz J Pharm Sci,* 55: 95-104.

MARRACHE F, PENDYALA S, BHAGAT G, BETZ KS, SONG Z, WANG TC (2008) Role of bone marrow-derived cells in experimental chronic pancreatitis. *Gut,* 57(8): 1113-1120.

MAS MR, ISIK AT, YAMANEL L, INAL V, TASCI I, DEVECI S, MAS N, COMERT B, AKAY C (2006) Antioxidant treatment with taurine ameliorates chronic pancreatitis in an experimental rat model. *Pancreas,* 33(1): 77-81.

MASHYAKHY M, ALKAHTANI A, ABUMELHA A, SHARROUFNA RJ, ALKAHTANY MF, JAMAL M, ROBAIAN A, BINALRIMAL S, CHOHAN H, PATIL VR, RAJ AT, BHANDI S, REDA R, TESTARELLI L, PATIL S (2021) Taurine augments telomerase activity and promotes chondrogenesis in dental pulp stem cells. *J Pers Med,* 11(6): 491.

MATSUSHITA K, MIZUSHIMA T, SHIRAHIGE A, TANIOKA H, SAWA K, OCHI K, TANIMOTO M, KOIDE N (2012) Effect of taurine on acinar cell apoptosis and pancreatic fibrosis in dibutyltin dichloride-induced chronic pancreatitis. *Acta Med Okayama,* 66(4): 329-334.

OBAFEMI TF, YU P, LI J, DAVIS JM, LIU K, CHENG B, ZHAO X, SHEN Q, YOUNES M, KO TC, CAO Y (2018) Comparable responses in male

and female mice to cerulein-induced chronic pancreatic injury and recovery. *JOP,* 19(5): 236-243.

QIN T, LIU CJ, ZHANG HW, PAN YF, TANG Q, LIU JK, WANG YZ, HU MX, XUE F (2014) Effect of the IκBα mutant gene delivery to mesenchymal stem cells on rat chronic pancreatitis. *Genet Mol Res,* 13(1): 371-385.

RASMUSSEN HH, IRTUN Ø, OLESEN SS, DREWES AM, HOLST M (2013) Nutrition in chronic pancreatitis. *World J Gastroenterol,* 19(42): 7267-7275.

ROBLES L, VAZIRI ND, LI S, MASUDA Y, TAKASU C, TAKASU M, VO K, FARZANEH SH, STAMOS MJ, ICHII H (2014) Dimethyl fumarate protects pancreatic islet cells and non-endocrine tissue in L-arginine-induced chronic pancreatitis. *PloS One,* 9(9): e107111.

ROY A, SAHOO J, KAMALANATHAN S, NAIK D, MOHAN P, POTTAKKAT B (2020) Islet cell dysfunction in patients with chronic pancreatitis. *World J Diabetes,* 11(7): 280-292.

SCUTERI A, MONFRINI M (2018) Mesenchymal stem cells as new therapeutic approach for diabetes and pancreatic disorders. *Int J Mol Sci,* 19(9): 2783-2796.

SHARMA S, RANA SV, RANA S, BHASIN DK, NADA R, MALHOTRA S (2017) Severe chronic pancreatitis due to recurrent acute injury: non-invasive chronic pancreatitis model of rat. *JOP,* 18(2): 107-120.

SHIRAHIGE A, MIZUSHIMA T, MATSUSHITA K, SAWA K, OCHI K, ICHIMURA M, TANIOKA H, SHINJI T, KOIDE N, TANIMOTO M (2008) Oral administration of taurine improves experimental pancreatic fibrosis. *J Gastroenterol Hepatol,* 23(2): 321-327.

SINGH VK, YADAV D, GARG PK (2019) Diagnosis and management of chronic pancreatitis: a review. *JAMA,* 322(24): 2422-2434.

SOLIMAN ME, KEFAFY MA, MANSOUR MA, ALI AF, ESA WA (2014) Histological study on the possible protective effect of pentoxifylline on pancreatic acini of l-arginine-induced acute pancreatitis in adult male albino rats. *Menoufia Med J,* 27(4): 801-808.

SUN Z, GOU W, KIM D, DONG X, STRANGE C, TAN Y, ADAMS DB, WANG H (2017) Adipose stem cell therapy mitigates chronic pancreatitis via differentiation into acinar-like cells in mice. *Mol Ther,* 25(11): 2490-2501.

SWENTEK L, CHUNG D, ICHII H (2021) Antioxidant therapy in pancreatitis. *Antioxidants (Basel),* 10(5): 657.

WHITCOMB DC, FRULLONI L, GARG P, GREER JB, SCHNEIDER A, YADAV D, SHIMOSEGAWA T (2016) Chronic pancreatitis: an international draft consensus proposal for a new mechanistic definition. *Pancreatology,* 16(2): 218-224.

YANG L, SHEN J, HE S, HU G, SHEN J, WANG F, XU L, DAI W, XIONG J, NI J, GUO C, WAN R, WANG X (2012) L-cysteine administration attenuates pancreatic fibrosis induced by TNBS in rats by inhibiting the activation of pancreatic stellate cell. *PLoS One,* 7(2): e31807.

YUSOP N, BATTERSBY P, ALRAIES A, SLOAN AJ, MOSELEY R, WADDINGTON RJ (2018). Isolation and characterisation of mesenchymal stem cells from rat bone marrow and the endosteal niche: a comparative study. *Stem Cells Int,* 2018: 6869128.

ZHANG W, ZHAO J, PING F, LIU Z, GU J, LU X (2016) Effect of dimethyl fumarate on rats with chronic pancreatitis. *Asian Pac J Trop Med,* 9(3): 261-264.

ZHAO H, HE Z, HUANG D, GAO J, GONG Y, WU H, XU A, MENG X, LI Z (2016) Infusion of bone marrow mesenchymal stem cells attenuates experimental severe acute pancreatitis in rats. *Stem Cells Int,* 2016: 7174319.

ZHOU C, LI M, QIN A, LV S, ZHU X, LI L, DONG Y, HU C, HU D, WANG S (2013) Reduction of fibrosis in dibutyltin dichloride-induced chronic pancreatitis using rat umbilical mesenchymal stem cells from Wharton's jelly. *Pancreas,* 42(8): 1291-1302.

ZHOU Q, MELTON DA (2018) Pancreas regeneration. *Nature,* 557(7705): 351-358.

A cluster of dysmorphologies in a male human body: The value of anatomical variants in health sciences student training

Pieter-Jan Bosman, Surasha M. Surandernath, Baron Quinton, Daniel Ziqubu, Muhammad Khan, Faatimah Asmal, Beverley Kramer

School of Anatomical Sciences, Faculty of Health Sciences, University of the Witwatersrand, Johannesburg, South Africa

SUMMARY

The human body is known to contain many variations in its normal structure which, while of interest to teachers of anatomy, may be vexing to health sciences students when compared to the description of "normal" anatomy in their textbooks. However, these variations, and even dysmorphologies, pose interesting and sometimes challenging learning experiences to students during dissection of the body. Such an instance occurred for undergraduate medical students in the School of Anatomical Sciences, University of the Witwatersrand, South Africa, when three unrelated dysmorphologies were discovered while undertaking a full dissection of a donor's body. An aberrant right subclavian artery was found in the thoracic cavity and two further dysmorphologies, a supernumerary kidney and accessory indentations on the diaphragmatic surface of the liver presented on dissection of the abdominal cavity. The aberrant right subclavian conformed with previous descriptions of the anomaly. However, the supernumerary kidney lacked a ureter, was lobulated and contained large blood-filled spaces, with histological evidence of urinary tubules in the intervening connective tissue. The accessory hepatic indentations varied in depth, with the deeper one forming a fissure and the less deep indentation, a sulcus. While the described dysmorphologies vary in their incidence, the occurrence of a cluster of three within one body provided a significant opportunity for the students to review the normal anatomy, and especially the complex development of the structures, as well as the clinical significance of each.

Key words: Accessory hepatic indentations – Dysmorphologies – Morphological anatomy – Right aberrant subclavian artery – Supernumerary kidney

INTRODUCTION

The morphology of the human body is complex and may be further complicated by variations in the arrangement and/or position of organs and other structures. While variations are not considered to be abnormal (Willan and Humpherson, 1999), they present a distinctive learning perspective for the health sciences student from that

Corresponding author:
Professor Emeritus Beverley Kramer. School of Anatomical Sciences, Faculty of Health Sciences, University of the Witwatersrand, Johannesburg, South Africa. Phone: +27825545529. E-mail: beverley.kramer@wits.ac.za

Submitted: February 7, 2023. **Accepted:** March 28, 2023

https://doi.org/10.52083/CZAA2387

depicted in anatomical textbooks and demonstrate the uniqueness of each individual. Variations of structures may include dysmorphologies, which are expressions of human teratology or alterations of normal morphology (Merriam-Webster; Richtsmeier, 2017) of congenital origin. When these dysmorphologies occur, they provide the student with a unique atlas within each body and an irreplaceable learning experience. Variations and dysmorphologies discovered during the dissection of the human body furnish students with insight into what they may stumble upon in clinical practice. While variations and dysmorphologies may generally not affect the function of the relevant organ (Kachlík et al., 2020), their identification may play a significant role in diagnosis as well as minimising misdiagnosis in clinical practice.

A unique learning experience arose for a group of medical students in their second year of study while undertaking full body dissection of a donor body as part of their anatomy course in the School of Anatomical Sciences, Faculty of Health Sciences, University of the Witwatersrand, South Africa. Three major dysmorphologies were noted during the dissection. One of these abnormalities occurred in the thoracic cavity, while the remaining two were located in the abdominal cavity. In the thoracic cavity the absence of the brachiocephalic trunk as a major branch of the aortic arch was accompanied by an aberrant right subclavian artery as the distal-most branch of the aortic arch. In the abdomen, a third (supernumerary) kidney without a ureter was present on the left side. Finally, two accessory hepatic indentations were noted on the diaphragmatic surface of the liver.

This study thus describes three unusual dysmorphologies occurring together in one individual and reviews their development and clinical relevance as pertinent to variations which may occur in the human body.

MATERIALS AND METHODS

Permission to undertake the study was provided by the Collections Committee of the School of Anatomical Sciences, University of the Witwatersrand, and by an ethics waiver from the Human Research Ethics Committee (Medical), University of the Witwatersrand (W-CBP-220504-01).

A South African white male presented for dissection. The individual – aged 74 years – had donated his body for teaching and learning to the School of Anatomical Sciences, Faculty of Health Sciences, University of the Witwatersrand. The cause of death of the individual as noted on the death certificate listed “cutaneous squamous cell carcinoma with metastases in the brain, liver, lung”. A secondary diagnosis was also provided which stipulated: “brain (occipital and parietal area), numerous pulmonary nodules, liver”.

The dissection of the body was carried out in full as per the instructions detailed in the practical manual “Practical Anatomy” (Kieser and Allan, 2020). The length, breadth, and depth of the kidneys as well as the length and depth of the liver indentations were measured using a manual sliding vernier scale calliper with an accuracy of 0.05mm. Photos of the morphological structures of interest were captured using a Nikon DSLR D90 camera.

Segments of the supernumerary kidney were removed for histological investigation and fixed in 10% neutral buffered formalin for 48 hours. Following fixation, the tissue was routinely dehydrated through a graded series of alcohols, cleared in xylene, and embedded in wax. Sections of the wax-embedded tissue were cut on a microtome at 5µm and placed on silane-coated glass slides. The sections were then rehydrated through a graded series of alcohols and stained with haematoxylin and eosin, and following cover-slipping with Entellan®, were examined with a Zeiss (Primo Star) compound microscope to allow for a general appraisal of the tissue. Following analysis by a histologist, the sections were independently appraised by a pathologist, and the diagnosis was confirmed.

RESULTS

The three major abnormalities found during the dissection of the body included an aberrant right subclavian artery, a supernumerary kidney, and accessory hepatic indentations. Each structure presented with distinct and clearly divergent morphology from the expected anatomy.

Aberrant Right Subclavian Artery

Generally, three major arteries arise from the aortic arch: the brachiocephalic trunk (which branches into the right subclavian artery and right common carotid artery), the left common carotid artery, and finally, the left subclavian artery. In the male body dissected in this study, four major branches arising from the aortic arch were observed. The brachiocephalic trunk was absent and instead, four large arteries arose directly from the aortic arch. These were (from proximal to distal) the right common carotid artery, the left common carotid artery, the left subclavian artery, and most distally, the right aberrant subclavian artery (Figs. 1a, b, c).

The right common carotid artery, which originated most proximally on the superior aspect of the arch, continued in a right superolateral direction, passing anterior to the trachea at the level of T3. The artery then passed along the right inferior margin of the thyroid gland and continued superiorly, parallel to the larynx. The next branch arising from the aortic arch was the left common carotid artery, which originated from the superior aspect of the aortic arch and continued superiorly along the left margin of the thyroid gland and travelled parallel to the larynx. Next, the left subclavian artery originated from the left superolateral aspect of the aortic arch and passed superolaterally, posterior to the left anterior scalene muscle. There-

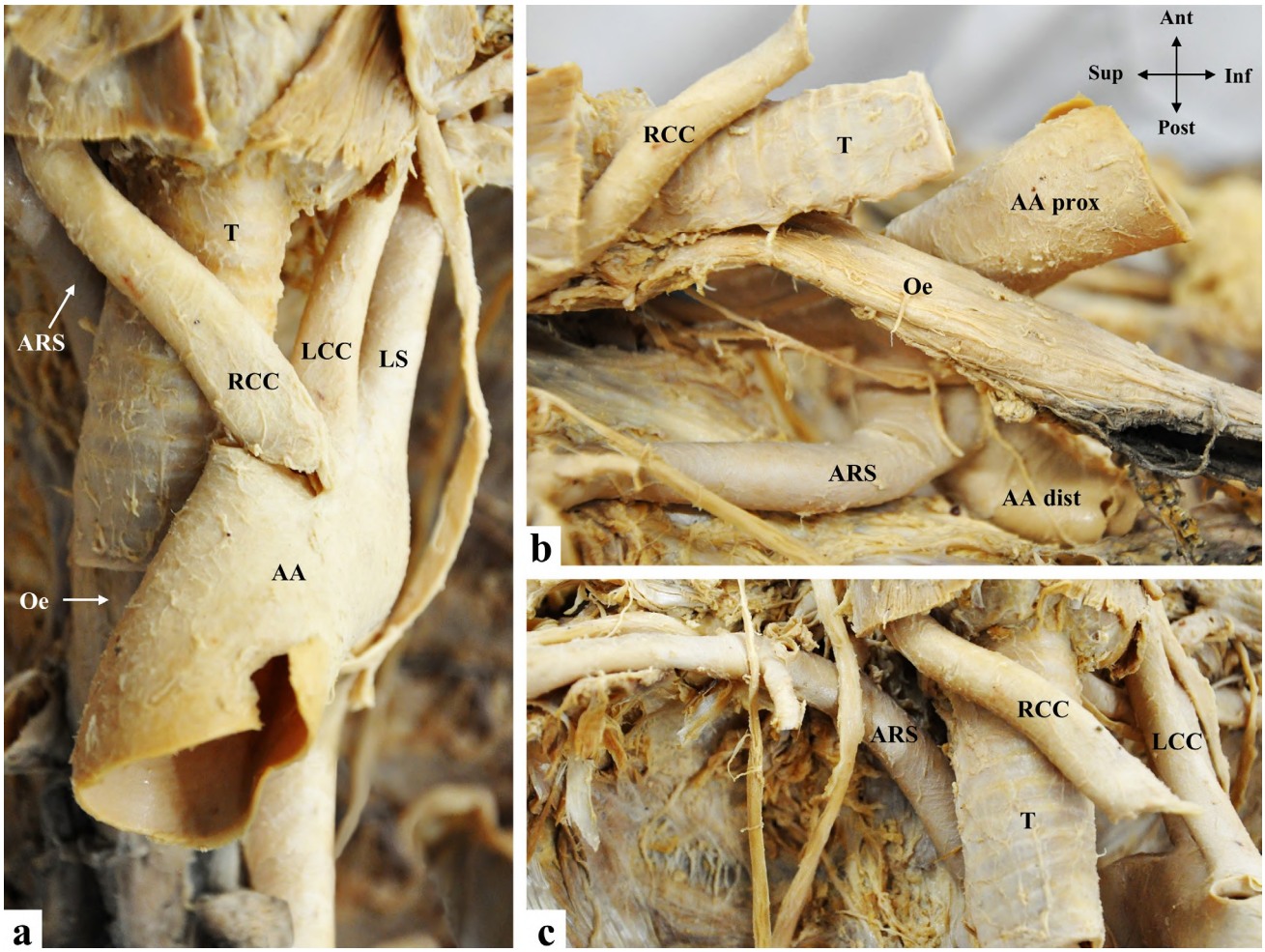

Fig. 1.- Photographic representation of right aberrant subclavian artery. **1a:** Anterior view of the aortic arch (AA) showing its four major branches: Right common carotid artery (RCC), left common carotid artery (LCC), left subclavian artery (LS), and the aberrant right subclavian artery (ARS) running posterior to the trachea (T) and oesophagus (Oe). **1b:** Right lateral view showing the origin of the aberrant right subclavian artery (ARS) from the aortic arch (AA). Proximal (AA prox) and distal (AA dist) parts of the arch are indicated. The right common carotid artery has been separated from the aorta. Note the position and course of the aberrant right subclavian posterior to the trachea (T) and oesophagus (Oe). **1c:** Anterior view of the superior thoracic region displaying the course of the aberrant right subclavian artery (ARS) posterior to the trachea (T) (oesophagus cannot be seen in this view). The aortic arch has been reflected out of view.

after, it continued laterally to the external border of the first rib, where it became the left axillary artery as expected.

The aberrant right subclavian artery arose from the aortic arch as the distal-most branch, where it originated from the posteromedial aspect (Fig. 1b). It continued in a right superomedial direction, passing posterior to the oesophagus at the level of T3, then superolaterally to the external border of the first rib and continued into the right upper limb (Fig. 1c).

Supernumerary Kidney

Two normal kidneys plus a third ectopically-placed kidney were found in the body upon dissection. The left and right normal kidneys occurred retroperitoneally against the posterior abdominal wall in the left and right lumbar regions, respectively. The normal kidneys occupied an oblique position, had a smooth surface and were ovoid in shape, lying on either side of the vertebral column between the levels of T12 and L3. As expected, the right kidney occurred more inferiorly than the left within these vertebral levels due to the presence of the liver in the upper right quadrant of the abdomen. A left and a right ureter, respectively, were found originating from each kidney. These too were retroperitoneal and ran inferiorly after exiting each renal hilum, then passed over the bifurcation of the common iliac arteries and entered the bladder along the later-

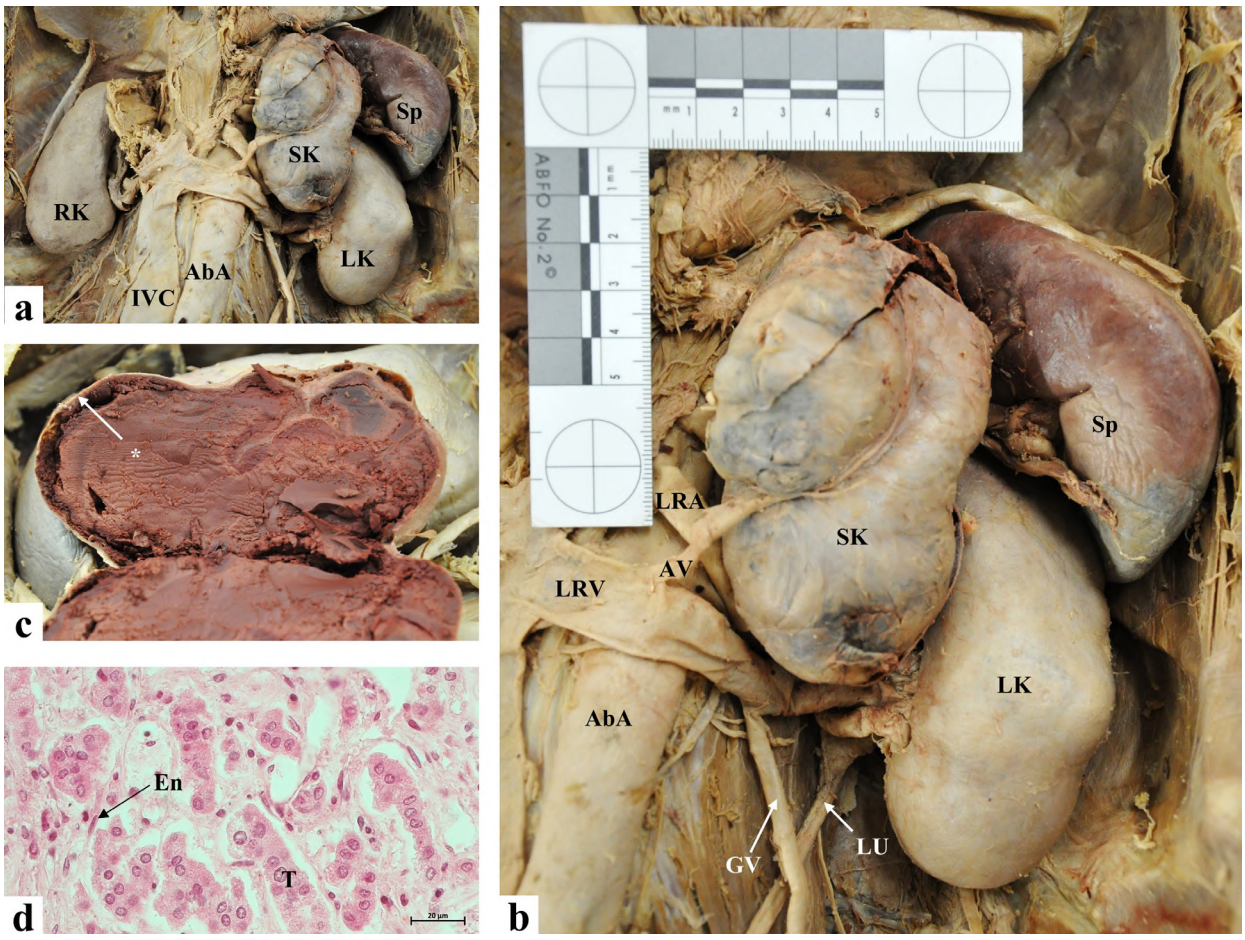

Fig. 2.- Photographic representation of the supernumerary kidney. **2a:** Anterior view of the abdominal retroperitoneal organs in situ including the supernumerary kidney to show the anatomical arrangement of the two normal kidneys and the supernumerary kidney (SK). The liver, stomach, and intestines have been removed. The diaphragm has been reflected. IVC – Inferior vena cava; RK – Right kidney; LK – left kidney; AbA – abdominal aorta. **2b:** Anterior view of the left retroperitoneal region of the abdomen, including the supernumerary kidney (SK) and its accessory vein (AV) – a tributary of the left renal vein (LRV). Note the lobulated appearance of the supernumerary kidney compared to the normal left kidney (LK). Sp – Spleen; LU – Left ureter of normal kidney; GV – Gonadal (testicular) vein; AbA – Abdominal aorta; LRA – Left renal artery. Note the absence of a ureter and/or renal pelvis in relation to the supernumerary kidney. **2c:** A sagittal section of the supernumerary kidney showing the renal capsule (*) and blood-filled cavities. **2d:** Histological section of the supernumerary kidney showing tubules reminiscent of the nephric loops. T – Tubules; En – Endothelium of a peritubular blood vessel. Light microscopy (x40), scale bar = 20 µm.

al wall of the pelvis. The left and right suprarenal glands were topologically normal and their anatomical relations with each respective kidney were typical.

A third, supernumerary kidney (Figs. 2a, b) was found anteromedial to the left kidney and was contained in its own capsule (Fig. 2c) with its longitudinal axis in the same plane as the longitudinal axis of the left kidney. It occupied a region posterior to the stomach, pancreas, and jejunum. The inferior margin of the supernumerary kidney was positioned more superiorly than the inferior margin of the left kidney. While the structure was retroperitoneal, a large protuberance which occurred on the anterior aspect of the supernumerary kidney, bulged the peritoneal lining.

The supernumerary kidney resembled the basic ovoid shape of a normal kidney, but its surface was lobulated, reminiscent of its embryonic state. It was 103 mm in length (greatest length measured along its longitudinal axis; compared with the normal kidneys: R = 113 mm; L = 117 mm), 57 mm wide (R = L = 52 mm), and with an anteroposterior depth of 48 mm (R = 39 mm; L = 45 mm).

While a slight indentation reminiscent of a hilum was noted on the supernumerary kidney, there was no evidence of typical hilar structures, namely a renal pelvis, calyces, or a ureter, nor any evidence of tearing of the latter had it been present. This was further confirmed on sectioning. The supernumerary kidney was drained by a small tributary of the left renal vein. This tributary exited the supernumerary kidney on its anterior surface. The origin of the supernumerary kidney's arterial supply, however, is unclear and is likely to have been inadvertently severed during dissection.

Large blood-filled spaces were evident in the histological sections of the tissue, but no glomeruli nor collecting ducts were found. Connective tissue

Fig. 3.- Diaphragmatic surface of the liver showing the deep accessory hepatic fissure (AHF) on the left, and the more superficial accessory hepatic sulcus (AHS) to the right.

strands occurred between the blood-filled spaces and contained blood vessels and tubules reminiscent of the nephric loops (Fig. 2d). The tissue was confirmed by a pathologist to be nephric tissue.

Accessory Hepatic Fissure and Sulcus

In addition to the major hepatic fissures which were evident on dissection, two accessory indentations were noted on the diaphragmatic surface of the liver of the dissected body. These indentations were respectively termed as a fissure, due to its depth, and the other a sulcus, as it was more superficial/lacked depth. The deeper left accessory indentation (fissure) measured 77 mm in length, 4.5 mm average width, and extended into the parenchyma to a depth of 14 mm. The right depression (sulcus) was shallow and appeared to be slightly longer than the fissure. Both indentations ran in a supero-inferior direction – parallel to each other (Fig. 3). The respective midlines of the accessory hepatic fissure and sulcus were separated by 29 mm. No supernumerary/aberrant ribs were present, and no hypertrophied bands of diaphragmatic muscle were found.

DISCUSSION

The occurrence of multiple dysmorphologies in a human body present with an opportunity for students and staff in anatomy to discover the wide anatomical variation that can occur. These manifestations also better prepare students for their future role as clinicians, when variations and abnormalities may present unexpectedly in their patients – especially during surgery. Any variations and dysmorphologies found during dissection are therefore an excellent learning experience and should be considered carefully in preparation for making diagnoses and developing treatment options in future patients.

Aberrant Right Subclavian Artery

The fourth (aberrant) branch of the aortic arch observed in this dissection resembles the anatomy previously described as *arteria lusoria* (Molz and Burri, 1978; Polguj et al., 2014) or *arteria subclavia aberrans retrooesophagus* (Kachlík et al., 2020). This congenital abnormality has a female predominance (Molz and Burri, 1978; Polguj et al., 2014) and is the most common embryological abnormality of the aortic arch (Darwazah et al., 2015; Polguj et al., 2014), having an incidence ranging between 0.16-4.4% (Freed and Low, 1997; Natsis et al., 2017; Ramaswamy et al., 2008; Rosa et al., 2003). This abnormality is said to have been first described by Hunauld in 1735 (Freed and Low, 1997).

Developmentally, the aortic sac gives rise to the pharyngeal arch arteries (Allan and Kramer, 2009). Six pairs of bilateral arteries leave the aortic sac and pass through each pharyngeal arch before joining the dorsal aorta. However, the number of arch arteries is dynamic, as the pharyngeal arches develop and regress at various stages (Benson et al., 1992), with the fifth arch being rudimentary.

The right and left dorsal aortae receive the pharyngeal arch arteries bilaterally. The dorsal aortae remain paired at the level of the pharyngeal arches, but merge caudally to create the descending aorta (Rosen and Bordoni, 2022). Seven bilateral cervical intersegmental arteries originate from the dorsal aortae. The left subclavian artery arises entirely from the left seventh intersegmental artery, while the right subclavian artery normally arises from the right fourth pharyngeal arch artery proximally, and the right seventh intersegmental artery distally (Rosen and Bordoni, 2022).

An aberrant right subclavian artery results when the right fourth pharyngeal arch artery regresses, leading to the loss of the right subclavian's typical proximal section (Polguj et al., 2014). Consequentially, the seventh right segmental artery serves as the sole source of the artery resulting in an independent branch originating from the aorta and an independent origin for the right common carotid artery. In 60% of cases of aberrant right subclavian artery, an aortic diverticulum known as Kommerell's diverticulum is present (Domínguez-Massa et al., 2019), which is a fragment of the right aortic arch present at the origin of the aberrant right subclavian artery (Domínguez-Massa et al., 2019; Freed and Low, 1997).

Individuals with an aberrant right subclavian artery may be asymptomatic, and are often dis-

covered accidentally (Darwazah et al., 2015). In cases where the aberrant artery compresses the oesophagus, thereby creating a physiological constriction, dysphagia lusoria may occur (Polguj et al., 2014), which is of clinical significance. However, the aberrant right subclavian artery presents with symptoms in only 7-10% of adult patients (Delap et al., 2000) and thus must be considered during surgical procedures involving the oesophagus (Mahmodlou et al., 2014). In patients in which progressive dysphagia presents, it is imperative to be aware of the possible courses of the aberrant artery such as the usual retro-oesophageal course or the uncommon route anterior to the trachea or oesophagus, ensuring an effective and encompassing surgical approach. Furthermore, anomalies such as non-recurrent right inferior laryngeal nerve, right sided aortic arch and a common origin of the common carotid arteries have been reported in association with an aberrant right subclavian artery (Epstein and DeBord, 2002).

Supernumerary Kidney

While renal abnormalities are not uncommon, a supernumerary kidney is rare (Kumar et al., 2019; Mejia et al., 2018; Sureka et al., 2013) with less than 100 cases said to have been reported in the literature (Ardalan, 2016; Sureka et al., 2013). The first case was described by Martius in 1656 (Krakhotkin et al., 2021). The incidence of supernumerary kidney has not been calculated due to its infrequent appearance (Tada et al., 1981), although the introduction of CT scans and MRI are now likely to document this variant more frequently. Most supernumerary kidneys are said to be located on the left-hand side (Krakhotkin et al., 2021; Tada et al., 1981) and are equally distributed in males and females (Ardalan, 2016; Tada et al., 1981). However, few cases of a supernumerary kidney without a ureter have been reported in the literature (Ardalan, 2016; Gray and Skandalakis, 1972).

During human development, a mesonephros develops prior to the formation of the normal adult kidney (metanephros) and undergoes an almost identical development to that of the metanephros (Allan and Kramer, 2009). Two important constituents are present during the normal development of both the mesonephric and the metanephric kidney, the ureteric bud (from the mesonephric duct) and the nephrogenic cord (Allan and Kramer, 2009). The metanephrogenic blastema, which arises from a condensation of nephrogenic cord mesoderm, induces the cells of the ureteric bud to differentiate and develop the renal collecting system. Simultaneously, the ureteric bud induces the metanephrogenic blastema to differentiate into the renal excretory system, consisting of the renal corpuscle, the nephric loops, and the proximal and distal convoluted tubules. The collecting duct system, derived from the ureteric bud, develops into the collecting ducts, major and minor calyces, renal pelvis, and the ureter. While one of the earliest studies of kidney development by Felix (1911) provided information on the steps of the development of the nephron in the mesonephros, the information was based mainly on comparative embryology and described mesoureters originating from the mesonephric (Wolffian) ducts. Recently, Landsman and Ludwig (2005) through their study of serial sections of human embryos have definitively shown that the cone of the mesonephric duct becomes the mesoureter (and subsequently the ureter of the adult kidney).

Initially, the metanephric (adult) kidney develops in the pelvic region, but progressively ascends until each kidney encounters the suprarenal gland. During the ascent of the kidneys, the hilum of each kidney rotates from initially facing anteriorly to finally facing medially in the adult. Thus, all nephric hilar structures normally exit/enter the kidney on its medial surface. In the case of the supernumerary kidney found in this study, an accessory renal vein exited the supernumerary kidney anteriorly, perhaps indicating that the normal rotation did not occur.

During the developmental ascent of the kidneys, their blood supply progressively changes. Initially the artery to each respective kidney originates from the corresponding common iliac artery (Allan and Kramer, 2009). With cranial migration of each kidney, the early blood supply degenerates and is replaced by intermediate renal arteries that originate from the distal part of the aorta. When the kidneys finally encounter the suprare-

nal glands, cranial migration of the kidney ceases, the intermediate blood supply degenerates, and the final arterial supply (adult renal artery) originates from the abdominal aorta. In some cases, these intermediate vessels fail to degenerate and present as accessory renal arteries or veins (Gupta et al., 2012).

The lobulated appearance of the dissected kidney, while reminiscent of an embryonic kidney that naturally smooths out due to growth of the nephrons over time (Shanthi D'Sa et al., 2022), is believed to be due to the masses of blood-filled spaces. Tubules within the connective tissue strands of the supernumerary kidney confirmed the diagnosis of a kidney by a histopathologist.

The supernumerary kidney found upon dissection in this study may be the result of the abnormal division of the nephrogenic cord into two metanephrogenic blastemata (Kumar et al., 2019; N'Guessan and Stephens, 1983) with or without division of the ureteric bud or a splitting of the ureteric bud (Ardalan, 2016). Generally, the supernumerary kidney may have a partially or completely duplicated ureter (N'Guessan and Stephens, 1983). However, it cannot be determined whether the supernumerary kidney found in this study developed *ab initio* or resulted from the splitting of the nephrogenic cord into two metanephrogenic blastemata (Kumar et al., 2019; N'Guessan and Stephens, 1983).

A supernumerary kidney on the left side was reported in a 45-year-old male in 1911 (Dixon, 1911). In this case, however, the supernumerary kidney presented with a distinct ureter. Few cases of supernumerary kidneys without ureters have been described in the literature although reference to detached masses of metanephrogenic tissue without ureters have been reported and are said to undergo differentiation. These masses were designated as "beinieren" by Neckar-Sulmer (1914) (see Gray and Skandalakis, 1972). It is highly probable that the supernumerary kidney found in the dissected body was not functional during the individual's lifetime and is likely to have been asymptomatic (Ardalan, 2016).

Clinically, upon analysis and interpretation of various non-invasive imaging techniques, supernumerary kidneys may be misdiagnosed. Rehder et al. (2019) suggest that the primary reason for an initial incorrect diagnosis of supernumerary kidney in 78% of the cases studied may be attributed to the relatively unfamiliar nature of a supernumerary kidney. Furthermore, supernumerary kidney is not regarded as a differential diagnosis. Rehder et al. (2019) further argue that there is currently no universally accepted approach to diagnose supernumerary kidneys consistently and accurately. Two major reasons for the importance of detecting and correctly interpreting cases involving a supernumerary kidney are provided by Rehder et al. (2019), including the importance of preventing the performance of unnecessary procedures, and more importantly, avoiding complications of superfluous surgical procedures as a result of incorrect diagnoses.

Accessory Hepatic Fissure and Sulcus

The topography of the accessory hepatic fissure and sulcus found in the dissected body is consistent with those described by Macchi et al. (2003) and are sometimes termed "cough furrows" (Nayak et al., 2017). Zahn (1882) as cited by Macchi et al. (2003) most likely provided the earliest description of accessory fissures of the liver. These indentations are said to occur frequently (Auh et al., 1984; Ono et al., 2000).

"Weak zones" that correspond to the margins between terminal branches of adjacent segmental portal veins may be the origin of hepatic indentations (Macchi et al., 2003). These weak zones in the superficial hepatic parenchyma are said to be particularly impressionable, and thus, as a result of pressure from the diaphragm on the liver, cause the formation of hepatic sulci or fissures (Macchi et al., 2003). In certain pathologies (such as the metastases to the lung found in the dissected body) that prompt a chronic increase in diaphragmatic activity, the increased pressure acts mainly at the preformed weak zones, which results in the portal fissures or "cough furrows" (Macchi et al., 2003).

Large variations in the incidence of accessory fissures on the diaphragmatic surface of the liver have been reported, ranging from 2% (Saritha et al., 2015) to 63% (Auh et al., 1984). The notice-

able discrepancy in incidence could be attributed to factors that may lead to the formation of these accessory hepatic indentations on the weaker regions of the liver, for example pressure from the ribs or the diaphragmatic muscle (Reddy et al., 2016). An understanding of these indentations and their causes may be of significance in the precise diagnosis and interpretation of sonography and/or CT imaging (Auh et al., 1984), as these indentations may be confused with hepatic cysts or haematomae. Knowledge of the presence of these indentations is of importance in preparation for hepatic segmental resections and transplantation procedures (Reddy et al., 2016).

Limitations of the study

Medical records of the donor body are not available to the authors. The study was limited by the unavailability of photographic records of rare supernumerary kidneys without a ureter, with which the present case could be compared.

CONCLUSION

Dysmorphologies found in the human body during dissection such as those described in this article are of vast importance in that they add to knowledge on human variability, allow for in-depth discussion of their embryological development and provide a clinical focus and basis for studying morphological anatomy. In addition, when variants of this nature are discovered by health sciences students themselves during dissection, it provides a vital lesson of the uniqueness of each human body. This experience will remain with the students far into their clinical years and may remind them of the difficulties in, and importance of, diagnosing structures clearly before surgical intervention is contemplated.

ACKNOWLEDGEMENTS

The authors sincerely thank those who donated their bodies to science so that anatomical research and teaching can be performed. Results from such research can potentially increase scientific knowledge and improve patient care. Therefore, these donors and their families deserve our highest respect. We would also like to acknowledge the following individuals for their assistance: Dr C Hammond (Cardiothoracic surgeon), Dr R Wadee (Pathologist), Dr E Hutchinson (photographs), Mrs H Ali (histology), and Mr P. Legodi (demographic information on the donor).

REFERENCES

ALLAN J, KRAMER B (2009) Organogenesis. In: *The Fundamentals of Human Embryology: Student Manual* (2nd ed). Wits University Press, pp 32-164.

ARDALAN M (2016) Kidney, urinary bladder, and ureter. In: Tubbs R, Shoja M, Loukas M (eds.). *Bergman's Comprehensive Encyclopedia of Human Anatomic Variation*. John Wiley and Sons, Inc., pp 1315-1331.

AUH YH, RUBENSTEIN WA, ZIRINSKY K, KNEELAND JB, PARDES JC, ENGEL IA, WHALEN JP, KAZAM E (1984) Accessory fissures of the liver: CT and sonographic appearance. *Am J Roentgenol*, 143(3): 565-572.

BENSON MT, DALEN K, MANCUSO AA, KERR HH, CACCIARELLI AA, MAFEE MF (1992) Congenital anomalies of the branchial apparatus: Embryology and pathologic anatomy. *Radio Graphics*, 12(5): 943-960.

DARWAZAH AK, EIDA M, KHALIL RA, ISMAIL H, HANBALI N (2015) Non-aneurysmal aberrant right subclavian artery causing dysphagia in a young girl: Challenges encountered using supraclavicular approach. *J Cardiothor Surg*, 10: 92.

DELAP TG, JONES SE, JOHNSON DR (2000) Aneurysm of an aberrant right subclavian artery presenting as dysphagia lusoria. *Ann Otol Rhinol Laryngol*, 109(2): 231-234.

DIXON AF (1911) Supernumerary kidney: The occurrence of three kidneys in an adult male subject. *J Anat Phys*, 45(2): 117-121.

DOMÍNGUEZ-MASSA C, BERBEL-BONILLO A, PÉREZ-GUILLEN M, MONTERO-ARGUDO JA (2019) Dissected aberrant right subclavian artery with Kommerell diverticulum. *Rev Portug De Cardiol*, 38(10): 737. e1-737.e4.

DYSMORPHOLOGY *Merriam-Webster Medical Dictionary*. Retrieved 22 January 2023, from https://www.merriam-webster.com/medical/dysmorphology.

EPSTEIN DA, DEBORD JR (2002) Abnormalities associated with aberrant right subclavian arteries: A case report. *Vasc Endovasc Surg*, 36(4): 297-303.

FELIX W (1911) Die Entwicklung der Harn- und Geschlechtsorgane. In: Keibel F, Mall FP (eds.). *Handbuch der Entwicklungsgeschichte des Menschen*, vol 2. Hirzel, Leipzig, pp 732-955.

FREED K, LOW VH (1997) The aberrant subclavian artery. *Am J Roentgenol*, 168(2): 481-484.

GRAY SW, SKANDALAKIS JE (1972) *Embryology for surgeons: The embryological basis for the treatment of congenital defects*. W.B. Saunders, Company (Philadelphia, London, Toronto), pp 443-518.

GUPTA A, GUPTA R, SINGAL R (2012) Congenital variations of renal veins: Embryological background and clinical implications. *J Clin Diag Res*, 5(6): 1140-1143.

JANDA GM, NEPPLE KG, COOPER CS, AUSTIN JC (2009) Supernumerary kidney in a child with OEIS Complex. *Urol*, 74(2): 305-307.

KACHLÍK D, VARGA I, BÁČA V, MUSIL V (2020) Variant anatomy and its terminology. *Medicina*, 56(12): 713.

KIESER J, ALLAN J (2020) *Practical Anatomy: The human body dissected* (2nd ed.). Wits University Press.

KRAKHOTKIN DV, CHERNYLOVSKYI VA, PIKHOVKIN DN, ERMOLAEV AN, BUGAEV RA (2021) Left supernumerary kidney: A rare case presentation. *Radiol Case Rep*, 16(3): 615-617.

KUMAR M, KUMAR G, BARWAL K, RAINA P (2019) Right supernumerary kidney: A rare entity. *Urol Case Rep*, 23: 97-98.

LUDVIG KS, LANDMANN L (2005) Early development of the human mesonephros. *Anat Embryol*, 209: 439-447.

MACCHI V, FELTRIN G, PARENTI A, DE CARO R (2003) Diaphragmatic sulci and portal fissures. *J Anat*, 202(3): 303-308.

MAHMODLOU R, SEPEHRVAND N, HATAMI S (2014) Aberrant right subclavian artery: a life-threatening anomaly that should be considered during esophagectomy. *J Surg Tech Case Rep*, 6(2): 61-63.

MEJIA M, LIMBACK J, RAMIREZ A, BURT JR (2018) A case of supernumerary kidney. *Cureus*, 10(12): e3686.

MOLZ G, BURRI B (1978) Aberrant subclavian artery (arteria lusoria): sex differences in the prevalence of various forms of the malformation. *Virchows Archiv A, Path Anat Histol*, 380(4): 303-315.

NATSIS K, DIDAGELOS M, GKIOULIAVA A, LAZARIDIS N, VYZAS V, PIAGKOU M (2017) The aberrant right subclavian artery: Cadaveric study and literature review. *Surg Radiol Anat*, 39(5): 559-565.

NAYAK SB, PADUR AA, KUMAR N, GEORGE BM (2017) Accessory grooves on the diaphragmatic surface of the liver: A cadaveric study. *J Clin Diag Res*, 11(5): 5-7.

N'GUESSAN G, STEPHENS FD (1983) Supernumerary kidney. *J Urol*, 130(4): 649-653.

ONO ML, MURAKAMI G, SATO TJ, KAKU SW (2000) Hepatic grooves and portal segmentation. *Kaibogaku Zasshi*, 75(6): 517-523.

POLGUJ M, CHRZANOWSKI Ł, KASPRZAK JD, STEFANCZYK L, TOPOL M, MAJOS A (2014) The aberrant right subclavian artery (arteria lusoria): the morphological and clinical aspects of one of the most important variations--a systematic study of 141 reports. *Sci World J,* 2014: 292734.

RAMASWAMY P, LYTRIVI ID, THANJAN MT, NGUYEN T, SRIVASTAVA S, SHARMA S, KO HH, PARNESS IA, LAI WW (2008) Frequency of aberrant subclavian artery, arch laterality, and associated intracardiac anomalies detected by echocardiography. *Am J Cardiol*, 101(5): 677-682.

REDDY N, MITTAL PS, JOSHI SS, JOSHI SD (2016) accessory fissures of liver and their clinical significance. *J Evol Med Dent Sci*, 5(82): 6125-6128.

REHDER P, REHWALD R, BÖHM JM, GRAMS AE, LOIZIDES A, PEDRINI M, STÜHMEIER J, GLODNY B (2019) Supernumerary kidneys: A clinical and radiological analysis of nine cases. *BMC Urol*, 19(1): 93.

RICHTSMEIER JT (2017) Dysmorphology. In: *Reference Module in Life Sciences*. Elsevier.

ROSA P, GILLESPIE DL, GOFF JM, O'DONNELL SD, STARNES B (2003) Aberrant right subclavian artery syndrome: A case of chronic cough. *J Vasc Surg*, 37(6): 1318-1321.

ROSEN RD, BORDONI B (2022) Embryology, Aortic Arch. [Updated 2022 Feb 10]. In: StatPearls [Internet]. Treasure Island (FL): StatPearls Publishing; 2022 Jan. Accessed 3rd February 2023.

SARITHA S, RAMANI N, NAGAJYOTHI D, YESENDER D (2015) Cadaveric study of morphological variations in the human liver and its clinical importance. *Int J Med Sci Clin Invent*, 2(6): 1020-1031.

SHANTHI D'SA D, VASUDHA TK, ANUP RAO K (2022) Genetic and embryological basis with clinical implications of lobulated kidney: A cadaveric study. *Int J Adv Res*, 10(3): 695-699.

SUREKA B, MITTAL MK, MITTAL A, SINHA M, THUKRAL BB (2013) Supernumerary kidneys - a rare anatomic variant. *Surg Radiol Anat*, 36(2): 199-202.

TADA Y, KOKADO Y, HASHINAKA Y, KADOWAKI T, TAKASUGI Y, SHIN T, TSUKAGUCHI I (1981) Free supernumerary kidney: a case report and review. *J Urol*, 126(2): 231-232.

WILLAN PL T, HUMPHERSON JR (1999) Concepts of variation and normality in morphology: Important issues at risk of neglect in modern undergraduate medical courses. *Clin Anat*, 12(3): 186-190.

Tibial vascular grooves: ambulatory physical activity and overall muscle activation

Luis Ríos[1], Isabel Pérez-Rubio[1], María Benito[2], Francisco Pastor[3]

[1] Unit of Physical Anthropology, Department of Biodiversity, Ecology and Evolution, Faculty of Biological Sciences, Universidad Complutense de Madrid.

[2] Department of Legal Medicine, Psychiatry and Pathology, Faculty of Medicine, Universidad Complutense de Madrid.

[3] Department of Anatomy and Radiology, Faculty of Medicine, Universidad de Valladolid.

SUMMARY

The vascular grooves on the lateral surface of the tibial diaphysis have been suggested as a qualitative indicator of mobility and physical activity. We study here the association between these grooves and an external index of cross-sectional circularity of the tibia, a biomechanical variable related to mobility. Three Iberian skeletal samples were selected for study, representing the Chalcolithic, Early Modern and Contemporary periods, a time span where a significant decrease in ambulatory activity has been documented in European samples. For each tibia, the circularity index and the presence of vascular grooves were recorded. The Chalcolithic sample presented a higher circularity index compared with the other two samples, indicating higher levels of ambulatory physical activity. It also presented a higher frequency of vascular grooves. The association between the circularity index and the presence of vascular grooves .was significant, but considerable overlapping in the index was observed between tibiae with few and several grooves. These grooves are associated to the tibialis anterior muscle, which is activated during the gait cycle but also in what has been called "active rest" postures, and possibly in other nonambulatory activities involving foot hyperdorsiflexion. The age- and sex-related changes in the vascular system could be also important in the interpretation of these grooves. These grooves might be partially related to levels of ambulatory activity, but we conclude that its presence cannot be used alone as a qualitative marker of mobility. Its use as a general indicator of overall lower limb muscle activity should be explored.

Key words: Osteology – Tibia – Physical activity – Muscle activation – Vascular

INTRODUCTION

The study of the patterns of mobility of past populations through the application of engineering principles to the diaphyses of limb bones has been a major development in the study of human skeletal remains (Larsen, 2018; Ruff, 2018). These studies are mostly based on the analysis of the cross-sectional properties of the diaphysis, although other variables of bone shape can be studied, like its longitudinal curvature (Brzobohatá et al., 2019). In addition to these well-established, quantitative techniques, it is discussed whether qualitative assessment of traits like entheseal changes can be confidently used as markers of

Corresponding author:
Luis Ríos. Unit of Physical Anthropology, Faculty of Biology, Universidad Complutense de Madrid, José Antonio Novais 12, 28040 Madrid; Phone: +34 91 394 5137. E-mail: lurios01@ucm.es

Submitted: February 23, 2023. **Accepted:** March 28, 2023

https://doi.org/10.52083/QAWR7133

physical activity (Villotte and Knusel, 2013). The relation of the size of the nutrient foramen on the diaphysis of limb bones with ontogenetic and mobility patterns has been studied in other organisms such as birds and kangaroos (Allan et al., 2014; Hu et al., 2018). In relation to the vascular system and the qualitative assessment of traits, it has been recently proposed that the vascular grooves in the human femur and tibia could be related to mobility and/or weight-bearing activity patterns (Soltysiak, 2015; Trujillo-Mederos et al., 2013). These authors observed a significant relationship between robusticity indices related to body size and mobility, and the presence of vascular grooves in the femur and tibia. A limitation of these studies was that they analyzed the intern sample variation of these variables, in Prehispanic individuals from the Canary Islands (Trujillo-Mederos et al., 2013), and in commingled remains from the Middle-East from the first half of the fourth millenium BCE (Soltysiak, 2015).

We present here the study of three Iberian skeletal samples spanning a chronological interval during which a decrease in ambulatory physical activity has been previously documented in European populations (Macintosh et al., 2014; Ruff et al., 2015). Basing our study on these previous findings, we would expect significant differences between the selected samples in the biomechanical parameters related to mobility. If these differences are observed, then the samples would be fit to test the hypothesis that the presence of vascular grooves in the tibia is a qualitative indicator of mobility, since we would expect more vascular grooves on the sample with biomechanic indices pointing to higher levels of mobility. Due to the complex nature of the variance in biological phenomena, the findings will be discussed in a broader context, considering other factors beyond levels of mobility.

MATERIAL AND METHODS

Three samples from different chronologies were selected: Carracasla and Wamba, curated at the Laboratory of Osteology, Faculty of Biological Sciences, Universidad Complutense de Madrid (UCM); and the documented collection from the Department of Legal Medicine, Psychiatry and Pathology, Faculty of Medicine, UCM. Carracasla is an archaeological collection recovered from the caves of the karstic system of Prádena de la Sierra (Province of Segovia, Spain). The radiocarbon date of one of these caves has resulted in 2460-2040 years cal BC, thus belonging to what is termed the North Plateau Chalcolithic (Carmona Ballestero, 2014). The minimum number of individuals of the Chalcolithic sample was 39 (epiphyses-fused right humeri), and the metric study of the 43 available pelvises (23 right pelvises, 21 left pelvises), indicated the presence of at least six women (right pelvises) and eight men (left pelvises) (Brůžek et al., 2017). Wamba is a collection named following its place of origin, the Church of Santa María de Wamba (Province of Valladolid, Spain), where a large secondary ossuary deposit was formed, dating from the 16th to 17th century, representing people affiliated with that church (López-Bueis, 1999). In this Early Modern sample, the presence of both sexes has been reported (López-Bueis, 1999), and the tibiae were selected based on visual assessment of size and robusticity with the objective of including both sexes. In these two disarticulated samples, right and left tibiae were selected for study, since each tibia probably represents one person. The documented collection is composed of skeletons of known sex and age of people who died in the city of Madrid at the end of the last century. This cemetery collection, with identification number EML-001/002, was initiated through a legal agreement between the Funeral Services of the Government of the Autonomous Community of Madrid and the Universidad Complutense de Madrid, for educational and research purposes, and complying with current legislation and personal data protection law, similar to other skeletal collections from cemeteries (Cardoso 2006; Belcastro et al., 2017).

For the present study, the three samples are named as Chalcolithic (Carracasla), Early Modern (Wamba), and Contemporary (documented). Skeletons from the Contemporary collection were divided into two age groups in the variable AGE, younger and older than 40 years. This age limit was selected due to the changes observed beyond that age in the cardiovascular system (Oxborough et al., 2014; Scuteri et al., 2014). The sex and age

composition presented an overrepresentation of people older than 60 years and more women than men for younger ages. In this sample of complete skeletons, right and left tibiae were studied, but for comparison with the other two samples, the left tibiae were selected. Sample sizes are described in detail in Table 1. Only tibiae with completely fused epiphyses, without any observable pathological condition, were selected.

To illustrate the presence of vascular grooves in the tibia, we show in Fig. 1a the dissection of the leg from a body donation with code 16/99, from the body donation program of the Department of Anatomy and Radiology, Faculty of Medicine, Universidad de Valladolid. The vascular grooves are associated to the arteries arising from the anterior tibial artery, which supply the tibialis anterior muscle (Fig. 1a). Two features of each vascular groove were recorded: position (medial, lateral or posterior side), and intensity (shallow, deep). The differentiation between shallow and deep grooves was made as follows: if the groove was completely visible at plain sight with tangential natural light, the groove was classified as deep; if additional artificial tangential light was needed to observe

Table 1. Sample sizes by collection, side, sex ad age group.

Collection	Right	Left	Female	Male	20-40 years	40+ years	Total
Chalcolithic	25	20	-	-	-	-	45
Early Modern	30	34	-	-	-	-	64
Modern	78	77	50	105	55	100	155

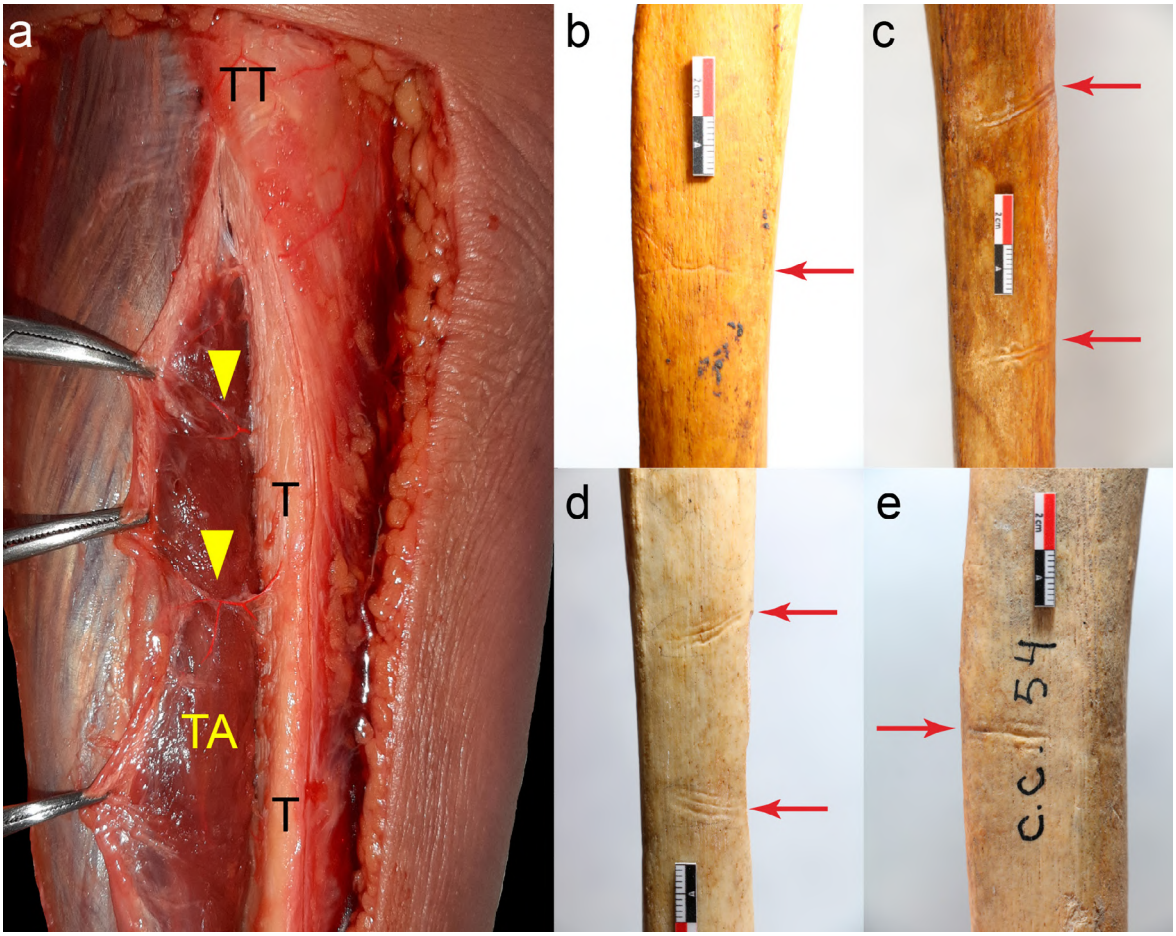

Fig. 1.- Left (**a**): Dissection undertaken at the Faculty of Medicine, Universidad de Valladolid, where the tibial tuberosity (TT) and anterior border of the tibial diaphysis (T) can be observed, as well as the tibialis anterior muscle (TA), and the transverse arteries associated to the vascular grooves of the tibial surface (yellow triangles). Right: A shallow vascular groove is shown in **b** (tibia from the Contemporary collection), while deep grooves are shown in tibia from the Contemporary (**c**), Early Modern (**d**), and Chalcolithic (**e**) samples. All vascular grooves are indicated with red arrows.

Table 2. Descriptive statistics (mean and standard deviation) of the SV (Dmax/Dmin), by collection, sex and age group.

Collection	Total		Female		Male		20-40 years		40+ years	
	Mean	S.D.	Mean	S.D.	Mean	S.D.	Mean	S.D.	Mean	S.D.
Chalcolithic	1.56	0.14	-	-	-	-	-	-	-	-
Early Modern	1.41	0.12	-	-	-	-	-	-	-	-
Modern	1.42	0.11	1.39	0.12	1.39	0.12	1.41	0.09	1.43	0.12

Table 3. Percentage of tibiae by total number of grooves and number of deep grooves, by collection.

	Number of grooves							
Sample	**0**	**1**	**2**	**3**	**4**	**5**	**6**	**7**
Chalcolithic	0,0	2,6	17,9	17,9	25,6	20,5	10,3	0,0
Early Modern	7,8	18,8	26,6	25,0	12,5	3,1	3,1	3,1
Contemporary	13,0	15,6	32,5	19,5	14,3	2,6	2,6	0,0
	Number of deep grooves							
Sample	**0**	**1**	**2**	**3**	**4**			
Chalcolithic	41,0	33,3	12,8	12,8	0,0			
Early Modern	48,4	37,5	6,3	6,3	1,6			
Contemporary	61,0	22,1	9,1	3,9	3,9			

the full extent of the groove, it was classified as shallow. The aspect of the vascular grooves in four tibiae are shown in Figs. 1b-e. The total number of grooves (NG), and the number of deep grooves (DG) per tibia were recorded. Two ordinal variables were created from these data: NG2, with two categories (0-3 grooves, 4-7 grooves); DG2, with two categories (0-1 deep grooves, 2-4 deep grooves). These tresholds for NG2 and DG2 were exploratory, and based on the rationale that an increased number of vascular grooves, or deep vascular grooves, could be associated with higher levels of the index variable of shape (see below).

Cross-sectional properties of the diaphyses that take into account the cross-section (medullary or solid), are usually analyzed to obtain, among others, measurements of bone's resistance to bending and torsional loads (second moments of area, and polar second moments of area), that allow to reconstruct mobility patterns (Ruff, 2018). External measurements of the diaphyses are also useful to study mobility patterns (Laffranchi et al., 2020; Wescott, 2006), since a reasonable correspondence has been observed between indices derived from them with those calculated upon medullary or solid cross-sections of the diaphyses (Stock and Shaw, 2007). The maximum and minimum diameter (Dmax and Dmin) at the tibial midshaft were measured with a digital caliper, and the index variable of shape SV (Dmax/Dmin) was calculated, as an alternative to the shape ratio or index of cross-sectional circularity obtained from the second moments of area (Imax/Imin) from the cross-section of the diaphysis (Macintosh et al., 2014; Stock and Shaw, 2007).

Regarding statitistical methods, first, since the shape variable SV (Dmax/Dmin) is a ratio, it was log transformed for achieving a log-normal distribution for statistical analysis. A one-way ANOVA with Tukey's HSD test for multiple comparisons was used to study the variation between the three samples in the quantitative variable SV. The Kruskall-Wallis test and the pairwise comparisons with Bonferroni correction were used to study the differences between the three samples in the number of vascular grooves, an ordinal variable. The Student's t-test for independent samples was used to study the association between the SV (quantitative variable) and the presence of vascular grooves (ordinal variables). Finally, the association of sex and age with the vascular grooves was studied with the chi-square test.

RESULTS

Descriptive statistics for the SV are shown in Table 2 (mean and standard deviation). For the NG and DG variables, percetange of tibiae by number of grooves is shown in Table 3. The one-way ANOVA (F(2,181)=[24.415], p< .001), and Tukey's HSD test for multiple comparisons, revealed that the mean value of the log-transformed SV was significantly higher in the Chalcolithic sample in comparison with the two other samples (p<.001), which did not differ between them (p=.977) (Fig. 2a). The vascular grooves were located mostly in the lateral side (90.71%), and middle third (82.67%) of the tibiae. The Kruskall-Wallis test (H=19.237, p=.001), and the pairwise comparisons with Bonferroni correction revealed that the

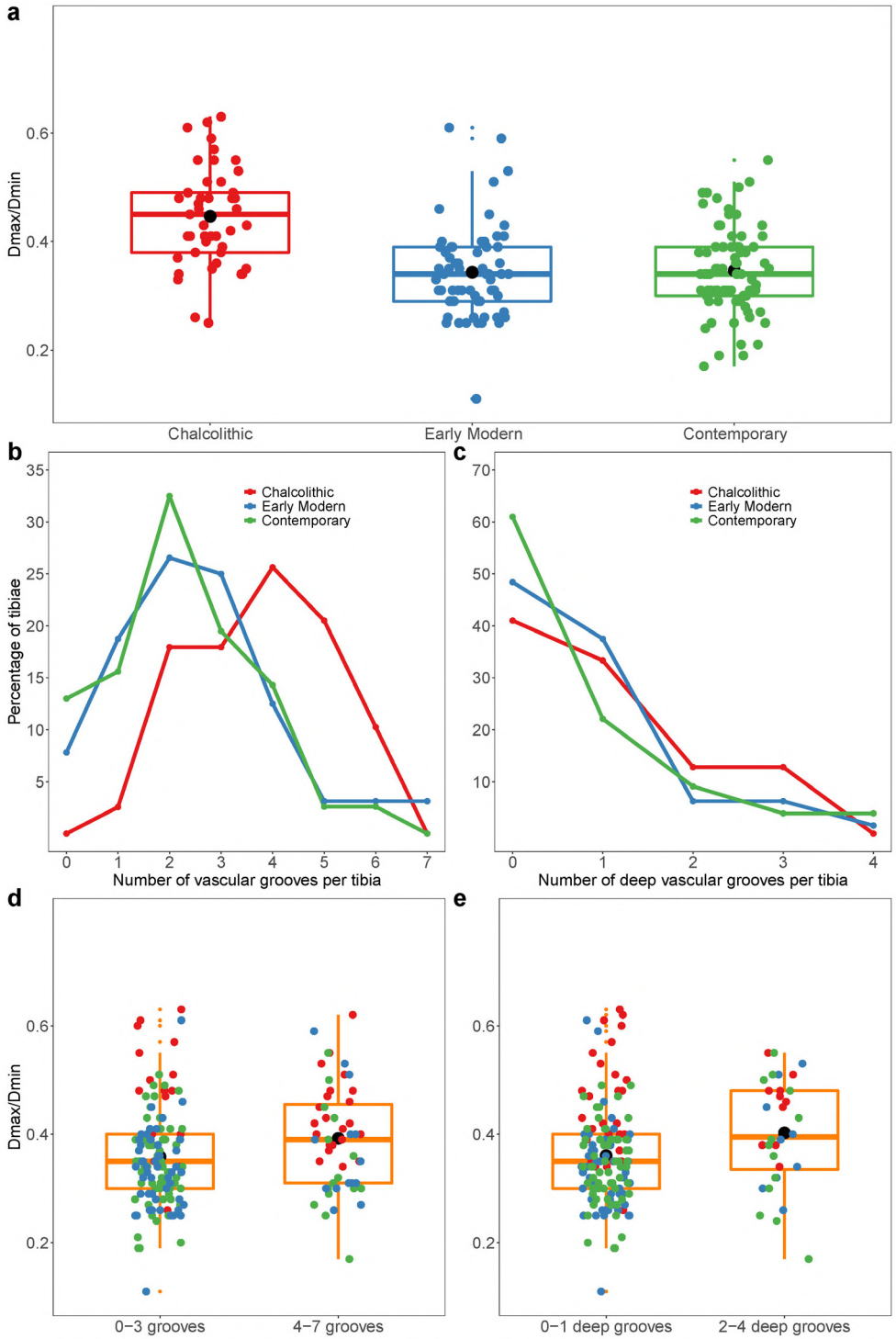

Fig. 2.- Box plot graph of the values of log-transformed SV by collection (**a**). Distribution of the tibiae by number of vascular grooves (**b**), and number of deep grooves (**c**), in percentages and by collection. Box plot graph of the values of the log-transformed SV, grouping the tibiae in two categories of total number of grooves (**d**), and number of deep grooves (**e**).

Chalcolithic sample presented a different distribution than the two other samples (p=.000, Early Modern; p=.002, Contemporary), with higher percentages of tibiae with more vascular grooves (Fig. 2b). The same test was used for the number of deep grooves (H=3.910, p=.142), and no differences were observed between the samples, although there were more tibiae with a higher number of deep grooves in the Chalcolithic sample (Fig. 2c). To study the association between the SV and the presence of vascular groups, the variables NG2 and DG2 were selected, and the Student's t-test for independent samples was used. The group of tibiae with more vascular grooves presented a significant higher value of SV for the total number of grooves or NG2 (t(176)=-2.272, p=.024), and

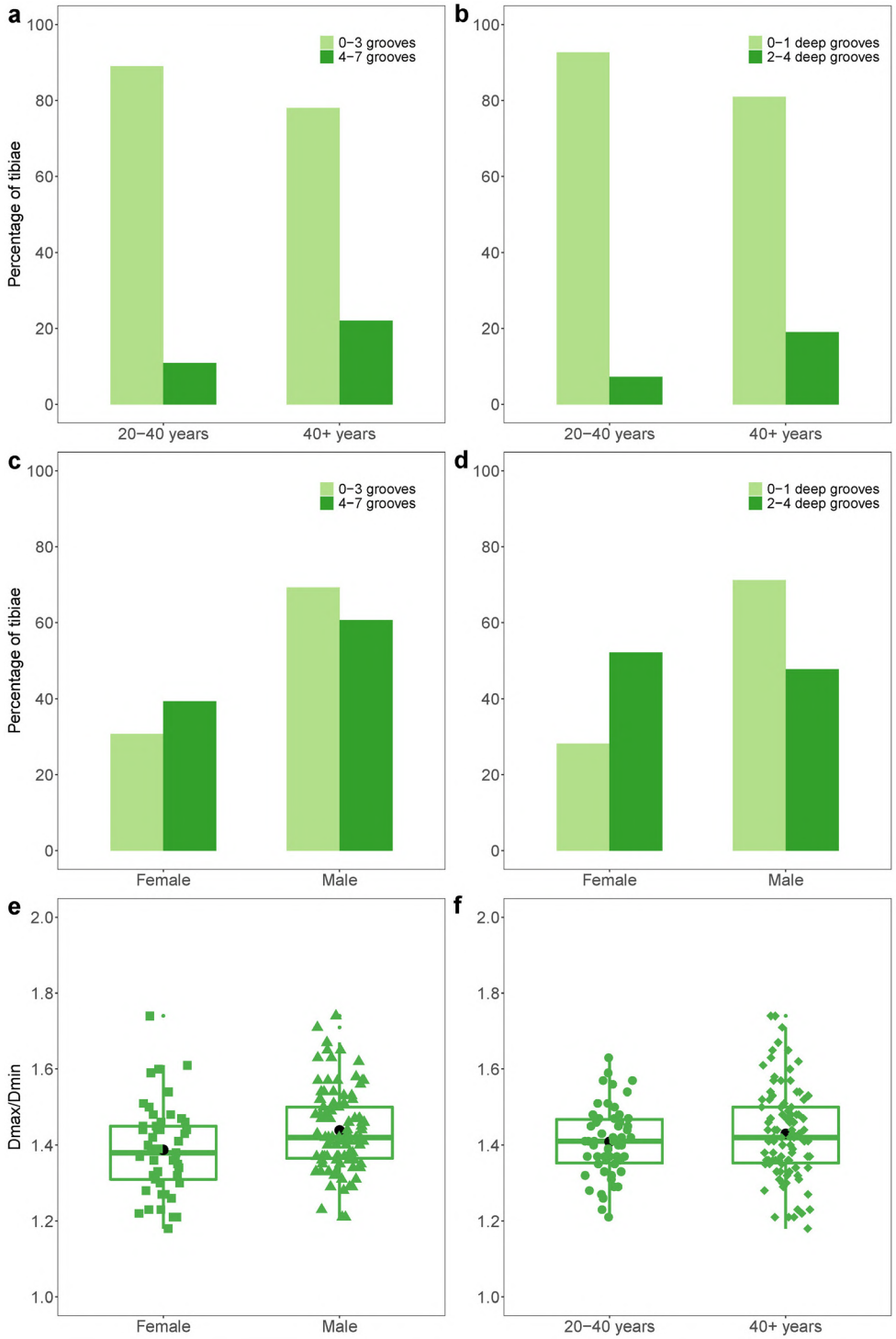

Fig. 3.- Bar graphs representing the changes associated with age in the categories of total number of groups (**a**), and deep grooves (**b**). Sexual differences in the total number of groups (**c**), and deep grooves (**d**), is also presented. Sexual differences and age changes in the values of the SV are also shown (**e** and **f**, respectively).

for the number of deep grooves or DG2 (t(176)=-2.351, p=.020) (Fig. 2d,2e).

The association of sex and age with the vascular grooves and the SV could be studied only in the Contemporary documented collection (Fig. 3). The chi-square test was used to study the relation between sex and age and the variables NG2 and DG2. The relation between sex and NG2 was significant (p=.006), while the relation with DG2 was not significant (p=.077). In both cases, women presented more tibiae with a higher number of total and deep grooves than men. The relation between the variable AGE and NG2 and DG2 was not significant (NG2, p=.086, continuity correction p=.134; DG2, p=.049, continuity correction p=.084). In both cases, tibiae in the older age group presented a higher number of total and deep grooves. With regard to the SV, the independent t-test revealed a significant difference between the sexes, with higher values for males (t(150)=-2.825, p=.005). No significant difference in SV was observed between the AGE groups (t(150)=-1.087, p=.279).

DISCUSSION

Previous biomechanical analyses have shown a temporal decrease in the values of some biomechanical properties of the cross-section of the femur and tibia in European samples from the Upper Paleolithic or Neolithic to the Early Medieval or very recent periods, associated with a decrease in ambulatory physical activity or mobility (Macintosh et al., 2014; Ruff et al., 2015). Lower circularity, or high values of the index Imax/Imin, has a strong association with high levels of terrestrial mobility, and a temporal change from lower to higher circularity of the tibia has been observed in these studies (Macintosh et al., 2014). The difference in the SV (Dmax/Dmin) between the Chalcolithic sample and the other two samples agreed with these previous results. We thus considered that the selected samples are useful to test the hypothesis of the presence of tibial vascular grooves as a qualitative marker of mobility. The Chalcolithic sample also presented a higher frequency of total number of vascular grooves, and a less marked increase in the number of deep grooves, than the two other samples, and there was a significant association between the SV and the vascular grooves. These results would support the suggestions of previous authors related to mobility (Soltysiak, 2015; Trujillo-Mederos et al., 2013), but Figs. 2D,2E indicate a more complex relation between the SV and the vascular grooves. There is a considerable overlap of values of the SV between the categories of vascular grooves, with tibias with a high value of the SV but with a lower number of total and deep grooves, and vice versa. Beyond the variation associated to the SV, the presence of vascular grooves in the diaphysis of the tibia is clearly related to other factors.

The vascular grooves studied in the present work were located mostly in the lateral side (90.7%) of the middle third of the tibia (82.67%), associated to the tibialis anterior muscle, whose most known function is foot dorsiflexion, very important in balance control and during the gait cycle (Ruiz-Munoz and Cuesta-Vargas, 2014). This well-known function of the tibialis anterior offers support to the hypothesis linking the vascular grooves with high levels of mobility, but this muscle is also involved in nonambulatory activity. Raichlen et al. (2020) examined the physical patterns of inactivity in a hunter-gatherer population, the Hadza of Tanzania, and observed that they present levels of nonambulatory time similar to those found in industrialized populations, averaging 9.9 hours of nonambulatory rest. But the Hadza often spent this time in what the authors termed “active rest” postures, which require higher levels of muscle activity than the most common posture in industrialized societies, chair sitting. One of these postures is full squatting (defined by these authors as squatting with heels in ground contact and buttocks elevated from the ground), which elicited higher levels of activity for the tibialis anterior, soleus and vastus lateralis, compared with chair sitting, as measured by electromyography (Raichlen et al., 2020). For the tibialis anterior, this activation reached almost 40% of the activation during walking. These findings are relevant from a bioarchaeological perspective, since a decline in the osteological indicators of squatting has been observed in European populations at least during the last twenty centuries (Boulle, 2001), and similar temporal changes have been observed in samples from other regions (Dlamini and Mor-

ris, 2005). As summarized by Boulle (2001), the temporal decrease in squatting could correspond to changes in interior space organization, including the increasing presence of furniture, as well as changes in some laboral activities, with less requirement of foot hyperdorsiflexion. The activation of the tibialis anterior in full squatting, and the temporal decrease of this posture, could also be associated to the variability of the frequency of vascular grooves observed in the present study. In this regard, the tibialis anterior could have been also involved in past populations in nonambulatory activities requiring foot hyperdorsiflexion. The patterns of mobility, resting posture like full squatting, and nonambulatory activities requiring foot hyperdorsiflexion, all involving the activation of the tibialis anterior, have changed through human history, and all could have a potential impact on the expression of vascular grooves on the tibia in skeletons from different periods. The difference in the SV and the distribution of the vascular grooves between the Chalcolitic sample and the other two samples would indicate a more physically active, both ambulatory and non-ambulatory, lifestyle in the former.

Other factors could be also important, like sex and age, although their effect could only be explored in the Contemporary sample. Men who lived in Madrid during the twentieth century presented higher values of the SV than women, although with a considerable overlap between sexes. Gendered division of labour has been an important factor shaping the mobility patterns in twentieth-century Western societies. Differences have been documented in work-related mobility as well as in what is termed maintenance work and mobility, associated to diverse, fundamental, non-remunerated tasks (Best and Lanzendorf, 2005). Sex also influenced the expression of vascular grooves, with women presenting a higher frequency of deep grooves than men. With regard to age, we observed an increase in the frequency of deep grooves after 40 years. Blood pressure and arterial stiffness increase with age (AlGhatrif et al., 2013; Scuteri et al., 2014), as well as muscular artery diameter, specially in women (Xu et al., 2017), and our results could be also reflecting these facts.

In conclusion, the Chalcolithic sample presented a significantly different diaphyseal shape of the tibia when compared with the Early Modern and Contemporary samples, indicating higher levels of mobility, as expected from previous works. It also presented a higher frequency of vascular grooves. But although the association between the shape of the tibia and the vascular grooves was significant, the presence of vascular grooves cannot be used to infer high levels of mobility. These vascular grooves are associated to the tibialis anterior muscle, which is activated during the gait cycle but also in what has been called “active rest” postures, and possibly in other nonambulatory activities involving foot hyperdorsiflexion. The age- and sex-related changes in the vascular system could be also important in the interpretation of these grooves. The presence of vascular grooves might be partially related to higher levels of mobility, but we conclude that it cannot be used alone as a qualitative marker of mobility in skeletal samples. Its use as a general indicator of overall lower limb muscle activity, both ambulatory and non-ambulatory, should be explored.

ACKNOWLEDGEMENTS

The authors sincerely thank those who donated their bodies to science so that anatomical research and teaching could be performed. Results from such research can potentially increase scientific knowledge and can improve patient care. Therefore, these donors and their families deserve our highest respect.

REFERENCES

ALGHATRIF M, STRAIT JB, MORRELL CH, CANEPA M, WRIGHT J, ELANGO P, SCUTERI A, NAJJAR SS, FERRUCCI L, LAKATTA EG (2013) Longitudinal trajectories of arterial stiffness and the role of blood pressure: the Baltimore longitudinal study of aging. *Hypertension,* 62(5): 934-941.

ALLAN GH, CASSEY P, SNELLING EP, MALONEY SK, SEYMOUR RS (2014) Blood flow for bone remodelling correlates with locomotion in living and extinct birds. *J Exp Biol,* 217(16): 2956-2962.

BELCASTRO MG, BONFIGLIOLI B, PEDROSI ME, ZUPPELLO M,TANGANELLI V, MARIOTTI V (2017) The History and Composition of the Identified Human Skeletal Collection of the Certosa Cemetery (Bologna, Italy, 19th-20th Century). *Int J Osteoarchaeol,* 27(5): 912-925.

BEST H, LANZENDORF M (2005) Division of labour and gender differences in metropolitan car use: An empirical study in Cologne, Germany. *J Transp Geogr,* 13(2): 109-121.

BOULLE EL (2001) Evolution of two human skeletal markers of the squatting position: A diachronic study from antiquity to the modern age. *Am J Phys Anthropol,* 115(1): 50-56.

BRŮŽEK J, SANTOS F, DUTAILLY B, MURAIL P, CUNHA E (2017) Validation and reliability of the sex estimation of the human os coxae using freely available DSP2 software for bioarchaeology and forensic anthropology. *Am J Phys Anthropol,* 164(2): 440-449.

BRZOBOHATÁ H, KRAJÍČEK V, VELEMÍNSKÝ P, VELEMÍNSKÁ J (2019) Three-dimensional geometry of human tibial anterior curvature in chronologically distinct population samples of Central Europeans (2900 BC–21st century AD). *Sci Rep,* 9(1): 4234.

CARDOSO HFV (2006) Brief communication: The collection of identified human skeletons housed at the Bocage Museum (National Nuseum of Natural History), Lisbon, Portugal. *Am J Phys Anthropol,* 129(2): 173-176.

CARMONA BALLESTERO E (2014) Dataciones radiocarbónicas de contextos calcolíticos al aire libre en la cuenca media del Arlanzón (Burgos, España). *Spal Revista de Prehistoria y Arqueología*, 23: 27-48.

DLAMINI N, MORRIS AG (2005) An investigation of the frequency of squatting facets in later stone age foragers from South Africa. *Int J Osteoarchaeol,* 15(5): 371-376.

HU Q, NELSON TJ, SNELLING EP, SEYMOUR RS (2018) Femoral bone perfusion through the nutrient foramen during growth and locomotor development of western grey kangaroos (Macropus fuliginosus). *J Exp Biol,* 221(4): jeb168625.

LAFFRANCHI Z, CHARISI D, JIMÉNEZ‐BROBEIL S, AMILELLA M (2020) Gendered division of labor in a Celtic community? A comparison of sex differences in entheseal changes and long bone shape and robusticity in the pre‐Roman population of Verona (Italy, third-first century BC). *Am J Phys Anthropol,* 173(3): 568-588.

LARSEN CS (2018) Bioarchaeology in perspective: From classifications of the dead to conditions of the living.) *Am J Phys Anthropol*, 165(4): 865-878.

LÓPEZ-BUEIS I (1999) Marcadores de estrés musculoesquelético en los huesos largos de una población española (Wamba, Valladolid). Doctoral dissertation, Universidad Complutense de Madrid.

MACINTOSH AA, PINHASI R, STOCK JT (2014) Lower limb skeletal biomechanics track long-term decline in mobility across similar to 6150 years of agriculture in Central Europe. *J Archaeol Sci*, 52: 376-390.

OXBOROUGH D, GHANI S, HARKNESS A, LLOYD G, MOODY W, RING L, SANDOVAL J, SENIOR R, SHEIKH NSTOUT M (2014) Impact of methodology and the use of allometric scaling on the echocardiographic assessment of the aortic root and arch: a study by the Research and Audit Sub-Committee of the British Society of Echocardiography. *Echo Res Pract,* 1(1): 1-9.

RAICHLEN DA, PONTZER H, ZDERIC TW, HARRIS JA, MABULLA AZP, HAMILTON MT, WOOD BM (2020) Sitting, squatting, and the evolutionary biology of human inactivity. *Proc Natl Acad Sci USA,* 117(13): 7115-7121.

RUFF CB (2018) Biomechanical analyses of archaeological human skeletons. In: Katzenberg MA, Grauer AL (eds.). *Biological anthropology of the human skeleton*. John Wiley & Sons, USA, pp 189-224.

RUFF CB, HOLT B, NISKANEN M, SLADEK V, BERNER M, GAROFALO E, GARVIN HM, HORA M, JUNNO J-A, SCHUPLEROVA E, VILKAMA R, WHITTEY E (2015) Gradual decline in mobility with the adoption of food production in Europe. *Proc Natl Acad Sci USA*, 112(23): 7147-7152.

RUIZ-MUÑOZ M, CUESTA-VARGAS AI (2014) Electromyography and sonomyography analysis of the tibialis anterior: a cross sectional study. *J Foot Ankle Res,* 7: 1-7.

SCUTERI A, MORRELL CH, ORRÙ M, STRAIT JB, TARASOV KV, FERRELI LAP, LOI F, PILIA MG, DELITA, LA ASPURGEON H (2014) Longitudinal perspective on the conundrum of central arterial stiffness, blood pressure, and aging. *Hypertension,* 64(6): 1219-1227.

SOLTYSIAK A (2015) Vascular grooves on human femora and tibiae as a potential activity-related trait. *Int J Osteoarchaeol,* 25(3): 345-351.

STOCK JT, SHAW CN (2007) Which measures of diaphyseal robusticity are robust? A comparison of external methods of quantifying the strength of long bone diaphyses to cross‐sectional geometric properties. *Am J Phys Anthropol,* 134(3): 412-423.

TRUJILLO-MEDEROS A, ARNAY-DE-LA-ROSA M, GONZÁLEZ-REIMERS E, CARMONA-CALERO E, GONZÁLEZ-TOLEDO JM, CASTAÑEYRA-RUIZ M, ORDÓÑEZ AC, CASTAÑEYRA-PERDOMO A (2013) Tibial marks in bare tibiae: relationship with robusticity indices. *Eur J Anat,* 17(1): 9-16.

VILLOTTE S, KNÜSEL CJ (2013) Understanding entheseal changes: definition and life course changes. *Int J Osteoarchaeol*, 23(2): 135-146.

WESCOTT DJ (2006) Effect of mobility on femur midshaft external shape and robusticity. *Am J Phys Anthropol,* 130(2): 201-213.

XU X, WANG B, REN C, HU J, GREENBERG DA, CHEN T, XIE LJIN K (2017) Age-related impairment of vascular structure and functions. *Aging Dis*, 8(5): 590-610.

Morphological integration and modularity of the human hand

Alexander Ermolenko

Doctor Chuchkalov Ulyanovsk Regional Clinical Center of Specialized Types of Medical Care, Ulyanovsk, Russian Federation

SUMMARY

Morphological modularity is a concept that refers to the level of covariance between the components of a structure. Morphological modules are independent subsets of correlated features; in particular, in the human hand, these are the metacarpus (metapodium) and fingers (acropodium). The human hand has been studied as an integral morphological structure for a long time, but its modularity has not been evaluated within the framework of an integrative approach. The aim of this study is to assess the hypothesis of modularity of the metapodium and acropodium of the human hand in the context of their spatial conjugacy using geometric morphometry. Using geometric morphometric methods to determine the shape and location, both modules were examined in samples from 100 digital X-ray images of the right hands of men and women, using 16 two-dimensional landmarks. The modules were compared using partial least squares analysis and the Escoufier coefficient (RV). Against the background of weak allometric effects (4.6-4.86%, $p<0.05$), there is a moderate correlation between the blocks of landmarks of the metapodium and acropodium ($RV=0.5$, $p<0.05$). Partial Least Squares analysis demonstrates that the shape of the hand is more influenced by the shape of the acropodium, and the change in the shape of the metapodium turned out to be more conservative than that of the acropodium. The observed integration of metapodium and acropodium into human hands in this study indicates the plasticity of the hand, especially its fingers in the context of the diversity of its shape.

Keywords: Human hand – Geometric morphometry – Morphological modularity – Morphological integration

INTRODUCTION

The human hand is functionally integrated as a whole, but its morphological integration is rather heterogeneous. The hand consists of several parts – metacarpus (metapodium) and fingers (acropodium)– which differ from each other in the context of development or function (Wagner and Chiu, 2001). This coordination into subunits or modules is known as morphological integration (Klingenberg and Marugán-Lobón, 2013). Integration and modularity relate to the degree of covariance between parts of a structure that represent separate areas from a developmental perspective (Adams and Felice, 2014). Some authors have proposed the metapodium and acropodium as two different human hand modules, since they are units whose parts are strongly integrated internally, but poorly integrated with each other, although hand modules can never be completely independent of each

Corresponding author:
Alexander Ermolenko. 28 Koryukin st., Ulyanovsk, Russian Federation, 432063. Phone: +79372753757. E-mail: osteon@yandex.ru

Submitted: March 4, 2023. **Accepted:** March 28, 2023

https://doi.org/10.52083/CFCN4789

other (von Cramon-Taubadel, 2022). On the other hand, modules can limit or enhance the potential of the hand to evolve into new forms, which is probably observed during the evolution of thoracic limbs in primates and humans in particular. At the same time, the metapodium and acropodium form rays that determine the shape of the hand, while in various representatives of primates, including humans, the latter are characterized by a variety of forms (Patel and Maiolino, 2016).

Thus, the idea of the modular structure of the hand is of interest in the context of the form of the latter – whether the geometry of the metapodium and acropodium can change in space without any negative consequences for the structure of the hand as a whole. The hypothesis was that there may be an ontogenetic difference between these parts of the hand, and the shape of the acropodium will affect the variability of the shape of the hand to a greater extent than the metapodium, since it has a more complex structure.

The aim of this study was to assess whether the metapodium and acropodium are two spatially conjugate parts of the hand, corresponding to a single integrated block, or form two separate modules, by using Geometric Morphometry (GM).

MATERIALS AND METHODS

Sample

Digital images of radiographs of the right hands (anterior-posterior projection, fingers in the position of reduction) of 50 men (average age 46.3 ± 1.1 years) and 50 women (average age 49.2± 0.9 years) were taken from the archive of digital images of the Department of Radiation diagnostics of the Doctor Chuchkalov Ulyanovsk Regional Clinical Center of Specialized Types of Medical Care. The criteria for inclusion in the study: the absence of fractures of the metacarpal bones and phalanges of the fingers, developmental anomalies, deformities and bone and joint pathology.

Digitization and Landmarking

On each digital image of the radiograph, 16 landmarks were located using TPSDig2 v. 1.40, which represented the metapodium and acropodium modules (Fig. 1) (Rohlf, 2015).

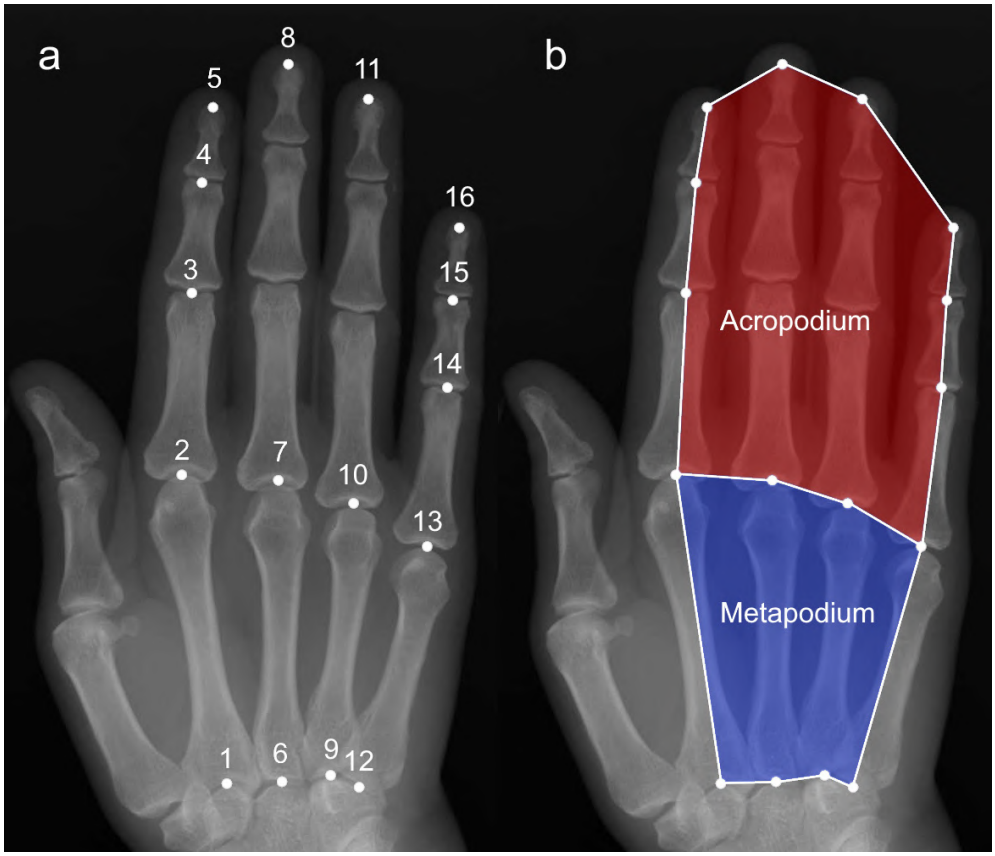

Fig. 1.- Landmark positions (**a**) and configuration of modules (**b**).

Geometric morphometric analysis

The two-dimensional coordinates of the metapodium (n=100) and acropodium (n=100) landmarks were subjected to Generalized Procrustes analysis (GPA) in order to optimally align the configuration of the landmarks in the general shape space and eliminate effects unrelated to the shape (position, orientation, scale) (Pavlinov and Mikeshina, 2002). As a result of the GPA for each configuration of landmarks, the Procrustean distance (the square root of the sum of the squares of the distances between the landmarks of this configuration) is obtained, which is a measure of the shape space and the centroid size (Centroid Size, CS is the square root of the sum of the squares of the distances between each landmark and the center of gravity, or-centroid), which is a size variable.

The evaluation of allometry (the relationship between shape and size) was carried out using multivariate regression of shape (Procrustean coordinates) as a dependent variable on size (CS) as an independent variable (Klingenberg, 2016).

Partial Least Squares analysis (PLS) was used to evaluate the interaction between modules, which allows us to study models of integration of parts within individual configurations of landmarks (Klingenberg and Marugán-Lobón, 2013). The average values of each individual's configurations were used to calculate covariance matrices between individuals. Since the degree of covariance between metapodium and acropodium is a criterion for assessing the integration and modularity of morphometric data, a measure for quantifying covariance between sets of landmarks is of critical importance. To estimate the strength of covariance between modules, the Escoufier coefficient (RV) was used, which is a multidimensional generalization of the square of the Pearson correlation coefficient (Adams, 2016). The RV coefficient is a scalar measure of the strength of the relationship between two sets of variables, which demonstrates the overall magnitude of the association between sets of variables relative to covariance within sets of variables (Klingenberg, 2009). Thus, RV values close to 0 indicate low covariance between sets of landmarks, and RV values close to 1 indicate a large covariance between them (Abdi and Williams, 2013).

MorphoJ 1.07a and OriginPro 2022 (Mann-Whitney test) were used for all statistical analyses (Klingenberg, 2011; Seifert, 2014).

RESULTS

As expected, the CS of the studied hand modules in men is larger than in women (U=2134, $p<0.05$), while the CS acropodium exceeds the size of the metapodium regardless of gender (U=2500, $p<0.05$) (Fig. 2).

Multidimensional regression of the coordinates of the Scroll depending on CS showed that that al-

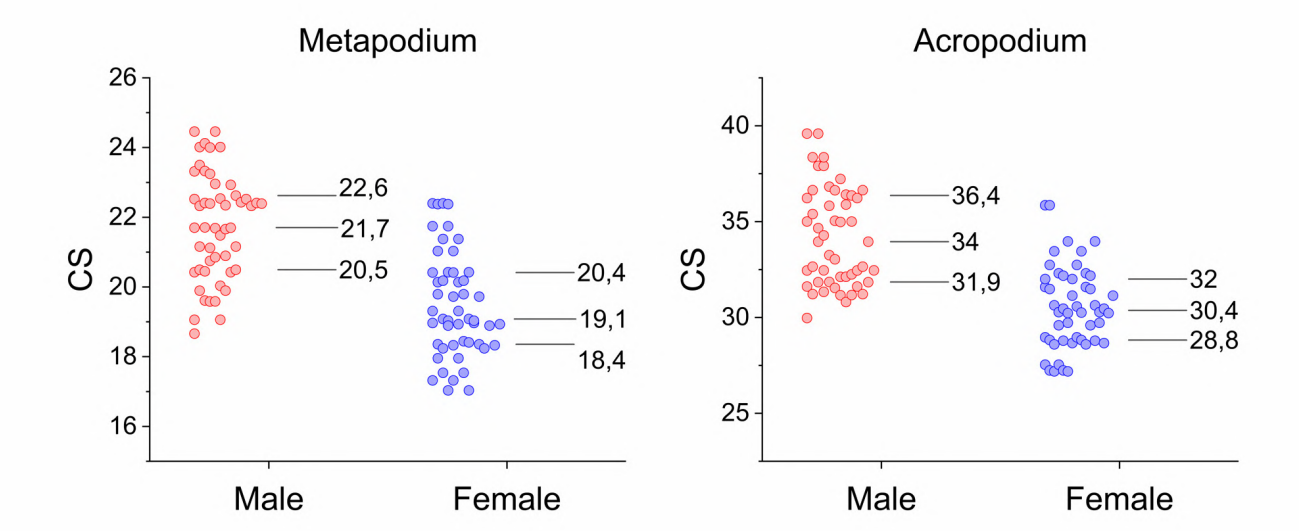

Fig. 2.- Plots of CS (Me, 25-75%).

lometry is statistically significant (10,000 random permutations). Metapodium accounted for 4.6% (p=0.0013), and acropodium accounted for 4.86% (p=0.0021) of the shape change explained by size.

The PLS results demonstrate a moderate degree of correlation between the two reference blocks (RV=0.5, p<0.0001, 10000 rounds of randomization) and the hypothesis of no covariance was rejected, which indicates the relationship between the modules. For the entire dataset, the first axis (PLS1) describes 75.2% of the total square of the covariance, indicating that it represents the main covariance of the two modules. PLS demonstrates that the shape of the hand is more influenced by the shape of the acropodium, and the change in the shape of the metapodium turned out to be more conservative than that of the acropodium (Fig. 3, Table 1).

DISCUSSION

In this study, the GM method was used to determine whether the two parts of the hand – metapodium and acropodium – are morphologically integrated or independent of each other, since integration determines the degree of their structural connection, which is significant in the context of hand morphogenesis (Adams and Felice, 2014). One of the aspects of morphological integration is that high integration of modules leads to a decrease in the diversity of the structure that these modules form, since non-weak integration between modules allows the latter to change more freely; within the framework of variation they do not have a negative impact on the structure as a whole (Zelditch and Goswami, 2021). The observed integration of the metapodium and acropodium into human hands in this study indicates the plasticity of the hand, especially its

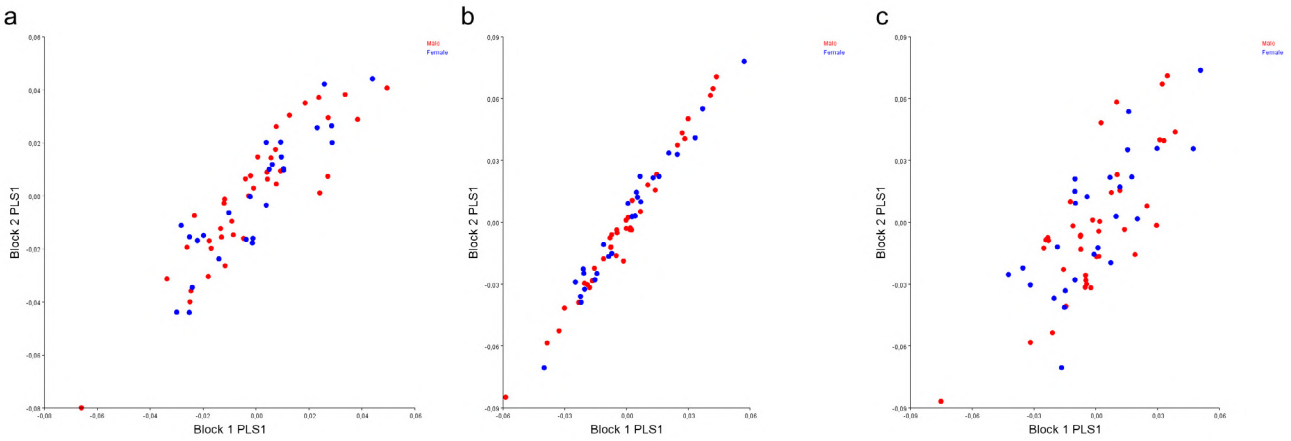

Fig. 3.- Results of two-block PLS (scatter plot of the PLS1). Hand (Block 2)/Metapodium (Block 1) (**a**). Hand (Block 2)/Acropodium (Block 1) (**b**). Acropodium (Block 2)/Metapodium (Block 1) (**c**).

Table 1. Angular comparison of hand shape vectors and covariance between two blocks of modules.

Integration	Angular value	p-value
Shape – Hand/Metapodium	26.9°	<0.00001
Shape – Hand/Acropodium	4,65°	<0.00001

fingers in the context of the diversity of its shape (Patel and Maiolino, 2016). Integration between the metapodium and acropodium in the aspect of hand shape disproportions in humans is more pronounced than in other primate species, which can be explained by the relatively independent ability to change during locomotor adaptation of the upper limbs (von Cramon-Taubadel, 2022). In the evolutionary context, one of the aspects of the phylogenetic transformation of the shape of the hand due to changes in proportions between the metapodium and acropodium is biomechanical – progressive functional improvement of the functions of the hand (thumb opposition, precision finger grip of small objects) (Patel and Maiolino, 2016; von Cramon-Taubadel, 2022). The results of testing alternative hypotheses demonstrate that a high degree of integration between modules leads to a smaller transformation of the shape of the biological object as a whole, while less integrated modules cause greater variability in shape (Klingenberg and Marugán-Lobón, 2013).

ACKNOWLEDGEMENTS

The author expresses gratitude to the radiology department of the Doctor Chuchkalov Ulyanovsk Regional Clinical Center of Specialized Types of Medical Care for providing digital images of hand radiographs.

REFERENCES

ABDI H, WILLIAMS LJ (2013) Partial least squares methods: partial least squares correlation and partial least square regression. *Methods Mol Biol*, 930: 549-579.

ADAMS DC (2016) Evaluating modularity in morphometric data: Challenges with the RV coefficient and a new test measure. *Methods Ecol Evol*, 7(5): 565-572.

ADAMS DC, FELICE RN (2014) Assessing trait covariation and morphological integration on phylogenies using evolutionary covariance matrices. *PLoS One*, 9(4): e94335.

KLINGENBERG CP (2009) Morphometric integration and modularity in configurations of landmarks: Tools for evaluating a priori hypotheses. *Evol Dev*, 11(4): 405-421.

KLINGENBERG CP (2011) MorphoJ: an integrated software package for geometric morphometrics. *Mol Ecol Resour*, 11(2): 353-357.

KLINGENBERG CP (2016) Size, shape, and form: concepts of allometry in geometric morphometrics. *Dev Genes Evol*, 226(3): 113-137.

KLINGENBERG CP, MARUGÁN-LOBÓN J (2013) Evolutionary covariation in geometric morphometric data: analyzing integration, modularity, and allometry in a phylogenetic context. *Syst Biol*, 62(4): 591-610.

PATEL BA, MAIOLINO SA (2016) Morphological diversity in the digital rays of primate hands. In: Kivell T, Lemelin P, Richmond B, Schmitt D (eds). *The Evolution of the Primate Hand. Developments in Primatology: Progress and Prospects*. Springer, New York, pp 55-100.

PAVLINOV IJA, MIKESHINA NG (2002) Principles and methods of geometric morphometrics. *Zh Obshch Biol*, 63(6): 473-493.

ROHLF FJ (2015) The tps series of software. *Hystrix, It J Mamm*, 26: 9-12.

SEIFERT E (2014) OriginPro 9.1: scientific data analysis and graphing software-software review. *J Chem Inf Model*, 54(5): 1552.

VON CRAMON-TAUBADEL N (2022) Patterns of integration and modularity in the primate skeleton: a review. *J Anthropol Sci*, 100: 109-140.

WAGNER GP, CHIU CH (2001) The tetrapod limb: a hypothesis on its origin. *J Exp Zool*, 291(3): 226-240.

ZELDITCH ML, GOSWAMI A (2021) What does modularity mean? *Evol Dev*, 23(5): 377-403.

Topographic morphometry of the pineal gland of the rat. A 24-hours period, light-dark cycle and seasonal study

Francisco Martínez Soriano, Arantxa Blasco-Serra, Eva M. González-Soler, Salvador Hernández-Sánchez, Alfonso A. Valverde Navarro

Department of Human Anatomy and Embryology, Faculty of Medicine, University of Valencia (Spain)

SUMMARY

Classical studies pointed out to a possible division of rodents' pineal parenchyma in various regions and layers, also observing variations in nuclear sizes that could depend on luminosity cycles. The aim of this study is to analyze the morphological changes of nuclear sizes of pinealocytes that occur in the pineal gland of albino rats during different hours of the day, seasons and photoperiods, taking into account the different layers and regions. We studied differences on karyometric indices of pinealocytes of the peripheral (cortical) and central (medullary) layers of pineal gland in order to analyze the circadian and seasonal modifications, and establish whether these are indicative of functional differences between proximal, intermediate, and distal portions. Results showed that the total karyometric values of the distal area are clearly higher than those of the other two areas, and in turn those of the intermediate area are also significantly higher than those of the pars proximalis; and also, that there are significant differences between the peripheral and central karyometric indices of all the pineal regions analyzed. Moreover, there are significant evolutionary circadian, photophasic and seasonal differences between regions and the pineal layers analyzed.

Key words: Karyometric indices – Pineal gland – Circadian rhythms – Morphologic variations

INTRODUCTION

The pineal gland (named "pineal" by Galen because of its resemblance to pine nuts), also known as *conarium*, or *epiphysis cerebri*, is a small neuroendocrine organ present in the nervous system of vertebrates. It is located in the ceiling of the diencephalon, behind splenium corpus callosum, between habenularis and posterior commissures. Its main function is the rhythmic synthesis and release, during the dark hours of the day–night cycle, of melatonin. This control of melatonin production is known as an endogenous circadian timing system which is suppressed by light. This relationship between luminosity and the physiology of the pineal gland has been known for a long time (Wurtman and Axelrod, 1964, Axelrod et al., 1965, Merrit and Salkowski, 1959, Wurtman and

Corresponding author:
Francisco Martinez Soriano. Department of Human Anatomy and Embryology, Faculty of Medicine, University of Valencia, Av. Blasco Ibáñez 15, E-46010 Valencia, Spain. Phone: 34.96.386.48.08; Fax: 34.96.386.41.59. E-mail: martinfr@uv.es

Submitted: February 15, 2023. **Accepted:** April 6, 2023

https://doi.org/10.52083/XDNS9336

Ozaki, 1978). This circadian rhythm, or "clock", controls a number of behaviors such as the sleep–wake cycles, feeding, and cognition rhythms. Nocturnal secretion of melatonin is present in all species analyzed so far, but is interpreted differently depending on whether the animal is nocturnal or diurnal, and it guarantees a time-sensitive and ecologically well-adapted behavior of humans and animals (Macchi and Bruce, 2004; Sapède and Cau, 2014; Koch et al., 2015; Shoja et al., 2016). Moller and Baeres described that the main cell type in mammals' pineal gland are pinealocytes (95%), followed by glial cells (astrocytic and phagocytic subtypes). Pinealocytes are responsible for the synthesis and secretion of melatonin (Moller and Baeres, 2002; Aulinas et al., 2019).

The pineal gland has been studied from different morphological viewpoints in an attempt to establish links with the corresponding physiological rhythms parameters. Its size and anatomy vary significantly among vertebrates; but among them, it should be noted that the anatomy of the rodent pineal gland is considered, by diverse morphological characteristics, more complex (Quay and Renzoni, 1966; Becker and Vollrath, 1983; Matsushima et al., 1983; Cimas et al., 1992; Sakai et al.,1996; Borjigin et al., (2012).

In view of the variable length of the pineal gland in rodents, a classification in different types was proposed (Vollrath, 1979, 1981). The long, rod-like pineal organs that read the cerebellum and are closely related to the skull, belong to types A, AB, ABC, etc. The pineal gland of the rat is classified in this last type (Fig. 1).

In a similar line, various classical morphological and physiological animal studies suggest a possible division of the pineal gland parenchyma into an external ("cortex") and central ("medullar") layers (Quay and Renzoni 1966, Romijn, 1975, Matsushima el al.1983, Semm, 1983, Cimas et al. 1992, Hira, 1998), and revealed variations in nuclear size during different point-time.

Such size variations were also established between the peripherical (cortical) and central (medullary) gland regions. Although such cortico-medullary differences have not been confirmed by all authors of that time (Welsh et al., 1979, Heidbüchel and Vollrath,1983), they have been suggested by others, especially in relation to rodents (Milline et al.,1968, Blumfield and Tap, 1970, López-Iglesias et al., 1987; Martínez-Soriano et al., 2002). Some authors (Diehl et al, 1984) have reported cortico-medullary differences, although these were found to depend of the pineal region considered. In turn, Becker and Vollrath (1983) reported rhythmic differences in pinealocyte nuclear size within the peripheral but not in the central gland layer; besides, studies in different seasons (Popova et al, 1975) have shown the central and peripheral regions of the pineal gland differ in responsive capacity.

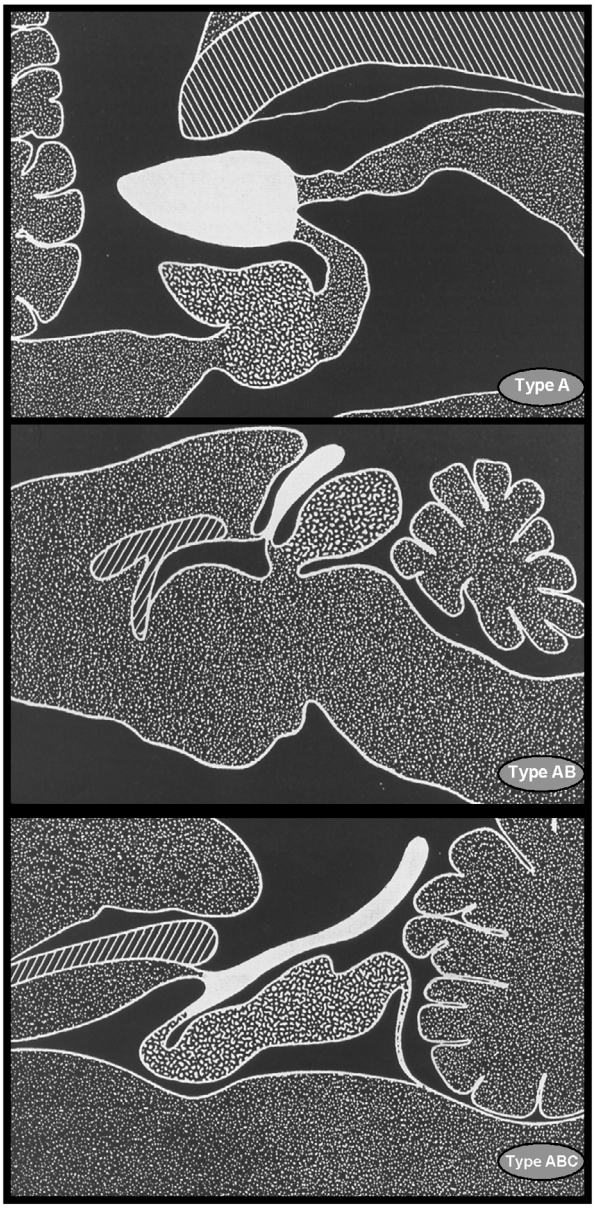

Fig. 1.- Different types of pineal gland in rodents. Based on the studies of Vollrath, 1979 and 1981.

This study attempts to establish that these karyometric differences may be a consequence of varying conditions in natural luminosity. To do this, we have studied the variations that the karyometric index of the pinealocytes of the peripheral and central layers could experience during the established photoperiods in order to be able to analyze the 24-hour periods and seasonal modifications and establish if these are indicative of functional differences between the proximal (*pars proximalis)*, intermediate (*pars intermediate)*, and distal (*pars distalis)* areas of the rat's pineal gland.

MATERIALS AND METHODS

Animals

120 adult male Wistar rats that weighed 280 ± 20 g were used for this experiment. Only male rats have been used to avoid the complex interactions that melatonin and the estrous cycle of female rats may have had in the experiment (Chuffa et al., 2013).

Animals were housed in the Central Research Unit of the University of Valencia, with a controlled cycle of 12 hours light/12 hours darkness under natural circadian and seasonal luminosity (light/dark cycle) (i.e. 08:00-18:30 pm during the short photoperiod (Winter and Autumn) and 07:00-21:30 pm. for the long photoperiod (Spring and Summer), as established from Valencia Meteorological Centre information), and constant temperature (22 ± 2 °C) and humidity (55 ± 10%). All the animals came from litters born on similar dates. Animal experimentation was carried out in accordance with the European Community's Council Directive and was approved by the Ethics Committee of the University of Valencia. Animals were weighed weekly to determine any possible differences between groups. Rats were divided in four groups of 30 rats for each season. Water and food were given ad libitum.

Animals were sacrificed in groups of five, every four hours (06:00, 10:00, 14:00, 18:00, 22:00 and 02:00). This was carried out in Autumn (20/21 October), Winter (2/3 February), Spring (20/21 April) and Summer (1/2 July).

Perfusion

Animals were sacrificed after anesthesia with an intraperitoneal injection of sodium Nembutal (10%). Afterwards, they were perfused with 5% glutaraldehide following saline cleansing. Once removed, the pineal bodies were fixed and refixed in osmium tetroxide.

Electron microscopy study

Once the pineal glands were obtained, they were post-fixed in osmium tetroxide for 90 minutes and dehydrated with graded series of acetone, stained with 5% uranyl acetate and 1% phosphotungstic acid in 70% acetone, and finally embedded in Epon resin. Afterwards, tissue was cut transversely with an ultramicrotome into thin sections and (1 µm) stained with toluidine blue (Fig. 2).

Measurements of 100 peripheral (cortical) and 100 central (medullar) pinealocyte nuclei have been previously reported to be sufficiently representative for each animal (Cimas et al., 1992). These 100 nuclei were selected from four sections taken from the *pars distalis*, *intermediate* and *proximalis*. Nuclear size measurements were made in two layers of the gland (central and peripheral layers), which have different staining aspects (Romijn, 1975). Only clearly visible pinealocyte nuclei were considered. All four selected sections were at least 15 µm away from the preceding one to avoid including the same pinealocyte nucleus in more than one section.

Nuclear measurements were performed following Martínez-Salvador et al. (2018). Once the visual field of the preparation to be analyzed was acquired, the contour of the nuclei object of analysis was drawn using an electronic pencil, and then, all the content of the screen was eliminated, except that of the surface of the drawing. Then, VISILOG program estimated nuclear volume (V) using Jacobj's formula with the following karyometric indices: longer diameter (A), shorter diameter (B) and a constant (*k*). $V = \prod/6 \times A \times B2 \times k$. (Jacobj, 1935).

To obtain the value of *k*, we took a Neubauer camera and photographed a square of it, which we subjected to the same computer process as the pieces to be studied. This gave us figures 1720 times higher than expected. Since a 1000x mag-

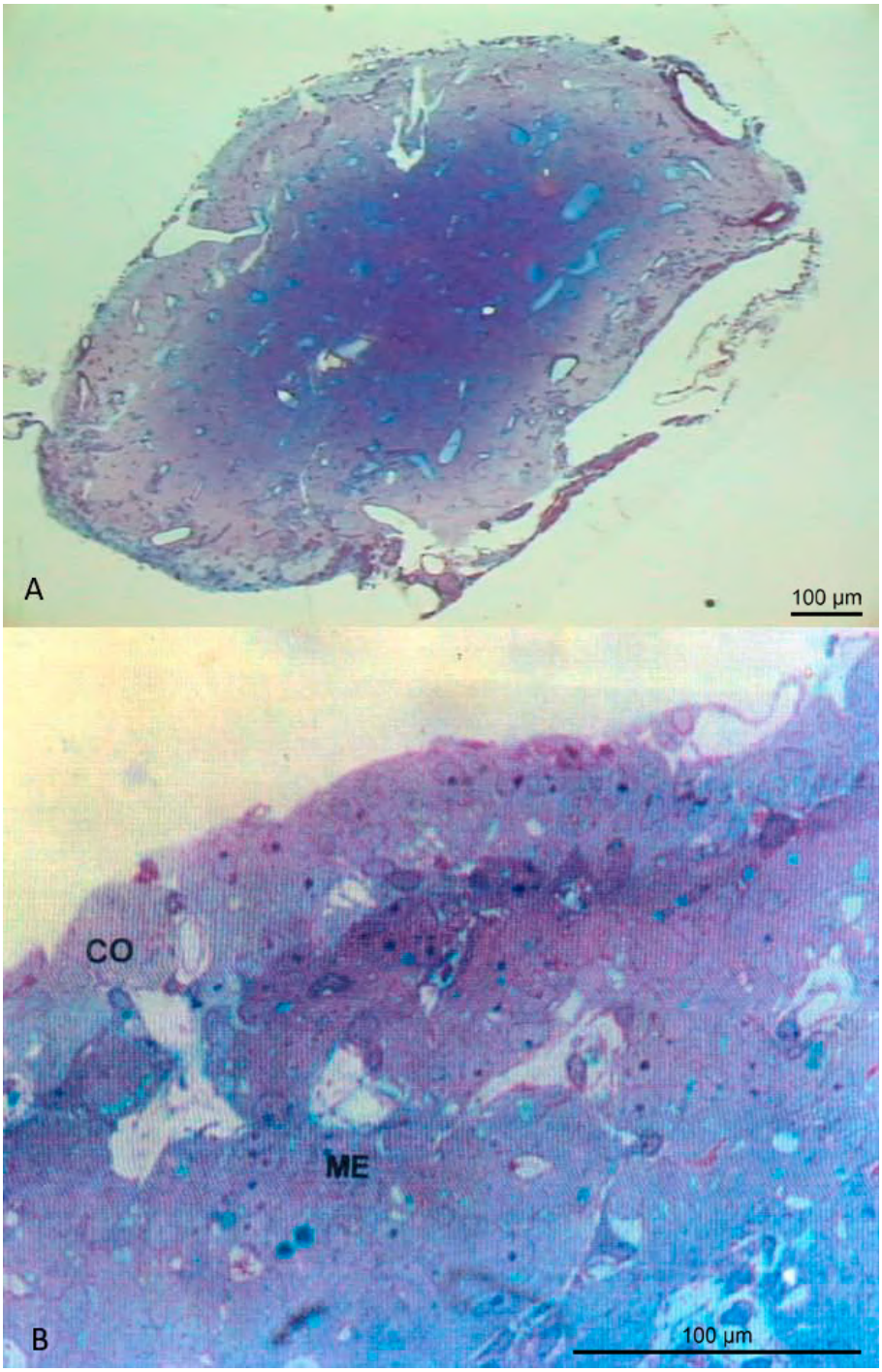

Fig. 2.- Immunohistochemical preparations (toulidine blue) of a pineal gland showing the difference between the cortical and medullary layers. CO: Cortical layer. ME: Medullary layer. Scale bars = 100 µm.

nification objective was used for the photographs, *k* would correspond to 1/1000, that is, to 1.72 the value of the constant that we need.

Statistical analysis

Statistics were done after a descriptive study. A comparative analysis of the variables was carried out by contrast and significance tests. Any P-values lower than 0.05 were considered statistically significant. An analysis of variance (ANOVA) or a Kruskall-Wallis test (depending on descriptive statistics) was used when comparing the means of more than two variables.

RESULTS

General Analyses

A general analysis of the mean volumes of the three regions shows that karyometric indices of

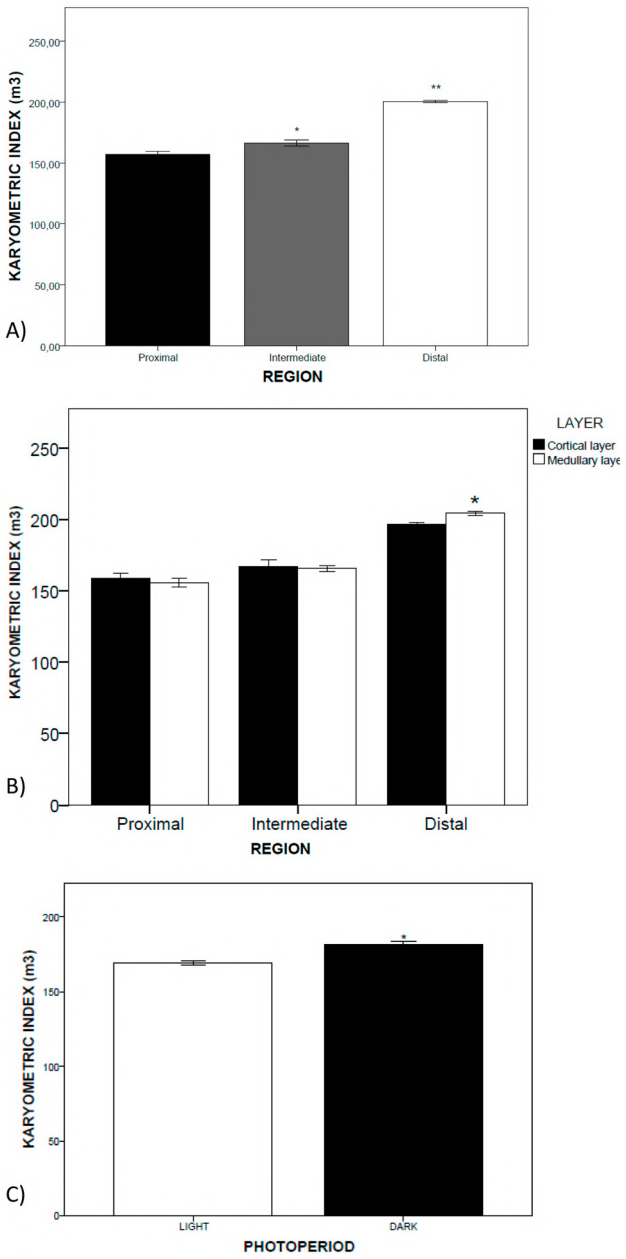

Fig. 3.- A) General comparison of karyometric indexes by regions. It can be seen that distal region has significant higher values than proximal and intermediate region. All data are presented as the mean +/- 2 SEM. *p<0,05 in respect to proximal region. **p<0,05 in respect to proximal and intermediate regions. **B**) General comparison of karyometric indexes by regions and layers. It can be seen that in the distal region, medullary layer values are significantly greater than the cortical ones, while cortical layer's karyometric indices in the intermediate and proximal tend to be higher. All data are presented as the mean +/- 2 SEM. *p<0,05 in respect to cortical layer of distal region. **C**) General comparison of karyometric indices depending on the photophase. There are statistically significant differences between the light and dark phases. All data are presented as the mean +/- 2 SEM. *p<0,05 in respect to light phase.

the distal region (or *pars distalis*) are significantly greater than those of the intermediate (or *pars intermediate*) and proximal (or pars *proximalis*) regions, being this last the region with the lowest karyometric indices (F=485,32, p<0,05) (Fig. 3A).

On the other hand, and once the sample has been segregated according to layers, a general analysis by layers shown that, in the p*ars distalis*, the medullary layer values are greater than the cortical ones (F = 76.140; p <0.01), while in the case of karyometric indices in the intermediate and proximal regions (or *pars*), cortical layer tend to be higher than the medullary, during dark phase, (F = 0.402; p> 0.05 and F = 1.517; p> 0.05; respectively). On the contrary, values of medullar layer are higher that cortical, but not in a significant manner (Fig. 3B).

General analyzes focused on karyometric indices depending on the photophase (light or dark), independently of other variables, show higher values in the dark photoperiod (t=-9,549; p<0,01) (Fig. 3C).

Proximal Region (*Pars proximalis*)

24-hour evolution

a. Cortical layer

Results show that evolution of karyometric indices throughout 24 hours is different, and constant alternating ascending and descending changes between the different time points of seasons can be observed. A substantial oscillation can be observed from 6 to 10 AM (Fig. 4).

b. Medullary layer
Circadian evolution of karyometric indices in the medullary layer happens to be different and alternating, but follows a more regular line compared to cortical layers (Fig. 4).

Seasonal Evolution

Focusing analytically on a seasonal analysis, results show that karyometric indices of medullary layer decrease progressively since the spring with respect to indices of the cortical layer, which slightly increase. This tendency becomes statistically significant in the summer (F=5,699; p<0,05) (Fig. 5).

Photophasic evolution

A more exhaustive analysis, taking into account the cell layers, results show a tendency of the karyometric indices to be higher in the medullary layer on the light photoperiod, with respect to the cortical layer (t=-3,396; p<0,01). Otherwise, karyometric indices of the medullary layer are smaller with respect to the cortical layer in the dark photoperiod (t=2,264; p<0,05) (Fig. 6).

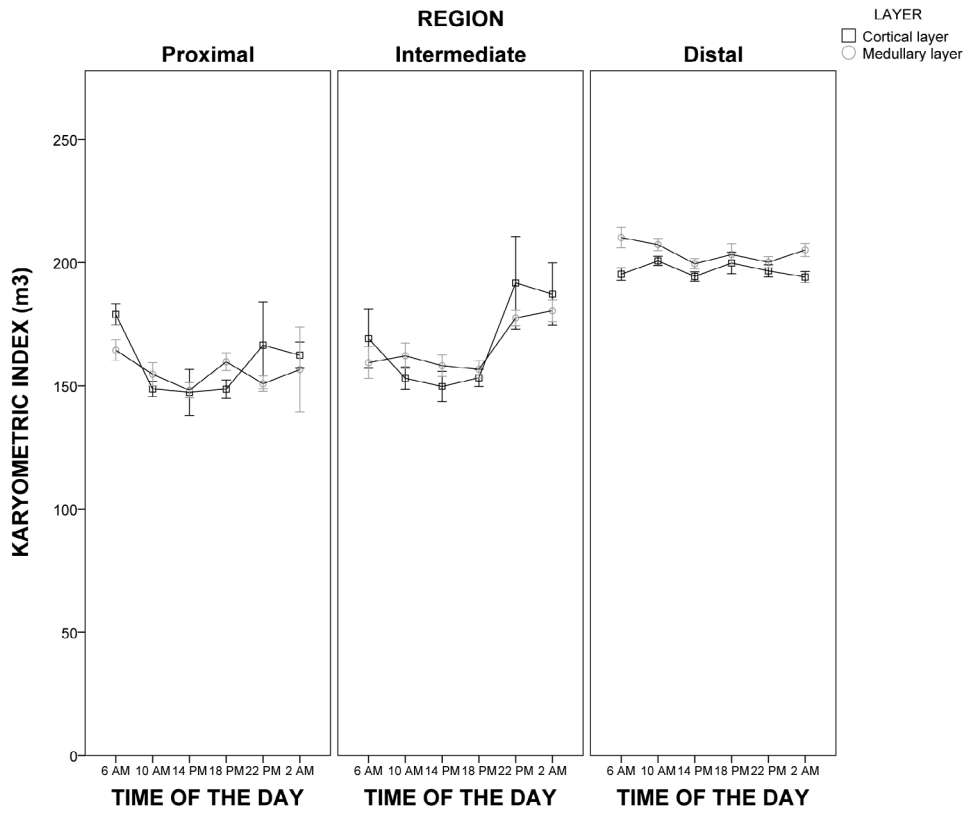

Fig. 4.- Evolution of karyometric indices in layers throughout 24 hours and divided by regions. All data are presented as the mean +/- 2 SEM.

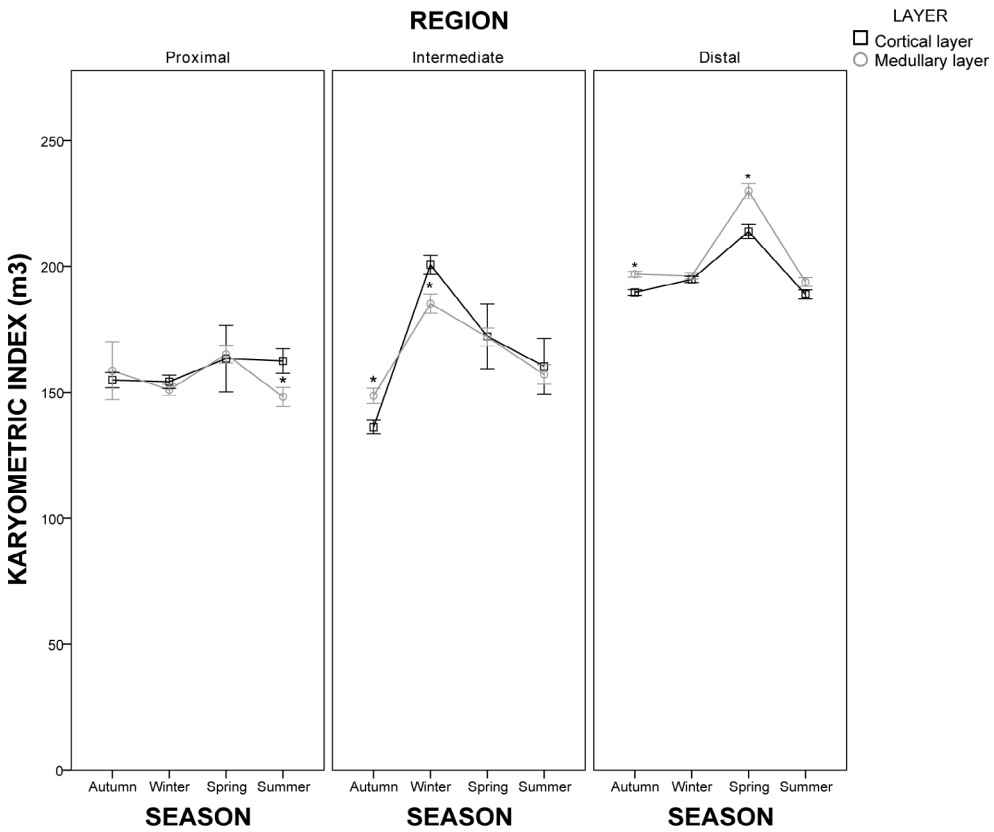

Fig. 5.- Seasonal evolution of karyometric indices in layers and divided by regions. A decrease of values can be seen on the medullary layers in respect to cortical layers on proximal region on summer and winter; on the other side, parallel curves can be appreciated on intermediate and distal regions, with some statistically significant points on the autumn-winter period (intermediate region) and in autumn and spring (distal region). All data are presented as the mean +/- 2 SEM. *p<0,05 in respect to cortical layer.

Intermediate Region (*Pars Intermediate*)

24-hour evolution

a. Cortical layer
Evolution of karyometric indices throughout 24 hours is different, observing a substantial oscillation from 18 to 22 PM (Fig. 4).

b. Medullary layer
Circadian evolution of karyometric indices in the medullary layer happens to be different and alternating, but, again, follows a more regular line compared to that of the cortical layer. Nevertheless, a similitude with changes in the cortical layer's karyometric indices can be seen on the 18-22 PM oscillation (Fig. 4).

Seasonal Evolution

In this area the values of both layers are very similar throughout the long photoperiod seasons, and results show an evolution curve overlapping in the spring-summer period, and those of the peripheral layer become greater in the winter. Results show significant differences between layers in the autumn (t= -3,52, p<0,05) and winter (t=4,03, p<0,05), the short photoperiods (Fig. 5).

Photophasic evolution

General results for the region show statistically significant differences between the light and dark photoperiods. Taking into account the cell layers, results show high medullary layer karyometric indices with respect to the cortical layer during the light period (t=-2,066; p<0,05); and on counterpoint, karyometric indices of the medullary layer are smaller with respect to the cortical layer in the dark photoperiod (t=2,105; p<0,05) (Fig.6).

Distal Region (*Pars Distalis*)

24-hour evolution

a. Cortical layer
Results show that karyometric indices' curves are very similar independently of the time of the day (Fig. 4).

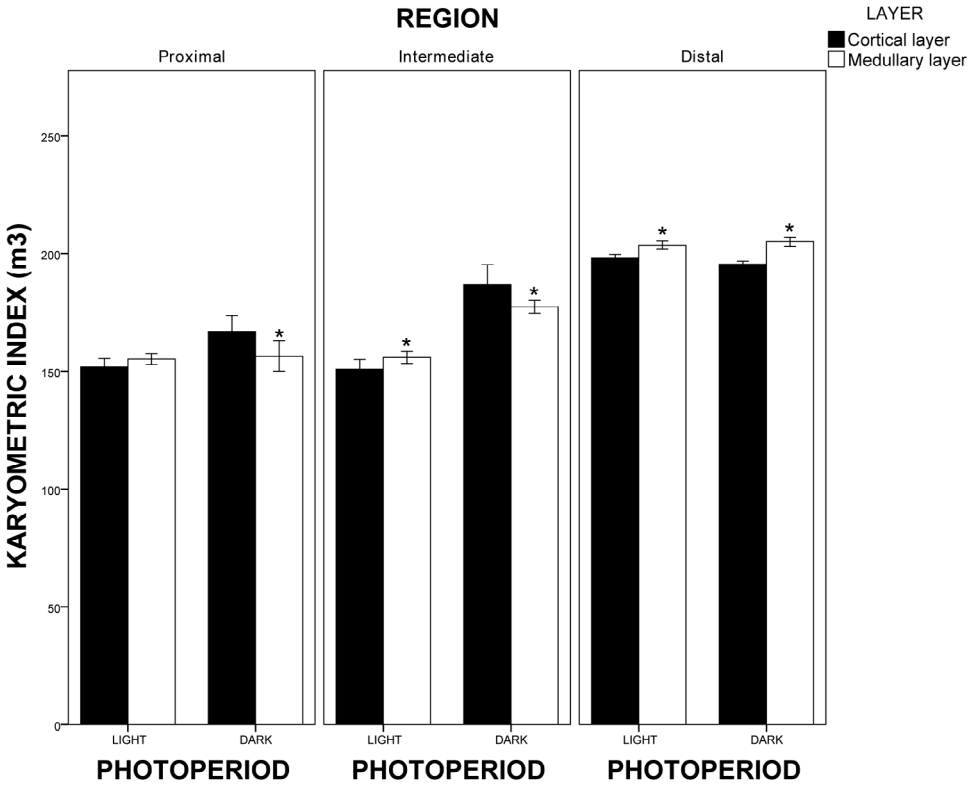

Fig. 6.- Photophasic evolution of karyometric indices in layers and divided by regions. In the proximal region, it can be seen that there is an increasing tendency of these indexes on the cortical layer in darkness in respect to the light photoperiod. This is the opposite in the medullary layer. Also, indexes are higher in the medullary layer on the light photoperiod, in respect to cortical layer; on the contrary, they are higher in the cortical layer on the dark photoperiod. In the intermediate region, values are significantly higher in both layers in the dark photoperiod. In the distal region, results show that indexes are similar in both light and dark photoperiods. Nevertheless, there's a significant decrease of values on the cortical layer in respect to medullary layer in the dark photoperiod. All data are presented as the mean +/- 2 SEM. *p<0,05 in respect to cortical layer.

b. Medullary layer
   In the medullary layer, it can be observed that the general evolution of the circadian curves is very similar to those of the cortical layer (Fig. 4). Interestingly, even though the curves are quite regular and have no large oscillations, karyometric indices are higher during all day than those seen in the other regions.

Seasonal Evolution

Results show that the karyometric indices' curves are similar, practically parallel. Nevertheless, results also show that the medullary layer has higher values; these differences are statistically significant on autumn and spring (Fig. 5).

Photophasic evolution

General results for the region did not show statistically significant differences between the light and dark photoperiods. Nevertheless, there are significant differences: in both photoperiods (light and dark), the medullary layer's karyometric indices are higher than those of the cortical layer (t=-4,489; p>0,05; t=-8,138; p<0,01; respectively) (Fig. 6).

DISCUSSION

Starting by analyzing the general aspects of the results, we can observe that the total karyometric values of the distal region are clearly higher than those of the other two regions, and in turn those of the intermediate region are also slightly (but significantly) higher, over those of the pars proximalis (Fig. 3). Within each of these three regions there are also differences, since while in the distal region the medullary layer values are higher than the cortical ones, in the intermediate and proximal portion the cortical values tend to be higher, but no statistically significant differences are found in between them (Fig. 3).

If we go on to analyze the variations that occur in the cortical and medullary layers of each of the pineal regions throughout the four seasons, (Fig. 5), two interesting circumstances are observed: the first is that, while in the distal and intermediate portions the evolution of both layers maintains a certain parallelism throughout all the seasons, in the proximal part the behavior during spring and summer is different (and opposite), and it becomes parallel in the autumn and winter seasons, which would suggest an influence of the short photoperiod seasons on the functioning of both layers in this pineal segment. Another aspect to highlight along the same lines is that, while in the distal region the values of maximum cortical and medullary activity occur in the spring season, in the intermediate season they occur in the winter season; and in the proximal region, it is maximum in the spring for the medullary layer and in the summer for the cortical layer, which indicates that the seasonal influence is not produced in a uniform way over the entire gland. Likewise, these variations are another piece of data that points to the difference in functional behavior between all the factors analyzed in this work, variations that undoubtedly seem to be determined by the photophysical characteristics (geomagnetic variations, wavelengths of solar radiation...) of seasonal evolution, which influence each one of the pineal regions differently (Gerasimov et al., 2014).

Differences between the medullary and cortical layers also exist in each of the regions according to photoperiods, since while in the distal part the karyometric indices of the medullary layer are always higher in both photophases, in the intermediate and proximal region the medullary layer's values are higher during the light photoperiod, but the cortical layer's values are higher during the dark period (Fig. 4). All these data point to the global existence of differences in the karyometric indices between the three pineal portions analyzed, and also to differences between the peripheral and central layers of each of the pineal regions analyzed, differences that seem to be mediated by the photophase.

Analyzing more specifically the 24-hour period evolution of the cortical and medullary layers (Fig. 6), we observe that the cortical layer of the proximal and intermediate regions tends to show the higheest oscillations, and has a different evolution than the medullary layer. Otherwise, both the scortical and medullary layer of the distal region follow a similar evolution, being the medullary layer's karyometric indices higher than those of the cortical layer; and these indices of the distal region are higher than those expressed by the other regions.

In view of all these circumstances, it seems evident that the behavior of the cortical and medullary layers in each of the pineal segments is different, and that seasonal, circadian and photophasic factors are not the only ones that must be intervening in this difference. In any case, these results support and reaffirm the importance of the effect of the season, the photophase and the 24-hour variations according to the topographic location of the pinealocyte within the gland. This would explain the discordant results of the different experts in the field regarding the variation of the karyometric indices both in the peripheral (cortical) or central (medullary) layer, since, they may be different depending on the time, the season and the region in which the measurement is made: thus, , while in the proximal and intermediate parts the cortical values seem to be higher, in the distal region the higher values are the medullary ones.

Our results coincide in supporting the existence of two zones/layers: peripheral (cortical) and central (medullary); and three regions (pars): proximal, intermediate and distal, which would be functionally different in the pineal gland of the rat, as pointed out by the team of Hira (Hira et al., 1988); this functionality would be determined by a combined influence of the geomagnetic and photophasic aspects of the 24-hour rhythms, seasons and light-dark photophases, as suggested in turn by the Cimas and Martínez-Soriano teams (Cimas et al., 1992; Martínez-Soriano et al., 2002). In this sense, Matsushima's team (Matsushima et al., 1993) showed that the volumes of pinealocytes in the pineal glands of rats subjected to a magnetic field during the months of April and October experienced volumetric differences between both layers and regions, in a proximal-distal direction and even between day and night, but these differ-

ences were vaguely significant in the intermediate zone. Photophasic differences were quite evident in the month of April and disappeared during the month of October. Authors concluded by suggesting that the influence of a magnetic field could exert a control mechanism of the day/night rhythms of the pinealocytes of the rat's pineal gland.

Some other published data would support this hypothesis: it is known that 90% of pineal cellularity is made up of pinealocytes, and within this population two subtypes have been described, α and β: while α constitutes 5% of pinealocyte population, β constitutes the remaining 85 (Pévet, 1977; Moller and Baeler, 2002). Receptors for adrenergic (Adrb1, Adra1b, Drd4) and cholinergic (Chrna3, Chrnb4) agonists have been found in them, and both express high levels of up to 49 different transcriptionists, which are found in the pineal gland and in the retina (Coon et al., 2019). Pinealocytes α have the specialized role of the methylation of N-acetyl-serotonin-methyl-transferase (ASMT), which is produced and released by pinealocytes β, so both constitute a fundamental set in the elaboration of melatonin, with transcriptional changes that occur between night and day, especially in β-type pinealocytes (Mays et al., 2018).

It is also known that melatonin receptors are widely expressed not only in the Central Nervous System (CNS), but in numerous peripheral tissues, which determines that the circadian rhythm of circulating pineal-derived melatonin can have important effects on the temporary functional organization of almost all peripheral organs, without this influence being necessarily involved in the feedback through the Suprachiasmatic Nucleus (Hardeland, 2013).

Pituitary adenylate-cyclase activating polypeptide (PACAP) is a neuropeptide that was isolated in the hypothalamus and localized in the central and peripheral nervous systems. Specific receptors for it have been found in the pinealocyte membrane and in nerve fibers that access the pineal gland. This neuropeptid stimulates the secretion of melatonin (Liu and Moller, 2000; Moller and Baeres, 2003).

On the other hand, it is also known that the distal pineal region receives a large number of vegetative afferent terminals from the superior cervical ganglion, via *nervus pinealis*. As these terminals descend towards the proximal region of the pineal gland, they decrease in number and practically almost disappear. On the contrary, numerous fibers of central origin are present in the proximal region, which attach to the pineal through the habenular and posterior commissures. Furthermore, the evident differences in the structure of both regions already suggest that both of them may be functionally different, the intermediate region being a transition zone between the other two.

Our results support the data provided in previously cited works and reaffirm the importance of the effect of season, photophase and 24-hour periods on the topographic location of the pinealocyte within the gland. Furthermore, this is thefirst study carried out in rats in a systematic way (together with Hira et al., 1998, and to the best of the authorss knowledge) which, taking into account not only the photophasic, daily or seasonal factors, but also the layers), can establish that differences in the karyometric indices, found according to the most proximal or distal, could be a reason that explains the discordant results of the different authors regarding the greater or lesser volume of the karyometric indices of the peripheral or central zone, since, as already expressed above, these may be different depending on the time, season and the region in which the measurement is carried out: thus, it can be clearly observed that, while in the proximal and intermediate parts the cortical values seem to be higher, in the distal, on the contrary, the higher values are the medullary ones.

This morpho-functional topographic distribution is suggestive of the possible existence of several different layers or "organs" in the pineal parenchyma, and would justify the application and use of the term "pineal complex" to the whole, (as suggested by Vollrath, 1985) since it could be an organ with sub-organs of functional characteristics and different cyclic elements in its interior that respond to geomagnetic and photophasic influences. Electrophysiological data existing in the literature could support this opinion. Indeed, several classic authors pointed to the existence

of pineal zones with different registers, and even pinealocytes with different electrical activity at rest or activity, day/night or under the stimulation of different hormones and chemical substances (Dafny, 1975; Semm and Vollrath, 1979, 1980; Reuss and Vollrath, 1984; Reuss et al., 1984). The existence of circadian, ultradian and infradian rhythms (Vollrath, 1981) in melatonin secretion also points in this direction.

On the other hand, it is also interesting to note that, according to existing data in the literature (Quay and Renzoni, 1966; De la Guardia et al., 1988; Giménez-González et al., 1991; Guillot-Valls et al., 1995), the medullary layer of the pineal gland of the rat is more susceptible to changes such as magnetic field influences or luminosity of different natures, than the cortical layer; in this same way, Martínez-Soriano et al. argued that the combined, seasonal, photophasic and lunar synodic influences are more specific on the medullary zone than on the peripheral one (Martínez-Soriano et al., 2002). So, it can be deduced that latitude andthe variation of light radiation and geomagnetic action are factors that could influence pineal functioning, and therefore its nuclear dynamics (Quay,1963; Cuello and Tramezzani, 1969).

An interesting issue to point out as a limitation of the present study is the exclusive use of male animals. As already mentioned, the use of females has been avoided due to the well-known influence and interaction of melatonin and reproductive hormones in mammalian species (Ozaki et al., 1978; Tamura et al., 199; Chuffa et al., 2013; Takahashi et al., 2021). In fact, there are studies that, after surgical removal of the pineal gland in females, found interesting changes in cycle hormones, but in turn evidenced that there is melatonin synthesis in sites other than the pineal gland (Dardes et al., 2000). Given all these complicated but interesting interactions, and considering that their study was not part of this project, it was decided to dispense with females. Still, it would be interesting that these types of studies begin to be carried out also in females as a future line of research, and, in turn, compare these results with those already existing in males.

ACKNOWLEDGEMENTS

The authors thank Prof. Francisco Montes-Suay for his help in statistical analysis.

FUNDING

This work was supported by FIS (health research fund - Fondo de investigación en salud) grants, designed by Carlos III Health Institute (ISCIII), to the project “Chronobiology of the pineal gland. Morphometric and embryological analysis”, [Ref. P1031081].

REFERENCES

AULINAS A (2019) Physiology of the Pineal Gland and Melatonin. In: KR Feingold (ed.). Endotext. MDText.com, Inc.

AXELROD J, WURTMAN RJ, SNYDER SH (1965) Control of hydroxyindole-O-methytransferase activity in the rat pineal gland by environmental lighting. *J Biol Chem,* 240: 949-954.

BECKER UG, VOLLRATH L (1983) 24-hour variation of pineal gland volume: Pinealocyte nuclear volume and mitotic activity in male Sprague-Dawley rats. *J Neural Transm,* 56(2-3): 211-221.

BORSIGIN J, ZHANG L, CALINESCU AA (2012) Circadian regulation of pineal gland Rhytmicity. *Mol Cell Endocrinol*, 349: 13-19.

BLUMFIELD MG, TAPP E (1970) Measurements of pineal parenchymal cells and their nuclei in the albino rat at different ages. *Acta Morphol Neerl Scand,* 8: 1-8.

COON SL, CONG F, HARTLEY SW, HOLTZCLAW L, MAYS JC, KELLY M, KELLEY MW, MULLIKIN JC, RATH MF, SAVASTANO LE, KLEIN DC (2019) Single cell sequencing of the pineal gland: the next chapter. *Front Endocrinol,* 20(10): 590.

CHUFFA LG, SEIVA FR, FÁVARO WJ, AMORIN JP, TEIXEIRA GR, MENDES LO, FIORUCCI-FONTANELLI BA, PINHEIRO PF, MARTÍNEZ M, MARTÍNEZ FE (2013) Melatonin and ethanol intake exert opposite effects of circulating estradiol and progesterone and differentially regulate sex steroid receptors in the ovaries, oviducts and uteri of adult rats. *Reprod Toxicol,* 39: 40-49.

CIMAS C, MARTÍNEZ-SORIANO F, RUIZ A (1992) Circadian and seasonal corticomedullary variations in pinealocyte nuclear size: a comparative and statistical analysis. *Histol Histopathol,* 7: 679- 687.

CUELLO AC, TRAMEZZANI JH (1969) The epiphysis cerebri of the Weddell seal: its remarkable size and glandular pattern. *Gen Comp Endocrinol*, 12(1): 154-164.

DAFNY N, MCCLUNG R, STRADA SJ (1975) Neurophysiological properties of the pineal body. 1. Field potentials. *Life Sci,* 16: 611-620.

DARDES RC, BARACAT EC, SIMÕES MJ (2000) Modulation of estrous cycle and LH, FSH and melatonin levels by pinealectomy and sham-pinealectomy in female rats. *Prog Neuropsychopharmacol Biol Psychiatry*, 24(3): 441-453.

DE LA GUARDIA F, MARTINEZ SORIANO F, RUIZ TORNER A, OLCINA P (1988) Pinealocyte karyometric modifications in the albino rat following the application of magnetic fields. *Z Zellforch Microsk Anat Histochem,* 102(4): 609-618.

DIEHL BJM, HEIDBÜCHEL M, WELKER HA, VOLLRATH L (1984) Day/night changes of pineal gland volumes and pinealocyte nuclear size. Assesses over 10 consecutive days. *J Neural Transm,* 60: 19-29.

GERASIMOV AV, KOSTYUCHENKO AS, SOLOVIEVA AS, OLOVNIKOV AM (2014) Pineal gland as an endocrine gravitational lunasensor: manifestation of moon-phase dependent morphological changes in mice. *Biochemistry,* 79(109): 1316-1323.

GIMÉNEZ-GONZÁLEZ M, MARTÍNEZ-SORIANO F, ARMAÑANZAS E, RUIZ-TORNER A (1991) Morphometric and structural study of the pineal gland of the Wistar rat subjected to the pulse action of a 52 Gauss, (50 Hz) magnetic field. Evolutive analysis over 21 days. *J Hirnforsch,* 32(6): 779-786.

GUILLOT-VALLS MD, HERNÁNDEZ-GIL-DE-TEJADA T, MARTÍNEZ-SORIANO F (1995) A morphometric and statistical study of the effects of soft laser (He-Ne) irradiation on the pineal gland. *Histol Histopathol,* 10(2): 351-358.

HARDELAND R (2013) Chronobiology of melatonin beyond the feedback to the suprachiasmatic nucleus-consequences to melatonin dysfunction. *Int J Mol Sci,* 14(3): 5817-5841.

HEIDBÜCHEL V, VOLLRATH L (1983) Morphological findings relating to the problem of cortex and medulla in the pinal gland of rats and hamsters. *J Anat,* 136: 723-734.

HIRA Y, SAKAI Y, MATSUSHIMA S (1998) Quantitative light microscopic study on the heterogeneity in the superficial pineal gland of the rat. *Anat Rec,* 250(1): 80-94.

JACOBJ JL (1935) Die Zellkerngrösse beim Menschen. Ein Beitrag zur quantitativem Zytologie. *Z Zellforch Microsk Anat Histochem,* 38: 161-240.

KOCH M, FERREIRÓS N, GEISSLINGER G, DEHGHANI F, KORF HW (2015) Rhythmic control of endocannabinoids in the rat pineal gland. *Chronobiol Int,* 32(6): 869-874.

LIU W, MOLLER M (2000) Innervation of the rat pineal gland by PACAP-immunoreactive nerve fibers originating in the trigeminal ganglion: a degeneration study. *Cell Tissue Res,* 301(3): 369-373.

LÓPEZ-IGLESIAS C, ARIAS JC, ALVAREZ-URÍA M (1987) The rat pinealocyte during the strous cycle. A morphometric study. *Arch Anat Microsc Morphol Exp,* 75: 19-27.

MACCHI MM, BRUCE JN (2004) Human pineal physiology and functional significance of melatonin. *Front Neuroendocrinol,* 25(3-4): 177-195.

MARTÍNEZ-SALVADOR J, RUIZ-TORNER A, BLASCO-SERRA A, MARTÍNEZ-SORIANO F, VALVERDE-NAVARRO AA (2018) Morphologic variations in the pineal gland of the albino rat after a chronic alcoholisation process. *Tissue Cell*, 51: 24-31.

MARTÍNEZ-SORIANO F, ARMAÑANZAS E, RUIZ-TORNER A, VALVERDE-NAVARRO AA (2002) Influence of light/dark, seasonal and lunar cycles on the nuclear size of the pinealocytes of the rat. *Histol Histopathol,* 17: 205.212.

MATSUSHIMA S, MORISAWA Y, AIDA Y, ABE K (1983) Circadian variations in pinealocytes of the chinese Hamster, Cricetulus griseus. A quantitative electron microscopic study. *Cell Tissue Res,* 228: 231-244.

MATSHUSIMA S, SAKAI Y, HIRA Y (1989) Twenty-four changes in pinealocytes, capillary endothelial cells and pericapillary and intercellular spaces in the pineal gland of the mouse. *Cell Tissue Res,* (255): 323-332.

MATSUHIMA S, SAKAY Y, HIRA Y, KATO M, SHIGEMITSU T, SHIGA Y (1993) Effect of magnetic field on pineal gland volume and pinealocyte size. *J Pineal Res,* 14(3): 145-157.

MAYS J, KELLY MC, COON SL, HOLTZCLAW L, RATH ME, KELLEY MW, KLEIN DC (2018) Single-cell RNA sequencing of the mammalian pineal gland identifies two pinealocytes subtypes and cell type-specific daily patterns of gene expression. *PLoS One*, 22: 13(10): e0205883.

MERRIT JH, SULKOWSKI TS (1969) Alterations of pineal gland biorhythms by N-methyl-3-piperediyl benzilate. *J Pharmacol Exp Ther,* 166: 119-124.

MILLINE R, KRSTIC R, DEVECERSKI V (1968) Sur le comportement de la glande pinéale dans des conditions de stress. *Acta Anat,* 71: 352-402.

MOLLER M, BAERES FM (2002) The anatomy and innervation of the mammalian pineal gland. *Cell Tissue Res,* 309(1): 139-150.

MOLLER M, BAERES FM (2003) PACAP-containing intrapineal nerve fibers originate predominantly in the trigeminal ganglion: a combined retrograde tracing- and immunohistochemical study of the rat. *Brain Res,* 984(1-2): 160-169.

OZAKI Y, WURTMAN RJ, ALONSO R, LYNCH HJ (1978) Melatonin secretion decreases during the proestrous stage of the rat estrous cycle. *Proc Natl Acad Sci USA*, 75(1): 531-534.

PÉVET P (1977) On the presence of different populations of pinealocytes in the mammalian pineal gland. *J Neural Transm,* 40(4): 289-304.

POPOVA NK, KOLAEVA SG, DIANOVA I (1975) State of the pineal gland during hibernation. *Bull Exp Biol Med,* 79: 467-468.

QUAY W, RENZONI A (1966) Twenty-four hour rhythms in the pineal activity activity and nuclear and nucleolar dimensions. *Growth,* 30: 315-324.

RENZONI A, QUAY WB (1964) Daily karyometric and rnitotic rhythm of pineal parenchymal cells in the rat. *Am Zool,* 4: 416-417.

REUSS ST, VOLLRATH L (1984) Electrophysiological properties of rat pinealocytes: Evidence for Circadian and ultradian rhythms. *Exp Brain Res*, 55(3): 455-461.

REUSS ST, SEMM P, VOLLRATH L (1984) Electrophysiological investigations on the central innervation of the rat and guinea-pig pineal gland. *J Neural Transm*, 60(1): 41-43.

SAKAI Y, HIRA Y, MATSUSHIMA S (1996) Regional differences in the pineal gland of the cotton rat, Sigmodon hispidus: light microscopic, electron microscopic, and immunohistochemical observations. *J Pineal Res,* 20(3): 125-137.

SAPÈDE D, CAU E (2013) The pineal gland from development to function. *Curr Top Dev Biol,* 106: 171-215.

SEMM P, VOLLRATH L (1979) Electrophysiology of the guinea-pig pineal organ: Sympathetically influenced cells responding differently to light and darkness. *Neurosci Lett*, 12: 93-96.

SEMM P, VOLLRATH L (1980) Electrophysiological evidence for circadian rhytmicity in a mamalian pineal organ. *J Neural Transm,* 47: 181-190.

SEMM P (1983) Neurobiological investigations of the pineal gland and its hormone melatonin. In: Axelrod J, Fraschini F, Velo GP (eds). *The Pineal Gland and its Endocrine Role. NATO Advanced Science Institutes Series* (Series A: Life Sci), vol 65. Springer, Boston, MA.

SHOJA MM, HOEPFNER LD, AGUTTER PS, SINGH R, TUBBS RS (2016) History of the pineal gland. *Childs Nerv Syst,* 32(4): 583-586.

TAKAHASHI T, OGIWARA K (2021) Roles of melatonin in the teleost ovary: A review of the current status. *Comp Biochem Physiol A Mol Integr Physiol*, 254: 110907.

TAMURA H, NAKAMURA Y, TAKIGUCHI S, KASHIDA S, YAMAGATA Y, SUGINO N, KATO H (1998) Melatonin directly suppresses steroid production by preovulatory follicles in the cyclic hamster. *J Pineal Res*, 25(3): 135-141.

VOLLRATH L (1979) Comparative morphology of the vertebrate complex. In: Ariëns Kappers J, Pévet P (eds). *The pineal of vertebrates including Man*. Prog Brain Res, 52: 25-38. Elsevier, Amsterdam.

VOLLRATH L (1981) The Pineal Organ. Handbuch der Mikroskopischen Anatomie des Menschen VI/7. *J Anat,* 135(2): 440-442.

VOLLRATH L (1985) The pineal gland of Mammals. An organ or a complex? In: Mess B, Rúzsas Cs, Tima L, Pévet P (eds). *The pineal gland. Current State of Pineal Research*. ISBN: 0-444-80629-6. Elsevier Science Publisher, Amsterdam, Netherlands, pp 27-33.

WELSH MG, CAMERON IL, REITER RJ (1979) The pineal gland of the Gerbil Meriones unguiculatus. I. Morphometric analysis over 24- hour period. *Cell Tissue Res,* 294: 95-109.

WURTMAN RJ, AXELDOD J (1964) Light and melatonin synthesis in the pineal. *Fed Proc,* 23: 206.

WURTMAN RJ, OZAKI Y (1978) Physiological control of melatonin synthesis and secretion: Mechanism generating rhythms in melatonin, methoxytryptophol and arginine,vasotocin levels and effects on the pineal of endogenous catecholamines, the estrous cycle, and environmental lighting. *J Neural Transm*, 13: 59-70.

Possible protective role of neutraceuticals in chronic intervertebral disc degeneration – A histological study

Fareeha Mushtaq [1], Humaira Ali [2], Shan E. Rauf [3], Abdullah Qamar [4], Ayesha Ali [5], Rabya Khalid [6], Amna Shoaib [7]

[1] Rawal Institute of Health Sciences, Islamabad, Pakistan
[2] Swat Medical College, Saidu sharif, Swat, Pakistan
[3] Armed Forces Institute of Pathology, Rawalpindi, Pakistan
[4] Army Medical College, Rawalpindi, Pakistan
[5] Army Medical College, Rawalpindi, Pakistan
[6] Army Medical College, Rawalpindi, Pakistan
[7] Al Nafees Medical College, Islamabad, Pakistan

SUMMARY

The aim of the study was to observe the effects of immobilization on the histomorphology of rats' intervertebral disc (IVD) and observe the protective effects of widely used neutraceuticals, Omega 3 fatty acids and Co-enzyme Q 10 (CoQ10) on it. The animal experimental study was carried out in the National Institute of Health, Islamabad in collaboration with the Anatomy Department, Army Medical College, Rawalpindi. Forty Sprague Dawley rats, weighing 250-300g, were chosen and grouped into 4 equal sets. Control group A was fed normal lab diet. In experimental group B, along with the lab diet, an Ilizarov apparatus was applied to the rats' tails for immobilization. In experimental groups C and D, the rats' tails were immobilized and given Omega 3 fatty acids (260 mg/kg body weight) and CoQ 10 (150 mg/kg body weight) through oral gavage. At completion of the study, IVDs of rats were analysed to see the histologic changes in the nucleus pulposus (NP) and annulus fibrosus (AF).

All the samples showed normal findings for NP in control group A. Degenerative changes were more significant in group B (p-value = 0.001) as compared to group C (p-value=0.005) and D (p-value=0.003). All the samples showed normal findings for AF in control group A. Degenerative changes were more significant in group B (p-value =0.000) as compared to group C (p-value=0.011) and D(p-value=0.003). Chronic immobilization of vertebral column induces degenerative changes in the cellular and matrix content of Intervertebral discs. However, consumption of neutraceuticals mitigates the consequences.

Key words: Annulus Fibrosus – Disc degeneration – Intervertebral disc – Neutraceuticals – Nucleus pulposus

Corresponding author:
Fareeha Mushtaq. Rawal Institute of Health Sciences, Dept. of Anatomy, Ground C, Block 5, Askari towers1, DHA2, 45730 Islamabad. E-mail: dr.fareeha.shan@gmail.com

Submitted: February 24, 2023. **Accepted:** April 11, 2023

https://doi.org/10.52083/IWCU1147

INTRODUCTION

Neutraceuticals have gained significant scientific attention in the past few decades. Omega 3 fatty acids (n-3 FA) have been added to a huge amount of dietary supplements and in a wide range of food products. n-3 FA derived from fish oil are evolving as potent and safe disease-modifying nutrients (Moyad, 2005). Consumption of n-3 FA, eicosapentaenoic acid (EPA) and docosahexaenoic acid (DHA), in preclinical and clinical research have illustrated beneficial effects in managing the inflammatory diseases including rheumatoid arthritis (Cleland et al., 2006), inflammatory bowel disease (Calder, 2008), psoriasis and neurodegenerative disorders (Dyall and Micheal, 2008).The prostaglandins and leukotrienes produced by EPA are less pro-inflammatory than the ones derived from Arachdonic acid (Stamp et al., 2005). Omega 3FA also inhibits the stimulation and activity of the nuclear factor jB (NF-jB), the pro-inflammatory transcription factor (Singer et al., 2008). EPA and DHA also produce resolvins and protectins, which are potent anti-inflammatory lipids (Arita et al., 2005). Long-chain n-3 FA can be used as an important adjunct to NSAID therapy in various inflammatory diseases.

Coenzyme Q 10 is a component of electron transport chain and acts as an electron and proton carrier coupled to ATP production in mitochondria. It also performs functions as an effective antioxidant in its reduced form (ubiquinol) (Saini, 2011). The levels of CoQ10 in tissues are increased under the effects of oxidative stress, e.g., physical exercise, cold adaptation, whereas the levels decrease during aging and degeneration. CoQ10, present in food or taken as a dietary supplement, seems to elevate the ubiquinone level in blood. CoQ10 performs important functions such as it prevents free radical injury triggered by neutrophils in inflammatory diseases, and also offers protection against oxidative injury produced due to ischemia (Lee et al., 2013). So, the term 'vitamin Q' has been also suggested for CoQ10 because of its numerous therapeutic properties when administered as a

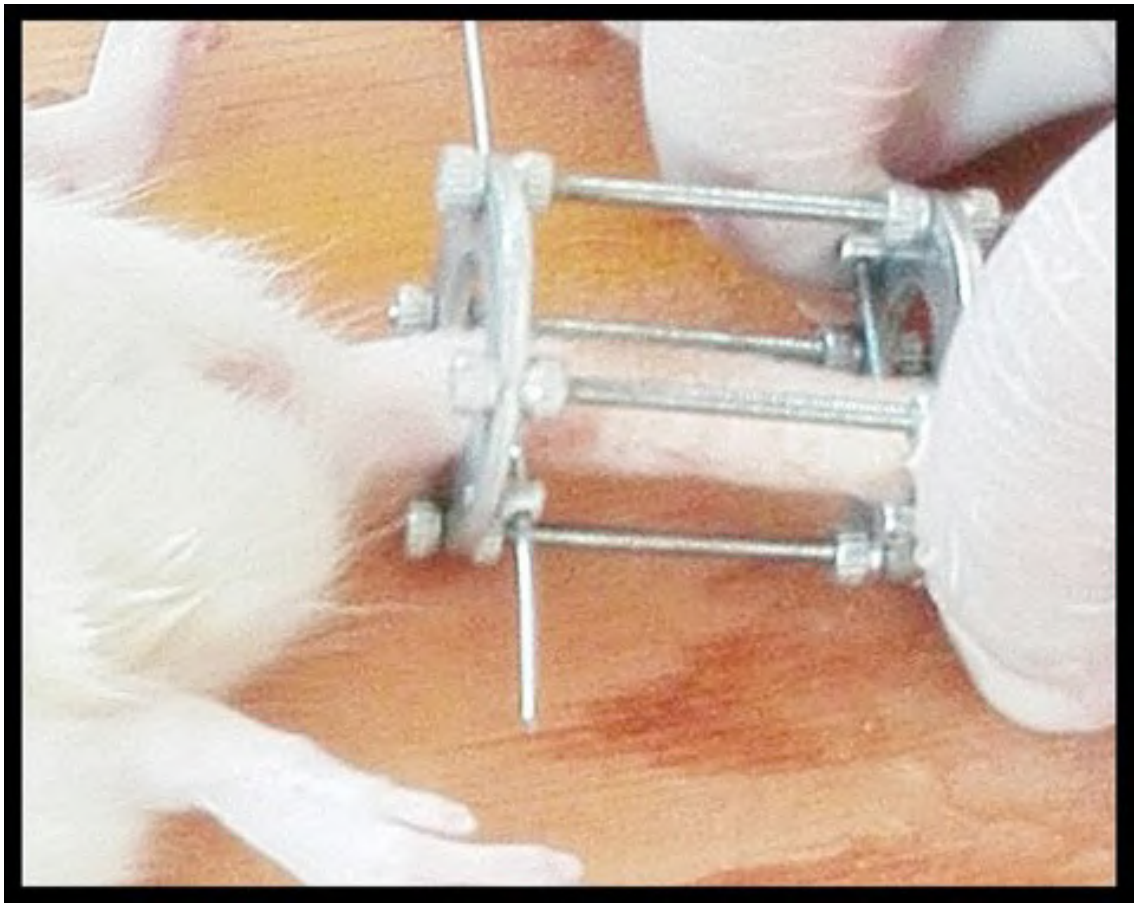

Fig. 1.- Application of an Ilizarov-type apparatus for rat tail segment immobilization.

dietary supplement (Bargossi et al., 1994). Animal studies offer mounting support for beneficial effects of CoQ10 supplements in various diseases, particularly neurodegenerative diseases, ageing and atherosclerosis (Turunen et al., 2004).

The intervertebral disc (IVD) is the avascular structure situated between the vertebrae of the spinal column. The disc is composed of a central soft, jell-like nucleus pulposus (NP) surrounded by the outer fibrous ring of annulus fibrosus (AF), sealed superiorly and inferiorly by the cartilaginous endplates (EP) (Whatley and Wen, 2012). Nutrients and metabolic by-products exchange mainly occurs through diffusion and convection with the surrounding. The NP is a gelatinous structure made up of water, extracellular matrix (ECM), and cellular elements. The AF is composed of 15-25 concentric rings of collagen fibrils arranged in a lamellar pattern parallel to each other. In each lamella layer, parallel running collagen fibre bundles are tilting at about 60° from the vertical axis, and in each successive lamellae the orientation is being reversed. Discrete translamellar bridging fibres radially join the adjacent lamellae (Chan et al., 2011). The morphology of the cellular components differs in AF and NP. The cells of the NP have a rounded appearance, and these chondrocyte-like cells are bounded inside a lacuna. On the other hand, the AF have cells with elongated fibroblastic appearance and are positioned in the same axis as the collagen fibrils, especially in the outer AF. The EP cells are chondrocytic (Wei et al., 2014).

Joint immobilization affects every connective tissue component of an articulation. It leads to degeneration of articular and periarticular connective tissue. Changes occur in biochemical elements of connective tissue, collagen, proteoglycans and hyaluronic acid. This brings about changes in the biomechanical and functional properties of the IVD. There is an increased risk for low back pain and disc degeneration with sedentary inactive lifestyle (Hagiwara et al., 2009).

This study was conducted to verify whether modification of diet with omega 3 FA and Co Q 10 could improve the histological parameters of chronic degenerative IVD disease in rats due to immobilization.

MATERIALS AND METHODS

Animals

This animal-based experimental study was completed in one year in the Army Medical College, Rawalpindi, in collaboration with the National Institute of Health (NIH)t, Islamabad, and Armed Force Institute of Pathology (AFIP), Rawalpindi. The necessary approval of the ethical committee of the Army Medical College, Rawalpindi, on animal experiments was taken (No. 02 / CREAM-A / 11 Aug, 2015). 40 mature Sprague-Dawley rats of about 3-4 months old, weighing between 250-300 grams, were taken for this study and divided into 4 equal groups. Animals were fed with standard lab diet and water for two months. Group-A (control): rats in this group were given standard lab diet and water ad libitum. Group-B: the animals' tails were immobilized by applying an Ilizarov-type apparatus (James et al., 1999). Group-C: the rats' tails were subjected to immobilization using an Ilizarov type apparatus. Animals were given standard lab diet, and omega 3FA was administered at a dose of 260 mg/kg body weight (Abdou et al., 2014). Group-D: the rats' tails were immobilized using Ilizarov apparatus and were administered Co-enzyme Q10 through oral gavage at a dose of 150 mg/kg/day (Kwong et al., 2002).

Method of vertebral disc immobilization

Before procedure, radiographs were taken to confirm the location of the 8^{th} and 10^{th} coccygeal vertebrae. Intraperitoneal injections of 10 mg/kg xylazine and 50 mg/kg ketamine were used to anesthetize the rats. An Ilizarov-type apparatus (Fig. 1) was applied to the rat's tail in order to immobilize the IVDs. Two K-wires were passed through the tagged locations of the two vertebrae. The wires were bonded to 35 mm diameter aluminium rings. Finally, four steel rods were passed longitudinally through four holes placed around the rings creating an Ilizarov-type apparatus (James et al., 1999).

After 8 weeks, rats were sacrificed and the immobilized segments (Co8-9 and Co10) of the vertebrae and complete IVDs were dissected. The removed part was then fixed in 10% formalin solution. The obtained sections were decalcified

and later infiltrated and embedded in paraffin wax. Five µm thick cross sections were obtained by using rotatory microtome. Then tissues were stained with Haematoxylin and Eosin (H&E) stain. This processing and staining methods were performed in histology unit of Armed Forces institute of Pathology. The tissue slides were studied under the light microscopic, and observations were documented with the help of two pathologists. 4X and 10X objectives were used to make observations for the qualitative and quantitative parameters. An established grading scale for NP and AF separately by Norcross et al. (2003) was used for histological score and grading (Tables 1 and 2).

RESULTS

Overall, during the experimental period all 40 animals remained healthy and alive. Changes were observed in NP and AF and were graded separately by using the histological grading scale ranging from 1 (severe disc degeneration) to 5 (normal disc). These scores are based on the cellularity and defects in the central nucleus pulposus and the orientation of collagen fibres and clefts in the annulus fibrosus. Three slides per specimen were observed and recorded.

On examination of NP, 100% specimens of Control Group A revealed normal disc and were placed in histological grade 5 of the Norcross et al.

Table 1. Grading Scale for Nucleus Pulposus established by Norcross et al. (2003).

	GRADING SCALE FOR NUCLEUS PULPOSUS (NP)
Score 5	Large, bulging central cavity with abundant NP material > 2/3rd IVD height; smooth borders with minimal disruption.
Score 4	Slightly reduced central cavity size with some NP material present ;> 1/3rd IVD height and < 2/3rd IVD height; minimal border disruption may be present.
Score 3	Markedly reduced and disrupted cavity with minimal NP material and compartmentalization; total cavity > 1/3rd IVD height and < 2/3rd IVD height.
Score 2	Severe disruption of NP with minimal cavity; total cavity < 1/3rd IVD height but > 0; consists only of a few small pockets lined by NP-like cells.
Score 1	Complete obliteration of cavity with no NP-lined pockets.

Table 2. Grading Scale for Annulus Fibrosus established by Norcross et al. (2003).

Score	GRADING SCALE FOR ANNULUS FIBROSUS (AF)
Score 5	Discrete, well-opposed lamellae bulging outward with no infolding; minimal preparation defects with simple radial clefting.
Score 4	Discrete, well-opposed lamellae bulging outward with no infolding; minimal preparation defects with simple radial clefting.
Score 3	Moderate to severe infolding of discrete, relatively well-opposed lamellae; moderate fragmentation of lamellae; AF fibers remain well organized.
Score 2	Severe infolding and distortion of poorly opposed lamellae; severe fragmentation of lamellae; small regions of disorganized fibrous material replacing central lamellae.
Score 1	Severe infolding, distortion, and fragmentation of lamellae; extensive amount of disorganized fibrous material replacing central lamellae.

Statistical analysis

Data were analysed by SPSS 21.0v. ANOVA was used for intergroup comparison of histological differences followed by Post Hoc Tukey Test. A confidence interval of 95% having p-value <0.05 was considered significant.

(2003) scale (Fig. 2a). In group B, the frequency of nucleus pulposus degeneration was higher when compared to control group A (p-value < 0.001), experimental group C (p-value =0.000) and D (p value=0.000), which was statistically significant (Table 3, Fig. 3a and Bar chart 1). In group C, 60% of the specimens had minimally disrupted cavity in comparison with group B, p =0.000, which was

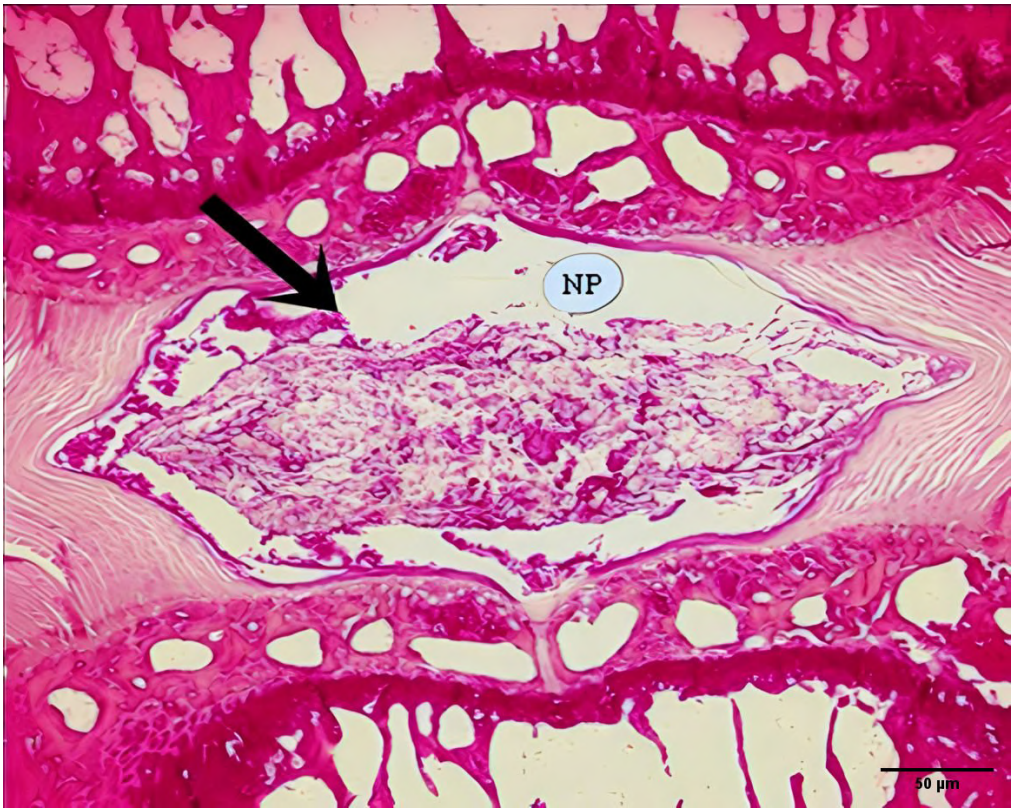

Fig. 2a.- Histological picture of the intervertebral disc of A4, an animal in the control group showing a large central NP (arrow) and smooth borders with AF. H&E staining. Scale bar: 50 µm.

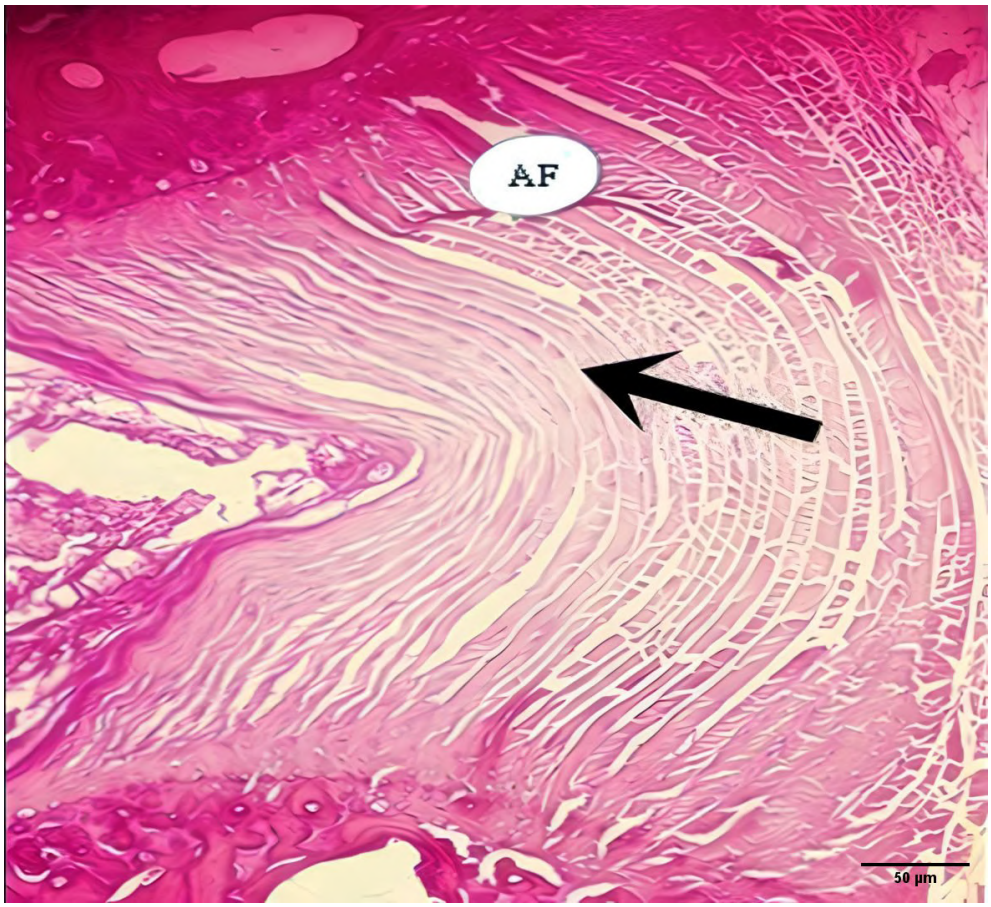

Fig. 2b.- Well organized, circumferential lamellae in AF (arrow). H&E staining. Scale bar: 50 µm.

Table 3. Comparison of Norcross et al. (2003) scoring for microscopic degeneration of nucleus pulposus (NP) between the control Group A and experimental Groups B, C and D.

Norcross scale for nucleus pulposus	Group A (n=10)	Group B (n=10)	Group C (n=10)	Group D (n=10)	Group A/B	Group A/C	Group A/D	Group B/C	Group B/D	Group C/D
Score 5	10	0	4	3	0.000*	0.005*	0.003*	0.000*	0.001*	0.250
Score 4	0	0	6	4						
Score 3	0	2	0	3						
Score 2	0	3	0	0						
Score 1	0	5	0	0						

statistically significant. The results were statistically insignificant when compared with group D (p =0.250) (Table 3, Fig. 4 and Bar chart 1). The results were statistically significant when group D was compared with group B (p-value =0.001), but in comparison with group C the results were statistically insignificant (p-value =0.250) (Table 3, Fig. 5 and Bar chart 1).

When AF was observed, all the specimens in control group A had well-opposed, discrete lamellae (grade 5). No infolding was observed in any of the specimens (Table 4, Fig. 2b and Bar chart 2). The frequency of AF degeneration was higher in group B when compared to control group A (p =0.000), experimental group C (p=0.001) and D (p =0.001), which was statistically significant (Table 4, Fig. 3b and Bar chart 2). In group C, only 20% of the specimens showed a moderate amount of fragmentation and infolding (grade 3). When compared to group B, p value=0.001 which was statistically significant. The results were statistically insignificant when compared with group D (p-value=0.753) (Table 4, Fig. 4 and Bar chart 2). The results were statistically significant when group D was compared with group B (p=0.001) but on comparison with group C the results were statistically insignificant (p =0.735) (Table 4, Fig. 5 and Bar chart 2).

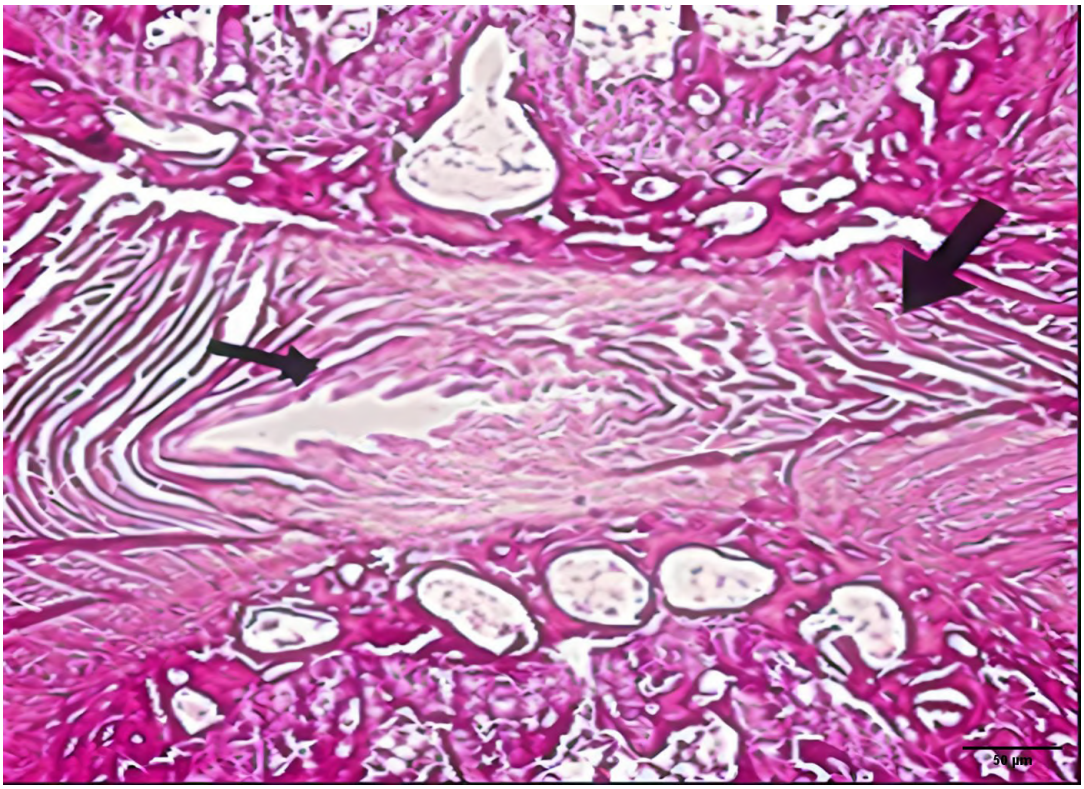

Fig. 3a.- Intervertebral disc of rat number B5 in the disc immobilized group B showing highly disrupted and reduced NP cavity (arrows). H&E staining. Scale bar: 50 µm.

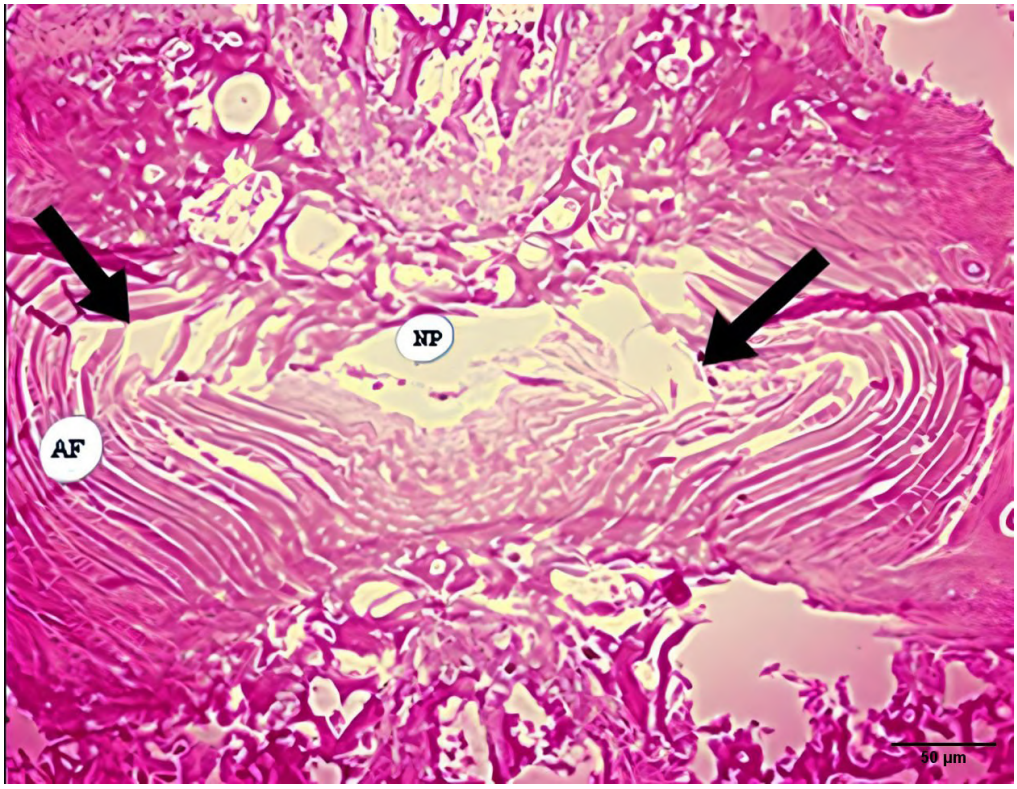

Fig. 3b.- Intervertebral disc showing, distortion, disruption and clefts in AF (left arrow) and highly reduced to obliterated NP cavity in B3 and B7 rats of group B (right arrow). H&E staining. Scale bar: 50 µm.

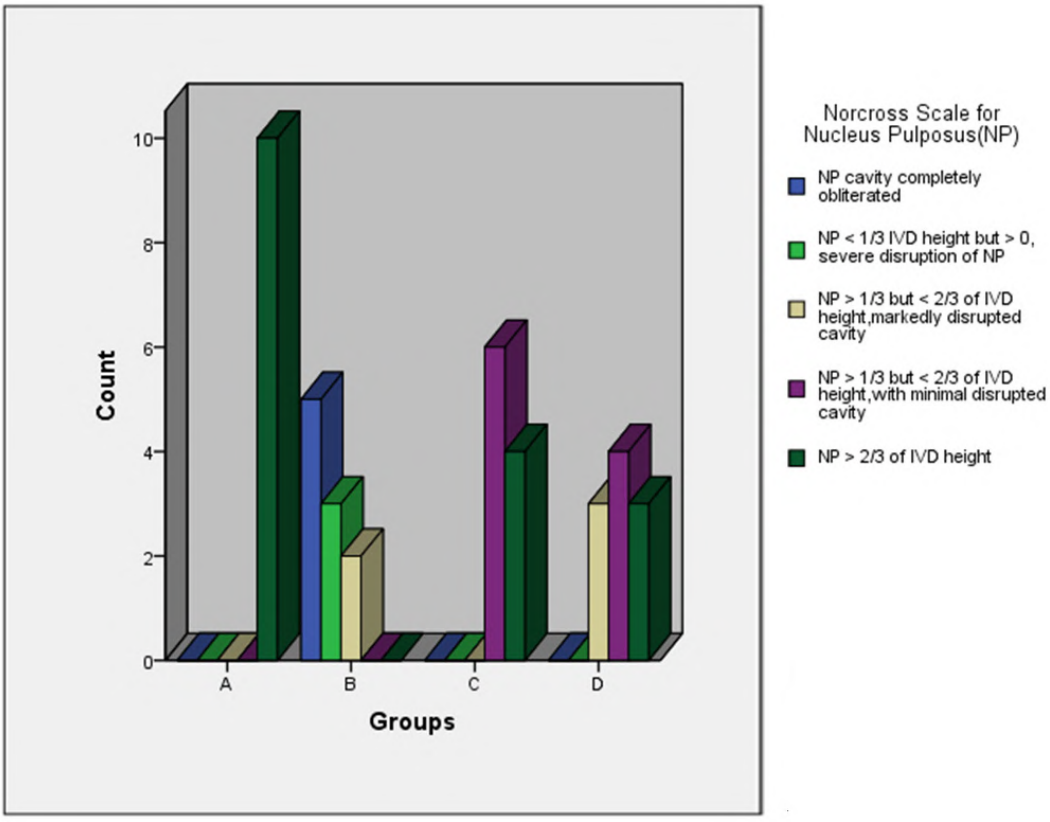

Bar chart 1. Clustered bar chart showing frequency of nucleus pulposus (NP)with scoring of degeneration (Norcross scale) among the control group A, disc immobilized group B, disc immobilized+Omg3 administered group C and disc immobilized+CoQ10 administered group D.

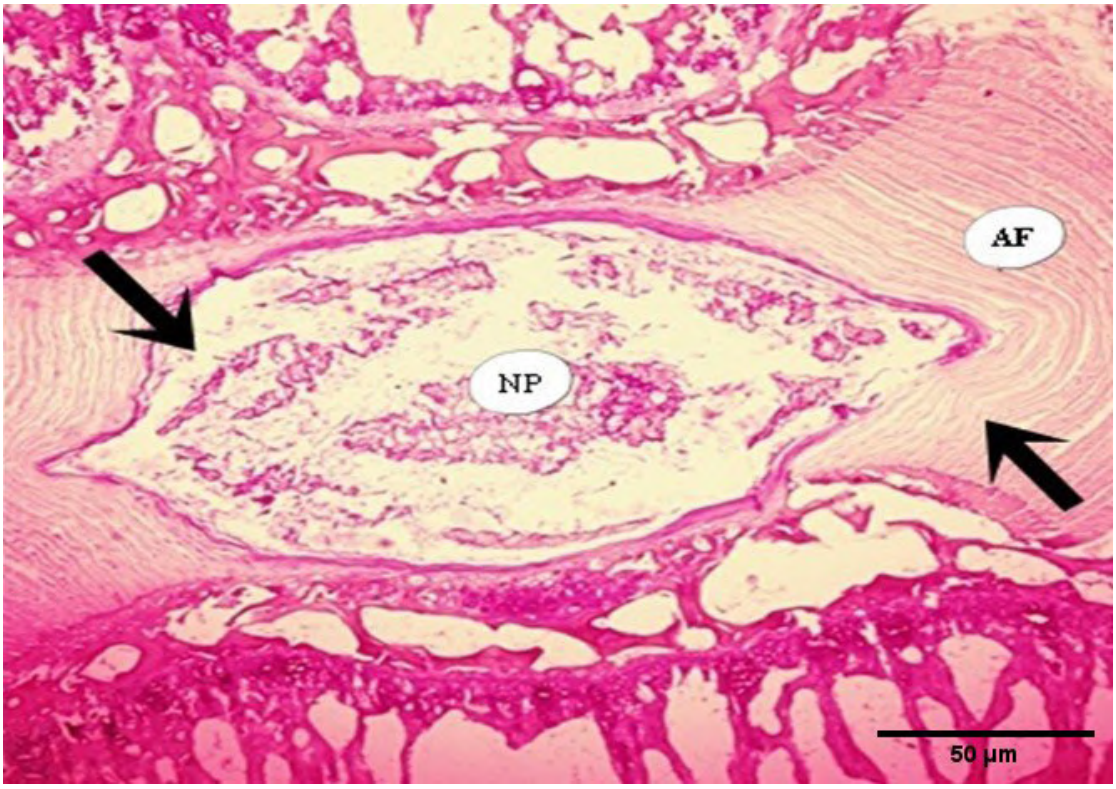

Fig. 4.- Histological section of the intervertebral disc of animal number C8 in the disc immobilized + omega 3 administered group C showing large NP cavity (left arrow) and discrete lamellae in AF (right arrow). H&E staining. Scale bar: 50 µm.

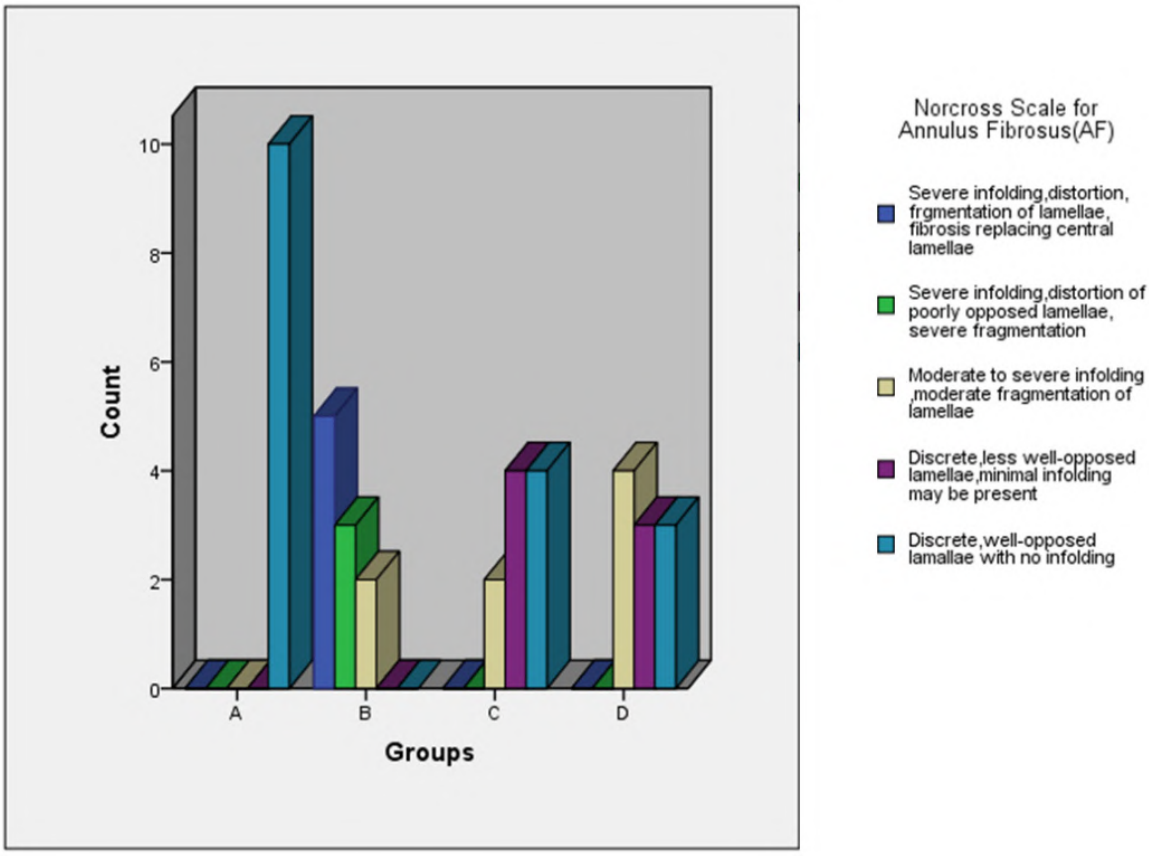

Bar chart 2. Clustered bar chart showing frequency of annulus fibrosus (AF) with scoring of degeneration (Norcross scale) among the control group A, disc immobilized group B, disc immobilized+Omg3 administered group C and disc immobilized+CoQ10 administered group D.

Table 4. Comparison of Norcross et al. (2003) scoring for microscopic degeneration of annulus fibrosus (AF) between the control Group A and experimental Groups B, C and D.

Norcross scale for annulus fibrosus	Group A (n=10)	Group B (n=10)	Group C (n=10)	Group D (n=10)	Group A/B	Group A/C	Group A/D	Group B/C	Group B/D	Group C/D
Score 5	10	0	4	4	0.000*	0.011*	0.003*	0.001*	0.001*	0.735
Score 4	0	0	4	3						
Score 3	0	2	2	3						
Score 2	0	3	0	0						
Score 1	0	5	0	0						

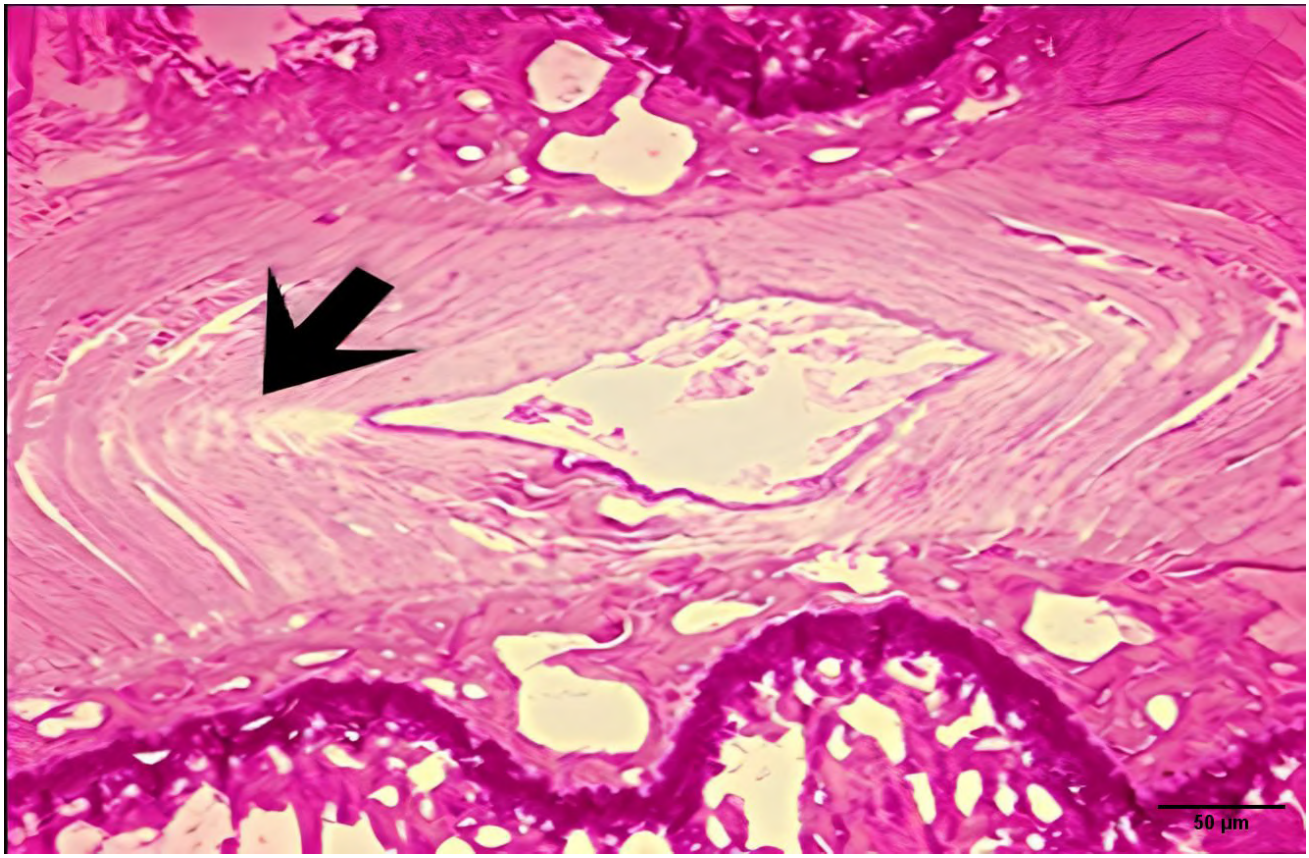

Fig. 5.- Intervertebral disc of animal number D3 in the disc immobilized+COQ10 administered group D showing slightly reduced NP cavity and minor fissures in inner lamellae of AF (arrow). H&E staining. Scale bar: 50 µm.

DISCUSSION

The histomorphological examination of nucleus pulposus of the intervertebral disc in experimental group B showed complete obliteration of nucleus pulposus (grade 1) in 50% and grade 2 in 30% of the specimens. The frequency of grade 1 and grade 2 degeneration was higher in disc-immobilized group B as compared to control group A, where all discs had normal histological features and showed no signs of degeneration (grade 5). Degeneration in nucleus pulposus was observed in the form of reduced height of NP as compared to intervertebral disc height and severity of disruption of NP cavity. These findings were consistent with a study performed on the rat intervertebral disc where disc degeneration caused damage to NP cavity and NP showed severe disruption and a slow on-going decline in cell count. This leads to decrease in the NP cavity until it is completely obliterated (Silveira et al., 2014). In group C, nucleus pulposus had mild degeneration (grade 4) in 40% specimens while 60% specimens showed no

signs of NP degeneration (grade 5). The decreased frequency of severity of degeneration of nucleus pulposus in group C was in consistency with a study performed by Berbert et al. (2005), where administration of omega 3 fatty acids reduced inflammation and resulted in decreased production of PGE2, thromboxane B2, LTB4 and LTE4 by inflammatory cells and consequently reduced degenerative changes in joints. Degeneration in nucleus pulposus was also found to be higher in the experimental group D as compared to control group A, however, the frequency of severity of degeneration in NP was greater in experimental group B as compared to group D. The degenerative changes in NP were less severe in group D as compared to group B, because CoQ10 has anti-oxidant action. It counters the free radical injury and the subsequent degeneration in the NP due to the oxidative stress caused by disc degeneration. This was in agreement with the study conducted on progressive neurodegenerative diseases where CoQ10 had a preventive role (Shults et al., 2004).

The histological examination of annulus fibrosus (based on Norcross scale) in intervertebral disc specimens in disc-immobilized group B showed highly disorganized, fragmented and infolded lamellae (grade 1) of the specimens. Fibrosis was also present in the central lamellae. The frequency of annulus disruption was higher in the experimental group B as compared to control group A. Studies have shown that degenerated IVD is in a chronic inflammatory state with increased expression of various inflammatory cytokines like interleukin 1 (IL-1), matrix metalloproteinase (MMP)-10, IL-8, tumour necrosis factor (TNF-α), IL-10, and prostaglandin E2 (PGE2). This leads to significant inflammation causing the annular damage (Wang et al., 2006). In group C, annulus fibrosus showed moderately fragmented and infolded lamellae (grade 3) in 20% specimens, mild changes were present in 40% (grade 2) while 40% specimens showed no signs of AF degeneration (grade 5). IVD degeneration is linked with apoptosis of cells in AF and ECM degeneration due to activation of the mitochondria-dependent apoptosome (Rannou et al., 2004). The ingestion of omega 3 fatty acids had a protective effect on the annulus fibrosus in group C. The results are in agreement with the study performed by Goldberg and Katz (2007). They proposed that consumption of Omega 3-rich fish oil reduced the number of painful and swollen joints. There was a marked reduction in production of pro-inflammatory factors like PG and leukotriene B_4. According to Calder (2002, 2008), n-3 PUFAs can influence transcription factors such as nuclear factor kappa B (NFκB) and peroxisome proliferator-activated receptors (PPARs) and alter inflammatory gene expression. The down-regulation of transcription factors plays a significant part in decreasing activity of a number of inflammatory signalling pathways (Calder and Grimble, 2002).

Degenerative changes in annulus fibrosus were also found to be higher in the experimental group D as compared to control group. However, the frequency of severity of degeneration in AF was lower in Co Q 10-treated group as compared to disc immobilized group B. Coenzyme Q10 is known as an effective anti-oxidant and proven to have outstanding capability to scavenge ROS. The CoQ10 had protective effect on the cells and matrix of AF in the experimental group D. This is supported by the fact that studies have shown that CoQ10 exert beneficial effect on osteoarthritis and suppresses pain and cartilage degeneration (Lee et al., 2013). Bauerova et al. (2010) proved that when treatment with CoQ 10 was provided in arthritis model, the high expression of pro-inflammatory cytokines, IL-1β, IL-6, and IL-15, decreased.

Owing to the therapeutic effects of n-3 PUFAs and CoQ10, in wide variety of chronic inflammatory and neurodegenerative diseases, they have become a focus of interest nowadays. However, further research is required to address important aspects such as how lifetime intake of n-3 PUFAs and CoQ10 can influence the progress of age-linked and chronic degenerative disorders for instance DDDD**.** More research is needed to claim them as preventive agents and establish their clinical efficacy in chronic IVD degeneration.

REFERENCES

ABDOU HM, HASSAN MA (2014) Protective role of omega 3 polyunsaturated fatty acid against lead acetate-induced toxicity in liver and kidney of female rats. *BioMed Res Internet*, Article ID 435857.

ADAM O, BERINGER C, KLESS T, LEMMEN C, ADAM A, WISEMAN M, ADAM P, KLIMMEK R, FORTH W (2003) Anti-inflammatory effects

of a low arachidonic acid diet and fish oil in patients with rheumatoid arthritis. *Rheumatol Int,* 23: 27-36.

ARITA M, BIANCHINI F, ALIBERTI J, SHER A, CHIANG N, HONG S, YANG R, PETASIS NA, SERHAN CN (2005) Stereochemical assignment, antiinflammatory properties, and receptor for the omega-3 lipid mediator resolvin E1. *J Exp Med,* 201(5): 713-722.

BARGOSSI AM, GROSSI G, FIORELLA PL, GADDI A, DI GIULIO R, BATTINO M (1994) Exogenous CoQ10 supplementation prevents plasma ubiquinone reduction induced by HMG-CoA reductase inhibitors. *Mol Aspects Med,* 15: s187-s193.

BAUEROVA K, PAULOVICOVA E, MIHALOVA D, DRAFI F, STROSOVA M, MASCIA C, BIASI F, ROVENSKY J, KUCHARSKA J, GVOZDJAKOVA A, PONIST S (2010) Combined methotrexate and coenzyme Q10 therapy in adjuvant-induced arthritis evaluated using parameters of inflammation and oxidative stress. *Acta Biochim Pol*, 57(10): 347-354.

BERBERT AA, KONDO CRM, ALMENDRA CL, MATSUO T, DICHI I (2005) Supplementation of fish oil and olive oil in patients with rheumatoid arthritis. *Nutrition*, 21: 131-136.

CALDER PC (2002) Dietary modification of inflammation with lipids. *Proc Nutr Soc*, 61(3): 345-358.

CALDER PC (2008) Polyunsaturated fatty acids, inflammatory processes and inflammatory Bowel diseases. *Mol Nutr Food Res*, 52: 885-897.

CALDER PC, GRIMBLE RF (2002) Polyunsaturated fatty acids, inflammation and immunity. *Eur J Clin Nutr*, 56(3): S14-S19.

CHAN WC, SZE KL, SAMARTZIS D, LEUNG VY, CHAN D (2011) Structure and biology of the intervertebral disk in health and disease. *Orthopedic Clinics*, 42(4): 447-464.

CLELAND LG, CAUGHEY GE, JAMES MJ, PROUDMAN SM (2006) Reduction of cardiovascular risk factors with long term fish oil treatment in early rheumatoid arthritis. *J Rheumatol*, 33: 1973-1979.

DYALL SC, MICHAEL-TITUS AT (2008) Neurological benefits of omega-3 fatty acids. *Neuromol Med*, 10(4): 219-235.

GOLDBERG RJ, KATZ J (2007) A meta-analysis of the analgesic effects of omega-3 polyunsaturated fatty acid supplementation for inflammatory joint pain. *Pain*, 129(1-2): 210-223.

HAGIWARA Y, ANDO A, CHIMOTO E, SAIJO Y, OHMORI-MATSUDA K, ITOI E (2009) Changes of articular cartilage after immobilization in a rat knee contracture model. *J Orthop Res*, 27(2): 236-242.

JAMES CI, PETER LM, IAN AFS, DAVID DA, MAURO A (1999) Compression-induced changes in intervertebral disc properties in a rat tail model. *Spine*, 24(10): 996-1002.

KWONG LK, KAMZALOV S, REBRIN I, BAYNE ACV, JANA CK, MORRIS P (2002) Effects of coenzyme Q 10 administration on its tissue concentrations, mitochondrial oxidant generation, and oxidative stress in the rat. *Free Radical Biol Med*, 33(5): 627-638.

LEE J, HONG YS, JEONG JH, YANG EJ, JHUN JY, PARK MK, JUNG YO, MIN JK, KIM HY, PARK SH, CHO ML (2013) Coenzyme Q10 ameliorates pain and cartilage degradation in a rat model of osteoarthritis by regulating nitric oxide and inflammatory cytokines. *PLoS One*, 8(7): e69362.

MOYAD MA (2005) An introduction to dietary/supplemental omega-3 fatty acids for general health and prevention: part II. In: *Urologic Oncology: Seminars and Original Investigations.* Vol. 23, No. 1, pp 36-48. Elsevier.

NORCROSS JP, LESTER GE, WEINHOLD P, DAHNERS LE (2003) An in vivo model of degenerative disc disease. *J Orthop Res*, 21: 183-188.

RANNOU F, LEE TS, ZHOU RH, CHIN J, LOTZ JC (2004) Intervertebral disc degeneration: the role of the mitochondrial pathway in annulus fibrosus cell apoptosis induced by overload. *Am J Pathol*, 164(3): 915-924.

SAINI R (2011) Coenzyme Q10: The essential nutrient. *J Pharm Bioallied Sci*, 3(3): 466-467.

SHULTS CW, FLINT BM, SONG D, FONTAINE D (2004) Pilot trial of high dosages of coenzyme Q10 in patients with Parkinson's disease. *Exp Neurol*, 188(2): 491-494.

SILVEIRA JW, ISSY AC, CASTANIA VA, SALMON CEG, NOGUEIRA-BARBOSA MH (2014) Protective effects of cannabidiol on lesion-induced intervertebral disc degeneration. *PLoS One*, 9(12): e113161.

SINGER P, SHAPIRO H, THEILLA M, ANBAR R, SINGER J, COHEN J (2008) Anti-inflammatory properties of omega-3 fatty acids in critical illness: novel mechanisms and an integrative perspective. *Intensive Care Med*, 34(9): 1580-1592.

STAMP LK, JAMES MJ, CLELAND LG (2005) Diet and rheumatoid arthritis: a review of the literature. In: *Seminars in arthritis and rheumatism* (Vol. 35, No. 2, pp 77-94). WB Saunders.

TURUNEN M, OLSSON J, DALLNER G (2004) Metabolism and function of coenzyme Q. *Biochim Biophys Acta (BBA)-Biomembranes*, 1660(1-2): 171-199.

WANG YJ, SHI Q, LU WW, CHEUNG KC, DAROWISH M, LI TF (2006) Cervical intervertebral disc degeneration induced by unbalanced dynamic and static forces: a novel in vivo rat model. *Spine (Phila Pa 1976)*, 31: 1532-1538.

WEI A, SHEN B, WILLIAMS L, DIWAN A (2014) Mesenchymal stem cells: potential application in intervertebral disc regeneration. *Translat Pediatrics*, 3(2): 71-90.

WHATLEY BR, WEN X (2012) Intervertebral disc (IVD): Structure, degeneration, repair and regeneration. *Materials Sci Engineer: C*, 32(2): 61-77.

Neurophobia: The inconvenient truth

Gerda Venter[1], Marius C. Bosman[1], Johanna C. Lubbe[2,3]

[1] *Department of Anatomy, Faculty of Health Sciences, University of Pretoria, Pretoria, Gauteng, South Africa*

[2] *Department of Education Innovation, Faculty of Health Sciences, University of Pretoria, Pretoria, Gauteng, South Africa*

[3] *Yehuda Elkana Center for Teaching, Learning and Higher Education Research, Central European University, Austria*

SUMMARY

Medical schools have implemented strategies in response to neurophobia to counteract the negative perception and improve neuroscience experiences for undergraduate medical students. In this study, we explored the attitudes, perceptions and preferred learning approaches of undergraduate and postgraduate medical students toward the teaching, facilitation, learning and assessment of neuroanatomy, as well as their perceptions on its relevance in the South African medical curriculum. A total of 299 undergraduate and five postgraduate students from the University of Pretoria participated in this study. We used a multi-method approach in which the undergraduate students completed an anonymous quantitative questionnaire, while the postgraduate students participated in a qualitative focus- group discussion. Undergraduate medical students preferred lecture notes to study from above any other type of literature and mainly used laptop computers as preferred electronic devices in preparation for their assessments. The favourite topic was cranial nerves, and the least popular was histology of the nervous system. Postgraduate students shared their undergraduate neuroanatomy experiences and provided constructive feedback and suggestions to undergraduate students and lecturing staff. Ineffective teaching methods and limited contact time remain factors that contribute to neurophobia in South Africa. Students perceive neuroanatomy as an interesting and important subject in their medical degree. However, changes are needed to modernize neuroanatomy and make it more accessible and student-friendly. The challenge then remains: how do we, as lecturers, modernize neuroanatomy in the medical curriculum to make it contemporary and clinically applicable?

Key words: Medical education – Neuroanatomy education – Neurophobia – Students' perceptions – Undergraduate education

INTRODUCTION

Human anatomy, which includes neuroanatomy, is regarded as a foundational subject of the medical curriculum (Sotgiu et al., 2020). If obstacles such as students' irrational fear towards the subject threaten the stability of this foundation, there will be dire consequences later in a medical students' career.

Students experience a fear toward neuroanatomy in their undergraduate medical training which can be attributed to their perception of neurosciences, limited exposure to neuroanatomy during their training, as well as the way in which this sub-

Corresponding author:
Gerda Venter. Department of Anatomy, University of Pretoria, Pretoria, Gauteng, South-Africa. Private Bag X323, Arcadia 0001, South Africa. Phone: +2712 319 2536. E-mail: gerda.venter@up.ac.za Orcid ID: 0000-0003-3471-4776

Submitted: March 11, 2023. **Accepted:** April 13, 2023

https://doi.org/10.52083/CUKT7497

ject is currently being presented and facilitated (Nham, 2012; Kam et al., 2013; Maranhão- Filho, 2014; Geoghegan et al., 2019). This leads to a deficit in their basic anatomy knowledge and, in turn, inhibits the application of basic neuroanatomy in the clinical environment (Nham, 2012). This deficiency of theory-practice integration could result in general medical practitioners who lack a sufficient level of applied theoretical knowledge of the human body. This may then have a direct influence on the way in which they assess, diagnose, treat, or refer patients with neurological disorders and diagnoses (Zinchuk et al., 2010; Gorgich et al., 2017). Therefore, the perceptions and attitudes of medical students towards neuroanatomy in the medical curriculum need to be explored, and measures put in place to address any negative perceptions.

Often, the perception of medical students is that neurosciences, including neuroanatomy and clinical neurology, are overwhelming in both content and context, and overly complex (Arantes et al., 2017). This, in turn, may lead to the development of an irrational fear towards the neurosciences (Maranhão-Filho, 2014; Geoghegan et al., 2019), known as neurophobia (Russell et al., 2015). The term 'neurophobia' was coined by Ralph Jozefowicz in 1994 (Josefowicz, 1994; Russell et al., 2015; Arantes et al., 2017). The irrational fear of the neurosciences has further been referred to as a "real and prevalent educational disease" (Kam et al., 2013) reported to manifest within the first two years of medical study (Geoghegan et al., 2019), affecting 50% of undergraduate medical students (Jozefowicz, 1994; Abushouk and Duc, 2016; Hall et al., 2018; Shelley et al., 2018), and has no gender preference (Jozefowicz, 1994). Neurophobia, as a symptom, has been recognized in a variety of countries such as Nigeria, United States of America, United Kingdom (McCarron et al., 2014), Saudi Arabia (Abulaban et al., 2015; Mohammed et at., 2018), Singapore (Kam et al., 2013), China (Lukas et al., 2017), Sri Lanka (Matthias et al., 2013), Brazil (Santos-Lobato et al., 2018), Trinidad and Tobago (Youssef, 2009), Portugal (Arantes et al., 2017), West India (Shiels et al., 2017), India (Shelley et al., 2018) and Sudan (Elnaeim et al., 2021).

Neurophobia is an all-inclusive term that describes the insights, beliefs, negative preconceptions, apprehensive feelings, dislikes, and disinterest that medical students have toward neuroscience education (Shelley et al., 2018). Unfortunately, even though neurophobia, its causes and possible prevention plans have been extensively described in the literature, some lecturing staff still view this as a trivial issue (Tarolli and Jozefowicz, 2018; Venter et al., 2022) and remain unwilling to acknowledge its existence.

Several factors influence the presence and severity of neurophobia. Causative and contributing factors to neurophobia can be divided into three risk categories. The first category is non-modifiable and includes all the preconceptions and past experiences that students have towards neurosciences before they start medical school (Fantaneanu et al., 2014). The second group consists of all the factors affecting the students during their pre-clinical years and include the students' inability to apply their basic science knowledge to the clinical environment (Nham, 2012), a lack of self-confidence in the approach and understanding of the elementary neurological concepts (Nham, 2012; Santos-Lobato et al., 2018), inadequate or inappropriate teaching techniques (Youssef, 2009; Nham, 2012; Kam et al.,2013; Abulaban et al., 2015; Mohammed et al., 2018; Venter et al., 2022), the complexity of neuroanatomy as a subject (Hudson, 2006; Nham, 2012; Kam et al., 2013; Shiels et al., 2017; Mohammed et al., 2018) and the habit of superficial learning instead of deep learning, as well as rote learning by students (Pandey and Zimitat, 2007; Sotgiu et al., 2020). The last group of contributing factors affects the medical students during their clinical training years and include the difficulty, complexity and length of the clinical examination (Nham, 2012), the lack of proper exposure to neurologically impaired patients and insufficient bedside teaching (Nham, 2012; Kam et al., 2013), the large number of rare and intricate diagnoses and, at times, the inability to have a conclusive curative treatment plan for many of the cases (Matthias et al., 2013). The second and third group of risk factors during the students' pre-clinical and clinical training years are modifiable (Fantaneanu et al., 2014)

and, therefore, the development of neurophobia can be classified according to intrinsic and extrinsic factors.

Intrinsic factors refer to the students and include the perception of neurology within the medical community (Nham, 2012; Tarolli and Jozefowicz, 2018), the students' perception of the complexity of neuroanatomy as a subject (Nham, 2012; Kam et al., 2013; Tarolli and Jozefowicz, 2018), their inability to apply basic scientific knowledge to the clinical environment (Nham, 2012), and a lack of self-confidence in the approach and understanding of the elementary neurological concepts (Nham, 2012; Geoghegan et al. 2019). Extrinsic factors include poor or insufficient teaching of neuroanatomy (Nham, 2012; Kam et al., 2013; Venter et al., 2022), and the limited exposure to the clinical environment and its relevance (Tarolli and Jozefowicz, 2018). In response to neurophobia, educational institutions have implemented various strategies to counteract this perception and improve neuroscience experiences for undergraduate students (Pakpoor et al., 2014). It is important to maintain high standards in neuroscience teaching, and this can only be upheld if the current cohort of undergraduate medical students are given the opportunity to develop the relevant knowledge, skills, and enthusiasm to cultivate an interest or career in the neurosciences (Geoghegan et al., 2019).

A study was therefore undertaken to explore undergraduate and postgraduate medical students' attitudes towards the teaching, facilitation, learning and assessment of neuroanatomy, as well as their perceptions on the relevance of neuroanatomy in the medical curriculum. The results reported in this study are part of a larger exploratory study into neuroanatomy within the South African medical curriculum.

MATERIALS AND METHODS

We used a multi-method approach which included both qualitative and quantitative research design characteristics. In a multi-method research approach, the objectives can run concurrently without one objective influencing, or depending on, another (Seawright, 2016).

Ethical approval

Permission to include students from the University of Pretoria was obtained from the Registrar and Deputy Dean of Teaching and Learning, in the Faculty of Health Sciences at the University of Pretoria. The questionnaires completed by the volunteering students were accompanied by a participant information leaflet which explained the details of the study, as well as the rights of the participant. All participants provided written informed consent prior to enrolment in the study. The anonymity of these participants was always maintained. The ethical consent required for this research project was acquired from the Research Ethics Committee of the University of Pretoria (Reference number: 587/2018) in October 2018.

Participants

We collected information from undergraduate and postgraduate medical students at the University of Pretoria. Email requests were sent to the undergraduate medical students to invite them to anonymously participate in a survey. These students had exposure to neuroanatomy during their previous years. Each volunteering student completed an anonymous electronic questionnaire. We further approached postgraduate medical students from the same institution, who were specializing in either Neurosurgery, Neurology or Psychiatry. They were invited to participate in a qualitative focus-group discussion.

Data collection

The questionnaires were developed by the researchers and validated by independent academic consultants and statisticians. These questionnaires were completed by the undergraduate students, contained mostly quantitative questions, and were designed to gather information on the perceptions of the students towards the current neuroanatomy teaching and facilitation approaches, as well as their perceived importance of neuroanatomy within the medical curriculum. Likert-scale-, matrix- and open-ended questions were included in the questionnaires.

The questionnaire requested information such as the year of study, other neuroanatomy expo-

sure, preferred teaching approaches and study materials including their use of electronic devices for studying neuroanatomy. Information regarding the students' view on the importance of neuroanatomy as part of their training was also requested. Eleven core categories previously identified by Moxham and co-workers (2015) were assessed in this questionnaire, and included questions on the development of the nervous system, histology of the nervous system, spinal cord, brainstem, cranial nerves, diencephalon and the pituitary gland, cerebral hemispheres, limbic system and reticular formation, autonomic system, ventricular system, meninges, and blood vessels. The perceptions on the importance and relevance of the eleven core categories were explored.

For the postgraduate students, we conducted a focus-group discussion t related to their undergraduate neuroanatomy experience, possible role-models, the reason for specializing in a neuroscience field, as well as their advice and suggestions to the current undergraduate students and lecturing staff. The focus-group approach worked well, since it allowed equal expression of the perspectives and views on the specific issues of neurophobia (Colucci, 2007; Bryman et al., 2014).

Data analysis

The data obtained from the undergraduate students' questionnaires was analysed with IBM SPSS, Statistics for Windows, Version 22.0 (IBM Corp., Armonk, NY) for the descriptive statistics and the statistical software SAS^{R}, Version 9.4 (SAS Institute) for the inferential statistics. The statistical significance was determined by a p-value of less than 0.05. The statistical analysis consisted mainly of descriptive statistics which included frequencies and means with standard deviations. Inferential statistical techniques such as the analysis of variance (ANOVA) were performed to find possible simultaneous relationships between continuous dependent variables and independent factors. Through the process of statistical model building, significant independent factors such as the year-group of students and time allocated to neuroanatomy could be identified to have a simultaneous influence on dependent variables such as preferred teaching approaches, literature used and neuroanatomy topics, as well as perceived importance of neuroanatomy within the medical curriculum.

All open-ended questions underwent thematic analysis by means of Atlas.ti^{TM} Version 8.0 software (Scientific Software, Berlin, Germany). The postgraduate focus-group discussions were transcribed and thematically analysed with the Atlas.ti^{TM} software. Relationships between the themes were identified, further analysed, and discussed (Lacey and Luff, 2001; Nowell et al., 2017).

RESULTS

Participants' characteristics

A total number of 299 undergraduate medical students and five (out of a possible 25) postgraduate students participated in this study. The undergraduate student sample self-identified as 101 males (34%) and 196 females (66%). Two students did not indicate the gender they associate with. The mean age of this group of students was 22.04 years, which ranged from 18-36 years.

The students had to indicate in which year they were registered. One hundred and twenty-four (124) students (41.4%) were in their second year of studies, 60 students (20.1%) in their third year, 66 students (22.1%) in their fourth year and 49 students (16.4%) in their sixth and final year. The first-year group was excluded from this study since they have not had any neuroanatomy experience within the medical curriculum at the time of data collection. The fifth-year group was also excluded from this study as they were used as part of a pilot study to test the relevance of the questionnaires.

Ten students (3.3%) indicated that they were repeating the current neuroanatomy module, while 14 students (4.7%) indicated that they had previously studied another degree that included neuroanatomy content. The postgraduate students consisted of four females and one male.

Study materials and electronic devices used

We explored different types of study materials used by the undergraduate students. The participants had to indicate whether they did or did not use the prescribed and recommended literature,

as well as other information sources. The results are summarised in Fig. 1.

Lecture notes provided to the students was the most preferred resource used (93.7%) in preparation for neuroanatomy assessments. Self-identified gender had a statically significant impact on the usage of lecture notes, as 63.6% females preferred lecture notes, compared to 30.1% males (p-value=0.0025). The prescribed literature (80.3%) and internet resources (77.9%) were other preferred resources used for studying neuroanatomy. One-way ANOVA models were built for the preferred use of prescribed literature and internet resources. Scheffe's and Bonferroni tests revealed that the year-group of the students had a statistically significant impact on the study materials used in their preparation for assessments. A statistically significant difference was found between the second-year group and the third-year group regarding the use of prescribed literature (p-value = 0.022). Approximately 53.2% of the second-year group of medical students used prescribed literature, in comparison to 16% of the third-year group.

The participants had to further indicate whether they used the specified electronic devices in their preparation for assessment. The most preferred electronic device was laptop computers, as indicated by 90% of the undergraduate participants. A statistically significant difference was noted in the usage of the second-year students and the final year students (p-value < 0.0001). Approximately 50% of the second-year students prefer to use their laptop computers, compared to the 9.8% of final-year students. Smartphones and handheld devices were preferred by about 50% of the participants. The data obtained are summarised in Fig. 2.

Preferred teaching approaches

The undergraduate respondents had to indicate their most and least favourite teaching approaches for neuroanatomy from a list provided. An 'Other' option was supplied where the respondents could include approaches not mentioned. The highest ranking for favourite teaching approaches were practicals containing wet brain specimens, as preferred by 77 students (25.8%) and dissection of cadaveric brain specimens, indicated by 64 students (21.4%). Video demonstrations of dissected brain specimens were preferred by 46 students (15.4%). Seven students (2.3%) indicat-

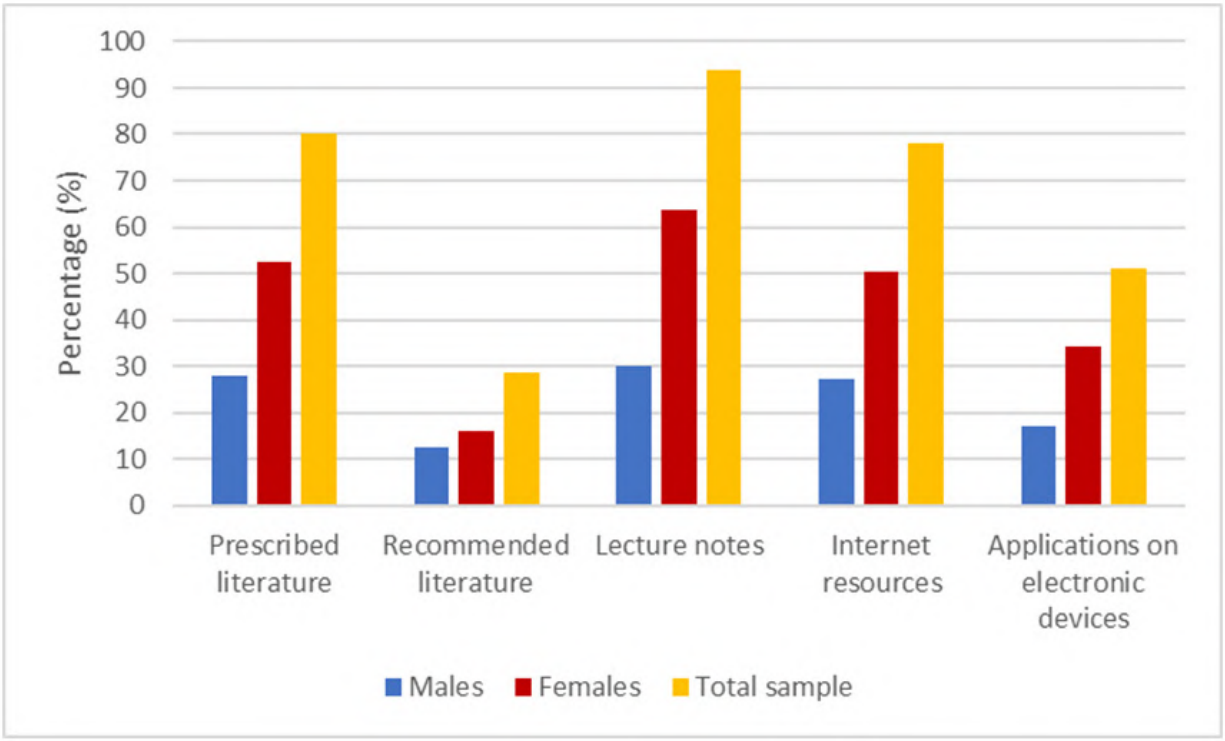

Fig. 1.- The use of literature by self-identified male and female students in their preparation for neuroanatomy assessments. Percentage values (%) are indicated.

ed the 'Other' option, which they described as a combination of the teaching approaches from the list provided. Teaching approaches that students disliked included didactic sessions (lectures) without the use of MS PowerPoint presentations, as indicated by 97 students (32.4%). Another unpopular approach was self-study or self-directed learning, which 60 students (20.1%) selected. Students were not asked to provide a rational for their choice. A possible follow-up study could be done to determine why this is not a favourite choice for students and whether the students' perceptions have changes after the COVID-19 lockdown, when they were forced into a higher level of self-directed learning. Table 1 summarises the results for preferred teaching approaches.

Preferred neuroanatomy topics

The undergraduate respondents were requested to indicate their most and least favourite neuroanatomy topics from a list provided, and then supplement their choice with a motivation. The most preferred neuroanatomy topic was cranial nerves, as indicated by 91 students (30.4%). Other preferred topics included blood vessels (21.4%), the cerebral hemispheres (19.4%) and the brainstem (12%). The rest of the topics had values lower than ten percent. The least favoured neuroanatomy topic was the histology of the nervous system, as indicated by nearly half of the students - 137 students (45.8%). Another unpopular topic was the development of the nervous system (19.7%). The results for all the topics are summarised in Table 2.

Students were further asked to indicate whether appropriate time was allocated to each of the topics during their contact sessions. The students agreed that enough time was allocated to the brainstem (70.8%), cranial nerves (77.5%), meninges (76.8%) and blood vessels (83.8%). They indicated that more time should be allocated to the histology of the nervous system (63.8%). We can assume that the dislike of the histology of the nervous system can be linked to the amount of time spent on this topic, since the students would prefer more time. The rest of the neuroanatomy topics had an almost 50/50 distribution between "enough time" and "not enough time" allocated to the assorted topics.

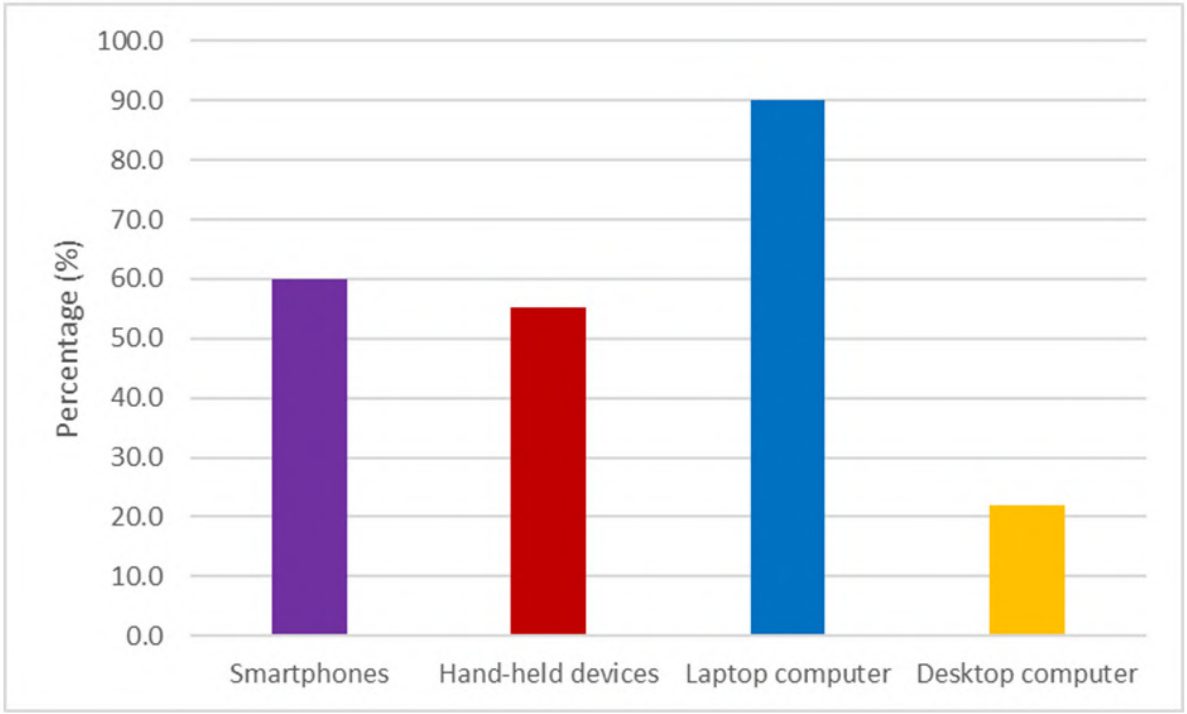

Fig. 2.- The use of electronic devices by students in their preparation for neuroanatomy assessments. Percentage values (%) are indicated.

Table 1. Teaching approaches in neuroanatomy as selected by undergraduate medical students.

Neuroanatomy teaching approaches	Indicated as most favourite (n=299)		Indicated as least favourite (n=299)	
	n	%	n	%
Lectures with MS PowerPoint presentations	56	18.7	22	7.4
Lectures without MS PowerPoint presentations	3	1	**97**	**32.4**
Video demonstrations	46	15.4	8	2.7
Computer-based practicals	-	-	24	8
Dissection of cadavers	64	21.4	13	4.3
Wet specimen / models practicals	**77**	**25.8**	13	4.3
Practical and lecture combined into a single session	21	7	14	4.7
Problem-solving scenarios	14	4.7	8	2.7
Self-study	9	3	60	21.1
Tutor-classes	-	-	29	9.7
Other	7	2.3	5	1.7

Table 2. The most- and least favourite neuroanatomy topics of undergraduate medical students.

Neuroanatomy topic	Indicated as most favourite (n=299)		Indicated as least favourite (n=299)	
	n	%	n	%
Development of nervous system	2	0.7	59	19.7
Histology of nervous system	2	0.7	**137**	**45.8**
Spinal cord	6	2	10	3.3
Brainstem	36	12	5	1.7
Cranial nerves	**91**	**30.4**	15	5
Diencephalon and pituitary gland	2	0.7	9	3
Cerebral hemispheres, limbic system and reticular formation	58	19.4	20	6.7
Autonomic system	14	4.7	17	5.7
Ventricular system	15	5	21	7
Meninges	8	2.7	6	2
Blood vessels	64	21.4	-	-

Relevance of neuroanatomy

The undergraduate respondents had to indicate whether they agreed or disagreed with statements regarding the importance of neuroanatomy within the medical curriculum. The statements were adapted from a previous study by Moxham and co-workers (2007). The results of these statements are summarised in Table 3. Most of the participants (97.7%) agreed that knowledge of neuroanatomy is essential for safe medical practice. Without this knowledge, the medical practitioner's effectiveness will be limited, as indicated by 83.9% of the participants. A two-way ANOVA model indicated that the year-group of the students and their self-identified gender had a simultaneous impact on the student's disagreement with the statement: "Neuroanatomy needs to modernize if it is going to be really useful in medicine". A statistically significant difference was noted in the students who disagreed with the statement in which 29.6% were males and 70.4% were females (p-value=0.011).

Table 3. The importance of neuroanatomy within the medical curriculum as perceived by undergraduate medical students.

Statement	Agreed with the statement (n=299)		Disagreed with the statement (n=299)	
	n	%	n	%
Neuroanatomy is an important component in my medical training.	293	97.9	5	1.7
Although neuroanatomy is interesting, the subject needs selective understanding in the clinical setting.	224	75.4	73	24.4
Neuroanatomy is necessary for safe medical practice.	**291**	**97.7**	7	2.3
Neuroanatomy is of some use in the clinical setting, but its importance may be exaggerated.	59	19.9	238	79.6
Neuroanatomy is only beneficial in certain medical specialities.	70	23.6	227	75.9
Neuroanatomy is so old-fashioned that is has no importance in contemporary medicine.	5	1.7	294	98.3
Neuroanatomy is time wasted in the medical curriculum.	6	2	292	97.7
Neuroanatomy needs to modernise if it is going to be really useful in medicine.	**110**	**37.2**	**186**	**62.2**
A very good doctor must have a good understanding of neuroanatomy.	279	93.3	20	6.7
It is impossible to conceive a good medical training without a major neuroanatomy component.	229	76.8	69	23.1
It is not possible to make a reasonable medical diagnosis without a sound knowledge of neuroanatomy.	204	68.7	93	31.1
Medicine would not exist without neuroanatomy.	235	78.6	64	21.4
Only a limited neuroanatomical knowledge is required for safe medical practice.	99	33.2	199	66.6
Rather than studying neuroanatomy, medical students should concentrate on clinical sciences.	44	14.8	254	84.9
Without knowledge of neuroanatomy, the doctor is of limited effectiveness.	**250**	**83.9**	48	16.1

Further significant differences were noted between the second-year group and third- year group of students (p-value = 0.025), as well as the second-year group and final- year group of students (p-value = 0.037). In the second-year group, 48.4% of the students disagreed with the statement, in comparison to the third-year group with 16.1% and the final-year group with 13.4%. We can then assume that female second- year students do not want modern changes to occur in the medical neuroanatomy curriculum, and that they are content with the current stance of neuroanatomy.

Advice from postgraduate students

The postgraduate student sample is small (five out of a possible 25 students) due to the small number of students who want to specialize in neurosciences for an MMed degree. These students had to elaborate on their undergraduate neuroanatomy experiences. Only one student (20%) had positive comments regarding his/her experience with the statement "*I find the neurosciences interesting, it's not difficult, just need to have enough time to study it, it can be fun.*" The rest of the group (80%) described their negative experiences which included "*very difficult and not easy to understand", "cannot remember anything about undergraduate neuroanatomy training besides that it was difficult and confusing" and "we had to rely on ourselves".*

This group was further asked to provide constructive feedback and suggestions on how to approach neuroanatomy. Most of the group suggested that the lecturing staff should make neuroanatomy more fun, accessible, and simplified to the students. Their advice to the students was mainly to understand the fundamentals of neuroanatomy and allocate enough time for study purposes. Only one of the participants indicated that she had a neuroanatomy role-model during her undergraduate training.

DISCUSSION

Neurological disorders constitute more than 6.4% of the health burden and 12% of mortality

globally (Ridsdae, 2009; Abulaban et al., 2015) The prevalence and impact of neurological conditions place a higher demand on the healthcare system to improve on neurological care. Therefore, doctors/physicians need to be better prepared in their approach and diagnosis to this specialty (Fantaneanu et al., 2014). Given these statistics, the effect that neurophobia has on medical students will greatly affect the treatment provided to patients who complain of neurological symptoms (Nham, 2012). Medical students consider neurology to be the most difficult, but also the most interesting of all the internal medicine specialties, especially after completion of that specific rotation (Hudson, 2006; Nham, 2012; McCarron et al., 2014). Neuroanatomy has even been mentioned as the main reason for this perception of difficulty (Arantes et al., 2017).

In this study, we explored the perceptions of medical students towards neuroanatomy, as well as its position and assumed importance within the undergraduate medical curriculum. This study forms part of a larger study which investigates neuroanatomy within the South African medical curriculum. The results of this study can be used to create awareness of the perceptions, preferences and needs of undergraduate medical students towards neuroanatomy and its teaching, facilitation, and assessment within the South African curriculum.

Study material and electronic devices

The respondents indicated that they prefer lecture notes, supplied by the lecturers, above any of the other forms of literature. Ninety percent (90%) of the students used laptop computers in their preparation for neuroanatomy assessments in comparison to smartphones and hand-held devices, which are only used by 55-59%. This contradicts assumptions that students prefer to use their smartphones and hand-held devices for studying, as these devices are always readily available.

Students mainly use electronic devices, including smart phones and hand-held devices, for information retrieval (Morris et al., 2016). In the UK, the successfully integrated use of hand-held devices in neuroanatomy practicals and learning support has been reported with an increased success-rate in the students' results (Morris et al., 2016). The students' perception of their learning and class enjoyment can be enhanced by integrating mobile learning opportunities within the curriculum (Morris et al., 2016). Medical students in Ireland deem internet sources for neuroanatomy as very useful, as indicated by 81.8%, especially in understanding the clinical relevance of neuroanatomy (Javaid et al., 2018).

Preferred teaching approaches

The undergraduate students prefer their contact sessions in neuroanatomy to be in the format of practicals with cadaveric brain specimens and plastic models, as well as dissections of human cadaveric brains. These students want to interact with the content instead of attending didactic lectures, especially those that do not include MS PowerPoint presentations. They want to be actively involved in their learning processes which is in line with the transferrable skills of the twenty-first-century student. However, self-directed learning is a very unpopular approach to neuroanatomy, according to these students. One can speculate that it can be ascribed to factors such as poor self-management, readiness, openness, work-drive and even access to resources which might be challenging (Lunyk-Child et al., 2001; Morris, 2019). A follow-up study with the same cohort of students is advisable to confirm these assumptions. Exposure to more complicated brain dissections is a valuable learning experience for students (Myers et al., 2018; Karamaroudis et al., 2020). In Ireland, senior medical students (already in their clinical years) valued the use of case-based learning more than prosected brain specimens, in comparison to the junior medical students (still in their basic sciences years) (Javaid et al., 2018). This supports the findings of this study.

Our findings concur with those reported in Saudi Arabia, in which 70.4% of students ascribed their lack of interest in neurology to bad teaching experiences (Abulaban et al., 2015). In the United Kingdom (UK), 35% of the participating medical students indicated that the time allocated for neurology and related content is insufficient (Pakpoor et al., 2014). Medical students from

Brazil, especially senior students, also indicated that more teaching was needed for neurosciences (Santos-Lobat et al., 2018). Students from West India indicated that they prefer educational interventions such as team-based learning, problem-based learning, and case- based teaching for neuroscience (Shiels et al., 2017).

Although the responsibility to engage in learning opportunities in neurosciences remains the responsibility of the student (Nham, 2012), the lecturer can contribute by making the subject interesting, contemporary, and engaging by using various student-centred teaching modalities and techniques. Furthermore, the lecturers need to guide the students into taking responsibility for their own learning through student-centred teaching and facilitation methods. Educational interventions in the early stages of a medical career may enhance long-term motivation and interest in the neurosciences (McCarron et al., 2015). Such interventions to expand the student's competency in neurology include more clinical or bedside teaching, more case discussions, additional teaching aids, as well as extra neurology and neuroanatomy lectures (Matthias et al., 2013).

Preferred neuroanatomy topics

The participants in this study indicated that cranial nerves, on average, was their most favourite neuroanatomy topic. We explored the reasons for this choice and five themes emerged from their answers. The participants indicated cranial nerves as a topic that is interesting and easy to understand. They see the topic's clinical relevance for their future careers, they understand how cranial nerves are integrated with the rest of the body, and they had a good teaching experience on this topic. Medical students in Ireland made similar statements, in which they rated the cranial nerves as an easy neuroanatomy topic, except for the cranial nerve nuclei (Javaid et al., 2018). The students indicated that their least favourite topic is the histology of the nervous system, and ascribed this to unconducive didactic teaching experiences, complex and uninteresting content, not enough time allocated, and, in their opinion, lack of clinical relevance.

Importance of neuroanatomy

Overall, the undergraduate medical students perceive neuroanatomy as an interesting and important, but not stand-alone component in their medical curriculum. They understand that a good foundational knowledge of neuroanatomy is necessary for safe medical practice, irrespective of the discipline. When asked whether neuroanatomy needs to be modernized, more than 50% of the students, mostly females, were in support of the statement, indicating the need to revamp the teaching approaches in the current medical neuroanatomy curriculum,. which might be ascribed to the fact that female students are more likely to be neurophobic (Kam et al., 2013), perceive neuroanatomy as complicated and not consider a future career in the neurosciences in comparison to male students (Abulaban et al., 2015). However, the perception of difficulty, with reference to the three-dimensional complexity of the brain might also affect the student's attitude towards neuroanatomy, and it is reported to affect females more than males (Clements-Stephens et al., 2009; Palomera et al., 2014). Furthermore, male students tend to be more reliant on images and prefer "hands-on" during contact sessions in comparison to females (Clements-Stephens et al., 2009).

As part of our own personal introspection, reflections and contemplations, the question that needs to be answered is: how can we, as lecturers, modernize neuroanatomy in the medical curriculum and subsequently prevent the development of neurophobia? Recommendations include more clinical relevance in the neuroanatomy content for the students (Pakpoor et al., 2014), as well as the inclusion of medical images, anatomical models, and virtual anatomy. We need to acknowledge that, by separating basic neuroscience from clinical sciences, and removing clinical relevance, the students become neurophobic as they struggle to implement the basic neuroanatomy concepts in the clinical environment, therefore enhancing the lack of theory-practice integration. Neurophobia is a result of our teaching and attitudes towards the content, as well as the use of a non-transformed, outdated curricula. We as lecturers, therefore, need to take ownership of the fact that we might be the cause of neurophobia among our under-

graduate medical students and, consequently, have to adapt our attitude and teaching methods towards the student's training in medical school (Ridsdale et al., 2007; Arantes et al., 2017; Shiels et al., 2017) We need to allocate more time to basic neuroscience concepts, as medical students worldwide indicated that more time is needed for basic neuroanatomy (Pakpoor et al., 2014: Santos-Lobato et al., 2018).

Our teaching approaches should be person-focused and student-friendly, as suggested by the postgraduate students. Lecturers should engage in student-centred teaching methods to assist students in overcoming/minimizing neurophobia. We, the lecturers, are not the centre-point of the teaching environment anymore, as we are mere facilitators in the learning process of our students. We can instil in them the enthusiasm for neuroanatomy and not drown them with cognitive and content overload or attempt to make content-experts of them in the early years of their medical degree (Palomera et al., 2014; Greville et at., 2016). We should provide them with the necessary tools and guidance, but they, themselves, must master the neuroanatomy content and apply it, when necessary, in the clinical environment.

In conclusion, a less than optimal teaching experience and limited contact-time for students remain crucial factors contributing to neurophobia, even in the South African medical schools. This affects how our students perceive neuroanatomy and its importance in the medical curriculum, irrespective of whether the students are undergraduates or postgraduates. If we, as lecturers, can address these issues at our institutions, we can start to make a difference in our students' lives regarding neurophobia. Dedicating more time to neuroanatomy is a challenging task to accomplish, as it implies that time must be negotiated and reduced from another discipline or subject to accommodate this change. Collaboration between the basic sciences departments and clinical departments is vital for such changes. Nonetheless, we can reflect on our teaching approaches and make the necessary changes to help our students overcome this fear for the neurosciences. After all, we want our students to be competent healthcare professionals with a sound foundation in neuroanatomy.

ACKNOWLEDGEMENTS

We would like to thank the students who participated in this study. The authors thank Ms Joyce C. Jordaan, a research consultant in the Department of Statistics, University of Pretoria, for her assistance with the statistical analysis of the data obtained in this study.

REFERENCES

ABULABAN AA, OBEID TH, ALGAHTANI HA, KOJAN SM, AL-KHATHAAMI AM, ABULABAN AA, BOKHARI MF, MERDAD AA, RADI SA (2015) Neurophobia among medical students. *Neurosciences (Riyadh),* 20(1): 37-40.

ABUSHOUK AI, DUC NM (2016) Curing neurophobia in medical schools: evidence-based strategies. *Med Educ Online*, 21(1): 32476.

ARANTES M, BARBOSA JM, FERREIRA MA (2017) Neuroanatomy education: The impact on perceptions, attitudes, and knowledge of an intensive course on general practice residents. *Anat Sci Educ*, 10(5): 465-474.

BRYMAN A, BELL E (2014) *Research Methodology: Business and Management Contexts*. Oxford University Press, Southern Africa (Pty) Limited.

CLEMENTS-STEPHENS AM, RIMRODT SL, CUTTING LE (2009) Developmental sex differences in basic visuospatial processing: differences in strategy use? *Neurosci Lett*, 449(3): 155-160.

COLUCCI E (2007) "Focus groups can be fun": The use of activity-oriented questions in focus group discussions. *Qualit Health Res*, 17(10): 1422-1433.

ELNAEIM M, BABIKER I, ELNAEIM A (2021) Neurophobia among medical students in Sudan. *J Neurol Sci,* 429.

FANTANEANU TA, MOREAU K, EADY K, CLARKIN C, DEMEULEMEESTER C, MACLEAN H, DOJA A (2014) Neurophobia inception: a study of trainees' perceptions of neurology education. *Canad J Neurol Sci*, 41(4): 421-429.

GEOGHEGAN K, PAYNE DR, MYERS MA, HALL S, ELMANSOURI A, PARTON WJ, BORDER S (2019) The National Undergraduate Neuroanatomy Competition: lessons learned from partnering with students to innovate undergraduate neuroanatomy education. *Neuroscientist,* 25(3): 271-280.

GORGICH EAC, SARBISHEGI M, BARFROSHAN S, ABEDI A (2017) Medical students' knowledge about clinical importance and effective teaching methods of anatomy. *Shiraz E-Medical J*, 18(12).

GREVILLE WJ, DYMOND S, NEWTON PM (2016) The student experience of applied equivalence-based instruction for neuroanatomy teaching. *J Educ Eval Health Prof*, 13: 32.

HALL S, STEPHENS J, PARTON W, MYERS M, HARRISON C, ELMANSOURI A, BORDER S (2018) Identifying medical student perceptions on the difficulty of learning different topics of the undergraduate anatomy curriculum. *Med Sci Educ*, 28: 469-472.

HUDSON JN (2006) Linking neuroscience theory to practice to help overcome student fear of neurology. *Med Teacher,* 28(7): 651-653.

JAVAID MA, CHAKRABORTY S, CRYAN JF, SCHELLEKENS H, TOULOUSE A (2018) Understanding neurophobia: Reasons behind impaired understanding and learning of neuroanatomy in cross disciplinary healthcare students. *Anat Sci Educ*, 11(1): 81-93.

JOZEFOWICZ RF (1994) Neurophobia: the fear of neurology among medical students. *Arch Neurol*, 51(4): 328-329.

KAM KQ, TAN GS, TAN K, LIM EC, KOH NY, TAN NC (2013) Neurophobia in medical students and junior doctors blame the GIK. *Ann Acad Med Singapore*, 42(11): 559-566.

KARAMAROUDIS S, POULOGIANNOPOULOU E, SOTIROPOULOS MG, KALANTZIS T, JOHNSON EO (2020) Implementing change in neuroanatomy education: organization, evolution, and assessment of a near-peer teaching program in an undergraduate medical school in Greece. *Anat Sci Educ*, 13(6): 694-706.

LACEY A, LUFF D (2001) *Qualitative data analysis*. Sheffield: Trent focus, pp 320-357.

LUKAS RV, COOPER B, MORGAN I, BRORSON JR, DONG H, SHERER R (2014) Attitudes toward neurosciences in medical students in Wuhan, China: a survey study. *World Neurosurg*, 82(3-4): 266-269.

LUNYK-CHILD OI, CROOKS D, ELLIS PJ, OFOSU C, O'MARA L, RIDEOUT E (2001) Self-directed learning: Faculty and student perceptions. *J Nursing Educ*, 40(3): 116-123.

MARANHÃO-FILHO P (2014) The healthy concern to improve neurological teachings. *Arq Neuropsiquiatr,* 72(10): 743-744.

MATTHIAS AT, NAGASINGHA P, RANASINGHE P, GUNATILAKE SB (2013) Neurophobia among medical students and non-specialist doctors in Sri Lanka. *BMC Med Educ*, 13: 1-7.

MCCARRON MO, STEVENSON M, LOFTUS AM, MCKEOWN P (2014) Neurophobia among general practice trainees: the evidence, perceived causes and solutions. *Clin Neurol Neurosurg,* 122: 124-128.

MCCARRON MO, STEVENSON M, LOFTUS AM, MCKEOWN P (2015) Reply to editorial–Neurophobia: A global and under-recognized phenomenon. *Clin Neurol Neurosurg*, (128): 132-133.

MOHAMMED A, MOHAMMED A, ABDULLAH A, MESHARI A, KHALID A, MOHAMMED A (2018) Assessment of attitude and perception toward neurology and neurosurgery specialties among medical students and interns attending college of medicine at university of Tabuk in Tabuk City, Saudi Arabia. *Egypt J Hosp Med,* 71(4): 2960-2962.

MORRIS TH (2019) Adaptivity through self-directed learning to meet the challenges of our ever-changing world. *Adult Learning*, 30(2): 56-66.

MORRIS NP, LAMBE J, CICCONE J, SWINNERTON B (2016) Mobile technology: students perceived benefits of apps for learning neuroanatomy. *J Comput Assist Learning*, 32(5): 430-442.

MOXHAM B, MCHANWELL S, PLAISANT O, PAIS D (2015) A core syllabus for the teaching of neuroanatomy to medical students. *Clin Anat*, 28(6): 706-716.

MOXHAM B, MOXHAM SA (2007) The relationships between attitudes, course aims and teaching methods for the teaching of gross anatomy in the medical curriculum. *Eur J Anat*, 11: 19-30.

MYERS M, HALL S, STEPHENS J, LOWRY J, SEABY E, PARTON W, BORDER S (2018) The National Undergraduate Neuroanatomy Competition: five years of educating, inspiring and motivating our future neurologists and neurosurgeons. *Eur J Anat,* 22(2): 183-193.

NHAM B (2012) Graded exposure to neurophobia: stopping it affect another generation of students. *Aust Gen Pract Training*, 3: 76.

NOWELL LS, NORRIS JM, WHITE DE, MOULES NJ (2017) Thematic analysis: Striving to meet the trustworthiness criteria. *Int J Qualit Meth*, 16(1): 1609406917733847.

PAKPOOR J, HANDEL AE, DISANTO G, DAVENPORT RJ, GIOVANNONI G, RAMAGOPALAN SV (2014) National survey of UK medical students on the perception of neurology. *BMC Med Educ*, 14(1): 1-5.

PALOMERA PR, MÉNDEZ JAJ, GALINO AP (2014) Enhancing neuroanatomy education using computer-based instructional material. *Comput Human Behav,* 31: 446-452.

PANDEY P, ZIMITAT C (2007) Medical students' learning of anatomy: memorisation, understanding and visualisation. *Med Educ*, 41(1): 7-14.

RIDSDALE L, MASSEY R, CLARK L (2007) Preventing neurophobia in medical students, and so future doctors. *Pract Neurol*, 7(2): 116-123.

RUSSELL S, VERNON STE, TALLANTYRE E (2015) Next generation neurology: e-learning. *ACNR,* 15: 18-19.

SANTOS-LOBATO BL, MAGALHÃES ÁB, MOREIRA DG, FARIAS FP, PORTO LK, PEREIRA RB, BRAGA TKK (2018) Neurophobia in Brazil: detecting and preventing a global issue. *Rev Brasil Educação Médica*, 42:121-128.

SEAWRIGHT J (2016) Better multimethod design: the promise of integrative multimethod research. *Security Studies*, 25(1): 42-49.

SHELLEY BP, CHACKO TV, NAIR BR (2018) Preventing "neurophobia": Remodeling neurology education for 21st-century medical students through effective pedagogical strategies for "neurophilia". *Ann Indian Acad Neurol*, 21(1): 9-18.

SHIELS L, MAJMUNDAR P, ZYWOT A, SOBOTKA J, LAU CS, JALONEN TO (2017) Medical student attitudes and educational interventions to prevent neurophobia: a longitudinal study. *BMC Med Educ,* 17(1): 1-7.

SOTGIU MA, MAZZARELLO V, BANDIERA P, MADEDDU R, MONTELLA A, MOXHAM B (2020) Neuroanatomy, the Achille's heel of medical students. A systematic analysis of educational strategies for the teaching of neuroanatomy. *Anat Sci Educ*, 13(1): 107-116.

TAROLLI CG, JÓZEFOWICZ RF (2018) Managing neurophobia: how can we meet the current and future needs of our students? *Seminars in Neurology* (Vol. 38, No. 04, pp 407-412). Thieme Medical Publishers.

VENTER G, LUBBE JC, BOSMAN MC (2022) Neurophobia: a side effect of neuroanatomy education? *J Med Syst*, 46(12): 99.

YOUSSEF FF (2009) Neurophobia and its implications: evidence from a Caribbean medical school. *BMC Med Educ*, 9(1): 1-7.

ZINCHUK AV, FLANAGAN EP, TUBRIDY NJ, MILLER WA, MCCULLOUGH LD (2010) Attitudes of US medical trainees towards neurology education:" Neurophobia"-a global issue. *BMC Med Educ*, 10(1): 1-7.

SUPPLEMENTARY MATERIAL: STUDENT QUESTIONNAIRE

Dear Student

I am a PhD student in the Department of Anatomy, University of Pretoria. You are invited to volunteer to participate in my research project, by completing the following questionnaire regarding the exploration of perceptions and attitudes of both staff and students towards neuroanatomy in the South African undergraduate medical curriculum. This letter provides you with information to help you decide whether you want to take part in this study. Before you agree you should fully understand what is involved. You should not agree to take part unless you are completely happy about what we are requesting from of you.

The aim of this study is to investigate the attitudes of anatomy lecturers, undergraduate and postgraduate students towards the teaching and learning of neuroanatomy in the medical curriculum. This study will further examine the perception of students on the importance of neuroanatomy as it relates to their future careers as well as the current teaching and assessment practices used by anatomy lecturers at South African Universities.

This study involves answering some questions regarding your personal opinion on the facilitation and learning of neuroanatomy and the relevance of neuroanatomy as part of your medical curriculum.

We would like you to complete an anonymous online questionnaire. This may take about 10 minutes. This will ensure confidentiality and anonymity. The Research Ethics Committee of the University of Pretoria, Faculty of Health Sciences granted written approval for this study (nr 587/2018). This study has been structured in accordance with the Declaration of Helsinki, of which a copy may be obtained from the primary investigator, should you wish to review it.

This questionnaire consists of the following two parts:

- Section A: General information which involves answering some questions about your age, current year of studies etc.
- Section B: Perceptions and attitudes towards neuroanatomy which involves answering some questions about your personal view on neuroanatomy and its place in the medical curriculum

Your participation in this study is voluntary. You can refuse to participate, omit questions or stop at any time without providing any reason. As you do not write your name on the questionnaire, you give us the information anonymously. Once you have submitted the questionnaire, you cannot recall your consent as we will be unable to trace (identify) your information-sheet. Therefore, you will also not be identified as a participant in any publication that results from this study.

There is no foreseeable physical discomfort or risk involved. If there are questions that are too sensitive for you to answer, you do not need to answer them. This study may help to make key recommendations towards the formation of a framework for a revised neuroanatomy module for undergraduate medical students, specific to the South African context.

Note: The implication of completing the questionnaire is that informed consent has been obtained from you. Thus, all information derived from you and all records from this study will be regarded as confidential (which will be depersonalised and anonymous) may be used for e.g. publication, by the researchers. If you have any questions concerning this study, you should contact the primary investigator, Mrs Gerda Venter at (+27)12 319 2536 or gerda.venter@up.ac.za.

We sincerely appreciate your help.
Gerda Venter

Consent to participate in this study:

- I confirm that the person requesting my consent to take part in this study has informed me about the nature and process, any risks or discomforts, and the benefits of the study.
- I have received, read and understood the attached written information leaflet about the study.
- I am aware that the information obtained in the study, including personal details, will be anonymously processed and presented in the reporting of results.
- I am participating willingly.

o I agree (1)
o I do not agree (2)

Q2 The gender I identify with:
o Male (1)
o Female (2)
o Prefer not to answer (3)
o Other (4) .....

Q3 My current age in years:
.....

Q4 I am currently completing the _____ of my medical degree.
o First year (1)
o Second year (2)
o Third year (3)
o Fourth year (4)
o Fifth year (5)
o Final year (6)

Q5 The neuroanatomy module(s) that I am currently registered for / completed:
.....

Q6 I am repeating this Neuroanatomy module.
o Yes (1)
o No (2)

Q7 Have you done any other Neuroanatomy course(s), excluding the ones in your medical degree?
o Yes (Please specify) (1) .....
o No (2)

Q8 Did you receive a study-guide for your Neuroanatomy modules in your medical degree?
o Yes (1)
o No (2)
o Not in all of the modules (please elaborate) (3) .....

Q9 Did you find the study-guide useful for: (Select the most relevant options)

	Extremely useful (1)	Useful (2)	Somewhat useful (3)	Not useful (4)
Administrative information (1)				
Assessments (2)				
Preparation for contact sessions (3)				
Overview of the syllabus (4)				

Q10 How often did you make use of the following types of study materials to study Neuroanatomy. (Select the most relevant options)

	All the time (1)	Most of the time (2)	Almost never (3)	Never (4)
Prescribed literature (1)				
Recommended literature (2)				
Lecture notes (3)				
Internet resources (4)				
Applications on electronic devices (5)				

Q11 How often did you make use of the following types of electronic devices to study Neuroanatomy. (Select the most relevant options)

	All the time (1)	Most of the time (2)	Almost never (3)	Never (4)
Smartphone (1)				
Hand-held devices (2)				
Laptop (3)				
Desktop computer (4)				

Q12 Indicate your liking / interest in the following Neuroanatomy topics. (Select the most relevant options)

	Do not like at all (1)	Like a little (2)	Like (3)	Like a lot (4)	Was not covered in this module (5)
Development of the nervous system (1)					
Histology of the nervous system (2)					
Spinal cord (3)					
Brainstem (4)					
Cranial nerves (5)					
Diencephalon and pituitary gland (6)					
Cerebral hemispheres, limbic system and reticular formation (7)					
Autonomic system (8)					
Ventricular system (9)					
Meninges (10)					
Blood vessels (11)					

Q13 Which Neuroanatomy topic is your MOST favourite?

o Development of the nervous system (1)
o Histology of the nervous system (2)
o Spinal cord (3)
o Brainstem (4)
o Cranial nerves (5)
o Diencephalon and pituitary gland (6)
o Cerebral hemispheres, limbic system and reticular formation (7)
o Autonomic system (8)
o Ventricular system (9)
o Meninges (10)
o Blood vessels (11)

Q14 Please supply the reason for choosing this specific topic as your MOST favourite (in the box below).

.....

Q15 Which Neuroanatomy topic is your LEAST favourite?

o Development of the nervous system (1)
o Histology of the nervous system (2)
o Spinal cord (3)
o Brainstem (4)
o Cranial nerves (5)
o Diencephalon and pituitary gland (6)
o Cerebral hemispheres, limbic system and reticular formation (7)
o Autonomic system (8)
o Ventricular system (9)
o Meninges (10)
o Blood vessels (11)

Q16 Please supply the reason for choosing this specific topic as your LEAST favourite (in the box below).

.....

Q17 In your opinion, was enough time allocated to the following Neuroanatomy topics? (Select only the appropriate boxes)

	Yes (1)	No (2)
Development of the nervous system (1)		
Histology of the nervous system (2)		
Spinal cord (3)		
Brainstem (4)		
Cranial nerves (5)		
Diencephalon and pituitary gland (6)		
Cerebral hemispheres, limbic system and reticular formation (7)		
Autonomic system (8)		
Ventricular system (9)		
Meninges (10)		
Blood vessels (11)		

Q18 Please evaluate the following teaching approaches for Neuroanatomy according to your liking / interest. (Select only the appropriate boxes)

	Do not like at all (1)	Like a little (2)	Like (3)	Like a lot (4)	Not used in this module (5)
Lectures with PowerPoint presentations (1)					
Lectures without PowerPoint presentations (2)					
Video demonstrations (3)					
Wet specimens / models demonstrations by a staff member (4)					
Computer-based practicals / tutorials (5)					
Dissection of human cadavers (6)					
Wet specimens / models practicals (7)					
Practical and lecture combined into a single session (8)					
Problem-solving scenarios (9)					
Self-study (10)					
Tutor classes (11)					
Other (12)					

Q19 If 'other' was selected, please specify. (Write your answer in the box below)

.....

Q20 Which teaching approach, for Neuroanatomy, was your MOST favourite? (Select only the appropriate box)

o Lectures with PowerPoint presentations (1)
o Lectures without PowerPoint presentations (2)
o Video demonstrations (3)
o Wet specimens / models demonstrations by a staff member (4)
o Computer-based practicals / tutorials (5)
o Dissection of human cadavers (6)
o Wet specimens / models practicals (7)
o Practical and lecture combined into a single session (8)
o Problem-solving scenarios (9)
o Self-study (10)
o Tutor classes (11)
o Other (please specify) (12) _____

Q21 Please supply the reason for choosing this specific approach as your MOST favourite (in the box below).

.....

Q22 Which teaching approach was your LEAST favourite? (Select only the appropriate box)

o Lectures with PowerPoint presentations (1)
o Lectures without PowerPoint presentations (2)

- o Video demonstrations (3)
- o Wet specimens / models demonstrations by a staff member (4)
- o Computer-based practicals / tutorials (5)
- o Dissection of human cadavers (6)
- o Wet specimens / models practicals (7)
- o Practical and lecture combined into a single session (8)
- o Problem-solving scenarios (9)
- o Self-study (10)
- o Tutor classes (11)
- o Other (please specify) (12) .....

Q23 Please supply the reason for choosing this specific approach as your LEAST favourite (in the box below).

.....

Q24 Regarding your attendance in this Neuroanatomy module: (Tick only the appropriate boxes)

	All the time (1)	Most of the time (2)	Half the time (3)	Almost never (4)	Never (5)	Not applicable for this module (6)
How often did you attend the Neuroanatomy lectures? (1)						
How often did you attend the Neuroanatomy practicals? (2)						
How often did you attend the Neuroanatomy practical-lectures? (3)						
How often did you attend the additional tutor classes / supplementary instruction sessions? (4)						

Q25 Indicate your level of agreement. (Select only the appropriate options)

	Strongly agree (1)	Agree (2)	Disagree (3)	Strongly disagree (4)
Neuroanatomy is an important component in my medical training. (1)				
Although Neuroanatomy is interesting, this subject needs selective understanding in the clinical setting. (2)				
Neuroanatomy is necessary for safe medical practice. (3)				
Neuroanatomy is of some use in the clinical setting, but its importance may be exaggerated. (4)				
Neuroanatomy is only beneficial in certain medical specialities. (5)				
Neuroanatomy is so old-fashioned that it has no importance in contemporary Medicine. (6)				
Neuroanatomy is time wasted in the medical curriculum. (7)				
Neuroanatomy needs to modernise if it is going to be really useful in Medicine. (8)				
A very good doctor must have a good knowledge of Neuroanatomy. (9)				
It is impossible to conceive a good medical training without a major Neuroanatomy component. (10)				
It is not possible to make a reasonable medical diagnosis without a sound knowledge of Neuroanatomy. (11)				
Medicine could not exist without Neuroanatomy. (12)				
Only a limited neuroanatomical knowledge is required for safe medical practice. (13)				
Rather than studying Neuroanatomy, medical students should concentrate on clinical sciences. (14)				
Without a knowledge of Neuroanatomy, the doctor is of limited effectiveness. (15)				

Q26 Please write comments regarding your Neuroanatomy experience in the box below.

.....

Q27 Please write any suggestions for the Neuroanatomy lecturers in the box below.

.....

The unfamiliar entity in an unfamiliar location - Stafne bone cavity (Ramus variant)

Karthikeya Patil, C.J. Sanjay, Namrata Suresh, Eswari Solayappan

Department of Oral Medicine and Radiology, JSS Dental College and Hospital, JSS Academy of Higher Education and Research, Mysore - 570 015, India

SUMMARY

Identifying Stafne bone cavities of the ramus mimics early diagnosis of cysts or tumours. In contrast, failure to recognize them can result in incorrect diagnoses and ineffective treatments. Clinical and radiological characteristics using orthopantomogram and cone beam computed tomography to make clinicians aware of such entities and help distinguish between this anatomical variant from benign tumours or cysts. This report attempts to broaden the understanding of this rare entity, as, to the best of our knowledge, only 10 cases of the ramus variant of Stafne bone cavities have been reported in the literature.

Key words: Pseudocyst – Salivary gland – Mandible – Developmental

INTRODUCTION

Preliminary radiographic evaluation of the dentomaxillofacial complex and its supporting structures is carried out by a panoramic radiograph, which has been widely accepted and clinically justified. Occasionally, this radiographic evaluation may reveal rare yet normal incidental findings. Recognition of such an entity and its characteristics in a radiographic image is detrimental to a patient's health care, the failing of which could result in an inaccurate diagnosis and treatment. One such occurrence is the Stafne bone cavity (SBC).

The Stafne bone cavity was first described by Edward Stafne (1942) as a unilateral, radiolucent, and asymptomatic cavity usually located between the lower first molar and the mandibular angle. It has been addressed by a plethora of names, including "cortical mandibular depression," "Stafne bone cyst," "Stafne bone cavity," "latent bone cyst," "aberrant salivary gland defect," "developmental bone defect of the mandible," and "idiopathic bone cavity" (Kaya et al., 2018). SBC is usually mistaken for a benign tumour or cyst because of its radiological features (Campos et al., 2004). SBCs are classified into three types: the anterior variant, the posterior variant, and the ramus variant. Only 10 cases of the ramus variant are reported in the scientific literature, which makes it a very rare entity.

In this article, we present two exceptional instances of Stafne Cavity: the ramus variant in the left sub-condylar region of the mandible was found during a routine panoramic radiographic evaluation, for which ethical clearance was

Corresponding author:
Dr Sanjay CJ, MDS. Department of Oral Medicine and Radiology, JSS Dental College and Hospital, JSS Academy of Higher Education and Research, Mysore - 570 015, India. Phone: +91 97425 65566. E-mail: drsanjaycj_dch@jssuni.edu.in - Orcid ID: 0000-0003-2830-1481

Submitted: February 11, 2023. **Accepted:** March 2, 2023

https://doi.org/10.52083/NUKD2624

obtained from the Institutional Ethics Committee with the JSSDCH IEC Research Protocol No: 22/2022.

CASE REPORT 1

A 14-year-old female patient presented with the chief complaint of forwardly placed upper front teeth. There was no history of mouth breathing, difficulty in speech, or mastication. The patient was healthy, and the medical history contained no systemic diseases or drug allergies. Intraoral examination revealed the full complement of permanent teeth except for the maxillary permanent canines, which were missing clinically. The patient was diagnosed provisionally with Angle's class I molar malocclusion with increased overjet. As a preliminary radiograph, the patient was subjected to panoramic radiography, which revealed erupting maxillary permanent canines and a well-defined homogeneous radiolucency with a thin sclerotic border measuring 1 cm in diameter in the posterior portion of the ramus, involving the left sub-condylar region (Fig. 1a). There were no perturbations to the adjacent structures, such as periosteal response or anatomical structural displacement.

The radiolucency was further investigated using Cone Beam Computed Tomography (CBCT).

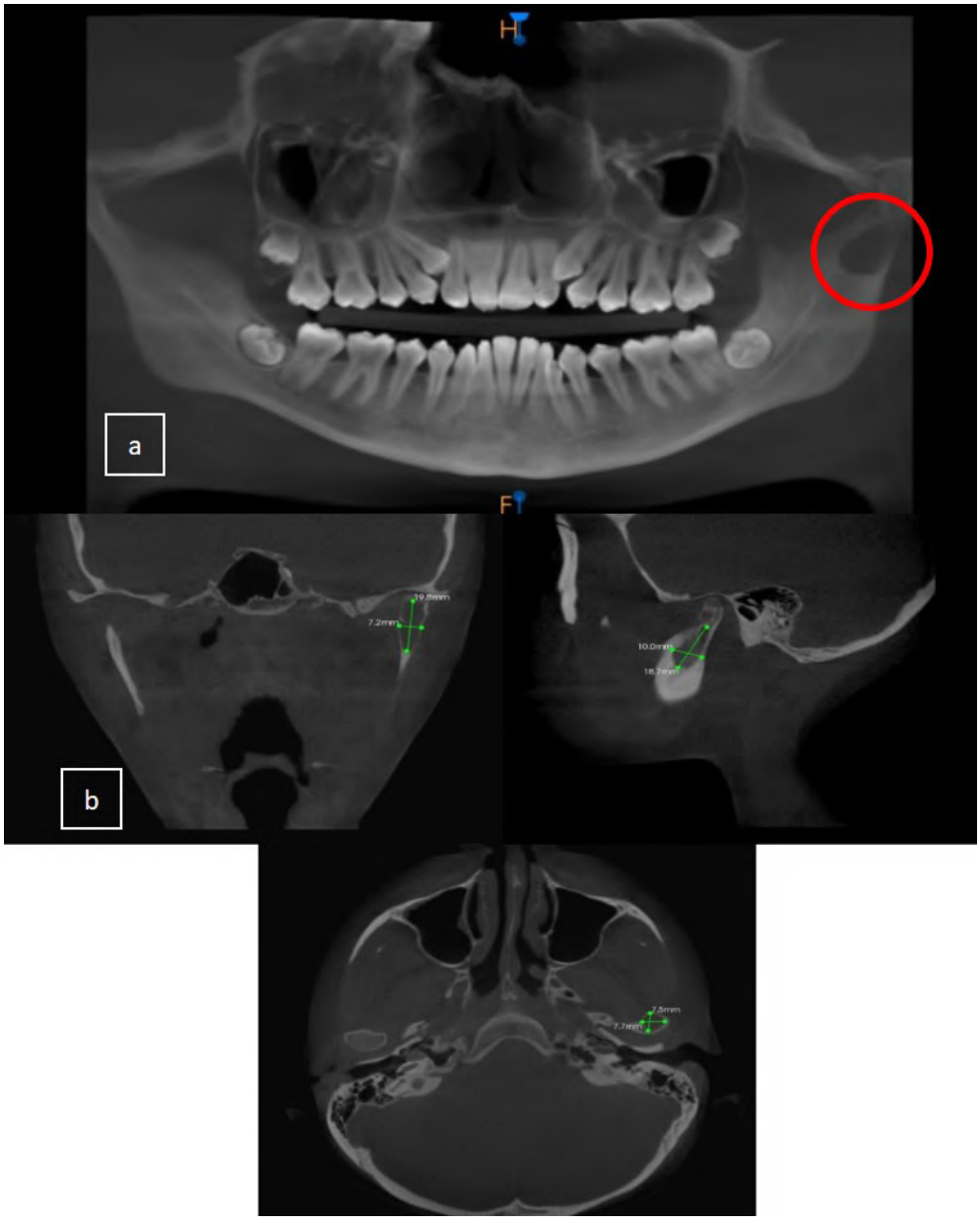

Fig. 1.- a: Orthopantomogram showing SBC of Ramus variant, noted in the left subcondylar region. **b:** CBCT showing SBC of Ramus variant.

This confirmed the uniform radiolucency with the measurement of 19.8 mm* 7.2 mm supero-inferiorly, and 7.5 mm*7.7 mm anteroposteriorly and did not signify central pathology at the left sub-condylar region. The mandibular canal was intact, and the lesion was 3 mm above the lingula (Fig. 1b).

CASE REPORT 2

Another 50-year-old male patient visited with the chief complaint of missing teeth in the right upper jaw. The patient was diabetic and was under medication. Intraoral examination revealed that the right first, second, and third permanent molars and upper right second premolar were missing. The patient had poor periodontal status and undesirable oral hygiene. A provisional diagnosis of chronic generalised periodontitis with a partially edentulous upper arch was made. A preliminary panoramic radiograph was advised as part of the periodontal treatment protocol, which depicted generalised horizontal and vertical bone loss. A well-defined, unilocular oval-shaped radiolucency was noticed on the posterior portion of the ramus below the neck of the condyle on the left side. The lesion was homogeneously radiolucent

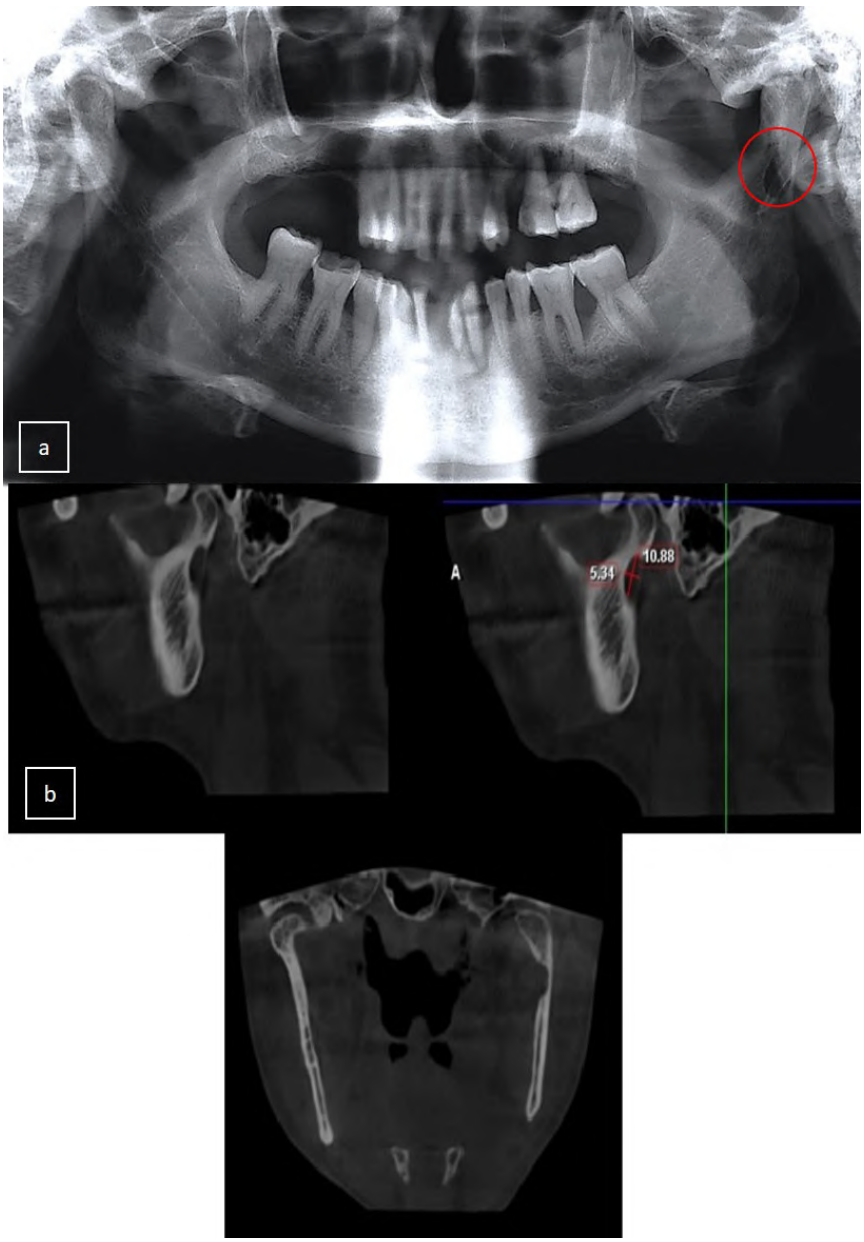

Fig. 2.- a: Orthopantomogram showing SBC of Ramus variant, noted in the posterior portion of the ramus below the neck of the condyle on the left side. **b:** CBCT showing well-defined semilunar radiolucency noted in the left medial surface of ramus below the level of subcondylar region.

without sclerotic borders and had a maximum diameter of one centimetre. There were no changes in the surrounding tissues, such as periosteal response or displacement of anatomical structures (Fig. 2a). CBCT was advised to further investigate the lesion that confirmed a well-defined, uniformly radiolucent lesion visible in the axial cross sections on the medial surface of the left ascending ramus, measuring about 10.8 x 5.3 mm with no sclerotic borders. In coronal sections, it appeared as a well-defined *semilunar radiolucency* involving the medial surface of the ramus below the level of left sub-condylar region (Fig. 2b).

DISCUSSION

A bone cavity or pseudocyst well recognized as the "Stafne bone cavity" (SBC) is primarily filled with salivary gland tissue, and may comprise of muscles, lymphoid tissue, blood vessels, fat, and/or connective tissue (Iwanaga et al., 2019). The nature of the contents of the bone cavity is determined by the local anatomical condition, as in the case of rare ramus variants, where ectopic adipose tissue development has been reported (Friedrich et al., 2012). SBC is thought to be a developmental lesion that often manifests in middle-aged to older adults, but is presumed to have its origin in intrauterine growth (Schneider et al., 2014). Stafne claimed that, during the development of the mandible, Meckel's cartilage was replaced by bone tissue and a fragment of the salivary gland was trapped. However, there are numerous hypotheses regarding its etiopathogenesis, but the most prominent one, which is commonly acknowledged by several authors, is that it occurs as a result of bone resorption caused by external pressure exerted by nearby salivary glands (Ariji et al., 1993). This hypothesis was supported by discovering large bone cavities packed with salivary gland tissue after examining 15 patients using CT scans and sialography. Certain authors, nevertheless, refuted this hypothesis by affirming the presence of some clear bone cavities with no sign of salivary gland tissue, as well as indicating similar findings on the buccal surface of the mandible, which are evidently distant from the salivary gland tissue (Friedrich et al., 2012). Clinically, it is asymptomatic, seldom palpable due to the missing bone surface, and self-limited in progression, but invasive procedures may be performed if it is incorrectly labelled as a tumour or a true cyst (Lucas et al., 2021). For instance, when it develops in an edentulous region of the mandible, the more anteriorly placed SBC variation might occasionally unintentionally resemble a remnant cyst (de Courten et al., 2002). The Stafne bone cavity (SBC) usually manifests radiologically as a well-defined, radiolucent lesion below the level of the mandibular canal in the molar-mandibular angle region.

Stafne Bone Cavities were classified into three variants according to their location (Sisman et al., 2012), as described:

- Anterior variant: The lesion present in the sublingual gland area, involving anterior region or body of the mandible.
- Posterior variant: The lesion present in the submandibular gland area, involving the posterior aspect of mandible, was the most typical site.
- Ramus variant: The lesion present in the parotid gland area, involving the ramus of the mandible.

In 1985, Wolf described the "ramus variety" of Stafne's bone cyst in the parotid area. Stafne bone cysts, which form as a result of unusual alterations in the ascending ramus, are benign, but their radiographic features may mimic some intrabony neoplasms (Bornstein et al., 2009). Furthermore, this entity should be distinguished from a pseudo foramen known as "medial sigmoid depression," which also manifests as a radiolucency found in the mandibular ramus (Langlais et al., 1983). The ascending mandibular ramus has been identified as the least prevalent site for Stafne's bone cavity, and two such cases are presented here.

Hisatomi et al. (2019) reviewed 91 instances with Stafne bone cavities, and discovered that the posterior variation was present in 0.10% to 0.48% of cases. Anterior variants are almost seven times less prevalent than posterior variants. However, in contradiction of the above statistics, we are reporting two cases with Stafne bone cavities of the ramus variant, which have been rarely reported previously in the literature (Table 1).

Table 1. Past literature reporting of Stafne Bone Cavities (Ramus variant).

Case No.	Author (year)	Age & Gender	Site	Imaging modalities performed
1.	Barker (1988)	60 year male	The posterior border of the left ascending ramus below the neck of the condyle	Panoramic
2.	Minowa et al. (2003)	63 year female	The posterior border of the right ascending ramus below the neck of the condyle	CT
3.	Minowa et al. (2003)	50 year male	Left mandibular ramus	CT, MRI
4.	Tarım Eratas et al. (2013)	55 year male	Right mandibular ramus at the junction of ramus and coronoid process	CBCT, MRI
5.	Campos et al. (2004)	14 year male	Right mandibular ramus	Panoramic, CT
6.	Anbiaee et al. (2016)	55 year male	Posterior and upper one-third of the right mandibular ascending ramus und1er the condylar neck	Panoramic, CBCT
7.	Melnichenko et al. (2016)	57 year female	Left mandibular ramus	CBCT
8.	Chen et al. (2016)	52 year male	Superior region of the left ascending ramus	Panoramic, CBCT
9.	Hisatomi et al. (2019)	52 year male	Superior posterior border of left mandibular ramus	Panoramic, MRI
10.	Lee et al. (2019)	57 year male	Left mandibular ramus	Panoramic, CBCT
11.	2023 (Current case)	14 year female	The posterior border of the left ascending ramus below the neck of the condyle	Panoramic, CBCT
		50 year male	The posterior border of the left ascending ramus below the neck of the condyle- lingual variant	Panoramic, CBCT

Although the ramus is extremely closely related to the external auditory meatus, it was challenging to palpate the jaw medially in these cases, and there was no palpable deformation of the mandibular cortex. No other symptoms were observed in either of the cases. Confirming the diagnosis of an SBC will be highly conducive when a rare or uncommon variation is suspected. Additional imaging, such as computed tomography or magnetic resonance imaging, as well as documentation of a radiolucency of unaltered size and appearance, would help to confirm the diagnosis. In a study on SBCs, Sisman et al. (2012) found that there was no discernible difference between CBCT and commonly used Multislice Spiral Computed Tomography (MSCT) in terms of accuracy. In addition, CBCT produces a lower radiation exposure dose than MSCT; therefore, it is preferred to avoid subjecting patients to radiation inadvertently. According to Katz et al. (2001), CBCT also provided detailed information about the conclusive diagnosis of SBC. As reported by More et al. (2015), an asymptomatic patient with a definitive radiographic diagnosis and periodic follow-ups are satiable, and a biopsy to confirm the diagnosis is redundant. Therefore, in the current cases, the CBCT analysis was sufficient to rule out SBC. When clinicians come across a radiolucency in panoramic radiography, Stafne's bone cavity is less often taken into consideration during differential diagnosis. However, as the lesion is asymptomatic and non-progressive, surgical intervention is unnecessary. The best long-term choice is generally considered to be periodic radiographic follow-up. The treatment of an anterior or posterior Stafne bone cavity does not require surgery. Atypical instances or any suspected lesions should be subjected to surgical examination or biopsy.

CONCLUSION

Stafne's bone cavity is a relatively uncommon anatomic anomaly that can typically be detected radiographically, although it can present a diagnostic challenge if it manifests in an unusual position. To prevent a misleading diagnosis, it must be distinguished from other cystic lesions. A surgical examination or biopsy should be performed on unusual cases or any suspected lesions. This case series attempted to further understand the occurrences of Stafne cysts, which could frequently be misdiagnosed as potentially lethal mandibular

cavities. Hence, they should not be missed out from the list of differential diagnoses, while considering cystic lesions involving the mandible.

REFERENCES

ARIJI E, FUJIWARA N, TABATA O, NAKAYAMA E, KANDA S, SHIRATSUCHI Y, OKA M (1993) Stafne's bone cavity. Classification based on outline and content determined by computed tomography. *Oral Surg Oral Med Oral Pathol*, 76(3): 375-380.

BORNSTEIN MM, WIEST R, BALSIGER R, REICHART PA (2009) Anterior Stafne's bone cavity mimicking a periapical lesion of endodontic origin: report of two cases. *J Endod*, 35: 1598-1602.

CAMPOS PS, PANELLA J, CRUSOÉ-REBELLO IM, AZEVEDO RA, PENA N, CUNHA T (2004) Mandibular ramus-related Stafne's bone cavity. *Dentomaxillofac Radiol*, 33: 63-66.

DE COURTEN A, KÜFFER R, SAMSON J, LOMBARDI T (2002) Anterior lingual mandibular salivary gland defect (Stafne defect) presenting as a residual cyst. *Oral Surg Oral Med Oral Pathol Oral Radiol Endod*, 94: 460-464.

FRIEDRICH RE, ZUSTIN J, SCHEUER HA, ASSAF AT, GRÖBE A (2012) A unilateral basal bone defect of the mandible occupied by fatty tissue: Stafne's cavity. *In Vivo*, 26: 1045-1048.

HISATOMI M, MUNHOZ L, ASAUMI J, ARITA ES (2019) Stafne bone defects radiographic features in panoramic radiographs: Assessment of 91 cases. *Med Oral Patol Oral Cir Bucal*, 24(1): e12-19.

IWANAGA J, WONG TL, KIKUTA S, TUBBS RS (2019) Stafne bone cavity: a rare cadaveric case report. *Anat Cell Biol*, 52(3): 354-356.

KATZ J, CHAUSHU G, ROTSTEIN I (2001) Stafne's bone cavity in the anterior mandible: a possible diagnostic challenge. *J Endod*, 27(4): 304-307.

KAYA M, UGUR KS, DAGLI E, KURTARAN H, GUNDUZ M (2018) Stafne bone cavity containing ectopic parotid gland. *Braz J Otorhinolaryngol*, 84: 669-672.

LANGLAIS RP, GLASS BJ, BRICKER SL, MILES DA (1983) Medial sigmoid depression: a panoramic pseudoforamen in the upper ramus. *Oral Surg Oral Med Oral Pathol*, 55: 635-638.

LUCAS M, LUCIANA M, ALINE N, MIKI H, JUNICHI A, EMIKO A (2021) Imaging features of Stafne bone defects on computed tomography: An assessment of 40 cases. *Imaging Sci Dent*, 51: 81-86.

MORE CB, DAS S, GUPTA S, PATEL P, SAHA N (2015) Stafne's bone cavity: a diagnostic challenge. *J Clin Diagn Res*, 9(11): ZD16-19.

SCHNEIDER T, FILO K, LOCHER MC, GANDER T, METZLER P, GRÄTZ KW, KRUSE AL, LÜBBERS HT (2014) Stafne bone cavities: a systematic algorithm for diagnosis derived from retrospective data over 5 years. *Br J Oral Maxillofac Surg*, 52(4): 369-374.

SISMAN Y, MILOGLU O, SEKERCI AE, YILMAZ AB, DEMIRTAS O, TOKMAK TT (2012) Radiographic evaluation on prevalence of Stafne bone defect: a study from two centres in Turkey. *Dentomaxillofac Radiol*. 41(2): 152-158.

Ascending pharyngeal artery supplying the posterior inferior cerebellar artery via the hypoglossal canal with preserved anastomosis to the vertebral artery: a rare variant of the persistent hypoglossal artery

Alexis Guédon [1, 2, 3], Bernard Moxham [3, 4], Odile Plaisant [2, 3], Emmanuel Houdart [1, 2]

[1] *Department of Neuroradiology, Lariboisière Hospital, AP-HP Nord, Paris, France*

[2] *Université Paris Cité, France*

[3] *Trans-European Anatomical Pedagogic Research Group (TEPARG)*

[4] *Cardiff School of Biosciences, Cardiff University, Wales, UK*

SUMMARY

Carotid-vertebrobasilar anastomoses are rare and usually discovered serendipitously; the persistent hypoglossal artery is the second most common, with an incidence of 0.29%. We present a very rare anatomical variant of a persistent hypoglossal artery. This variant was visualized on 2D and 3D angiography and on MRI.

In the case reported here, the hypoglossal branch of the neuromeningeal trunk of the ascending pharyngeal artery communicated with the posterior inferior cerebellar artery ("type 2 persistent hypoglossal artery variant" of Uchino's classification), but with a preserved junction with the vertebral artery, which is not hypoplastic ("ascending pharyngeal artery - vertebral artery anastomosis" of Lasjaunias' description). A review of the literature was performed on the "type 1-2 persistent hypoglossal artery variant" (11 cases) and schematic representations of the different anatomic variants are illustrated. The pharyngo-cerebellar artery and pharyngo-vertebral anastomosis are variants of the persistent hypoglossal artery, these relatively small branches may be missed, with a risk of cerebellar infarction during embolization.

Key words: Cerebellar arteries – External carotid artery – Vertebrobasilar system – Radiological anatomy – Interventional neuroradiology

INTRODUCTION

Carotid-vertebrobasilar (VB) anastomoses are rare and usually discovered serendipitously. However, they may have clinical significance, including aneurysm related to the anomalous artery (Tse et al., 2019), cerebral ischaemia owing to single arterial supply, and dangerous anastomoses in the case of embolization. Four types of

Corresponding author:
Dr Alexis Guédon. Service de Neuroradiologie Diagnostique et Interventionnelle, Hôpital Lariboisière, AP-HP Nord, 2 rue Ambroise Paré, 75010 Paris, France. Phone: +33 1 49 95 81 17 ; Fax: +33 1 49 95 83 56. E-mail: alexis.guedon@aphp.fr

Submitted: February 22, 2023. **Accepted:** March 14, 2023

https://doi.org/10.52083/OVDG1869

foetal anastomoses exist between the carotid artery and the VB system at 5 weeks gestation (at the 3-5 mm stage) (Padget, 1948); from the caudal to the cranial position: proatlantal intersegmental, hypoglossal, otic, and trigeminal arteries. During development, these primitive arteries regress, and/or fuse, to form the mature arterial system and with the development of the posterior communicating (PcomA) and vertebral (VA) arteries. Nevertheless, they can persist in some cases. The persistent trigeminal artery (PTA) is the most common persistent primitive carotid-VB anastomosis (Ota and Komiyama, 2022). Each persisting primitive artery can lead to several anatomical variations.

The persistent hypoglossal artery (PHA) is the second most common persistent carotid-VB anastomosis, with an incidence ranging from 0.027% (Lie and Foundation, 1968) in historic angiographic studies to 0.29% (Uchino et al., 2013) in a recent study based on 2074 CT angiographic images. Many cases have been reported since Batujeff (Batujeff, 1889) first reported in 1889 PHA in an autopsy case, and Begg (Begg, 1961) by angiography in 1961. Based on the work of Brismar (Brismar, 1976), three essential imaging diagnostic criteria are required to describe a PHA: 1) the PHA leaves the proximal ICA as an extracranial branch; 2) the PHA ascends posterior to the cervical ICA and passes into the posterior fossa via the hypoglossal canal; 3) the PHA joins the V4 segment of the ipsilateral VA or the caudal portion of the basilar artery (BA).

According to this description, a PHA is usually large and associated with an hypoplastic ipsilateral VA. Bilateral PHAs are rare (Murayama et al., 1985).

PHAs from the external carotid artery (ECA) have been reported recently. This extremely rare artery arises from the proximal ECA, and its proximal segment rises anterior to the cervical ICA. To our knowledge, 12 cases have been published (Welten et al., 1988; Nakamura et al., 2000; Meguro et al., 2007; Lee et al., 2010; Uchino and Saito, 2011; Nanto et al., 2012; Uchino et al., 2013; He et al., 2014; Sabouri et al., 2014; Yamamoto et al., 2019) (the homolateral VA was hypoplastic or absent in all cases). Based on this anatomical observation, Uchino proposed naming the usual PHA with an ICA origin as follows: “type 1 PHA”; and PHA with an ECA origin: “type 2 PHA” (Uchino and Saito, 2011). As proposed by Anderson and Sondheimer (Anderson and Sondheimer, 1976), entry into the hypoglossal canal is the discriminating factor differentiating the PHA from the persistent proatlantal artery (joining the VA via the foramen magnum) or the PTA (joining the BA via the prepontine cistern). In adults, the remnant of the PHA is the hypoglossal branch of the ascending pharyngeal artery (APA) (Lasjaunias et al., 1981, 2013). The APA normally arises from the posterior wall of the proximal ECA; after a short common trunk, the APA divides into the pharyngeal trunk anteriorly, the neuromeningeal trunk posteriorly and the inferior tympanic artery. The neuromeningeal trunk is intracranial, dividing into hypoglossal and jugular branches, entering the posterior fossa through the hypoglossal canal and the jugular foramen, respectively. The hypoglossal branch supplies the vasa nervorum of the hypoglossal nerve and the meninges of the posterior cranial fossa where it is in balance with the other arteries of this region (Hacein-Bey et al., 2002).

Among type 1-2 PHAs, a variant (“type 1-2 PHA variant”) may exist as a small PHA supplying only the posterior inferior cerebellar artery (PICA) without connecting to the BA. Similarly, for the “PTA variant”, the cerebellar artery originates from the PTA (anterior inferior cerebellar artery [AICA], superior cerebellar artery [SCA] and/or PICA) without persistent connection to the BA (Uchino, 2019).

We report here a very rare anatomical variation: a type 2 PHA variant with a persisting PICA-VA junction and without hypoplastic VA.

CASE REPORT

This anatomical variant was serendipitously discovered in our centre during a right lateral sinus stenting procedure for idiopathic intracranial hypertension syndrome with disabling pulsatile tinnitus caused by lateral sinus stenosis. Images were obtained from a preoperative brain MRI with 3D TOF sequence and cerebral arteriography per-

formed via the right radial approach during the stenting procedure with selective catheterisation of the right common carotid and vertebral arteries. The Institutional Review Board (IRB) committee approved the study. The procedures were carried out after obtaining an informed consent and in accordance with ethical standards.

In the case reported here, angiograms of the common carotid and vertebral arteries showed: 1) the VAs were co-dominant and of normal calibre; 2) the APA branched off as expected from the ECA and supplied the pharyngeal arteries; 3) the hypoglossal branch of the neuromeningeal trunk of the right APA was voluminous and fed the PICA through the right hypoglossal canal; 4) there was preserved hypoplastic communication between the VA and the PICA, with the connection occurring shortly after the exit of the hypoglossal canal,

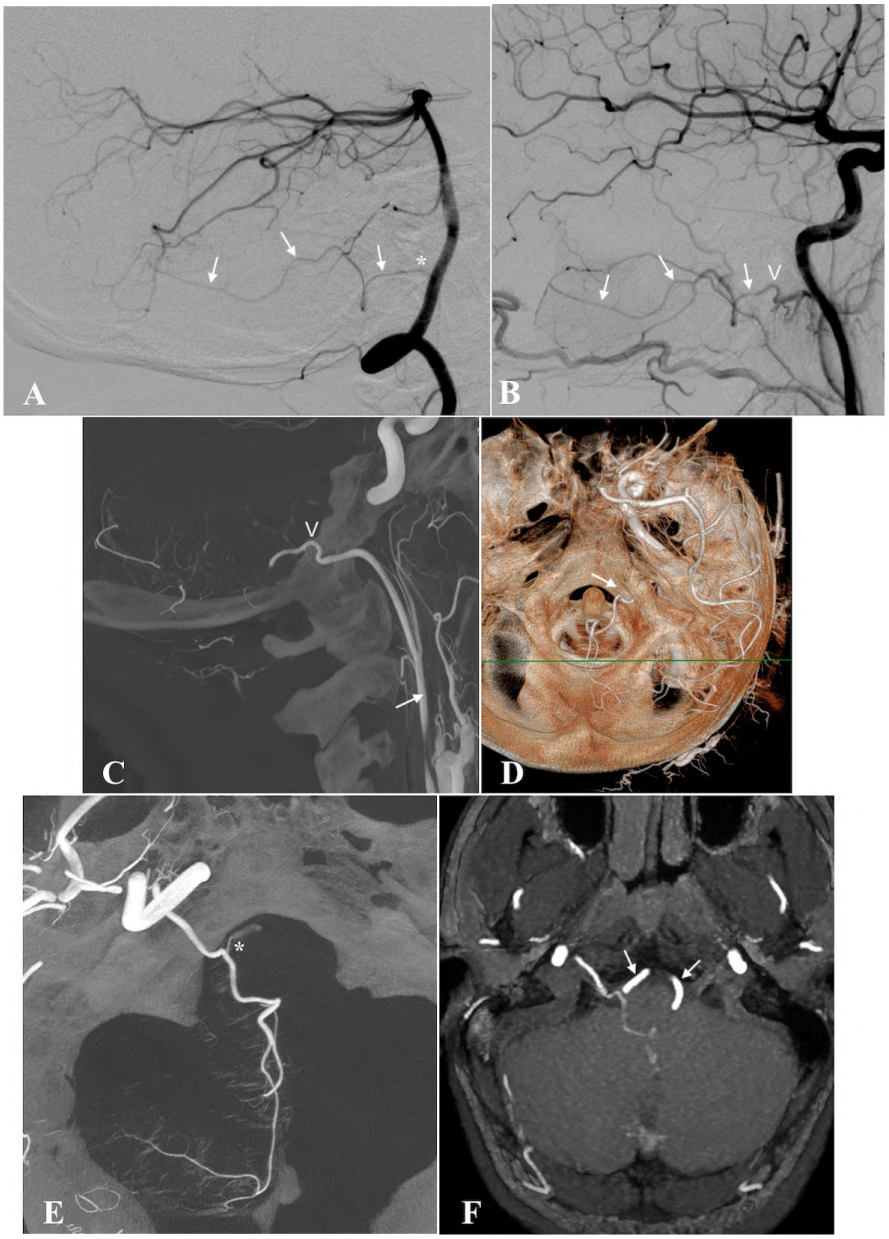

Fig. 1.- Case report illustration. **A**: Selective angiography of the right VA, lateral view, showing normal caliber of the V4 segment and persistence of a narrow communication (asterisk) with the right PICA (arrows); **B**: Selective angiography of the right CCA, lateral view, demonstrating the APA (hypoglossal) – PICA (arrows) anastomosis (arrowhead); **C**: 3D rotational DSA, lateral view, finding the APA (arrow) originating from the external carotid artery with the pharyngeal territory located anteriorly and posteriorly, through its hypoglossal branch (arrowhead), the neuromeningeal branch takes over the territory of the homolateral PICA; **D**: 3D-DSA volume rendering showing the emergence of the APA-PICA at the hypoglossal foramen (arrow); **E**: 3D-DSA with MIP, the persistent communication between PICA and V4 is visible (asterisk), **F**: 3D TOF MRI showing codominance and non-hypoplastic V4 segments on both sides (arrows), the V4-PICA communication is not visible. VA: vertebral artery, PICA: posterior-inferior cerebellar artery, CCA: common carotid artery, APA: ascending pharyngeal artery, DSA: digital subtraction angiography, MIP: maximum intensity projection, TOF: time-of-flight.

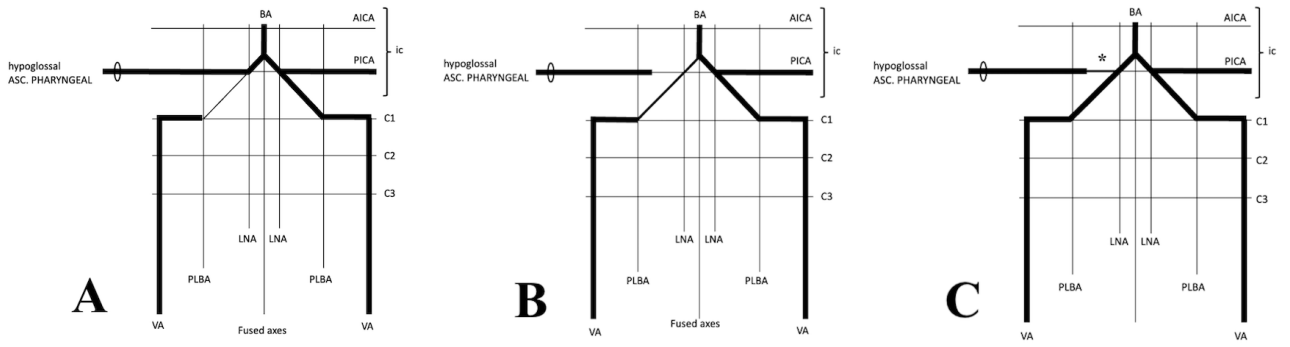

Fig. 2.- Frontal schematic representation of hypoglossal variations on the vertebrobasilar system. **A**: PHA; **B**: APA origin of PICA (pharyngo-cerebellar variety); **C**: Patient of this case report, APA (hypoglossal) – VA anastomosis with persistent of a hypoplastic stem of PICA (asterisk). On the three diagrams, the left PICA is represented supplied by the V4 segment (most frequent course, as in our patient).
PHA: persistent hypoglossal artery, VA: vertebral artery, PICA: posterior-inferior cerebellar artery, APA: ascending pharyngeal artery, LNA: longitudinal neural artery, PLBA: primitive lateral basilovertebral artery, BA: basilar artery, AICA: antero-inferior cerebellar artery, ic: intracranial.

there was no accessory PICA visible on the VA; 5) the APA terminated in the PICA and hemodynamically supplied the entire PICA territory, the supply of blood flow into the PICA by the VA was accessory (Fig. 1). This anatomical pattern represents an intermediate form between the type 2 PHA and the type 2 PHA variant, where there is no communication with the VB system (Fig. 2).

DISCUSSION

The hypoglossal canal is formed by the fusion of the intervertebral foramens of the area vertebralis (Karasu et al., 2009). The hypoglossal canal contains three important structures (Karasu et al., 2009): the twelfth cranial nerve, a meningeal branch of the APA, and a surrounding emissary venous plexus that communicates between the basilar venous plexus and the marginal sinus

Table 1. Type 1-2 PHA variant in the literature.

N°	Author	Year	Sex	PHA Variant	Side	Imaging	Homolateral VA	Associated arterial anomalies
1	Teal JS	1973	M	1	R	DSA	Hypoplastic	Ruptured AComA aneurysm, infraoptic course of the right ACA
2	Lasjaunias P	1981		1	R	DSA	Hypoplastic	Bilateral PHA
3	Murayama Y	1985	M	1	R	DSA	Hypoplastic	Bilateral PHA, ruptured PHA-BA aneurysm, right MCA aneurysm
4	Andoh K	2001	F	1	L	DSA, CTA	Hypoplastic	Right VA fusiform aneurysm, left MCA saccular aneurysm
5	Nakanishi N	2004	M	1	R	MRA, DSA	Absent	No
6	Kim JT	2009	F	2	L	MRA, CTA, DSA	Present	Occlusion of the left MCA with rich collateral supplies, severe stenosis of the right proximal MCA (Moya-Moya?)
7	Uchino A	2013	M	2	R	MRA, CTA	Present	Narrowing of entire right ICA
8			F	2	L	MRA, CTA	Absent	Right MCA aneurysm
9	Namba K	2017		2	R	DSA		
10	Patira R	2017	M	1	L	CTA	Absent	Bilateral PHA
11	Uchino A	2018	F	1	R	MRA	Absent	No

PHA: persistent hypoglossal artery, **VA**: vertebral artery, **BA**: basilar artery, **MCA**: middle cerebral artery, **ACA**: anterior cerebral artery, **AComA**: anterior communicating artery, **ICA**: internal carotid artery, **DSA**: digital subtraction angiography, **CTA**: computed tomography angiography, **MRA**: magnetic resonance angiography, **R**: right, **L**: left, **M**: male, **F**: female

around the foramen magnum. The hypoglossal artery and nerve are related to the rhombomere 8 and occipital somites 2-4 (Müller and O'Rahilly, 2011). The hypoglossal nerve is phylogenetically equivalent to a spinal nerve and not to a cranial nerve, although, given its evolutionary history, it is associated with the head into which it is secondarily included (Louryan and Vanmuylder, 2018).

To our knowledge, there are reports of 7 cases of type 1 PHA variant (Teal et al., 1973; Murayama et al., 1985; Andoh et al., 2001; Nakanishi et al., 2004; Uchino and Suzuki, 2018) and 4 cases of type 2 PHA variant (pharyngo-cerebellar artery) (Lasjaunias et al., 1981, 2013; Kim et al., 2009; Uchino et al., 2013) (Table 1). Most often, they are located on the right side (7/11) and the homolateral VA is hypoplastic or absent.

Lasjaunias et al. (1981, 2013) assume that the remnant of the PHA in adults is the hypoglossal branch of the neuromeningeal trunk of the APA. This hypothesis may explain the presence of a type 2 PHA. Normally, the hypoglossal branch of the APA supplies the meninges of the posterior fossa, the vasa nervorum of the hypoglossal nerve (XII), and a posterior descending branch contributes to the odontoid arch system providing anastomoses to the VA (Hacein-Bey et al., 2002). Whereas the lower cranial nerves are supplied by the VB system, the supply to their foraminal parts is mainly ensured by the neuromeningeal trunk of the APA (Lasjaunias et al., 2013). The dural branches of the jugular branch of the APA also rarely anastomose with the PICA though the jugular foramen (Effendi et al., 2016), although this does not represent a type of PHA variant (Uchino, 2019). According to Morris and Moffat (Moffat and Morris, 1956), the PHA is not identical to the embryonic hypoglossal artery. They suggest that the PHA is composite and is composed of three parts: 1) the primitive hypoglossal artery, 2) portions of the primitive lateral basilovertebral anastomosis (PLBA) (lateral anastomotic channel), and 3) the transverse anastomotic channels connecting the PLBA to the longitudinal neural artery (LNA). The type 1-2 PHA variant results from the persistence of the first and second parts, from involution or failure to develop of the third part and from disconnection of the PICA origin from the VA (Andoh et al., 2001).

Lasjaunias et al. (2013) theorize the existence of an "APA-vertebral anastomosis" with homolateral non-hypoplastic V4 segment of the VA. An illustration of this situation, similar to that for our patient, is provided on page 216 of the book *Surgical Neuroangiography* (Lasjaunias et al., 2013). This, to our knowledge, is the only other case. Recently, Bordes et al. (2021) report a case of hypoplasic pharyngo-vertebral anastomosis without homolateral V4 hypoplasia, but with PICA branched off the VA. This rare variant could be explained by a minimal persistence of the third portion of the PHA, or by the persistence of the origin of the PICA on the VA that is associated with a patent homolateral V4 segment of the VA. It is possible that the spatial resolution of MRA and CTA is insufficient to visualise a persistent hypoplastic communication with the VA (as in our case) and that, for some of the cases of type 1-2 PHA variant described in the literature where DSA is not performed, there is in fact a patent PICA-VA junction.

Unlike PHA, which is usually large, the type 1-2 PHA variant is a relatively small branch and may be missed, with a risk of cerebellar infarction during embolization. Thus, the existence of a type 1 PHA variant should not be ignored before planning a temporary intraoperative carotid occlusion for carotid endarterectomy, endovascular carotid occlusion, or balloon carotid artery occlusion testing. Recognition of a type 2 PHA variant is very important for endovascular treatment of a dural arteriovenous fistula of the hypoglossal canal/sigmoid sinus/jugular gulf fed by the APA, for preoperative embolization of a petroclival meningioma, and for preoperative or haemostatic embolization of pharyngeal tumours. The persistence of a PICA-VA junction could minimize these risks, provided that the flow via the VA is sufficient to compensate for the PICA territory.

REFERENCES

ANDERSON RA, SONDHEIMER FK (1976) Rare carotid-vertebrobasilar anastomoses with notes on the differentiation between proatlantal and hypoglossal arteries. *Neuroradiology*, 11(3): 113-118.

ANDOH K, TANOHATA K, MORIYA N, HAGIWARA H, LEE J, SATO M, YOSHIDA T, NAGASHIMA T (2001) The posterior inferior cerebellar artery arising from the extracranial segment of the internal carotid artery via the hypoglossal canal without an interposed segment of the basilar artery: A persistent primitive hypoglossal artery variant. *Clin Imaging*, 25(2): 86-89.

BATUJEFF E (1889) Eine seltene Arterienanomalie (Ursprung der A. basilaris aus der A. carotis interna). *Anat Anz*, 4: 282-285.

BEGG AC (1961) Radiographic demonstration of the « hypoglossal artery ». A rare type of persistent anomalous carotidbasilar anastomosis. *Clin Radiol*, 12: 187-189.

BORDES SJ, ZARRINTAN S, IWANAGA J, LOUKAS M, DUMONT AS, TUBBS RS (2021) Rare anastomosis between the ascending pharyngeal and vertebral arteries via the hypoglossal canal: A cadaveric case report. *Anat Cell Biol*, 54(3): 399-403.

BRISMAR J (1976) Persistent hypoglossal artery, diagnostic criteria. Report of a case. *Acta Radiol Diagn (Stockh)*, 17(2): 160-166.

EFFENDI K, MAGRO E, GENTRIC JC, DARSAUT TE, RAYMOND J, SEIZEUR R, BOJANOWSKI MW (2016) Anastomosis between the ascending pharyngeal artery and the posterior inferior cerebellar artery through the jugular foramen: a cadaveric observation. *Oper Neurosurg Hagerstown Md*, 12(2): 163-167.

HACEIN-BEY L, DANIELS DL, ULMER JL, MARK LP, SMITH MM, STROTTMANN JM, BROWN D, MEYER GA, WACKYM PA (2002) The ascending pharyngeal artery: branches, anastomoses, and clinical significance. *Am J Neuroradiol*, 23: 1246-1256.

HE S, RUSSIN JJ, ADAMCZYK P, GIANNOTTA SL, AMAR AP, MACK WJ (2014) A persistent primitive hypoglossal artery arising from the external carotid artery associated with subarachnoid hemorrhage. *World Neurosurg*, 82(1-2): 239.e1-239.e3.

KARASU A, CANSEVER T, BATAY F, SABANCI PA, AL-MEFTY, O (2009) The microsurgical anatomy of the hypoglossal canal. *Surg Radiol Anat*, 31(5): 363-367.

KIM JT, HEO SH, LEE SH, CHOI SM, PARK MS, KIM BC, YOON W, KIM MK, CHO KH (2009) An uncommon anastomosis of the posterior inferior cerebellar artery and the external carotid artery with the patent vertebrobasilar system. *Br J Radiol*, 82(981): e171-174.

LASJAUNIAS P, GUIBERT-TRANIER F, BRAUN JP (1981) The pharyngo-cerebellar artery or ascending pharyngeal artery origin of the posterior inferior cerebellar artery. *J Neuroradiol*, 8(4): 317-325.

LASJAUNIAS P, BERENSTEIN A, TER BRUGGE KG (2013) *Surgical Neuroangiography: Vol. 1: Clinical Vascular Anatomy and Variations* (Second ed.). Springer-Verlag, Berlin, Heidelberg.

LEE EJ, CHANG HW, CHO CH, KIM E, LEE SK, KWON JH (2010) Rare variant of persistent primitive hypoglossal artery in magnetic resonance angiography. *Surg Radiol Anat*, 32(8): 801-804.

LIE TA, FOUNDATION EM (1968) Congenital anomalies of the carotid arteries: including the carotid-basilar and carotid-vertebral anastomoses. an angiographic study and a review of the literature. *Excerpta Medica*.

LOURYAN S, VANMUYLDER N (2018) Apports de l'embryologie et de l'anatomie comparée à l'enseignement des nerfs crâniens. *Morphologie*, 102(337): 111-121.

MEGURO T, TERADA K, HIROTSUNE N, NISHINO S, ASANO T (2007) Unusual variant of persistent primitive hypoglossal artery. *Br J Radiol*, 80(960): e314-316.

MOFFAT DB, MORRIS ED (1956) Abnormal origin of the basilar artery from the cervical part of the internal carotid and its embryological significance. *Anat Rec*, 125(4): 701-711.

MÜLLER F, O'RAHILLY R (2011) The initial appearance of the cranial nerves and related neuronal migration in staged human embryos. *Cells Tissues Organs*, 193(4): 215-238.

MURAYAMA Y, FUJIMOTO N, MATSUMOTO K (1985) Bilateral persistent primitive hypoglossal arteries associated with a large ruptured aneurysm on one side. *Surg Neurol*, 24(5): 498-502.

NAKAMURA M, KOBAYASHI S, YOSHIDA T, KAMAGATA M, SASAKI T (2000) Persistent external carotid-vertebrobasilar anastomosis via the hypoglossal canal. *Neuroradiology*, 42(11): 821-823.

NAKANISHI N, SUGINO T, MORIKAWA K, OHKAWA N, FUKUSUMI A (2004) The posterior inferior cerebellar artery arising from the internal carotid artery directly: A variant of the persistent primitive hypoglossal artery. *No To Shinkei*, 56(3): 253-257.

NANTO M, TAKADO M, OHBUCHI H, MANDAI A, OSAKA Y, NAKAHARA Y, TENJIN H (2012) Rare variant of persistent primitive hypoglossal artery, arising from the external carotid artery. *Neurol Med Chir (Tokyo)*, 52(7): 513-515.

OTA T, KOMIYAMA M (2022) Vascular supply of the hindbrain: Basic longitudinal and axial angioarchitecture. *Interv Neuroradiol: J Peritherapeutic Neuroradiol Surg Proced Relat Neurosci*, 28(6): 756-764.

PADGET DH (1948) The development of the cranial arteries in the human embryo. (Contrib Embryol., Vol. 32). Carnegie Institution of Washington, USA.

SABOURI S, EBRAHIMZADEH SA, RAHIMIAN N (2014) Unusual variant of persistent primitive hypoglossal artery diagnosed by CT angiography: A case report and literature review. *Clin Neuroradiol*, 24(1): 59-63.

TEAL JS, RUMBAUGH CL, SEGALL HD, BERGERON RT (1973) Anomalous branches of the internal cartoid artery. *Radiology*, 106(3): 567-573.

TSE GH, MARTIN A, DYDE RA, COLEY SC (2019) Persistent hypoglossal artery aneurysm: Case report and qualitative systematic review. *Interv Neuroradiol*, 25(2): 164-171.

UCHINO A (2019) Carotid-vertebrobasilar anastomosis: Magnetic resonance and computed tomographic angiographic demonstration. *Jpn J Radiol*, 37(8): 565-578.

UCHINO A, SAITO N (2011) Persistent hypoglossal artery arising from the external carotid artery diagnosed by MR angiography. *Surg Radiol Anat*, 33(6): 543-545.

UCHINO A, SAITO N, OKADA Y, KOZAWA E, NISHI N, MIZUKOSHI W, INOUE K, NAKAJIMA R, TAKAHASHI M (2013) Persistent hypoglossal artery and its variants diagnosed by CT and MR angiography. *Neuroradiology*, 55(1): 17-23.

UCHINO A, SUZUKI C (2018) Variant of a persistent hypoglossal artery supplying only the posterior inferior cerebellar artery diagnosed by magnetic resonance angiography: A case report. *Surg Radiol Anat*, 40(7): 807-810.

WELTEN RJ, EIKELBOOM BC, ACKERSTAFF RG, LUDWIG JW (1988) A persistent hypoglossal artery arising from the external carotid artery. *Eur J Vasc Surg*, 2(4): 269-272.

YAMAMOTO R, MORI N, NAKAE Y, TANAKA F, JOHKURA K (2019) Anomalous anastomosis between the external carotid artery and vertebrobasilar artery via the hypoglossal canal: A case report and review of literature. *Surg Radiol Anat*, 41(7): 849-852.

Learning anatomy through dissection: emotional influence on the first-year medical student: a systematic review

Francisco Quiñonero[1,2,3], Cristina Mesas[1,2,3], Kevin Doello[1,3,4], Antonio J. Láinez-Ramos-Bossini[5], Gloria Perazzoli[1,2,3]

[1] Institute of Biopathology and Regenerative Medicine (IBIMER), Center of Biomedical Research (CIBM), University of Granada, 18100 Granada, Spain

[2] Department of Anatomy and Embryology, Faculty of Medicine, University of Granada, 18071 Granada, Spain

[3] Instituto Biosanitario de Granada (ibs. GRANADA), 18014 Granada, Spain

[4] Medical Oncology Service, Virgen de las Nieves Hospital, 18014 Granada, Spain

[5] Department of Radiology, Hospital Universitario Virgen de las Nieves, 18014 Granada, Spain

SUMMARY

The traditional study of anatomy is based on cadaveric dissection. However, in recent years new teaching methodologies have been introduced with the aim of increasing the ability of students to learn about the structures of the human body using computerized representations. Despite the increasing implementation of these new methodologies, universities around the world continue to base the practical teaching of anatomy on dissections. However, biomedical students begin to study dissections without having been exposed to a corpse previously, which poses a risk of generating stress. Using a systematic review process, we have observed that a large majority of students feel psychologically affected by this experience, leading to physiological consequences derived from anxiety and fear, although these decrease throughout the year due to a process of habituation. Therefore, it is necessary to reduce the amount of stress factors that can be found in the anatomy laboratory to increase the transfer of knowledge between professor and student.

Key words: Medical students – Anatomy – Dissection – Emotions

INTRODUCTION

For several centuries, the practical learning of anatomy has depended primarily on the use of dissection techniques in human corpses, an educational method widely used in universities around the world (Getachew et al., 2014). For years, different educational methods have been compared with the intention of elucidating which ones optimize anatomy learning. Several approaches have been carried out, including the use of small groups of students or computerized representations of anatomy, and even the debate between dissection and prosection has been raised. Despite all this, anatomy still needs

Corresponding author:
Dr. F. Quiñonero. Institute of Biopathology and Regenerative Medicine (IBIMER), Biomedical Research Centre (CIBM), University of Granada, Spain. Phone: +34-958249322; Fax: +34-958246296. E-mail: fjquinonero@ugr.es

Submitted: March 17, 2023. **Accepted:** April 11, 2023

https://doi.org/10.52083/OSUR2683

to be taught based on learning about the human body, this being fundamental for adequate professional development. Normally, anatomy teaching takes place during the first semesters of training of biomedical students, since it is a cornerstone for the subsequent development of more in-depth knowledge (Bernhardt et al., 2012).

However, there is one issue that may go unnoticed in our education system: how can we prepare young students of health science degrees to confront the study of anatomy using an anatomical subject? It should be noted that, at this early stage of their academic degree, most students have not had any prior contact with a corpse. The first exposure to a dead body can trigger various emotional reactions (Criado-Álvarez et al., 2017). In addition, stress is presented as a complex interaction between the student and his environment, generating around him events that can be positive, neutral, or negative. The most important manifestations of stress in the student are anxiety and depression, although the presence of low stress levels can lead to a lack of concentration and a decrease in motivation, and thus may influence their study habits and desire to work. It is important to note that stress has been shown to have a high impact in first-year students, who are focused on the exam stage due to a highly competitive environment and the absence of a well-defined study strategy. Conversely, students in higher clinical years show more concern for their professional future (Nechita et al., 2014).

The prosection of corpses is presented as an event that produces high levels of stress in students, generating physiological alterations such as palpitations, dizziness, or insomnia. Accordingly, generating a relaxed and favorable environment becomes essential to reduce the number of physiological alterations related to dissection in students (Anyanwu, 2015). Some studies have focused on trying to reduce the anxiety levels of students using different methods. One of them is based on an educational film about body donors; the students demonstrated increased levels of empathy and respect towards donors as a result, in addition to experiencing a reduction in anxiety levels, especially in those who were beginning to study anatomy (Iaconisi et al., 2019). Other studies have tried to improve anatomy learning using small tasks that students must perform in groups in each period, showing considerable acceptance by students, and improving the learning of the anatomical area being studied. This extra motivation could reduce stress in students (Kang et al., 2012). In addition to these techniques, some studies have focused on the use of background music in the dissection room to try to reduce the stress to which students are subjected when they are in front of the corpse, this methodology being capable of producing this fact and, in addition, increasing the grades obtained by the groups subjected to the experiment (Anyanwu, 2015; Bellier et al., 2020).

Considering this background, over the last few years there has been a lot of interest in studying the traumatic effects of dissection on students, in addition to the psychological implications that can undermine their education. A study conducted at Hawassa University on second- and third-year medical students found that approximately 20% and 30% of these students, respectively, had no symptoms when entering the dissection room. The most common symptoms observed in the rest of students were loss of appetite, dizziness, and nausea. Other less common symptoms included eye redness, shortness of breath, or skin irritations. The main cause of this symptomatology was the smell of the dissection room, followed by the feeling of touching the corpse and the fear triggered by being exposed to it (Getachew et al., 2014).

Our goal is to analyze the psychological and physiological impact of the educational method of human anatomy dissection in first-year medical students using a systematic review process.

MATERIALS AND METHODS

Study eligibility

The objective of this systematic review was to determine the psychological effects of exposure to cadavers on first-year medical students. For the implementation of this systematic review, we followed the guidelines of the *PRISMA (Preferred Reporting Items for Systematic reviews and Meta-Analyses)* declaration (Page et al., 2020).

Inclusion and exclusion criteria

Publications related to the psychological and physiological consequences of the use of anatomy teaching techniques in first-year medical students were included. Articles on repercussions caused by any educational method other than dissection were excluded. In addition, publications had to be focused on medical students. For this reason, publications focused on degrees other than Medicine (e.g., Dentistry, Occupational Therapy, Pharmacy, Physics, or Speech and Language Therapy) were excluded. Moreover, all publications that were not journal articles and outdated articles not available through database access were excluded. On the other hand, only articles published in English were included. There were no geographical restrictions.

Databases

The literature search was performed using various databases, including PubMed, SCOPUS, Web of Science (WOS) and ERIC, to locate education manuscripts. The keywords used in the search, which were adapted to each database, included "medical students", "anatomy", "dissection" and "emotions". Accordingly, the following search formula was used in PubMed: ("students, medical"[MeSH Terms] OR ("students"[Title/Abstract] AND "medical"[Title/Abstract]) OR "medical students"[Title/Abstract] OR ("medical"[Title/Abstract] AND "students"[Title/Abstract])) AND ("anatomy"[Title/Abstract] OR "anatomy"[MeSH Terms]) AND ("dissection"[MeSH Terms] OR "dissection"[Title/Abstract] OR "dissections"[Title/Abstract]) AND ("emotions"[MeSH Terms] OR "emotions"[Title/Abstract] OR "emotion"[Title/Abstract] OR "emotional"[Title/Abstract]). The search formula used in SCOPUS was: (TITLE-ABS-KEY (medical AND students) AND TITLE-ABS-KEY (emotions) AND TITLE-ABS-KEY (anatomy) AND TITLE-ABS-KEY (dissection). Furthermore, the formula used for WOS was: TS= anatomy AND TS= dissection AND TS=medical students AND TS=emotions. Finally, the search formula used in ERIC was: "anatomy AND dissection AND emotions AND medical students". Bibliographic citations between 1990 and 2023 were included.

Study selection

Two of the authors (F.Q, and C.M.) carried out the literature research, the review of the abstracts

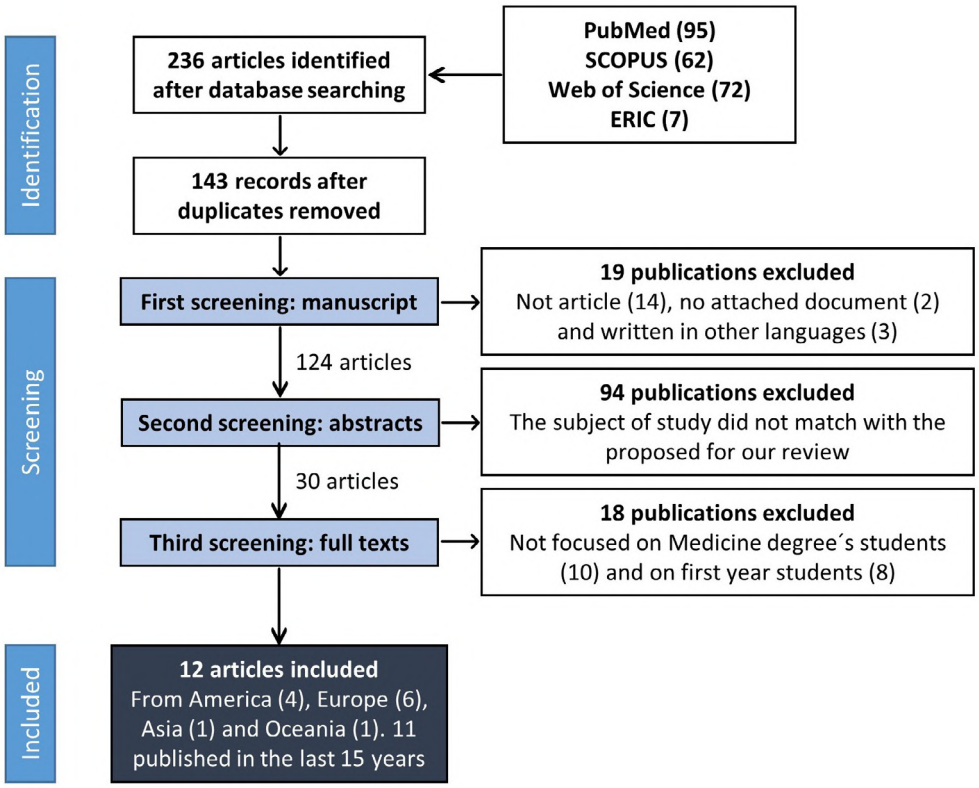

Fig. 1.- Flow diagram of the studies included in the review.

and the selection of the appropriate ones for full-text examination. After searching the databases described above, duplicated publications were eliminated. Following the application of the exclusion criteria, initial peer-reviewed screening was performed, considering the analysis of the publication title and summary. Finally, the screened articles were read in full, and those which met any exclusion criteria were discarded. In the event of a disparity between the two reviewers over inclusion, a third researcher was consulted to decide on its possible incorporation into the review.

The database search yielded 236 results, of which 93 were redundant, resulting in total of 143 articles being screened. Of these, 14 were excluded because they were not original research manuscripts, two because there was no attached document and 3 because they were written in other languages. In addition, 94 articles were excluded after reading the abstract, because they did not match the topic under study in our review. After full reading of the articles, 18 more were excluded (10 because they were not focused on medical students and 8 because they were not focused on first-year students). The final number of articles included in the review was 12 (Fig. 1).

RESULTS

Characteristics of the included studies

Studies carried out on Universities of Vermont, Minnesota, Oakland, Zulia (America), Castilla la

Table 1. Summary of features and results of articles included in the systematic review.

Reference	Year	University	Psychological and physiological consequences
Greene and Rosen	2020	Vermont University, USA	Nervousness, reflection on life, death, the donor and his family, concern for the body. They are altered by the smell of the dissection room.
Romo- Barrientos et al.	2019	University of Castilla la Mancha, Spain	Students show stress, anxiety, and fear. They are frightened by the observation of the corpse and report a strong smell in the practice room.
Chang et al.		Korea University, South Korea	Gratitude, intimate emotions after looking at corpses and respect for their altruism, responsibility, shock, apprehension, anxiety, and fear of death.
Wisenden et al.	2018	University of Minnesota, USA	Anxiety, mostly expressed in women compared to men.
Araujo-Cuauro		University of Zulia, Venezuela	Curiosity, fear, anguish, disgust, stress, sickness, and respect for the corpse. They manifest reactions of sweating, instability, tremor, paleness, and tachycardia.
Sandor et al.	2015	Universities of Bucharest, Debrecen, Pécs and Szeged, Hungary	Stress, post-practice thoughts about dead bodies, flashbacks, dreams about dead bodies, and fear of loneliness.
Hussein et al.		Oakland University	Sickness, fear, anxiety and depression, symptoms that decrease throughout the course.
Bob et al.	2014	Iuliu Hatieganu University, Romania	Fainting, dizziness, palpitations, tremors, sickness, sweating, loss of appetite, insomnia, recurrent images of corpses. They are altered by stimuli such as smell, vision and touch to corpses and are apprehensive.
Quince et al.	2011	University of Cambridge, United Kingdom	Apprehension, confusion, anxiety, sadness, enthusiasm, interest, and excitement. They get upset when they look at the corpse, coming to think of it afterwards.
Arráez-Aybar et al.	2008	Complutense University of Madrid, Spain	Curiosity, interest, anxiety, fear, pleasure, satisfaction, happiness, aversion, horror. Students develop arousal, nausea, palpitations, tremors, disturbed breathing, dry mouth, nausea, and dizziness.
Dempster et al.	2006	University of Northern Ireland, Ireland	Anxiety, sickness, appearance of nightmares, loss of appetite, increased thoughts about death and presence of recurrent images of corpses. Some students considered quitting the race.
Horne et al.	1990	University of Melbourne, Australia	Anxiety, dizziness depression, eye pain and sickness. In addition, the students reported a horrible smell of corpses.

Mancha, Complutense of Madrid, Iuliu Hatieganu, Cambridge, Northern Ireland, and several from Hungary (Europe), Korea (Asia) and Melbourne (Oceania) were included. Of the 12 articles selected, 11 had been published in the last 15 years, while the other one was published in 1990 (Table 1).

Psychological and physiological effects of the teaching of cadaveric dissection-based anatomy in first-year medical students

Initially, most students are emotionally prepared to attend the dissection room for the first time, a percentage that increases throughout the hands-on sessions. However, other studies reported that, although most students did not exhibit explicit "fear", 1/3 stated that they felt "several degrees of fear". In addition, half of the students had not witnessed any corpse before (Arráez-Aybar et al., 2008; David et al., 1990; Bob et al., 2014).

Studies indicated that, during the year, students' emotions and negative responses to exposure to the corpse decreased, especially anxiety and fear (Arráez-Aybar et al., 2008; Romo-Barriendos et al., 2019; Chang et al., 2018; Horne et al., 1990; Hussein et al., 2015; Dempster et al., 2006; Wisenden et al., 2018) and its consequences (nausea and nervous arousal, palpitations, tremors, tachycardia, paleness, nightmares, sweats and even shortness of breath) (Arráez-Aybar et al., 2008; David et al., 1990; Chang et al., 2018; Dempster et al., 2006; Araujo-Cuauro, 2018). This mixture of sensations disappears as the course progresses because they become accustomed to the dissection laboratory. However, certain negative emotions such as those derived from the smell of the dissection room increase throughout the year (Arráez-Aybar et al., 2008; Romo-Barriendos, et al., 2019; Araujo-Cuauro, 2018). In addition, several studies showed a decrease in positive emotions due to excessive workload and frequent examinations, difficulties in concentrating on the study, concerns about the future and financial problems, as well as personal problems such as partner relationships, family members and diseases (Sándor et al., 2015). Conversely, other studies found that these emotions remain unchanged or even increase (Chang et al., 2018; Greene and Rosen, 2021). Moreover, some authors observed that students express emotions of gratitude in relation to the donation process by appreciating the altruism of people and society (Chang et al., 2018) (Table 2).

Students also develop a perception of curiosity about dissection which remains invariable during the year. By the end of the year, almost all students indicated that they would "relive the experience", and that dissection-based teaching helped them reinforce the knowledge imparted in the theoretical classes. Students showed high satisfaction rates with practices, which remain unchanged throughout the year. However, a high percentage of students reflected on death after the first few months of internships due to their experience (Romo-Barriendos et al., 2019; Hussein et al., 2015). Upon completion of the anatomy course, students reported having a better understanding of anat-

Table 2. Consequences detected in the first expositions to the corpse in medical students.

Consequences	Number of studies (percentage)
Anxiety	8/12 (66%)
Sickness	6/12 (50%)
Fear	5/12 (42%)
Curiosity	4/12 (33%)
Concern for the body	4/12 (33%)
Reflection on life	4/12 (33%)
Stress	3/12 (25%)
Depression or sadness	3/12 (25%)
Respect for the corpse	2/12 (17%)
Nervousness	1/12 (8,5%)

omy, improved the development of psychomotor skills for clinical work, and were encouraged to further appreciate the human body and the spirit of organ donation (Hussein et al., 2015).

Students generally described the experience in the anatomy room as interesting, informative, challenging, exciting, enjoyable, and stimulating (Arráez-Aybar et al., 2008; Hussein et al., 2015) with the vast majority agreeing that cadaveric dissection is indispensable for the learning of anatomy (Bob et al, 2014; Araujo-Cuauro, 2018; Quince et al., 2011).

Modification of student behavior by prior exposure to the dissection laboratory

Prior exposure (PE) to laboratory practices by students did not increase positive responses. However, differences in negative emotions were found; these were significantly higher in students who had not previously been exposed to the laboratory (NE). During the year, NE students showed an increase in positive responses, while these did not vary significantly in PE pupils. Meanwhile, negative emotions decreased over time in NE students, but did not vary in PE students. At the end of the year, both groups expressed similar emotions in relation to the dissection process (Greene and Rosen, 2021).

DISCUSSION

The well-being of the student in his environment is essential for the correct process of education. Thus, it has been shown that the motivation of anatomy students is essential for optimizing the learning process (Abdel-Meguid and Khalil, 2017). The first contact with the corpse in the anatomical field can be frustrating for students who have just started their medical training. As shown in our review, lack of prior contact with a corpse leads to stress and fear in medical students through different mechanisms. The most frequent feelings described by students in these studies are anxiety (in 66% of the studies), sickness (50%) and fear (42%). One of the most interesting aspects is that, throughout the practical sessions in the anatomy laboratory, the students adapt, and their negative physiological and psychological feelings decrease, a factor that contributes to their learning. Although this learning curve is difficult for new students, most studies conclude that, by the end of the year, they enjoy the experience of learning about the body and that this type of education reinforces their theoretical knowledge on anatomy. Therefore, the experience of the anatomy student is positive after this training, endorsing its educational value. In addition, students who have previously been exposed to a dissection laboratory experience show fewer negative responses, which indicates that adaptation to these conditions reduces the stress caused by dissection and improves their learning experience. These results support those observed in other studies, in which implementation of training through prosection improves the theoretical and practical knowledge of students (Thompson et al., 2020).

The low number of articles obtained in our search may indicate that few anatomy professors have been interested in the consequences of exposure to a corpse for the first time in the novice student. However, the fact that most of the articles retrieved date from the last 15 years reveals an increasing interest in this topic. Therefore, it is essential to investigate new anatomy teaching methodologies capable of improving the environment in the dissection room, reducing the stress produced in the student, and increasing the knowledge acquired during the learning process. In our opinion, keeping dissection as a practical teaching method for human anatomy allows medical students to learn the structures in a real body, which makes it invaluable from an educational point of view.

CONCLUSION

Although students may think that they are prepared for dissection practices before they begin, exposure to corpses may affect them both psychologically and physiologically. Common symptoms during first exposures to a corpse include anxiety and fear reactions such as sweat, the presence of fainting or nausea, among others. However, habituation causes these reactions to decline over time, and reduces the percentage of students who show them at the end of the course. We stress the need for a greater number of studies in this field, since the physical and mental well-being of the student

is essential to allow for an optimal transfer of knowledge between the teacher and the trainee.

ACKNOWLEDGEMENTS

We thank the Scientific Instrumentation Center (C.I.C) from Granada University for technical assistance. This work was supported by the financial support from the CTS-107 Group from Junta de Andalucía.

REFERENCES

ABDEL MEGUID EM, KHALIL MK (2017) Measuring medical students' motivation to learning anatomy by cadaveric dissection. *Anat Sci Educ*, 10(4): 363-371.

ANYANWU EG (2015) Background music in the dissection laboratory: Impact on stress associated with the dissection experience. *Adv Physiol Educ*, 39(1): 96-101.

ARAUJO-CUAURO JC (2018) Reactions of the students of the first year of medicine in the practical study of the anatomy with the corpse before the dissection room and its influence on the learning process. *Avances en Biomedicina*, 7(2): 90-99.

ARRÁEZ-AYBAR LA, CASTAÑO-COLLADO G, CASADO-MORALES MI (2008) Dissection as a modulator of emotional attitudes and reactions of future health professionals. *Med Educ*, 42(6): 563-571.

BELLIER A, SECHERESSE T, STOECKLE A, DOLS AM, CHAFFANJON PC (2020) Impact of background music on medical student anxiety and performance during anatomical dissections: a cluster randomized interventional trial. *Anat Sci Educ*, 13(4): 427-435.

BERNHARDT V, ROTHKÖTTER HJ, KASTEN E (2012) Psychological stress in first year medical students in response to the dissection of a human corpse. *GMS J Med Educ*, 29(1): Doc12.

BOB MH., POPESCU CA, ARMEAN MS, SUCIU SM IHAELA, BUZOIANU AD (2014) Ethical views, attitudes and reactions of Romanian medical students to the dissecting room. *Rev Med Chir Soc Med Nat Iasi*, 118(4): 1078-1085.

CHANG HJ, KIM HJ, RHYU IJ, LEE YM, UHM CS (2018) Emotional experiences of medical students during cadaver dissection and the role of memorial ceremonies: A qualitative study. *BMC Med Educ*, 18(1): 1-7.

CRIADO-ÁLVAREZ JJ, GONZÁLEZ-GONZÁLEZ J, ROMO-BARRIENTOS C, UBEDA-BAÑON I, SAIZ-SANCHEZ D, FLORES-CUADRADO A, ALBERTOS-MARCO JC, MARTINEZ-MARCOS A, MOHEDANO-MORIANO A (2017) Learning from human cadaveric prosections: Examining anxiety in speech therapy students. *Anat Sci Educ*, 10(5): 487-494.

DAVID DJ, TILLER JW, EIZENBERG N, TASHEVSKA M, BIDDLE N (1990) Reactions of first-year medical students to their initial encounter with a cadaver in the dissecting room. *Acad Med*, 65(10): 645-646.

DEMPSTER M, BLACK A, MCCORRY N, WILSON D (2006) Appraisal and consequences of cadaver dissection. *Med Educ Online*, 11(1): 4592.

GETACHEW D (2014) Reaction of medical students to experiences in dissection room. *Ethiop J Health Sci*, 24(4): 337-342.

GREENE SJ, ROSEN L (2021) Tracking medical student emotionality in relation to whole body dissection and donation. *Clin Anat*, 34(1): 128-142.

HORNE DJ, TILLER JW, EIZENBERG N, TASHEVSKA M, BIDDLE N (1990) Reactions of first-year medical students to their initial encounter with a cadaver in the dissecting room. *Acad Med*, 65(10): 645-646.

HUSSEIN IH, DANY M, FORBES W, BARREMKALA M, THOMPSON BJ, JURJUS A (2015) Perceptions of human cadaver dissection by medical students: A highly valued experience. *Ital J Anat Embryol*, 120(3): 162-171.

IACONISI J, HASSELBLATT F, MAYER B, SCHOEN M, BÖCKERS TM, BÖCKERS A (2019) Effects of an educational film about body donors on students' empathy and anxiety levels in gross anatomy. *Anat Sci Educ*, 12(4): 386-398.

KANG SH, SHIN JS, HWANG YI (2012) The use of specially designed tasks to enhance student interest in the cadaver dissection laboratory. *Anat Sci Educ*, 5(2): 76-82.

NECHITA F, NECHITA D, PÎRLOG MC, ROGOVEANU I (2014) Stress in medical students. *Rom J Morphol Embryol*, 55: 1263-1266.

PAGE MJ, MCKENZIE JE, BOSSUYT PM, BOUTRON I, HOFFMANN TC, MULROW CD, SHAMSEER L, TETZLAFF JM, AKL EA, BRENNAN SE, CHOU R, GLANVILLE J, GRIMSHAW JM, HRÓBJARTSSON A, LALU MM, LI T, LODER EW, MAYO-WILSON E, MCDONALD S, ... MOHER D (2021) The PRISMA 2020 statement: an updated guideline for reporting systematic reviews. *BMJ*, 372: n71.

QUINCE TA, BARCLAY SI, SPEAR M, PARKER RA, WOOD DF (2011) Student attitudes toward cadaveric dissection at a UK medical school. *Anat Sci Educ*, 4(4): 200-207.

ROMO-BARRIENTOS C, CRIADO-ÁLVAREZ J, GONZÁLEZ-GONZÁLEZ J, UBEDA-BAÑON I, SAIZ-SANCHEZ D, FLORES-CUADRADO A, LUIS MARTÍN-CONTY J, VIÑUELA A, MARTINEZ-MARCOS A, MOHEDANO-MORIANO A (2019) Anxiety among medical students when faced with the practice of anatomical dissection. *Anat Sci Educ*, 12(3): 300-309.

SÁNDOR I, BIRKÁS E, GYORFFY Z (2015) The effects of dissection-room experiences and related coping strategies among Hungarian medical students. *BMC Med Educ*, 15(1): 73.

THOMPSON AR, MARSHALL AM (2020) Participation in dissection affects student performance on gross anatomy practical and written examinations: results of a four-year comparative study. *Anat Sci Educ*, 13(1): 30-36.

WISENDEN PA, BUDKE KJ, KLEMETSON CJ, KURTTI TR, PATEL CM, SCHWANTZ TL, WISENDEN BD (2018) Emotional response of undergraduates to cadaver dissection. *Clin Anat*, 31(2):224-230.

Eur J Anat, 27 (5): 651-652 (2023)

SynDaver®: as a tool for anatomical teaching and medical education

Manuel J. Uribe Miranda, Héctor M. Vargas Portilla, Yahair G. Mendoza Gallegos, Estefanía Hernandez Velázquez

Department of Neuroanatomy, School of Medicine, University Cuauhtémoc San Luis Potosí, Mexico

SUMMARY

The teaching of human anatomy is done through virtual dissection tables, 3D models and the use of synthetic cadavers as effective tools that can help integrate morphological, surgical and clinical processes. On the other hand, synthetic cadavers must remain submerged in running water with common table salt and liquid detergent, while not in use, to keep them fresh and flexible for dissections. In the anatomy laboratory of the University Cuauhtémoc San Luis Potosí, Mexico, we use this type of synthetic cadavers for practical classes. Various procedures are performed, such as dissection of the abdominal cavity, dissection of muscles of the dorsum, spine, face and neck, and suture workshop.

Key words: Anatomy – Cadaver – Education – Learning – Teaching

Mr. Editor,

Nowadays, the teaching of human anatomy is carried out through virtual dissection tables, 3D models, and the use of synthetic cadavers as effective tools that can help to integrate morphological, surgical, and clinical processes (Hecht and Larrazábal, 2018). Synthetic cadavers are very popular in America and Europe, where they are known by the SynDaver® brand. These models must remain submerged in running water with common table salt and liquid detergent, while they are not in use, to keep them fresh and flexible for dissections (Richardson et al., 2020; Gregory et al., 2020). On the other hand, this type of cadaver is increasingly being integrated into practical anatomy classes, becoming a useful tool when dissection practices are made in different anatomical planes, the vascular system, and the nervous system.

In the anatomy laboratory of the University Cuauhtémoc San Luis Potosí, Mexico, we use this type of synthetic cadavers for practical classes. Several procedures are performed, such as dissection of the abdominal cavity, dorsum muscles dissection, spine, face-and-neck and suture workshop (Fig. 1).

Corresponding author:
Manuel de Jesus Uribe Miranda. Calle 83, #328, Colonia: Prados de San Vicente Segunda Sección. 78394 San Luis Potosí, S.L.P. Mexico. Phone: 4444531930. E-mail: mdjum93@gmail.com

Submitted: March 17, 2023. **Accepted:** April 6, 2023

https://doi.org/10.52083/IQQT5640

Fig. 1.- Medical students dissecting dorsal muscles on the SynDaver model.

Taking the foregoing into consideration, anatomy students have been found to read more and perform better on final exams when dissecting these types of synthetic cadavers, compared to 3D models and anatomical drawings. Dissection facilitates learning, manual training and reduces errors in the surgical field in medical practice. We should preserve this type of practice and consider the synthetic cadaver an effective teaching-learning tool for the basics of anatomy.

Finally, the SynDaver® synthetic cadaver cost is very high. However, it allows medical students to know the morphology and tissue consistency in conditions similar to those of a real cadaver, but without the disadvantages of real cadavers such as their fixation in formaldehyde, as these solutions are toxic, carcinogenic and change the color of fresh tissues.

REFERENCES

GREGORY E, ZWAMBAG D, MCFALL K, ANDREWS D, RICHARDSON N (2020) Synthetic cadavers improved laboratory test grades in an undergraduate human anatomy course. *FASEB J*, 34(S1): 1-1.

HECHT P, LARRAZÁBAL A (2018) Uso de nuevos recursos tecnológicos en la docencia de un curso de anatomía con orientación clínica para estudiantes de medicina. *Int J Morphol*, 36(3): 281-828.

RICHARDSON N, ZWAMBAG D, MCFALL K, ANDREWS D, GREGORY D (2020) Exploring the utility and student perceptions of synthetic cadavers in an undergraduate human anatomy course. *Anat Sci Educ*, 14(5): 605-614.

SynDaver®: as a tool for anatomical teaching?

Response to the letter to the Editor: Syn Daver®: as a tool for anatomical teaching and medical education

Blanca Mompeó

Departamento de Morfología, Universidad de las Palmas de Gran Canaria, Gran Canaria, Spain

Dear Editor,

I have analyzed with great interest the letter to the Editor from Uribe et al. about the use and utility of SynDaver® synthetic cadaver.

Anatomical education has lately been changing to adapt to the current demands of the health science professions, and new teaching methodologies have supplemented traditional teaching methods due to the limited viability of time and human cadavers, the task of preparing and collecting embalmed cadavers, and the lack of instructors experienced in dissection.

Between the new tools, the SynDaver® synthetic cadaver seems to be becoming very popular in some anatomical departments for its versatility and easy conservation. The manufacturer considers that the artificial human tissue closely resembles the live human environment (Sakezles, 2009).

From my point of view, some questions concerning the SynDaver® synthetic cadaver deserve to be analyzed: 1. is the utility of synthetic cadavers different from the cheaper plastic models? 2. could this new resource replace the use of the human cadaver? 3. is it possible to dissect a synthetic cadaver?

Regarding the first point, although the SynDaver® synthetic cadaver is offered as a high- fidelity model, there is no proof of this material's effectiveness in gross anatomy teaching, considering its expensive cost. The letter's authors stated that students perform better on final exams when they dissect these types of material compared to 3D models and anatomical drawings, but there are no systematic studies about its effectiveness or comparison with other teaching resources. Supporting the synthetic cadaver effectiveness, the authors reference the work of Richardson et al. (2020), who explore this material's utility and student perception in an undergraduate human anatomy course. Using a systematic study, the authors demonstrated its utility by improving student grades by comparing synthetic cadavers and models with only models, but not with other teaching resources. Another referenced author exposes the tool as a new technologic resource to the study of anatomy with clinical orientation, considering that it is adequate to study larger anatomical structures, different organs, and topography, but they omit the proof of their efficacy (Hecht and Larrazabal, 2018).

Corresponding author:
Blanca Mompeó.E-mail: Blanca.mompeo@ulpgc.es

Submitted: April 9, 2023. **Accepted:** April 12, 2023

https://doi.org/10.52083/NVXC7226

On the other hand, the student perception is not always optimistic about the tool's utility in understanding the structures. While the synthetic cadaver could help understand the musculoskeletal relationship, it did not help understand the neurovascular structures (Mitchell et al., 2016). In my opinion, more studies are necessary to verify the efficacy of this material in teaching-learning anatomy, considering its cost.

Concerning the second point, despite the new technology used in its elaboration, the high- fidelity synthetic cadaver cannot become a substitute for human cadavers in teaching anatomy, not only because the structures, disposition, and joints between them are not genuine, but because many professional competencies derived from teaching anatomy, such as self-wareness, teamwork or reflective practice must be attributed to the use of cadaver dissection.

Concerning dissection, it is evident that the dissection in the SynDaver® synthetic cadaver is more a separation into pieces of its constitutive elements, such as it happens in the plastic models, than a dissection considered as a possibility to separate the structures along natural planes of cleavage, removing organs and identifying anatomical structures and its variability. Synthetic cadavers could be an option in learning-teaching anatomy, where several high-tech modalities are used for better understanding. However, it cannot replace cadaver-based instruction in anatomy in medical studies, and it is expensive concerning its usefulness.

REFERENCES

HECHT P, LARRAZÁBAL A (2018) Uso de nuevos recursos tecnológicos en la docencia de un curso de anatomía con orientación clínica para estudiantes de medicina. *Int J Morphol,* 36(3): 821-828.

MITCHELL T, NEWTON BW, TERREBERRY RR, VANCURA MX (2016) Video dissections to determine the usefulness of synthetic cadavers vs. real cadavers. *HAPS Educator,* 20(3): 115-118. doi:10.21692/haps.2016.026

RICHARDSON N, ZWAMBAG D, MCFALL K, ANDREWS D, GREGORY D (2020) Exploring the utility and student perceptions of synthetic cadavers in an undergraduate human anatomy course. *Anat Sci Edu,* 14(5): 605-614.

SAKEZLES C (2009) Synthetic human tissue models can reduce the cost of device development. *Med Device Technol,* 20(1): 32-34.

European Journal of Anatomy